Biomimetic mechanical control of pluripotent stem cell differentiation into pancreatic endocrine cells

by

Raymond Tran

Department of Chemical Engineering

McGill University

Montréal, Québec, Canada

December 2021

A thesis submitted to McGill University in partial fulfillment of the requirements to the degree of Doctor of Philosophy

Abstract

Insulin-producing beta cells derived from pluripotent stem cells could provide a virtually limitless cell supply to treat diabetes. This is accomplished using directed pancreatic differentiation protocols which deliver various stimuli through sequential changes of *in vitro* culture conditions to mimic events during embryonic development. Most protocols currently control the dosing of soluble signaling factors along with the formation of 3D cell aggregates. The cellular microenvironment of the developing pancreas is complex and involves many dynamic biophysical stimuli which are not well-studied in current differentiation protocols. This thesis focuses on biomimetic approaches to guide pancreatic differentiation, specifically on leveraging biomechanical stimuli seen and predicted during pancreatic morphogenesis. Three different approaches were used to recreate different aspects of pancreatic development, namely cell clustering during bud development, tissue geometry, and biomechanical forces. First, micropatterned surfaces were used to create well-defined, reproducible pancreatic cell clusters. Using this system, transcription factors which play a critical role in endocrine pancreas differentiation were upregulated in confined cultures, with distinct actin filament organization patterns emerging in the microwells. Next, to recreate the geometries seen during pancreatic morphogenesis, a novel technique to rapidly prototype micropatterned surfaces on-the-fly was developed. This technique was validated using human umbilical vein endothelial cells leading to novel insights regarding extracellular matrix removal in conventionally used wound healing assays. Later, this technique was used to generate micropatterns which mimicked sagittal sections of the developing pancreas. Lastly, an array designed to deliver equibiaxial strains was implemented to study the effect of biomechanical forces on pancreatic differentiation. The results suggest that biomechanical stimuli can promote endocrine differentiation and that these forces could originate *in vitro* from surrounding differentiating, clustering cells. Overall, these insights into the effect of the cell microenvironment during pancreatic development could lead to novel strategies for directed differentiation protocols which may lead to more cost-effective and efficient approaches.

Résumé

Les cellules bêta productrices d'insuline, dérivées de cellules souches pluripotentes, pourraient constituer une source de cellules pratiquement illimitée pour traiter le diabète. Pour ce faire, des protocoles de différenciation pancréatique ont été développés afin d'imiter les étapes du développement embryonnaire en livrant divers stimuli par le biais de changements séquentiels des conditions de culture in vitro. La plupart des protocoles contrôlent actuellement soit le dosage de facteurs de signalisation solubles ou la géométrie des cultures, i.e. la formation d'agrégats cellulaires en 3D. Le microenvironnement cellulaire du pancréas en développement est complexe et implique de nombreux stimuli biophysiques dynamiques qui ne sont pas bien étudiés dans les protocoles de différenciation actuels. Cette thèse se concentre sur des approches biomimétiques pour guider la différenciation pancréatique, en mettant l'accent sur l'exploitation des stimuli biomécaniques observés et prédits pendant la morphogenèse pancréatique. Trois approches différentes ont été utilisées pour recréer différents aspects du développement pancréatique, à savoir le regroupement des cellules lors du bourgeonnement pancréatique, la géométrie des tissus et les forces biomécaniques. Tout d'abord, des micro-motifs ont été utilisés pour créer des amas de cellules pancréatiques bien définis et reproductibles. Dans ce système, nous avons observé une augmentation significative de marqueurs essentiels au développement du pancréas dans les cultures confinées. De plus, nous avons observé une corrélation entre la réorganisation du cytosquelette d'actine et le processus de regroupement et de différenciation. Ensuite, nous avons cherché à recréer les géométries observées au cours de la morphogenèse pancréatique. Pour ce faire, nous avons mis au point une nouvelle technique permettant de rapidement fabriquer des surfaces microstructurées. Nous avons validé cette technique en utilisant des cellules endothéliales dérivées de la veine ombilicale humaine et avons découvert de nouvelles informations concernant l'élimination de la matrice extracellulaire dans les tests de blessure conventionnels. Ensuite, cette technique a été utilisée pour générer des micro-motifs qui imitent les sections sagittales du pancréas embryonnaire. Enfin, nous avons étudié le rôle des forces biomécaniques sur la différenciation du pancréas et recréé les contraintes prédites in vivo à l'aide d'un réseau conçu pour fournir des contraintes équibiaxiales. Cette étude suggère que les stimuli biomécaniques peuvent favoriser la différenciation endocrinienne et que in vitro, ces forces pourraient provenir des cellules en cours de différenciation et de regroupement. Dans l'ensemble, ces connaissances sur l'effet du microenvironnement cellulaire pendant le développement du pancréas pourraient conduire à l'élaboration de protocoles de différenciation plus efficaces tant au niveau de la qualité du produit que du coût de bioproduction.

Acknowledgements

I have met many intelligent, creative, and passionate people during my graduate studies, and I believe all of these interactions have helped me become the researcher I am today.

Firstly, I would like to thank my two co-supervisors, Dr. Chris Moraes and Dr. Corinne Hoesli, for taking a chance with me coming with little research experience into your labs. Chris, thank you for encouraging me to pursue my crazy, sometimes silly, ideas in the lab and reigning me back when necessary. Corinne, thank you for always being so supportive, for all your guidance, and for always inspiring new views from a different perspective. It has been a wonderful experience learning from you two, both inside and outside the lab. I know the skills I have taken from both of you will take me far.

Thank you to all the members of the Moraes lab that I have had the opportunity to work with. It was a great innovative environment, and I enjoyed all the work and play that went on in the lab. Steph, thank you for exposing me to many different hobbies which I have since grown to love and for all the adventures together. You have helped me grow enormously and I truly appreciate all you have done for me both in the lab and outside. Sanya, I am thankful to have had a great desk buddy during the first few years. Thanks for helping to start the fiesta committee and promoting a great lab atmosphere to work in. Wontae, I'm glad we were able to always get food and coffee together, most especially after long lab sessions. Sarah, thanks for taking me out for fun times into the wilderness and showing me trees in their natural habitat. Camille, thanks for being there to relate with PSC culture and keeping up lab morale. Sonya, I really enjoyed our conversations during office visits and dim sum. Carley, thanks for always being a joy to be around in the lab – I really appreciate you keeping me on track writing this thesis. Gabe, thanks for always being an engaging part of the lab, offering valuable insight, and a fun person to work with in general.

Thank you to the Hoesli lab – although I didn't work much with many of you it was nice to be part of such a welcoming, friendly lab environment. Jonathan, I am glad we had so many overlapping terms in the lab so that we could have our many outdoor adventures and occasional discuss science. Also, thank you very much for your help in translating my multiple abstracts into French. Mohamed, it has been wonderful experiencing the ups and downs of research with you and I will never forget the autoclave floods we have been through together. Brenden and Julia, I enjoyed all

the times I was fortunate enough to bump into you guys in the lab. Thanks for always being so willing to let me take you away from work to chat even when you had a million things to do. A special thank you to Natalie, Karen, and Nia, who supported me from the beginning of graduate studies and got the Hoesli lab up and running before we got there.

Thank you to Lisa D. for your tireless effort keeping the lab running, we are very fortunate to have you. Frank, I always enjoyed our conversations throughout our time here and thank you for always being willing to help out - I truly appreciate all you do for the labs and the program.

Thank you to all the undergraduate researchers I've had the pleasure to work with throughout my time at McGill. In particular, Si Da, Yanqing, and Andre thank you for your help getting my research off the ground; it has been a pleasure and a great experience to supervise all of you.

I would also like to thank all of the funding sources that have aided me throughout the course of my studies. Thank you to NSERC, Diabète Québec, the Quebec Cell, Tissue and Gene Therapy Network – ThéCell, the Montreal Diabetes Research Center (MDRC), the Juvenile Diabetes Research Foundation (JDRF), the McGill Regenerative Medicine Network (MRM), and the Centre québécois sur les matériaux fonctionnels (CQMF).

Finally, thank you to all my family that have never stopped supporting me on this journey.

Copyright Acknowledgements

I further acknowledge the following publishing companies for granting me the rights to use the full text and figures of my published works in the following chapters:

- Chapter 2: **Frontiers Media**, Frontiers in Bioengineering and Biotechnology 2020
- Chapter 4: **Nature Publishing,** Scientific Reports 2020
- Chapter 5: **IOP Publishing**, Biofabrication 2021

Table of Contents

Preface

This thesis is written in the manuscript-based format. It contains one published review (Chapter 2), two published articles (Chapter 3 and 4), and one manuscript in preparation (Chapter 5).

First author publications originating from this thesis

1) Developmentally-inspired biomimetic culture models to produce functional islet-like cells from pluripotent precursors
   R Tran, C Moraes, CA Hoesli
   Front Bioeng Biotechnol 8 (2020). doi.org/10.3389/fbioe.2020.583970

2) Controlled clustering enhances PDX1 and NKX6.1 expression in pancreatic endoderm cells derived from pluripotent stem cells
   R Tran, C Moraes, CA Hoesli
   Sci Rep 10, 1 (2020). doi.org/10.1038/s41598-020-57787-0

3) Accessible dynamic micropatterns in monolayer cultures via modified desktop xurography
   R Tran, CA Hoesli, C Moraes
   Biofabrication 13, 2 (2021). doi.org/10.1088/1758-5090/abce0b

4) Biomechanical forces enhance PDX1 expression during pancreatic differentiation of pluripotent stem cells
   R Tran, Y Liu, A Khavari, AJ Ehrlicher, CA Hoesli, C Moraes
   Manuscript in preparation

Additional publications

1) Stem cells: to be born great, achieve greatness, or have greatness thrust upon them?
   R Tran, CA Hoesli, C Moraes
   Integrative Biology 8, 7 (2016). doi.org/10.1039/c6ib90021f

2) Production of Pluripotent Stem Cell-Derived Pancreatic Cells by Manipulating Cell-Surface Interactions
   R Tran, C Moraes, CA Hoesli
   Advanced Materials. Berlin, Boston: De Gruyter. (2019) DOI: 10.1515/9783110537734-010

3) Biomimetic Micropatterned Adhesive Surfaces To Mechanobiologically Regulate Placental Trophoblast Fusion
   Z Ma, LS Fagundes, **R Tran**, PK Parameshwar, N Kalashnikov, C Vaillancourt, C Moraes
   ACS Applied Materials & Interfaces 11, 55 (2019). DOI: 10.1021/acsami.9b19906

4) Architectural control of metabolic plasticity in epithelial cancer cells
   M Al-Masri, K Paliotti, **R Tran**, R Halaoui, V Lelarge, S Chatterjee, L Wang, C Moraes, L McCaffrey.
   Commun Biol 4, 371 (2021) doi.org/10.1038/s42003-021-01899-4

Original Contributions to Knowledge

The body of this thesis focuses on utilizing a biomimetic approach to guide pancreatic differentiation of pluripotent stem cells (PSCs). In particular, I engineered methods to **recreate cell clustering, geometry, and biomechanics** observed during pancreatic differentiation and development, while looking mainly at the expression of the pancreatic and duodenal homeobox 1 transcription factor, PDX1. By taking a multifaceted, interdisciplinary approach, I have uncovered several novel insights and made the following original contributions to the field.

First, in **Chapter 2**, I provide an overview on the various cues present in the developmental cellular microenvironment which could influence directed differentiation protocols from both a biochemical and a biomechanical perspective. Following this, I bring a new perspective by looking at advances which control microenvironmental cues *in vitro* and frame these developments in the context of biomimicry of the developing pancreas.

Then, in **Chapter 3**, I demonstrate a novel method to reliably generate high-density 2D clusters of pancreatic endoderm cells, using an agarose-based micropatterning system, and confirm previous reports that clustering and increased cell density improves pancreatic differentiation. This method is an improvement over conventional protocols that require the forced formation of 3D cell aggregates, which are difficult to handle, technically challenging to study, and prone to sample loss. Using this technique, I reveal novel insights into the phenotype and behaviour of pancreatic cells during differentiation. In particular, I show that cytoskeletal rearrangements are required to promote pancreatic differentiation, measured by PDX1 expression, even before endocrine specification.

Complex micropatterns could better mimic morphogenesis but the required equipment and specialized techniques to generate these platforms are not broadly accessible. To address this need, in **Chapter 4,** I develop a novel, accessible, easy to use technique, termed SuBScribing (substractive bioscribing), to generate various biologically relevant micropatterns on-the-fly (in less than 90 minutes) using a modified desktop craft cutter. SuBScribing could be easily employed in labs for less than $1000 as it does not require expensive, specialized equipment or reagents, allowing for broader testing of micropatterns with a variety of cell lines. This technique is flexible in its operation and can be modified to perform micropatterned co-cultures, to create dynamic changes in micropattern geometry on live cell cultures, or to perform controlled wounding assays.

Together these features could lead to many other innovations in other biology labs. Using this technique, I find that mechanical scratching of epithelial layers could remove underlying extracellular matrix (ECM), which may have implications on previous wound healing studies. Furthermore, I reveal that overall migration is faster in lower aspect geometries and is highly dependent on scratching path due to ECM removal. Using the SuBScribing technique, I demonstrate that curved geometries promote PDX1 expression over straight geometries, suggesting the curvature of the developing pancreas plays a role in fate decisions.

In **Chapter 5**, I predict the presence of biomechanical forces involved in pancreatic morphogenesis *in vivo* and find evidence of heterogenous, cell-generated forces *in vitro*. With this knowledge, I take a novel approach to directed differentiation by incorporating timed mechanical stimuli in addition to an established pancreatic differentiation soluble signalling factor cocktail. Here I show that the average PDX1 expression increases in pancreatic endoderm cells when exposed to physiological stress profiles for 48 hours, implying that biomechanical stimuli plays a role in guiding endocrine differentiation. To my knowledge, this work is the first to introduce dynamic, mechanical actuation onto an established cell monolayer during directed pancreatic differentiation protocols. Other published works detach and seed differentiating pancreatic cells onto substrates with different stiffness or ECM composition, and the process of cell detachment could change cell behaviour. Here, my innovation could potentially give temporal control over the mechanical stimuli applied to a pre-existing layer of cells, which may lead to multifaceted, next generation directed differentiation protocols.

Finally, in **Chapter 6**, I integrate the combined results from my thesis, discuss limitations and other implications of my results, and finally propose other avenues for future research.

Contribution of Authors

Manuscript 1 (Chapter 2): Developmentally-inspired biomimetic culture models to produce functional islet-like cells from pluripotent precursors

Raymond Tran – researched, wrote initial draft, prepared figures, edited the manuscript

Christopher Moraes – edited the manuscript

Corinne A. Hoesli – edited the manuscript

Manuscript 2 (Chapter 3): Controlled clustering enhances PDX1 and NKX6.1 expression in pancreatic endoderm cells derived from pluripotent stem cells

Raymond Tran – project conceptualization, designed and conducted experiments, data analysis, investigation, write original draft, reviewed and edited the manuscript

Christopher Moraes – project conceptualization, resources, supervision, edited the manuscript

Corinne A. Hoesli – project conceptualization, resources, supervision, edited the manuscript

Manuscript 3 (Chapter 4): Accessible dynamic micropatterns in monolayer cultures via modified desktop xurography

Raymond Tran – project conceptualization, designed and conducted experiments, data analysis, investigation, write original draft, edited the manuscript

Corinne A. Hoesli – project conceptualization, resources, supervision, edited the manuscript

Christopher Moraes – project conceptualization, resources, supervision, edited the manuscript

Manuscript 4 (Chapter 5): Biomechanical forces enhance PDX1 expression during pancreatic differentiation of pluripotent stem cells

Raymond Tran – project conceptualization, designed and conducted experiments, data analysis, investigation, write original draft, edited the manuscript

Yanqing Liu – developed the initial FEBio finite element simulations which led to Figure 5-1 after modifications

Adele Khavari – provided Sylgard 527-soluble fluorescent tracking beads and assisted in traction force microscopy experiment design which led to Figure 5-3

Allen J. Ehrlicher – provided Sylgard 527-soluble fluorescent tracking beads, assisted in traction force microscopy experiment design which led to Figure 5-3

Corinne A. Hoesli – project conceptualization, designed and conducted experiments, data analysis, investigation, write original draft, edited the manuscript

Christopher Moraes – project conceptualization, designed and conducted experiments, data analysis, investigation, write original draft, edited the manuscript

List of Figures

List of Tables

Chapter 1

1.1 Introduction

1.2 Rationale

During development of tissues and organs, the cellular microenvironment is dynamically changing and undergoes many changes in presence of soluble signalling molecules, extracellular matrix (ECM) composition, matrix stiffness, and geometries. As tissues develop and cells differentiate, they undergo shape changes at the micro and macro scale. Pancreas development involves complex branching morphogenesis which occurs in tandem with endocrine specification, suggesting the resulting biomechanical changes associated with morphogenesis may impact differentiation. While current pancreatic directed differentiation protocols were designed to mimic sequential developmental stages and biochemical stimuli, they do not target biomechanical stimuli that accompany pancreas developmental stages *in utero*. These cues may be key to generating glucose-responsive insulin-producing cells in an efficient, reliable way but are not well captured in the state of the art. Thus, biomimicry of the developing pancreatic microenvironment during directed differentiation of pluripotent stem cells may aid the downstream production of functional insulin-producing beta cells.

1.3 Thesis Objectives

This thesis aims to investigate biomimetic approaches, using the developing pancreas as inspiration, to design new cultures systems which improve the early outcomes of endocrine differentiation protocols. The success of these aims could lead to novel insight into pancreatic morphogenesis and differentiation which may guide novel directed differentiation strategies in the future.

The specific aims of this thesis are to:

1) create a platform which can mimic *in vivo* cell clustering during pancreatic differentiation. I accomplish this by culturing cells on an array of circular micropatterns where 2D, self-aggregating cell clusters are generated during pancreatic differentiation, circumventing common issues of cell loss, to improve efficiencies.
2) develop a technique to generate geometries which resemble that of developing pancreatic branches and buds. Generating micropatterned surfaces is currently time-consuming, requires technical expertise, and specialized equipment and reagents. To address these issues, I developed an accessible technique which can generate agarose-based micropatterns on-the-fly using a modified hobby craft cutter, allowing us to prototype geometries observed in the developing pancreas.
3) investigate the effect of biomechanical stimuli during pancreatic differentiation. To accomplish this, I first use finite element simulations to predict stresses present during pancreatic morphogenesis. With this information, I then construct micro-scale devices to apply physiological levels of stress onto differentiating PSC-derived pancreatic cells *in vitro*.

Overall, this work aims to improve pancreatic differentiation protocols by incorporating biomimetic approaches during directed differentiation. Specifically, I explore the effect of clustering, geometry, and forces during pancreatic development.

Chapter 2

The following chapter begins with a comprehensive review of the state of the art in biochemical and biomechanical approaches applied to pancreatic differentiation protocols, for the goal of producing insulin-secreting beta cells. In this chapter, I look at these approaches from a biomimetic perspective to highlight the various biomechanical factors present during pancreas development and their role in pancreatic differentiation. The main text from this chapter was published in *Frontiers in Bioengineering and Biotechnology* by Frontiers Media in October 2020.

2.1 Developmentally-inspired biomimetic culture models to produce functional islet-like cells from pluripotent precursors

Raymond Tran, Christopher Moraes*, Corinne A. Hoesli*

Affiliations

[1] Department of Chemical Engineering, McGill University, 3610 rue University, Montreal, QC, Canada

[2] Department of Biomedical Engineering, McGill University, 3775 rue University, Montreal, QC, Canada

[3] Rosalind and Morris Goodman Cancer Research Center, McGill University, Montreal, QC, Canada

*Corresponding authors & equal contribution

E-mail: chris.moraes@mcgill.ca; corinne.hoesli@mcgill.ca

2.2 Abstract

Insulin-producing beta cells sourced from pluripotent stem cells hold great potential as a virtually unlimited cell source to treat diabetes. Directed pancreatic differentiation protocols aim to mimic various stimuli present during embryonic development through sequential changes of *in vitro* culture conditions. This is commonly accomplished by the timed addition of soluble signaling factors, in conjunction with cell-handling steps such as the formation of 3D cell aggregates. Interestingly, when stem cells at the pancreatic progenitor stage are transplanted, they form functional insulin-producing cells, suggesting that *in vivo* microenvironmental cues promote beta cell specification. Among these cues, biophysical stimuli have only recently emerged in the context of optimizing pancreatic differentiation protocols. This review focuses on studies of cell-microenvironment interactions and their impact on differentiating pancreatic cells when considering cell signaling, cell-cell and cell-ECM interactions. We highlight the development of *in vitro* cell culture models that allow systematic studies of pancreatic cell mechanobiology in response to extracellular matrix proteins, biomechanical effects, soluble factor modulation of biomechanics, substrate stiffness, fluid flow and topography. Finally, we explore how these new mechanical insights could lead to novel pancreatic differentiation protocols that improve efficiency, maturity, and throughput.

2.3 Introduction

Cell therapies involve the transplantation of human tissues or cells to treat illnesses that progressively damage or degrade functional tissues. These treatments are typically limited by access to a reliable and cost-effective cell source. For a successful transplant, allogeneic matching requires identification, procurement and transport of donor material; and variations in quality of the donated tissue may affect therapeutic potential. Therefore, the large-scale production of biological material for cell therapies is a rapidly growing area of interest. The primary goal of such research is to produce adequate quantities of functional therapeutic cells in a cost-effective manner.

Treatment of type 1 diabetes by islet transplantation is one example of a currently approved cell therapy. Here, donor islets are used to replace the insulin-secreting functionality lost from the autoimmune destruction of pancreatic beta cells. The Clinical Islet Transplantation Consortium trial (CIT-07) reported that 87.5% of patients were free from severe hypoglycaemic events and achieved normal or near normal glycaemic control at the 1 year end point (Foster et al., 2018). As with other cell therapies, the supply of donor islets greatly limits availability of this treatment. Islet transplantation typically requires a dose of greater than 5000 islet equivalents (IE) per kg body weight (Shapiro et al., 2017). To achieve the 500,000 - 1,000,000 IE/patient, islets are typically pooled from multiple deceased donors. Furthermore, the viability and function of the recovered islets is dependent on extraction techniques and post-mortem handling (Negi et al., 2012; Paraskevas et al., 2000; Rosenberg et al., 1999).

The production of insulin-secreting beta-like cells from pluripotent stem cells (PSCs) is a potential solution to the donor supply issues of islet transplantation. The first report of stem-cell derived insulin-producing cells via spontaneous differentiation was almost two decades ago and reported only 1-2% insulin^{+} cells (Assady et al., 2001). However, subsequent studies demonstrated that insulin staining and glucose-stimulated release can be due to insulin uptake from cell culture media (Hansson et al., 2004; Rajagopal et al., 2003; Sipione et al., 2004). Therefore, later studies reported C-peptide and/or pro-insulin content as well as more careful assessment of function and insulin granules instead of just insulin as a marker (D'Amour et al., 2006; Naujok et al., 2009; Sipione et al., 2004). More recent developments have been more successful, and rely on directed differentiation protocols which involve guiding stem cells through stages of pancreas development by mimicking the soluble signals present *in vivo*. These protocols are long and typically last more than 20 days (Hogrebe et al., 2020; Millman et al., 2016; Nair et al., 2019; Rezania et al., 2014).

One of the first major breakthroughs was homogenous induction of PSCs into the endoderm lineage (up to 80% endoderm cells) (D'Amour et al., 2005) and subsequently into cell populations with significant C-peptide and proinsulin content (D'Amour et al., 2006). Since then, the efficiency of monohormonal beta cell induction has increased (~40% NKX6.1^{+}/C-peptide^{+}) (Hogrebe et al., 2020). However, producing functional cell populations from PSCs remains an issue (Pagliuca et al., 2014; Rezania et al., 2014; Velazco-Cruz et al., 2019, 2020; Veres et al., 2019). Maturation of PSC-derived pancreatic progenitors can be accomplished when transplanted *in vivo* (Rezania et al., 2012; Robert et al., 2018) but typically requires cell aggregation *in vitro* (Nair et al., 2019; Toyoda et al., 2015). Hence, current strategies to improve directed differentiation protocols involve optimizing the duration of each differentiation stage as well as incorporating various aspects of the developmental microenvironment (Hogrebe et al., 2020; Mamidi et al., 2018a; Nair et al., 2019; Nostro et al., 2015).

This review will primarily focus on recent biomimetic approaches which exploit biochemical and biomechanical cues to promote the differentiation of pancreatic cells. We will first address directed differentiation protocols relying on soluble factors, followed by a discussion of more recent advances which mimic biophysical features of the developmental microenvironment, by manipulating cell-cell or cell-substrate interactions.

2.4 Directed pancreatic differentiation and cell signaling

Directed differentiation is the process of guiding stem cells through development to produce a desired, mature cell population. Classically, this is done by the timed addition of soluble factors to mimic conditions present during stages of development. In the context of pancreatic beta cell manufacturing, protocols emulate the multistep transition from pluripotent stem cells to definitive endoderm lineage, then towards the specification of the primitive gut tube and the subsequent pancreatic developmental steps (Figure 2-1A) (Benitez et al., 2012; Dassaye et al., 2016; Jennings et al., 2015; Pan & Wright, 2011). Each stage of development is accompanied by the nuclear expression of key transcription factors such as PDX1 or NKX6.1, which are commonly accepted as the first pancreatic and beta cell lineage markers respectively (Figure 2-1B) (Offield et al., 1996, p. 1; Schaffer et al., 2013, p. 1). Ultimately, the end goal of these protocols is to produce monohormonal, insulin-producing cells that have glucose-sensing capability comparable to native islets.

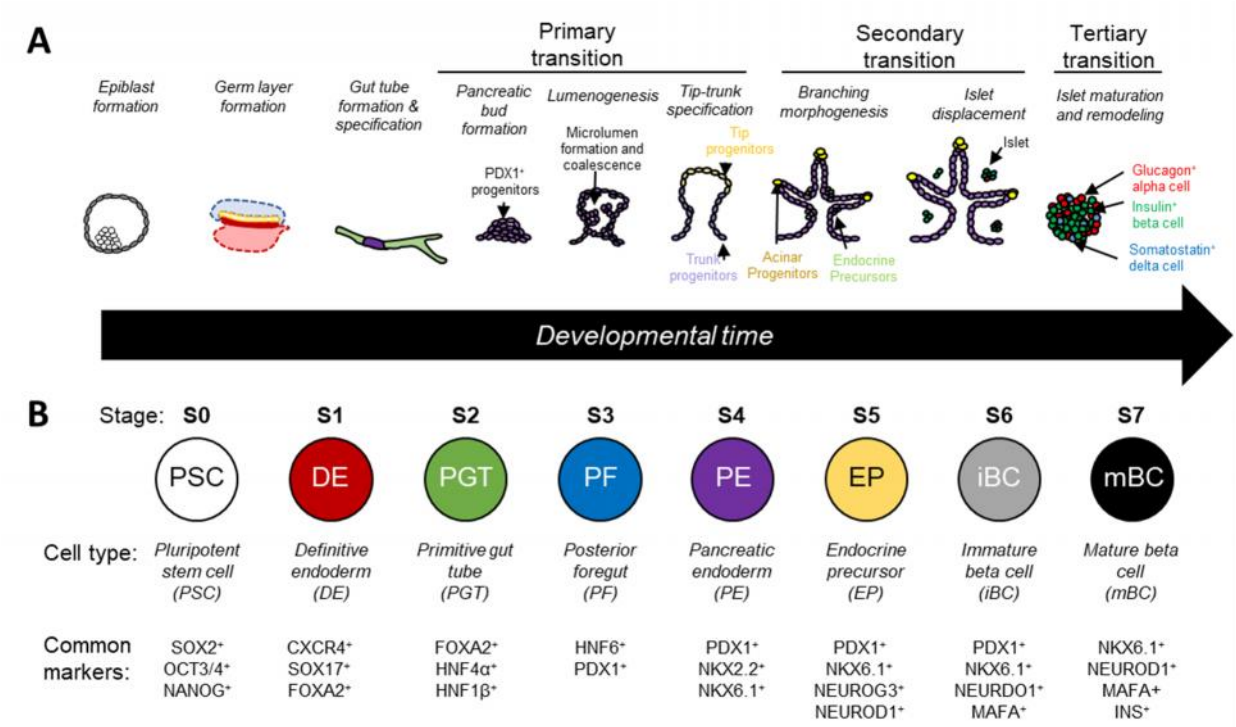

Figure 2-1*: (A) Illustrative schematic of pancreas development which is characterized by three main transitions. Primary transition involves bud formation and specification of different pancreatic cell types. Secondary transition involves branching of the pancreatic bud, further specification of endocrine precursors, and the delamination of islet cells. Tertiary transition involves remodeling of islet architecture and further maturation. (Benitez et al., 2012; Dassaye et al., 2016; Jennings et al., 2015; Pan & Wright, 2011) (B) Directed differentiation protocols recreate stages of differentiation in a step-by-step manner and look for expression of key transcription factors. Based on data presented by Rezania et al., 2014.*

In addition to soluble biochemical signals, other components of the cellular microenvironment are known to play a critical role during embryonic development. Stimuli from the microenvironment include biophysical cell-cell interactions and cell-extracellular matrix (ECM) interactions (Discher et al., 2009), which can interact with soluble factor signalling in a synergistic manner. However, the *in vivo* microenvironment, particularly during embryonic development, is particularly complex and difficult to mimic with current knowledge and culture systems.

Embryonic development is guided via highly dynamic signals from the surrounding cell microenvironment with remarkable precision and robustness. As cells differentiate, they relay different signals to neighbouring cells by secreting soluble factors and matrix proteins. The soluble signaling cues associated with pancreatic differentiation have been well studied using animal models and include the Wnt, Activin/Nodal, fibroblast growth factor (FGF), bone morphogenetic protein (BMP), retinoic acid, and sonic hedgehog (Shh), and Notch signaling pathways (Hashemitabar & Heidari, 2019). However, relatively little attention has been paid to the physical stimuli present during embryonic development. Biomechanics and cell/tissue mechanobiology play a large role in guiding cell behaviour especially during early embryogenesis (Heisenberg & Bellaïche, 2013). The pathways through which biomechanical cues translate to differentiation are not as well understood *in vivo*. Studies of developmental mechanobiology are challenging, and these parameters are often not considered as it is unclear what mechanics are present during human embryogenesis. Furthermore, the complexity of the *in vivo* microenvironment makes it difficult to control these biomechanical signals and to delineate their effects on differentiation from other correlated stimuli. Therefore, the field relies mainly on studies of biochemical pathways with *in vivo* mouse models or *in vitro* human models for information.

Cells respond to mechanical stimuli through mechanotransduction mechanisms, in which biomechanical stimuli are converted into biochemical signals (C. S. Chen, 2008; Martino et al., 2018; Moraes et al., 2011; Wolfenson et al., 2019). Reciprocally, cells alter the mechanics of their surrounding tissues by exerting contractile forces (H. Wang et al., 2014; Wozniak & Chen, 2009) and depositing or degrading the ECM proteins (Bonnans et al., 2014; Rozario & DeSimone, 2010). External biomechanical stimuli can promote cytoskeletal reorganization and subsequent changes in protein activity or localization, gene expression (N. Wang et al., 2009), proliferation (Frank et

al., 2016), and differentiation (Fang et al., 2019; Saha et al., 2006). Mechanotransduction could occur via mechanosensitive pathways such as Hippo signalling (Piccolo et al., 2014) which is heavily involved in development by regulating tissue growth (George et al., 2012), death (Sharma et al., 2017), and cell fate (Rosado-Olivieri et al., 2019). Properly designed novel cell culture substrates to control these aspects of cell-cell and cell-environment interactions could help drive cells toward desired cell fates. Biomechanical cues could be incorporated into cell culture systems to reduce the cost of soluble factors added in differentiation or the time required to produce a desired cell type. Therefore, in the following sections, we review the interactions between cells and biophysical components in the developmental microenvironment, to build a roadmap towards more advanced beta stem cell specification platforms (Figure 2-2).

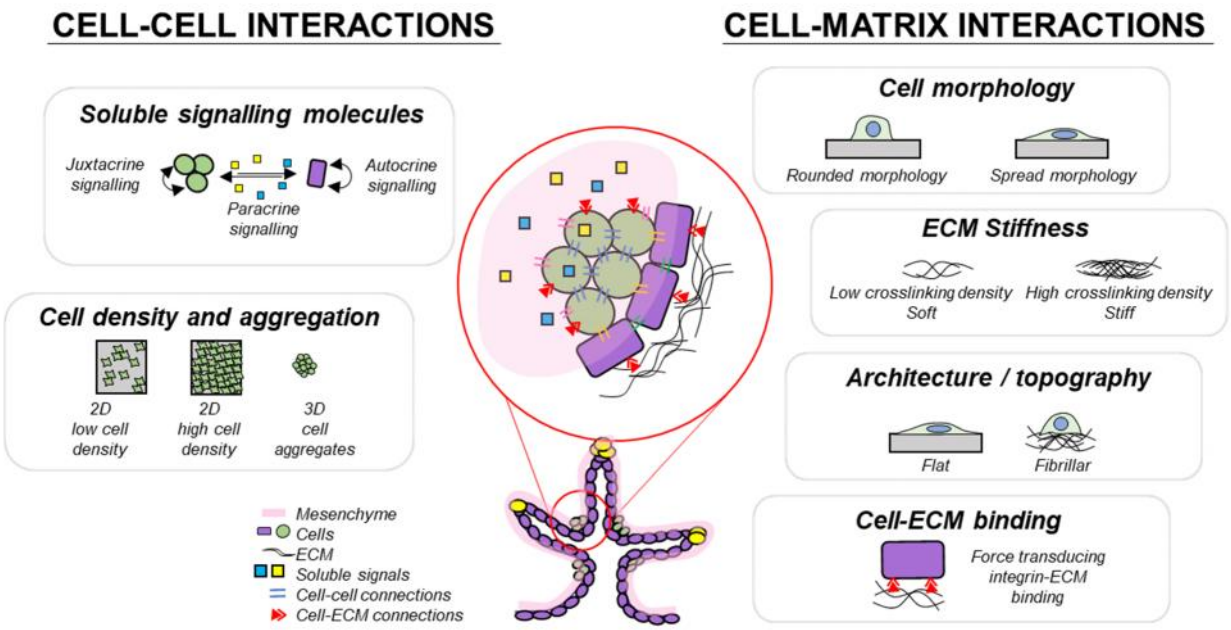

***Figure 2-2**: Summary of some cell interactions present during pancreas development which may play a role in guiding endocrine differentiation.*

2.5 Cell-cell interactions

Resident cells communicate with their neighbours during development by secreting soluble signalling molecules which can bias differentiation (Basson, 2012). The developmental microenvironment contains multiple transient cell types which each have different roles in the differentiation process. Within this environment, cells actively uptake soluble signalling factors and nutrients to form concentration gradients which are dependent on tissue thickness, vascularization, and oxygenation. In each of the following sections, we describe approaches to pancreatic differentiation that rely on controlling the soluble factor environment, optimizing cell seeding density, and forming pancreatic aggregates, all of which mimic aspects of developmental processes.

2.5.1. Soluble factor-based directed differentiation

The *in vivo* cellular microenvironment is much more intricate than can be modelled by current *in vitro* systems. Although directed differentiation protocols that focus solely on the timed addition of soluble signaling factors can generate insulin-producing cells (Hogrebe et al., 2020; Millman et al., 2016; Pagliuca et al., 2014; Rezania et al., 2014; Yung et al., 2019), these protocols typically produce some polyhormonal cells which have a transcriptome similar to fetal beta cells (Hrvatin et al., 2014), while monohormonal insulin-producing cells are more similar to adult pancreatic beta cells (Pagliuca et al., 2014). This may explain why earlier protocols produced cells with impaired glucose-sensing capabilities (Rezania et al., 2014), which may be due to metabolic bottlenecks in glycolysis (Davis et al., 2020). Furthermore, variation in differentiation efficiency between PSC lines (Nostro et al., 2015; Osafune et al., 2008) and in handling procedures between research groups represents a significant challenge for clinical translation. Interestingly, when immature NKX6.1^{+} pancreatic progenitors are transplanted into immunocompromised mice, they form functional insulin-producing cells (Kroon, 2008; Rezania et al., 2012) and are able to provide long-term glycaemic control when encapsulated within immunoprotective alginate polymers (Vegas et al., 2016). This suggests that some missing elements of the *in vivo* microenvironment have the potential to further improve mature beta cell production for therapeutic use.

The presence of other cell types found in native islets can improve insulin response. Glucose-stimulated insulin secretion is regulated by paracrine glucagon signaling from neighbouring alpha cells (Kelly et al., 2011; Samols et al., 1965; Svendsen et al., 2018; Trimble et

al., 1982). Human islets that are dispersed and reaggregated into controlled-size aggregates can restore glycaemic control in diabetic mice, suggesting that functional insulin response can be achieved with the appropriate co-culture (Yu et al., 2018). Soluble factors from mesenchymal stromal/stem cells (MSCs) in Transwell® cultures also improves proliferation, pancreatic differentiation, and engraftment function via IGF1 signalling (X. Y. Li et al., 2019). The presence of human amniotic epithelial cells within islet organoids grafted into a type 1 diabetes mouse model had enhanced blood glucose control and increased percentage diabetic reversal (96% vs 16%) after 1 month compared to animals transplanted with only islet cells (Lebreton et al., 2019). In directed differentiation, the addition of endothelial cells has also been shown to induce maturation of hESC-derived pancreatic progenitor cells towards insulin-expressing cells (Jaramillo et al., 2015). Overall, the addition of other cell types may improve current differentiation protocols, but it is currently not well understood whether these effects originate from paracrine signalling or cell-cell contacts.

Cell proliferation and other cell attributes such as metabolic rates can change the soluble factor microenvironment, including the level of dissolved oxygen available to cells. Control of oxygen and other nutrient levels therefore might be a useful strategy to improve cell functionality. Beta cells have a high oxygen demand and the oxygenation of islets is critical for survival (Komatsu et al., 2017a) and function (B. Ludwig et al., 2012). Differentiation of PSCs under increased oxygen tension promoted differentiation into pancreatic progenitors and subsequently, insulin-producing cells over normoxic conditions (Hakim et al., 2014; Heinis et al., 2010). Bioreactors providing feed-back control over nutrient and other biomolecular concentrations could improve the reproducibility of PSC pancreatic differentiation protocols.

2.5.2. Cell density effects on differentiation and function

Regulation of cell density is paramount to achieve controlled differentiation towards the desired cell lineage. High initial cell seeding densities promotes the differentiation of PSCs into definitive endoderm cells (Gage et al., 2013) as well as into downstream endocrine lineages (Takizawa-Shirasawa et al., 2013). Pancreatic differentiation arising from high cell density protocols is correlated with the downregulation of Rho-associated kinases (ROCK) and non-muscle myosin II (NM II) mRNA and proteins. This effect was independent of cell proliferation. At similar cell densities, inhibition of ROCK-NM II pathways improved pancreatic differentiation

over controls, suggesting that this effect is due to aggregation (Toyoda et al., 2017). High cell density cultures may therefore better recapitulate the local cell density in the developing pancreas, thereby increasing bias towards pancreatic endocrine fate. The mechanism by which high density cultures promotes pancreatic differentiation may include increased cell-to-cell contact, changes in oxygen tension, or increased soluble factor signalling. While the exact mechanisms remain to be elucidated, this general approach may be valuable for pancreatic differentiation protocols.

2.5.3. Cell aggregation

2.5.3.1. Effects of cell aggregation on beta cell differentiation and function

Forcibly aggregating pancreatic cells could capture many of the effects of high density culture, and may also better mimic the 3D environment and cell-cell signaling found *in vivo* to ultimately produce a more relevant phenotype *in vitro* (Antoni et al., 2015; Glieberman et al., 2019; Hohwieler et al., 2017). *In vitro,* spontaneous, cell-mediated clustering of pancreatic endoderm cells has been observed in 2D cultures (Nostro et al., 2015; Tran, Moraes, et al., 2020b). A potential candidate driving this clustering behaviour *in vivo* is the secretion and chemotaxis of FGF2, which further promotes differentiation into hormone producing, islet-like clusters (Hardikar et al., 2003). Thus, most directed differentiation protocols to generate functional beta-like cells rely on culturing differentiating and maturing pancreatic endoderm cells as aggregates (Nair et al., 2019; Pagliuca et al., 2014). The benefits of forced aggregation in directed differentiation may have origins in the biomimicry of pancreatic development where cell clusters are formed in primary transition and islet clustering.

Cell aggregation is important for proper functionality of beta cells (insulin response to glucose challenges) perhaps due to improved paracrine signalling and cell-cell contacts (Chowdhury et al., 2013; Lecomte et al., 2016). Paracrine signaling is necessary for proper crosstalk between the various hormonal cells (alpha, beta, delta, gamma cells) in native islets (Caicedo, 2013). Insulin secretion is also aided by calcium-driven electrical coupling of islet cell clusters (M. G. Pedersen et al., 2005; Sabatini et al., 2019). PSC-derived pancreatic aggregates encapsulated within a 3D matrix showed increased insulin secretion after 6 days compared to encapsulated single cells and cells cultured on a flat 2D surface, suggesting these functionalities may be closely linked to aggregation and paracrine signaling (J. Kim et al., 2019). Forced aggregation of PSC-derived pancreatic progenitor cells increases the proportion of $NKX6.1^{+}$ cells over standard 2D cultures (Toyoda et al., 2015). In their later work, Toyoda et al. demonstrated

that inhibition of Rho-associated kinases (ROCK) and non-muscle myosin II (NM II) increased the fraction of NKX6.1^{+} cells by emulating an aggregate phenotype even in low density cultures, suggesting that the physical act of aggregation may not be necessary (Toyoda et al., 2017). In addition to this, recent studies have shown that insulin-secreting cells can be produced in planar, non-aggregate protocols by the timed depolymerization of the actin cytoskeleton (Hogrebe et al., 2020).

2.5.3.2. Technologies to study cell aggregation

Proper control of aggregate size is an important design consideration since mass transfer limitations arise in larger aggregates and gradients in soluble signaling factors begin to play a role in specification. *In vitro*, larger non-vascularized islets may develop central necrosis due to high metabolic demand and low oxygenation (Avgoustiniatos & Colton, 1997; Komatsu et al., 2017b). To avoid core hypoxia, finite element models can be used to determine the optimal aggregate size in suspension (Buchwald, 2009) and encapsulation systems (Avgoustiniatos & Colton, 1997; Song & Millman, 2016). The average diameter of human islets is around 100 – 400 µm (Hellman, 1959; Ionescu-Tirgoviste et al., 2015; Suszynski et al., 2014). When islets and stem cell-derived beta cells are dissociated and re-aggregated, the optimal diameter to maintain viability and function was shown to be 100 – 150 µm (Hilderink et al., 2015; Song & Millman, 2016) while also improving survivability and function, perhaps due to improved nutrient availability (Yu et al., 2018). Therefore, creating aggregates of uniform size is crucial for reproducible production of functional insulin-producing cells.

Several groups have developed methods to reproducibly create endocrine cell aggregates of defined size to improve functionality (Velazco-Cruz et al., 2019; Nair et al., 2019; B. Gao et al., 2019). Culturing pancreatic cells on microporous scaffolds can improve differentiation towards insulin secreting beta-like cells over suspension cultures by guiding formation of consistently sized aggregates (Youngblood et al., 2019). Physical confinement of 3D MIN6 aggregates in 2% alginate beads promotes glucose-stimulated insulin secretion but decreases proliferation compared to adherent 2D culture (Hoesli et al., 2011). Micropatterned culture can be used to promote cell-driven clustering of PSC-derived NKX6.1^{+} cells with defined sizes while maintaining ease of handling associated with 2D cultures. Clustered cells from micropatterned confinement have increased PDX1 and NKX6.1 protein expression when compared to unconfined cells and this effect was further correlated with local cell density increases (Tran, Moraes, et al., 2020b). Agarose

microwells (Hilderink et al., 2015), pyramid-shaped polystyrene wells (M. Ungrin & Zandstra, 2011), or hydrogel micropockets (L. Zhao et al., 2019) have also been used to generate cell aggregates of controlled size. The production of uniformly sized cell aggregates in a scalable matter may be the key to producing mature cells for cell therapies in a consistent manner. Within these aggregates, cells deposit insoluble ECM proteins and dynamically change the surrounding microenvironment, which suggests that the architecture of these clusters and in general, the surrounding surfaces could play a large role in differentiation.

2.6 Cell-matrix interactions

The ECM presents cues to surrounding cells in the form of biochemical signals, growth factors, and biophysical signals (Nakayama et al., 2014). Native ECM found *in vivo* is extremely complex and contains hundreds of different proteins with varying composition depending on region. Combinatorial protein arrays are useful to study the interactive and additive effects of different ECM components on stem cell behaviour (Alberti et al., 2008; Flaim et al., 2005; Guilak et al., 2009; LaBarge et al., 2009). However, the architecture of native ECM is equally important and also plays a role in guiding stem cell differentiation through cell-generated force feedback mechanisms (Trappmann et al., 2012). In the developing embryo, the ECM structure and composition is dynamically evolving, which constantly changes the biochemical and biophysical cues presented to developing cells (Rozario & DeSimone, 2010). Understanding the different aspects of the ECM and their role in differentiation during each stage of pancreas development (Table 2-1) could help the development of novel biomimetic culture systems to better guide the production of functional insulin-secreting cells.

2.6.1. Biochemical effects of ECM Proteins

The presence of ECM proteins produced within a cell and ECM pre-adsorbed or conjugated onto culture substrates, is essential for successful differentiation. These proteins can also bind growth factors which can affect presentation to the cells and improve growth factor stability (Belair et al., 2014; Taipale & Keski-Oja, 1997). The ECM components of the microenvironment can influence survival, adhesion, proliferation and guide downstream cell fate decisions (Gattazzo et al., 2014; Guilak et al., 2009). The ECM of the human adult islet is composed mainly of laminin, collagen IV, fibronectin, and other types of collagen; whereas the embryonic pancreas ECM is fundamentally distinct and is primarily comprised of vitronectin, fibronectin, and collagen IV (Stendahl et al., 2009). Designing cell culture systems with combinations of ECM proteins found

in the pancreas could therefore help improve pancreatic cell function and differentiation (Table 2-1, Column 5).

Several works have shown that islets and other pancreatic cells have improved functionality when cultured in matrices that recapitulate those found *in vivo*. Collagen and fibronectin have been shown to promote beta cell survival, while laminins are responsible for beta cell specification and insulin secretion (Arous & Wehrle-Haller, 2017). Islets encapsulated in hydrogels containing collagen IV and laminin show improved glucose-stimulated insulin secretion response (J. Kim et al., 2019; Weber & Anseth, 2008). Incorporating ECM-derived peptides such as RGD, LRE, PDSGR has also been shown to improve viability and glucose-stimulated insulin secretion in alginate encapsulated islets (Llacua et al., 2016; Medina et al., 2020).

Coating cell culture substrates with ECM protein to mimic the biochemical effects of these ECM proteins can guide directed differentiation of PSCs towards the endocrine lineage. Directed differentiation of PSCs in 2D conditions usually begins on a Matrigel-coated surface (Hogrebe et al., 2020; Rezania et al., 2014; Tran, Moraes, et al., 2020b). However, Matrigel suffers from batch-to-batch variability which could affect differentiation outcomes. Purified ECM proteins (Amit et al., 2004; T. E. Ludwig et al., 2006), recombinant proteins (G. Chen et al., 2011; Y. Wang et al., 2014), or synthetic matrices (such as functionalized polyethylene glycol (PEG) or alginate) (Aisenbrey & Murphy, 2020) could serve as alternatives to Matrigel for PSC maintenance. Synthetic matrices and recombinant protein alternatives require more study in the context of pancreatic differentiation. Therefore, understanding the effect of constituent proteins in Matrigel and their effect on pancreatic differentiation is a necessary step to effectively guide differentiation outcomes. The synergistic role of various ECM protein mixtures can be screened combinatorically using protein arrays thus allowing for optimization of pancreatic differentiation protocols. For example, PSCs cultured on substrates coated with collagen I or in combination with collagen II and fibronectin reduced the time required for high purity endoderm differentiation (Rasmussen, Petersen, et al., 2016). Fibronectin has previously been shown to downregulate the pluripotency of PSCs and enhance endoderm differentiation, which leads to the pancreatic lineage downstream (Brafman et al., 2013; Taylor-Weiner et al., 2013). Combinations of the main pancreatic ECM components, including fibronectin, collagen IV, and laminin, further promote ESC differentiation

into pancreatic lineages (Malta et al., 2016; Narayanan et al., 2013). Further downstream, the composition of ECM protein coatings can also guide pancreatic cell fate decisions. Fibronectin-coated surfaces promote differentiation to ductal lineage whereas adhesion onto laminin-coated surfaces guides endocrine differentiation into $NGN3^+$ cells (Mamidi et al., 2018a).

Although Matrigel alternatives can be used to promote the initial stages of differentiation, downstream cell types may require a more complex environment. Embryonic murine pancreatic progenitors cultured in Matrigel gels could form organoid structures but not on synthetic 3D matrix alternatives (Greggio et al., 2013). PEG-based hydrogels functionalized with laminin 1 facilitated maintenance and expansion of murine pancreatic progenitors but on non-functionalized synthetic hydrogels, murine pancreatic progenitors did not expand and lost pancreatic character (Greggio et al., 2013). Similarly, the bioinert PEG hydrogels maintained the viability of rat-derived pancreatic progenitors for 7 days, but failed to obtain glucose-responsive behaviour, further suggesting the importance of ECM interaction (Amer et al., 2015; Mason & Mahoney, 2008). Pancreatic progenitor cells isolated from adult murine pancreas can also be cultured in methylcellulose (Jin et al., 2016) or laminin gels (Jin et al., 2013) to generate insulin-positive cells.

***Table 2-1**: Compiled effects of substrate stiffness and architecture on various pancreatic differentiation platforms.*
*Fn denotes fibronectin, Lam denotes laminin, Col denotes collagen, pdECM denotes pancreatic decellularized extracellular matrix. * Stiffness of polystyrene shown for reference. Taken from Gilbert et al., 2010. ☥ Cell morphology details taken from previous work from same group (Maldonado, 2015)*

Author	Cell Type	Differentiation Type	Platform	ECM coating	Apparent Modulus (kPa)	Cell Morphology	Relative Stiffness	Impact
Architecture								
Ghanian et al. (2015)	hESCs	Directed S0 → S1	Electrospun poly(ε-caprolactone)	Matrigel	Not reported	Clumped	-	hESCs cultured on small diameter nanofibers adopted a clumped morphology and had improved definitive endoderm differentiation.
			Tissue culture polystyrene (control)	Matrigel	3 x 10^6*	Spread	Stiff	
Maldonaldo et al. (2017)	iPSCs	Directed S0 → S3	Electrospun poly(ε-caprolactone)	Col I	20	Round, 3D colonies ☥	Soft	"Soft" nanofibers promoted posterior foregut and pancreatic differentiation. "Stiff" surfaces promoted mesodermal differentiation while downregulating pancreatic differentiation.
			Electrospun polyether-ketone-ketone	Col I	300	Spread, flattened 2D colonies ☥	Stiff	
			Tissue culture polystyrene (control)	Col I	3 x 10^6*		Stiff	
Substrate stiffness								
Narayanan et al. (2013)	hESCs	Spontaneous differentiation	Hyaluronic acid hydrogels	Col IV, Fn, Lam	1.3 - 3.5	Not reported	Soft	Optimal differentiation with 2.1 kPa gels and a 1/3/3 mixture of Col IV, fibronectin, and laminin.
			Tissue culture polystyrene (control)	RIN5F ECM	3 x 10^6*	Not reported		
Rasmussen et al. (2016b)	hESCs	Directed S0 → S3	High aspect ratio polycarbonate nanopillars	Fn	34.6	Small, tight 2D clusters. Elongated and aligned with nanopillars	Soft	Poor hESC adhesion on soft nanopillars. "Soft" surfaces promoted endoderm (S1) differentiation. Control had significantly higher PDX1 protein expression (S3) compared to test conditions.
			Low aspect ratio polycarbonate nanopillars	Fn	2800	Spread	Stiff	

			Tissue culture polystyrene (control)	Fn	3 x 10^6*	Spread	Stiff	
Richardson et al. (2016)	hESCs	Directed S0 → S3	Low concentration barium alginate capsules	N/A	3.9 ± 1.3	Larger circular 3D colonies	Soft	"Soft" capsules increase hESC proliferation and were highly PDX1+ (S3). Localized deposition of Col I and Lam in "soft" capsules. "Stiff" capsules support endodermal (S1) differentiation but downregulates pancreatic differentiation.
			High concentration barium alginate capsules	N/A	73.2 ± 22.4	Small, growth restricted 3D colonies and large, elongated 3D colonies	Stiff	
Kim et al. (2019)	Rat islets and PSCs	Directed S0 → S7	dECM bio-ink	Human pdECM	3	Not reported	-	Insulin secretion and maturation were enhanced in cells cultured in pdECM bioinks compared to 2D tissue culture polystyrene (TCPS), alginate gels, and collagen gels
			Collagen gel	Col I	100	Not reported	-	
			Tissue culture polystyrene (control)	-	3 x 10^6*		-	
Hogrebe et al. (2020)	PSCs	Directed S0 → S7	Tall collagen I gel	Col I	N/A	Not reported	Soft	Decreased stiffness via increasing gel height promotes overall endocrine induction (increases *NGN3, NKX2.2, NEUROD1* and decreases *SOX9, NKX6.1* expression)
			Short collagen I gel	Col I	N/A	Not reported	Stiff	
Pennarossa et al. (2018)	Mouse dermal fibroblasts	Transdifferentiation	Polyacrylamide hydrogels	Col I	0.1	2D epithelioid structure in small, scattered clusters	Soft	Improved transdifferentiation towards monohormonal pancreatic endocrine cells on soft substrates
			Tissue culture polystyrene (control)	Col I	3 x 10^6*	3D spherical structures	Stiff	

Separating the principal components of the ECM may lead to more efficient and cost-effective differentiation but synergistic effects of the complete matrix may be lost. Differentiation could be improved by using decellularized pancreatic ECM (dpECM), thus retaining ECM proteins composition . Utilizing decellularized pancreas matrix scaffolds in bioartificial pancreas designs could also be a fruitful strategy to improve islet functionality by retaining pancreas stiffness and matrix architecture (Goh et al., 2013; Guruswamy Damodaran & Vermette, 2018). Hydrogels composed of decellularized human pancreata can support the proliferation and differentiation of pancreatic progenitors into insulin-positive cells (Sackett et al., 2018; Wan et al., 2017). Pancreatic tissues derived from iPSC cultured in 3D bioprinted inks primarily composed of dpECM had increased Pdx1, insulin, and glucagon expression compared to collagen controls (J. Kim et al., 2019). Cell culture with the addition of collagen V, which was present in dpECM but not in Matrigel, enhanced islet organoid generation and glucose-responsive function (Bi et al., 2020). Overall, designing cell culture systems which recapitulate the *in vivo* ECM protein landscape could have significant impact to produce functional PSC-derived beta cells.

In addition to the combinatorial effects of individual ECM components, the composition of the ECM is dynamically changing during development. While one composition may promote early pancreatic differentiation, the same composition may hinder downstream differentiation stages. During hESC differentiation, ECM and MMPs are secreted which remodels the exogenous ECM on the culture substrate (Brafman et al., 2013). PSCs cultured on substrates supplemented with ECM proteins did not significantly improve beta cell maturation over 1-2 weeks, perhaps due to the contribution of cell-deposited ECM proteins. In self-organized PSC-derived beta cell clusters, cells deposit ECM which is largely composed of collagen IV, laminin, and fibronectin (Youngblood et al., 2019). This suggests guiding cell differentiation with ECM may not be a fruitful strategy in 3D aggregates or over longer time scales but could be used to improve initial differentiation after seeding.

2.6.2. Biomechanical effects

2.6.2.1. Soluble factor-based modulation of mechanotransducive machinery

More recent differentiation strategies can achieve dynamic glycaemic control in PSC-derived cells has been achieved by aggregating insulin-positive clusters (Nair et al., 2019; Velazco-Cruz et al., 2019), maturation through transplantation (Motté et al., 2014; Robert et al., 2018), or by timed activation of TGF-β signalling in aggregates (Velazco-Cruz et al., 2019). All these

promising protocols present a combination of biochemical and biomechanical stimuli applied to the PSC-derived pancreatic progenitor cells. Mechanotransduction occurs via complex machinery within a cell that involves interplay between ECM connections (e.g. integrins, adherens), cytoskeletal organization, and the nuclear envelope (Eyckmans et al., 2011). Rather than mimic soluble factors present *in vivo*, a recent successful strategy has been to target specific mechanotransduction-associated pathways during directed differentiation to promote pancreatic differentiation and thus improve the capacity to produce insulin-secreting cells. Such factors include H1152 (a ROCK II inhibitor) (Ghazizadeh et al., 2017), verteporfin (Rosado-Olivieri et al., 2019), and latrunculin A (disrupts microfilament organization) (Hogrebe et al., 2020). Nuclear activation of YAP, which affects the mechanosensitive Hippo pathway, is inversely correlated with expression of pancreatic and endocrine markers, PDX1 and NGN3 respectively (Mamidi et al., 2018a). Timed inhibition of YAP with verteporfin enhances endocrine differentiation while depleting the pancreatic progenitor population which may have benefits for downstream transplantation (Rosado-Olivieri et al., 2019). Depolymerizing the actin cytoskeleton with latrunculin A allowed endocrine differentiation that was previously not possible in 2D adherent cultures, perhaps suggesting that mechanosensing via the cytoskeleton is important in this process (Hogrebe et al., 2020). Altogether, this suggests that components of the *in vivo* cellular microenvironment are crucial for differentiation protocols and investigating how cells interact the surrounding extracellular matrix may be important in improving pancreatic differentiation protocols.

2.6.2.2. Biomechanical cell interactions

Cells interact with ECM proteins by binding with integrin receptors spanning across the cell membrane. These receptors can then activate downstream integrin-related signaling pathways that alter cell function and bias cell specification. In pancreas development, integrin-ECM signaling regulates collective cell migration and function (Hammar et al., 2004; Shih et al., 2016; R. Wang & Rosenberg, 1999). When pluripotent, hESCs express integrin domains α6 and β1 for laminin binding but this is downregulated after definitive endoderm differentiation (Wong et al., 2010). Differentiation towards definitive endoderm lineage with fibronectin and vitronectin is regulated by increased expression of integrin receptors α5, αV, β5 (Brafman et al., 2013; Wong et al., 2010). Further downstream, ECM-integrin α5 signaling associated with fibronectin binding promoted differentiation to pancreatic duct while disruption of this pathway enhanced endocrine

differentiation (Mamidi et al., 2018a). Although not yet studied in the context of mechanosensing for pancreatic differentiation, other surface receptors, such as stretch-activated ion channels (Y.-S. Liu et al., 2015; Nourse & Pathak, 2017), growth factor receptors (Tschumperlin et al., 2004), and cadherins (Ganz et al., 2006; Mui et al., 2016) could also play a role in guiding differentiation.

The surrounding ECM matrix also propagates stress (H. Wang et al., 2014) which allows cells to sense biomechanical cues through ECM-bound integrins (D'Angelo et al., 2011). Cells can also apply traction forces on the ECM through their integrin connections. Cells with high spread area also generate higher tractions forces (Han et al., 2012; Rape et al., 2011). Thus, these biomechanical interactions with ECM proteins may guide pancreatic differentiation through cell-generated forces caused by changes in the actin cytoskeleton organization. Integrin signalling drives cell-generated traction forces which are required for endoderm specification (Taylor-Weiner et al., 2015). Pathway analysis of single hiPSC-derived pancreatic cells encapsulated in alginate further suggests that integrin-signalling is involved in the cells' ability to transduce mechanical confinement towards islet differentiation pathways (Legøy et al., 2020).

Cell morphology is guided by the ECM proteins of the culture substrate (Polte et al., 2004; Watt, 1986) which could affect differentiation by regulating gene expression through changes in endogenous tension (Kilian et al., 2010; J. Lee et al., 2016; McBeath et al., 2004). In differentiation of $NGN3^+$ endocrine progenitors, fibronectin promotes high cell spread area while laminin-coated surfaces were associated with lower spreading (Mamidi et al., 2018a). Aside from these biochemical signalling cues, cell behaviour is dependent on the fibrous architecture and the apparent stiffness of the ECM, which both provide biomechanical cues to influence cell behaviour. Therefore, it is important to try to decouple the specific ECM protein effects from the structural or mechanical stimuli provided by the ECM.

2.6.2.3. Fluid flow

Pancreatic islets are highly vascularized tissues which is important for efficient oxygenation and rapid insulin response (Carlsson et al., 1998; Jansson & Hellerström, 1983). Microfluidics can resolve time-dependent secretion and metabolism of islets which would normally not be possible with conventional static cultures (Nourmohammadzadeh et al., 2016; Rocheleau et al., 2004; Walker et al., 2020; Y. Wang et al., 2010). When cultured directly under high external flow rates, shear stress damages peripheral islet cells, reducing glucose-stimulated metabolism and calcium

response (Sankar et al., 2011; Shenkman et al., 2009; Silva et al., 2013). However, blood flow (Y. Wang et al., 2010) and islet culture in bioreactors (Minteer et al., 2014) also improves mass transfer to pancreatic islets (J. Wu et al., 2014), improving islet survival and function (Lock et al., 2011; Sankar et al., 2011) – particularly if the islets are protected from shear stress (Jun et al., 2019). Islets with endothelial cells co-cultured under external flow have higher endothelial cell survival compared to static culture which may improve islet functionality and health *ex vivo*, perhaps by mediating regeneration of islet ECM within aggregates (Jun et al., 2019; Sankar et al., 2011). Culture with low flow rates permits paracrine signalling between neighbouring islet hormone cells and the low shear rates may help microvilli maintenance, which was correlated to insulin secretion capabilities (Bendayan, 1992; Geron et al., 2015; Jun et al., 2019).

Signals from pancreatic vasculature are critical in specifying differentiation (Lammert et al., 2001) but the role of shear stress on differentiation is not well understood. There are many reports of pancreatic differentiation within stirred bioreactors (Mihara et al., 2017; Pagliuca et al., 2014; Schulz et al., 2012; Yabe et al., 2019) however little has been done to characterize the effect of shear stress on pancreatic differentiation within these systems. The differentiation of embryoid bodies under external flow promoted expression of beta cell specific markers, such as *NKX6.1* and *INS*, and improved glucose-stimulated insulin secretion sensitivity over static conditions (Tao et al., 2019). In the future it would be interesting to further investigate the biophysical effects of varying fluid flow rates on pancreatic differentiation and functionality.

2.6.2.4. Substrate stiffness

Cells interact with aspects of the ECM, such as stiffness, by anchoring and pulling on the substrate. These signals are then transmitted through intracellular structures, such as the actin cytoskeleton, leading to downstream effects which alter cell fate decisions. Engler et al. showed that the differentiation of mesenchymal stem cells towards neurogenic, myogenic, and osteogenic lineages could be controlled by culturing cells on substrates of physiologically relevant *in vivo* stiffness (Engler et al., 2006). High stiffness environments reduce insulin expression of MIN6 cells confined in 3D polyacrylamide scaffolds (Nyitray et al., 2014). Therefore, the stiffness of the culture substrate is a key criterion in biomaterial and culture system selection when optimizing pancreatic differentiation protocols based on insulin-producing cell yield, purity and function (Table 2-1, Column 6).

One approach could be to mimic the stiffness of the pancreas which may better recapitulate *in vivo* cell function. The stiffness of the adult human pancreas lies within 1.4 ± 2.1 – 4.4 ± 5.1 kPa (Sugimoto et al., 2014). In contrast, standard tissue culture polystyrene has a stiffness around 3 GPa (Gilbert et al., 2010). Stiffness tunable hydrogels that can be functionalized with ECM proteins, such as polyacrylamide or hyaluronic acid gels, constitute interesting alternatives to polystyrene. Culture of pancreatic progenitors on substrates mimicking the stiffness of the pancreas is a promising strategy to promote differentiation relative to stiff polystyrene. Pancreatic differentiation of hESCs on relatively soft surfaces resulted in increased protein expression of PDX1, and gene expression of pancreatic endoderm markers,*NKX2.2*, and *NKX6.1* (Maldonado et al., 2017; Narayanan et al., 2013). Similarly, hESCs encapsulated and differentiated in soft 3D alginate matrices were more viable, proliferative, and had increased PDX1 protein expression suggesting improved pancreatic commitment compared to stiffer gels (Richardson et al., 2016). Significant upregulation of pancreatic associated genes, such as *PDX1*, *INS*, and *GLUT2*, were observed during pancreatic differentiation of hESCs on soft hyaluronic acid hydrogels (Narayanan et al., 2013). hESC-derived beta cells co-cultured with endothelial cells on Matrigel gels formed self-assembled networks of islet organoids with functional glucose-stimulated insulin secretion while these organoids did not form on stiff tissue culture polystyrene (TCPS) coated with Matrigel or in suspension culture (Augsornworawat et al., 2019).

Changing stiffness in hydrogel systems could change the number of cell tethering sites due to increased crosslinking or ECM protein concentration, therefore proper controls are required (Trappmann et al., 2012). To decouple stiffness and substrate binding differences due to composition changes, substrates composed of pillars with controllable aspect ratio can be used to modulate the perceived stiffness while maintaining substrate composition. Nanopillars with a high aspect ratio are more flexible and perceived to be softer compared to those with a low aspect ratio, while maintaining substrate chemistry (Yang et al., 2011). Definitive endoderm differentiation from hESCs commitment is improved on high aspect ratio polycarbonate pillars and resulted in a more cluster-like morphology (Rasmussen, Reynolds, et al., 2016a). Controlling cell morphology via substrate stiffness could be another approach to guide differentiation by altering internal cytoskeletal tension, which in turn impacts the compressive forces applied on the cell nucleus thus affecting transcriptional activation (Driscoll et al., 2015; McBeath et al., 2004) (Table 2-1, Column 7). Transdifferentiation of mouse dermal fibroblasts towards monohormonal pancreatic endocrine

cells is improved on soft polyacrylamide gels (1 kPa) and this was correlated with generation of large cell clusters, actin reorganization, and deactivation of YAP compared to culture on stiff substrates (Pennarossa et al., 2018).

During development, the embryo undergoes dynamic changes in ECM stiffness, architecture, and composition. Although optimizing substrates for one stage of differentiation could provide potential insight into developmental mechanics, this may decrease the fraction of pancreatic cells obtained downstream. Using soft, high aspect ratio pillars that promote definitive endoderm differentiation resulted in lower fraction of $PDX1^+$ cells compared to flat, polycarbonate controls while the same substrates has decreased downstream pancreatic differentiation (Rasmussen, Reynolds, et al., 2016a). Conversely, the formation of $PDX1^+$ cells is promoted on soft electrospun fibers while the precursor mesendodermal cell differentiation is improved on stiffer substrates (Maldonado et al., 2017). Alginate encapsulation of single pancreatic progenitor cells at later stages of differentiation promoted an islet-like gene expression profile and increased the fraction of insulin-expressing cells compared to when PSCs were encapsulated at the beginning of differentiation, further suggesting stage specific optimization of these microenvironmental cues is required (Legøy et al., 2020). When comparing pancreatic differentiation results across multiple studies, the classification of "soft" versus "stiff" substrates in relation to the native microenvironment, the type of material, and the ECM used to facilitate cell adhesion must be considered (Table 2-1, Column 8).

2.6.2.5. ECM Architecture/topography

The topography of the culture substrate can mediate cell clustering which is thought to promote pancreatic differentiation. The fibrous nature of native ECM can be mimicked using electrospun scaffolds. The ECM provides structural adhesive binding sites which influences the shape cells adopt on a substrate. Scaffolds, such as electrospun nanofibers, can be used to manipulate stem cell fate decisions by mimicking the topography and fibrous nature of native ECM proteins (Fujita et al., 2012; J. Kim et al., 2013; Luo et al., 2015; Xin et al., 2007). Human ESCs differentiated on 200 nm poly(ε-caprolactone) (PCL) fibers had higher expression of endodermal lineage genes such as *SOX17* and *FOXA2*, compared to on larger fibers. Cells cultured on thin fibers adopted a clumped, rounded morphology while cells on fibers greater than 800 nm were more spread and anchored. Having a more clumped morphology could promote cell-cell interactions over cell-substrate interactions which may bias differentiation (Ghanian et al., 2015).

Microporous poly(lactide-co-glycolide) (PLG) and PEG scaffolds can promote aggregation into consistently sized clusters, which improves beta cell differentiation downstream (Youngblood et al., 2019). Culture on nanostructured zirconia substrates promotes clustering of dissociated human pancreatic islets, reduced actin cytoskeletal stress fiber formation, and increased the number of vinculin focal adhesions compared to flat substrates. These traits of zirconia substrates culture were correlated to improved islet survival, growth, and pancreatic differentiation (Galli et al., 2018). These studies suggest that careful selection of culture surface topography could be used to guide tissue organization, which may be a more economical, operator-free alternative to guiding cultures purely with biochemical cues or specialized aggregation techniques.

2.7 Conclusions and Perspectives

Methods to produce functional beta cells from PSCs have advanced by leaps and bounds over the past two decades through advances such as directed differentiation which aimed to mimic the stages of pancreas development. In addition to soluble factors, the interactions between PSC-derived pancreatic cells with each other and with the ECM alter biomechanical stimuli which guide cell fate decision. Therefore, several aspects of the developing microenvironment must be taken into consideration when designing next-generation culture techniques and devices.

For one, understanding the roles of ECM proteins and structure in guiding different stages of differentiation may be crucial in accelerating early stages of differentiation or during transition points in culture. However, these biochemical and structural effects may only have short-term influences on differentiation and may diminish as differentiating pancreatic cells secrete their own native ECM. This speaks to the dynamic nature of the surrounding cellular microenvironment which may temporally vary in both biochemical composition and stiffness. Second, it is important to consider the material and perceived stiffness when interpreting results; a soft substrate in one paper could still be much stiffer than that of the native pancreas. In addition, appropriate design of substrates by controlling stiffness, ECM functionalization, and nanotopography could promote aggregation and pancreatic differentiation. Cell aggregation is an integral part of many differentiation protocols and is clear to be important to obtaining functional beta cells, however, recent studies have shown aggregation may not be required for beta cell differentiation (Hogrebe et al., 2020). Therefore, investigating the functional or phenotypic differences between PSC-derived cells from aggregation culture and 2D protocols, if any, will be important proceeding with scale-up.

Studying and controlling the complex set of factors which guide pancreas development using *in vitro* models is challenging – particularly since stimuli from soluble factors, cell-cell interactions, and cell-ECM interactions are both interrelated and time-dependent. The progression of pancreatic differentiation will likely be dependent on gaining a fundamental understanding of development and then translating this knowledge to scalable technologies. For one, the dynamic nature of maturing cells changing the surrounding microenvironment, and the subsequent effect on differentiation is not well understood. Complex *in silico* models and improved culture systems may be required to tease apart the many confounded effects of the dynamic cellular microenvironment. Previously, mathematical models of the interactions between biomechanical stimuli and regulatory gene networks have been used to predict MSC (Peng et al., 2017) and pancreatic cell fate decisions (de Back et al., 2013; J. Wang et al., 2020; J. X. Zhou et al., 2011, 2016). Novel *in silico* models which deal with cell generated forces in aggregate culture (W. Lee et al., 2019) while varying stiffness or cell organization over time could help us understand how mechanotransduction changes throughout a differentiating aggregate. As we move to more complex aggregates and culture systems, *in silico* models of biomechanics could shed light onto correlations between cell differentiation and varying substrate parameters. It is still not well understood why stem cell-derived beta-like cell co-cultures with endothelial cells (Augsornworawat et al., 2019) have not been able to surpass protocols without co-culture (Hogrebe et al., 2020; Nair et al., 2019; Velazco-Cruz et al., 2019). The presence of flow during culture might be required to recapitulate the effects of endothelial cells on islet development since hemodynamic stimuli have profound impact on endothelial cell function including their secretome (Berthiaume & Frangos, 1995; Burghoff & Schrader, 2011; C. Wang et al., 2013). In addition, mimicking vascular flow through organized endothelial cell-islet co-cultures could better mimic *in vivo* stimulation, and better reproduce nutrient gradients throughout the aggregates.

To address these questions, some technologies that could be used to specifically identify the effect of these factors are highlighted in Figure 2-3 but the state of the art is currently limited in the ability to emulate the temporal changes that occur during development. Once each independent effect is better understood, dynamic culture systems which leverage cell-cell interactions and timed biomechanical cues alongside soluble factor timing could be key for optimal production of functional beta cells. Future *in vitro* models implementing smart materials with dynamically tunable biomechanical properties could give insight to how the changing

microenvironment could affect development. For example, synthetic scaffolds with defined ECM functionalization and degradation characteristics would allow for precise control of biochemical, topographical, and stiffness cues presented to differentiating cells. Such a technology could accelerate lengthy differentiation protocols and promote cell morphologies which allow for optimal beta cell organization. Alternatively, novel models which mimic dynamic shape changes in tissue morphogenesis (via novel 4D biomaterials) or stiffness (MMP-mediated degradation or UV-based) could better accommodate the constantly changing requirements for beta cell differentiation. Finally, as our knowledge progresses, increasingly complex co-culture systems involving defined compositions of PSC-derived endothelial, islet endocrine cells, and other cells present during development, may be the route to a functional cell source for islet transplantation.

Overall, better understanding the mechanobiology of pancreas development could lead to new strategies to more efficiently produce functional glucose-responsive, insulin-secreting cells for cell therapies. Interdisciplinary approaches combining advances in materials science and developmental biology could accelerate the development and scale up of culture systems tailored for diabetes cell therapy.

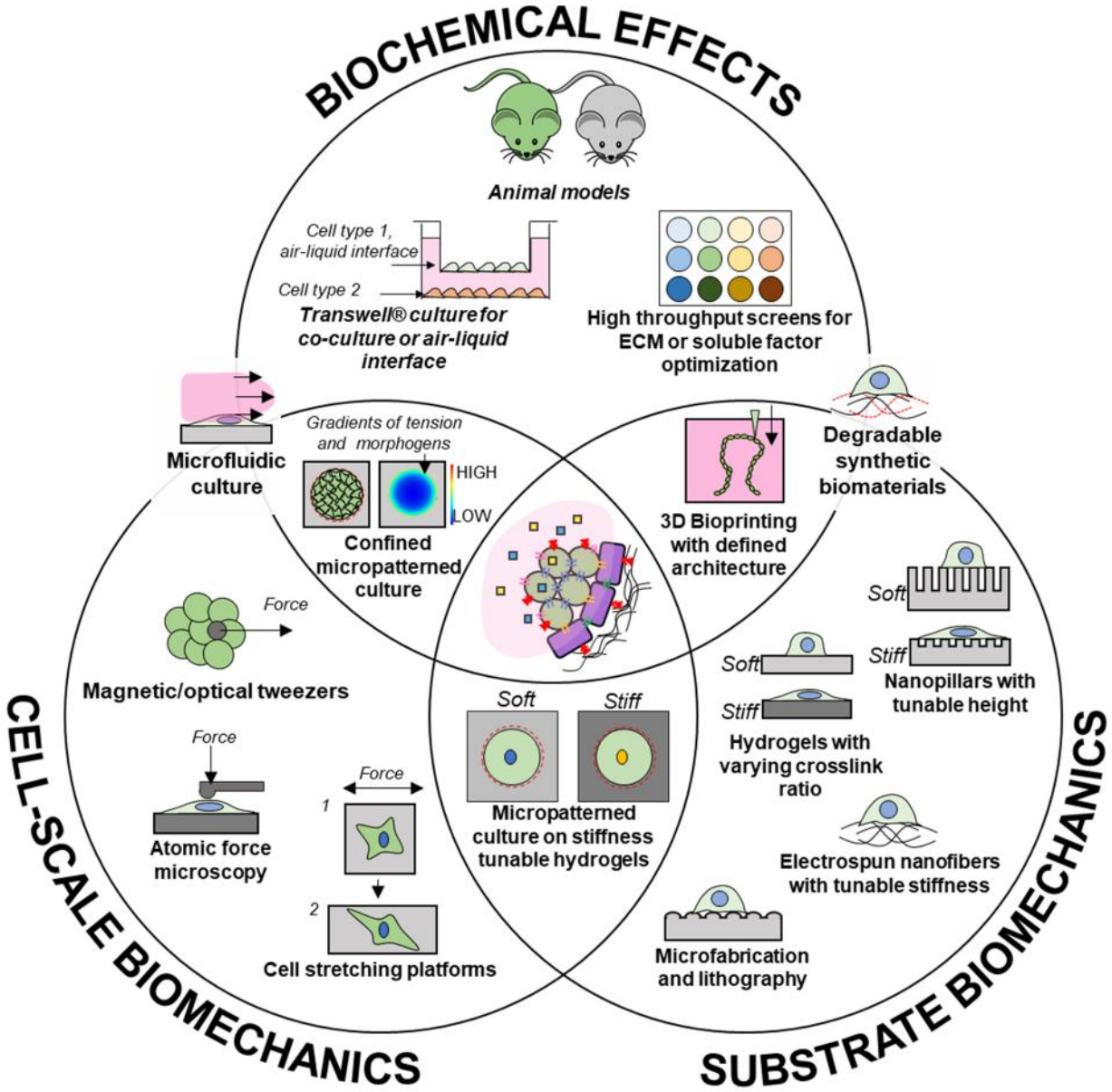

Figure 2-3: *Available technologies that could contribute to investigating independent aspects of pancreas development.*

2.8 Acknowledgements

We thank Jonathan Brassard for editing this manuscript and insightful discussion. The authors received funding from Canada's National Sciences and Engineering Research Council (NSERC, PGS-D award for RT, RGPIN-2015-05512 to CM and RGPIN-2015-05877 to CH) and the New Frontiers in Research Fund (NFRFE-2018-01546, CH) which supported this work. This work was undertaken, in part, thanks to funding from the Canada Research Chairs program (CH and CM) and the 'Fueling Biotechnology Partnerships' program from the Canadian Stem Cell Network. RT and CH are members of the Quebec Network for Cell, Tissue and Gene Therapy – ThéCell (a thematic network supported by the Fonds de recherche du Québec–Santé), of the Québec Center for Advanced Materials (CQMF), of PROTEO (The Quebec *Network* for Research on Protein Function, Engineering, and Applications), of the Cardiometabolic Health, Diabetes and Obesity Research Network (CMDO), and of the Montreal Diabetes Research Center (MDRC). RT, CM and CH are members of the McGill Regenerative Medicine Network.

Chapter 3

During development, the budding pancreas forms as a dense, stratified mass of cells from the posterior foregut which then evaginates into the surrounding mesenchyme, before branching and further developing to form the pancreas (Jennings et al., 2015). Pancreatic islets are also found as aggregates *in vivo* which allows for improved paracrine signalling and improved insulin response to glucose challenge (Chowdhury et al., 2013; Lecomte et al., 2016). Together, this highlights the importance of cell aggregation in forming functional insulin-secreting beta cells. As such, conventional directed differentiation of pluripotent stem cells into functional insulin-secreting cells typically requires formation of cell aggregates and subsequently, long-term suspension culture. In 2D planar differentiation protocols, circular clusters of pancreatic endoderm (PE/Stage 4) cells spontaneously formed stochastically throughout the culture, resembling the morphology of pancreatic buds *in vivo*. With this knowledge, I reasoned that confining differentiating posterior foregut (PF/Stage 3) cells within agarose-based micropatterns could more reproducibly form dense cell clusters which also reduces potential cell loss from user handling. The agarose micropattern platform thus allowed the study of cytoskeletal reorganization during the clustering and differentiation of PSC-derived pancreatic endoderm cells. This work was published in *Scientific Reports* by Nature Publishing in January 2020.

3.1 Controlled clustering enhances PDX1 and NKX6.1 expression in pancreatic endoderm cells derived from pluripotent stem cells

Raymond Tran[1], Corinne A. Hoesli[1,2]*, Christopher Moraes[1,2,3]*

[1] Department of Chemical Engineering, McGill University, 3610 rue University, Montreal, QC, Canada

[2] Department of Biomedical Engineering, McGill University, 3775 rue University, Montreal, QC, Canada

[3] Rosalind and Morris Goodman Cancer Research Center, McGill University, Montreal, QC, Canada

*Corresponding authors & equal contribution

E-mail: chris.moraes@mcgill.ca; corinne.hoesli@mcgill.ca

3.2 Abstract

Pluripotent stem cell (PSC)-derived insulin-producing cells are a promising cell source for diabetes cellular therapy. However, the efficiency of the multi-step process required to differentiate PSCs towards pancreatic beta cells is variable between cell lines, batches and even within cultures. In adherent pancreatic differentiation protocols, we observed spontaneous local clustering of cells expressing elevated nuclear expression of pancreatic endocrine transcription factors, PDX1 and NKX6.1. Since aggregation has previously been shown to promote downstream differentiation, this local clustering may contribute to the variability in differentiation efficiencies observed within and between cultures. We therefore hypothesized that controlling and directing the spontaneous clustering process would lead to more efficient and consistent induction of pancreatic endocrine fate. Micropatterning cells in adherent microwells prompted clustering, local cell density increases, and increased nuclear accumulation of PDX1 and NKX6.1. Improved differentiation profiles were associated with distinct filamentous actin architectures, suggesting a previously overlooked role for cell-driven morphogenetic changes in supporting pancreatic differentiation. This work demonstrates that confined differentiation in cell-adhesive micropatterns may provide a facile, scalable and more reproducible manufacturing route to drive morphogenesis and produce well-differentiated pancreatic cell clusters.

3.3 Introduction

Type 1 diabetes is caused by the autoimmune destruction of the insulin-producing beta cells found in the islets of Langerhans in the pancreas. Islet transplantation is a promising long-term cell-based therapy that provides insulin independence in more than 85% of recipients for at least 1 year(Hering et al., 2016; Shapiro et al., 2000). Access to islet transplantation remains limited by donor islet availability. Insulin-secreting cells derived from pluripotent stem cells (PSCs) are a possible source for these therapies, provided that robust differentiation protocols can be developed(Millman et al., 2016; Nostro et al., 2015; Pagliuca et al., 2014; Rezania et al., 2014). The efficiency of mature beta cell production from PSCs remains limited and variable between cell lines, protocols, and even batches within the same research group(Nostro et al., 2015; Rostovskaya et al., 2015; Toyoda et al., 2015). Although more mature beta cell clusters can be obtained via cell sorting and controlled aggregation, these additional processing steps may significantly reduce overall yields and are undesirable to maximize beta cell production(Nair et al., 2019). While early steps in the differentiation process are well-established and reasonably efficient, the successful production of pancreatic endoderm (PE) cells from pancreatic foregut (PF) cells is less consistent, and incomplete differentiation at this stage is expected to affect downstream specification(Jaramillo et al., 2014). Strategies to improve differentiation efficiency and PE cell yield from PF cells could substantially improve the robustness and overall efficiency of beta cell production from PSC sources.

PDX1 and NKX6.1 are the earliest markers of pancreatic and beta cell commitment, respectively(Offield et al., 1996; Sander et al., 2000, p. 2; Schaffer et al., 2013, p. 1), and play a critical role in pancreatic development towards functional insulin secretion capability(Fujimoto & Polonsky, 2009; T. Gao et al., 2014; Taylor et al., 2013a). Overexpression of PDX1 promotes differentiation towards insulin-expressing cells in pancreatic differentiation of mouse and human embryonic stem cells (hESCs) (Kubo et al., 2011; Lavon et al., 2006). Nuclear translocation of PDX1 through phosphorylation is required for activation and binding to the insulin promoter(Clark et al., 1993; Elrick & Docherty, 2001; Macfarlane et al., 1999) and other PDX1-binding DNA motifs(Marshak et al., 2000; Waeber et al., 1996; Watada et al., 1996). NKX6.1 represses the formation of multihormonal endocrine cells(Petersen et al., 2017) and higher NKX6.1 expression correlates with accelerated maturation of hESC-derived PE cells into insulin-expressing cells after engraftment in diabetic mice(Rezania et al., 2013). Functionally, PDX1 and NKX6.1 also

contribute to mature beta cells survival and synthesis of insulin(Fujimoto & Polonsky, 2009; S. B. Nelson et al., 2007; Schaffer et al., 2013). High yields of $PDX1^{+}/NKX6.1^{+}$ PE cells can be achieved by implementing a multicellular aggregation step(Pagliuca et al., 2014; Rezania et al., 2014; Toyoda et al., 2015). Current differentiation protocols involve cell release from the surface and then aggregate formation. These aggregates are typically heterogenous which may explain batch variability observed in insulin-producing cell yield, maturity, and purity. More advanced techniques such as microfluidic methods(Qin et al., 2019) or cell-repellent microwells can result in homogenous structures, but these are challenging to scale up, can require complex equipment and/or multiple manual operation steps which ultimately leads to significant loss of valuable cell material. These challenges all arise because they require cell detachment from adherent substrates prior to further processing and aggregation. Developing techniques that allow the formation of aggregates while maintaining adhesion might be a viable strategy to avoid these issues.

In this work, we propose that culture in adhesive micropatterns can be applied to direct and control cell clustering for efficient pancreatic differentiation in a scalable manner. Cells grown on small adhesive 2D micropatterned surfaces have previously been shown to form 3D aggregates of well-defined and uniform sizes when released(Bauwens et al., 2008; Leight et al., 2012). This suggests that micropatterned surfaces mechanically prime cells to form clusters, which may in itself be sufficient to improve PE cell yields. In this work we cultured adherent induced PSC (iPSC)-derived PF cells on micropatterned surfaces and demonstrated that sufficiently small patterns prompt clustering into multilayered structures during the PE transition, while cells are retained on the adherent surfaces. Cell-adhesive microwells induced higher levels of PDX1 and NKX6.1 nuclear transcription factor accumulation in the overall cell population, and this increase was associated with the clustering phenotype in which multilayer tissues are formed. Overall this system maintains the simplicity and ease of handling possible with simple adherent 2D culture systems, while enhancing differentiation efficiency and may hence provide a scalable route towards cell therapy manufacturing.

3.4 Results

3.4.1. Establishing pancreatic differentiation baseline in unconfined monolayer culture

To establish a baseline differentiation efficiency for iPSCs in our hands, pancreatic endoderm (PE) cells were produced using an established differentiation protocol in adherent unconfined monolayer culture (Figure 3-1A, Table S3-3) (Rezania et al., 2014). Commitment from pluripotent states towards pancreatic lineages was confirmed by the downregulation of pluripotency genes, OCT3/4 compared to iPSCs, as well as upregulation of definitive endoderm genes, SOX17 and FOXA2, relative to glyceraldehyde-3-phosphate dehydrogenase (GAPDH). After generation of PF cells, the mRNA levels of pancreatic genes, PDX1 and HNF6 increased to reach expression levels similar to healthy adult human islets, indicating commitment towards the pancreatic lineage during the differentiation process (Figure 3-1B). As expected, NKX6.1 mRNA levels were not increased after induction of the PF stage. Contrary to other reports(Nostro et al., 2015; Pagliuca et al., 2014; Rezania et al., 2014), NKX6.1 mRNA levels were also not upregulated in PE cells generated from standard unconfined cultures compared to undifferentiated iPSCs in our hands(Schaffer et al., 2013). The nuclear fluorescent intensity of immunostained cells indicated a measurable but highly variable nuclear expression of PDX1 in >90% of the cell population (Figure 3-1C).

Since only a small fraction of cells demonstrated increased nuclear PDX1 concentration at the PE stage, we asked whether there were any spatial patterns to the variable differentiation efficiency. When we analyzed the distribution of brightly labelled PDX1 cells (denoted $PDX1^{high}$) in monolayer culture after the transition from PF to PE, these differentiated cells were clustered together (Figure 3-1D, Figure S3-1), while the majority of cells expressed lower levels of nuclear PDX1. The size and position of these clusters appeared to be random, suggesting a stochastically-driven differentiation process that may lead to poor differentiation outcomes downstream. $PDX1^{high}$ clusters were circular in size and about 150 µm in diameter. Based on these observations, we then asked whether directing and controlling the formation of adherent cell clusters could improve pancreatic differentiation efficiency in the overall cell population and developed a micropatterning system to test this hypothesis.

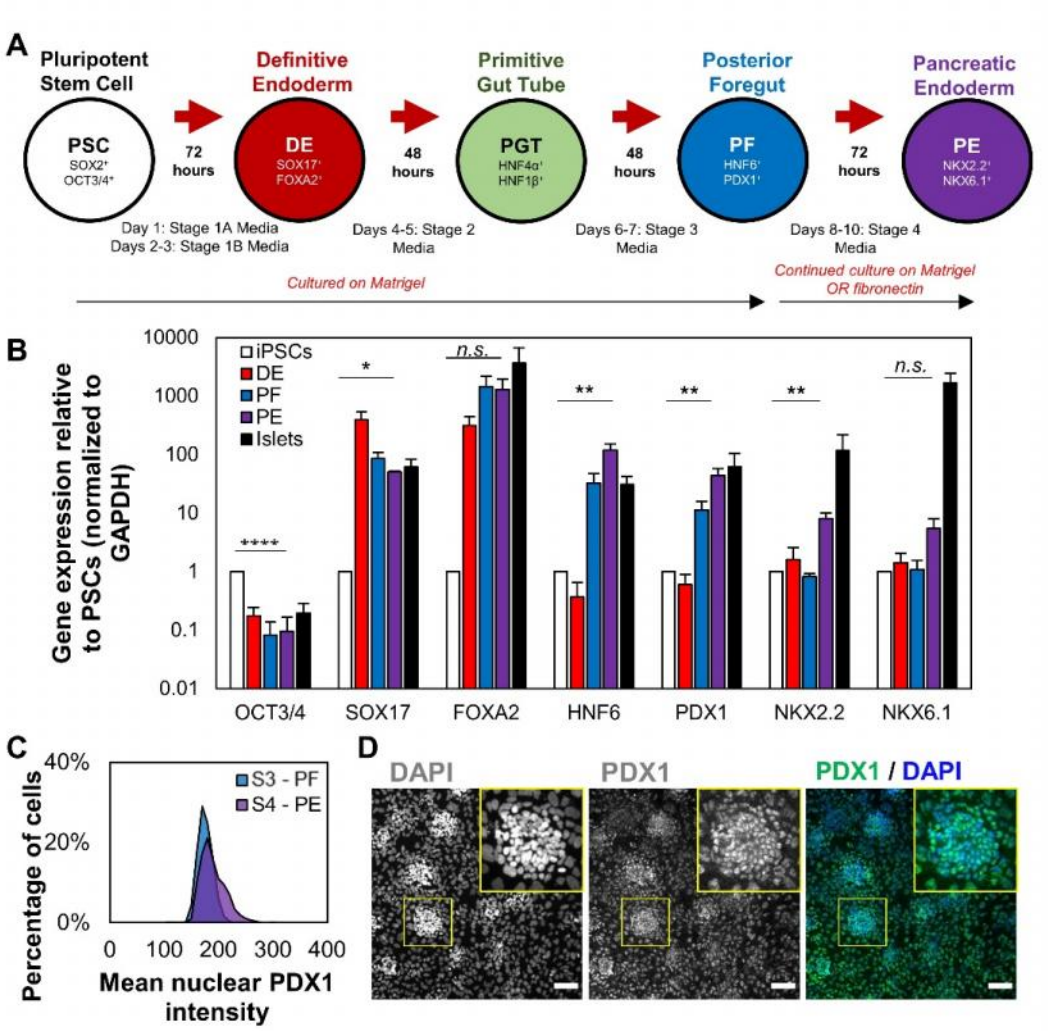

Figure 3-1: *Differentiation of iPSCs into PF cells on tissue culture plastic with timed addition of soluble factors without confinement. (A) The stages of development are mimicked by timed media changes and monitored by expression of key transcription factors. (B) Expression of key pancreatic transcription factors relative to GAPDH based on qPCR. No significant differences were found between -actin and GAPDH. Each bar represents the average of three separate differentiations (N=3). (C) Mean nuclear PDX1 intensity at the PF and PE stages of differentiation, showing a small proportion cells with higher PDX1 expression (PDX^{high}) emerging at the PE stage. (D) In monolayer cultures, roughly circular aggregates of PDX1^{high} cells were observed sporadically in culture. n.s = p>0.05, *=p<0.05, **=p<0.01, ****=p<0.001 for a one-way ANOVA. Full Tukey multiple comparisons post-hoc test results are shown in Table S1. Scale bars represent 100 µm.*

Table S3-1: *Significance testing summary for one-way ANOVA with Tukey post-hoc multiple comparison on qPCR data presented in Figure 1B. n.s.=p>0.05, *=p<0.05, **=p<0.01, ****=p<0.001.*

	OCT3/4	**SOX17**	**FOXA2**	**HNF6**	**PDX1**	**NKX2.2**	**NKX6.1**
Overall Significance	********	*****	**n.s.**	******	******	******	**n.s.**
iPSCs vs DE	****	*	n.s.	n.s.	n.s.	n.s.	n.s.
iPSCs vs PF	****	n.s.	n.s.	n.s.	n.s.	n.s.	n.s.
iPSCs vs PE	****	n.s.	n.s.	**	*	**	n.s.
DE vs PF	n.s.	n.s.	n.s.	n.s.	n.s.	n.s.	n.s.
DE vs PE	n.s.	*	n.s.	**	*	*	n.s.
PF vs PE	n.s.	n.s.	n.s.	*	n.s.	**	n.s.

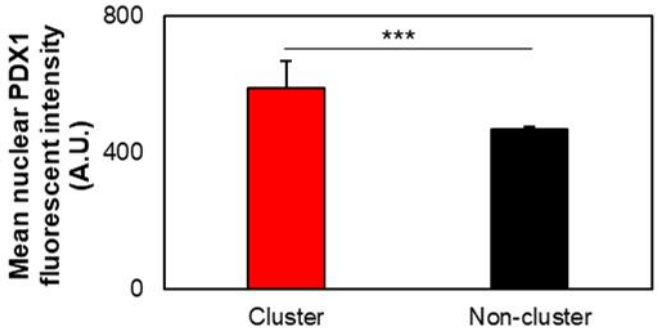

Figure S3-1: *Clustered (n = 7) pancreatic endoderm cells have elevated nuclear PDX1 fluorescent intensity than surrounding non-clustered cells. ***=p<0.005 for a Student's t-test.*

3.4.2. *Micropatterned adhesive islands prompt PF cell clustering and localized multilayer tissue formation*

To facilitate controlled cell clustering, circular cell-adhesive microwells were fabricated to spatially confine PF cells during differentiation in adherent culture, using an agarose-based microwell fabrication process (Figure 3-2A)(C. M. Nelson et al., 2007). Microwells with diameters ranging from 150 µm to 500 µm were successfully fabricated (Figure 3-2B) using standard soft lithography and replica molding processes, as previously demonstrated by others(Xia & Whitesides, 1998). The agarose patterning technique was suitable to spatially confine cells for the 72 hours required for the PE culture step (Figure 3-2C). Since local cell density is known to impact pancreatic specification (Gage et al., 2013; Toyoda et al., 2015), we quantified this parameter in controlled cluster cultures. To assess local cell density, each microwell was segmented into 4 concentric circles with equal area followed by nuclei enumeration (Figure 3-2D,E). In all microwells, the cell nuclei were primarily concentrated in the 3 innermost regions (Figure 3-2F). Furthermore, the overall microwell cell density decreased with increasing diameter, with the 500 µm microwells having the lowest cell density after 72 hours of confined culture. Increasing the initial seeding density did not appear to increase the cell density within 500 µm microwells over the 72 hours of culture (not shown).

To verify that microwell culture promotes controlled clustering into adherent multilayered microtissues, we visualized the 3D F-actin structure using confocal fluorescent microscopy. In the 150 µm microwells (Figure 3-2G,H), a 3D multilayered morphology was observed, resembling the clusters arising stochastically in unconfined monolayer cultures. This multilayered morphology was less pronounced in the 300 µm microwells and not present in the 500 µm microwells. Furthermore, at the edges of the 300 µm and 500 µm microwell colonies, the actin filaments appeared concentrated and aligned with the microwell boundary. This suggests that the actin structures under tension at the micropattern boundary act to cluster the cells, and this tension is sufficiently strong in the smallest patterns to promote cell-driven organization into a multilayer tissue. These results demonstrate that sufficiently small 2D micropatterns can be employed with iPSC-derived PF cells to produce adherent multilayered cell clusters in a predictive and controlled manner.

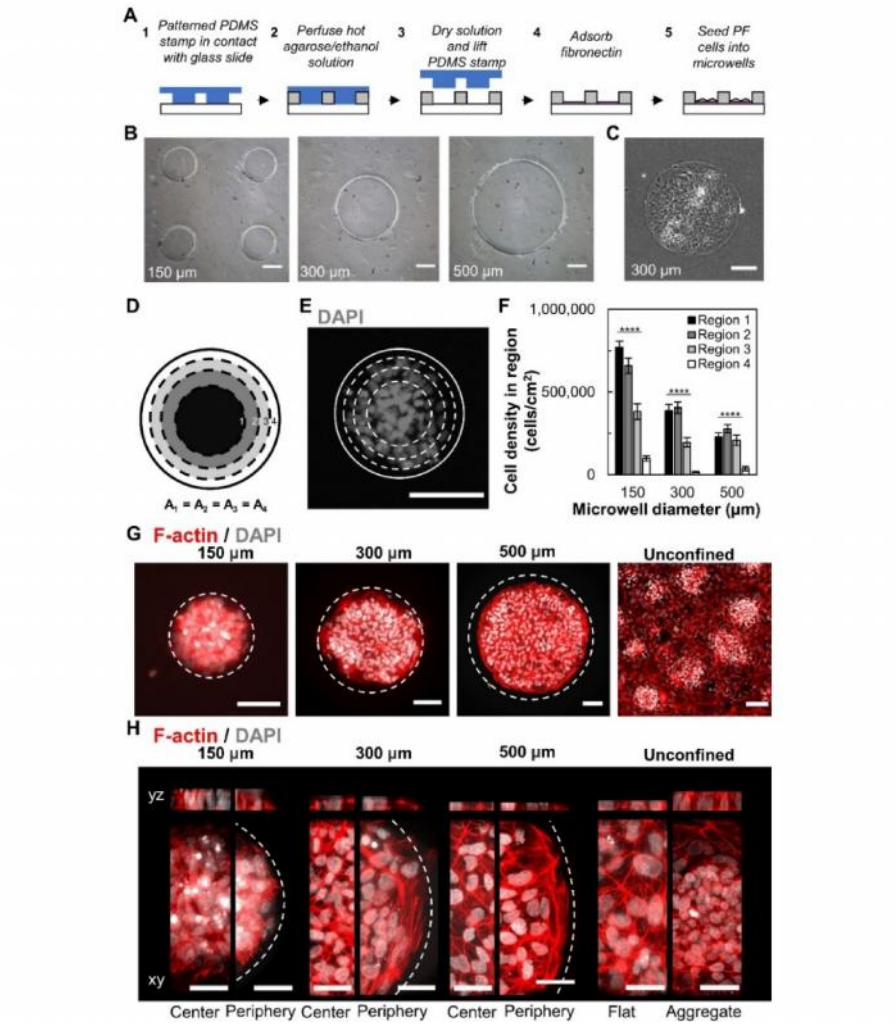

Figure 3-2*: Confined culture of iPSC-derived PF cells in micropatterns promotes clustering of cells in predictable patterns.(A) Process flow to microfabricate agarose microwells to spatially confine iPSC-derived PF cells. (B) Agarose microwells of 150 µm, 300 µm and 500 µm diameters were successfully fabricated with high between-well consistency in diameter. (C) Microwells facilitate confined cell clustering within 72 hours. (D) Areas of 4 concentric circles used for spatial analysis of cell density. (E) Nuclei are concentrated within inner radii of microwells. Each bar represents the average cell density from at least 10 microwells between at 3 separate experiments. (F) Local cell density in concentric microwell regions for 150 (n = 21), 300 (n = 13), and 500 (n = 9) µm microwells. (G) Cell densification occurs in 150 µm microwells similar to aggregates in unconfined culture. (H) Bulged morphology observed after 72 hours in 150 µm microwells but not in 300 µm or 500 µm microwells. Representative images of max intensity projection and 3D reconstructions in yz (top) and xy (bottom) plane. ****=p<0.001 for an one-way ANOVA performed on the iPSC-derived cells. Full Tukey multiple comparisons post-hoc test results are shown in. Scale bars represent 100 µm (B,C,E,G) and 50 µm (H).*

Table S3-2: *Significance testing summary for one-way ANOVA with Tukey post-hoc multiple comparison on cell density data presented in Figure* ***3-2****F. n.s.=p>0.05, **=p<0.01, ****=p<0.001.*

	Microwell Diameter (μm)		
	150	*300*	*500*
Overall Significance	****	****	****
Region 1 vs Region 2	**	n.s.	**
Region 1 vs Region 3	****	****	n.s.
Region 1 vs Region 4	****	****	****
Region 2 vs Region 3	****	****	****
Region 2 vs Region 4	****	****	****
Region 3 vs Region 4	****	****	****

3.4.3. *Controlled clustering of posterior foregut cells enhances pancreatic nuclear transcription factor localization*

To determine whether microwell culture promoted pancreatic differentiation during the transition from PF to PE, nuclear to cytoplasmic (N:C) expression ratios of PDX1 and NKX6.1 were evaluated via immunostaining based on mean fluorescence intensity (Figure 3-3A, Figure S2). N:C ratio was used as a metric since nuclear localization is required for transcriptional activity of these transcription factors and hence for the activation of downstream targets. After 72 hours in PE differentiation medium, cells cultured in the 500 µm microwells did not show any statistically significant increase in the mean N:C ratio for PDX1 or NKX6.1 over the unconfined control. However, the mean N:C ratio of PDX1 was significantly increased in the 150 µm and 300 µm diameter microwells, suggesting that islands with diameters smaller than 500 µm are required to observe significant effects of spatial confinement (Figure 3-3B). An overall increase in total nuclear fluorescent accumulation of PDX1 and NKX6.1 was also observed (Figure S3) and a similar trend in PDX1 and NKX6.1 fluorescent intensity of confined cells was observed (Figure S4). NKX6.1 expression was significantly increased on the 150 µm diameter microwells only. These results sugests that spatial confinement was sufficient to increase the nuclear amount of PDX1 and thus increase the amount of active transcription factors. Furthermore, differentiation into PE cells was confirmed by co-localization of PDX1 and NKX6.1 in 150 µm microwells (Figure S3-5). Hence, 150 µm diameter microwells are sufficiently small to produce clusters that simultaneously upregulate nuclear concentration of both target transcription factors.

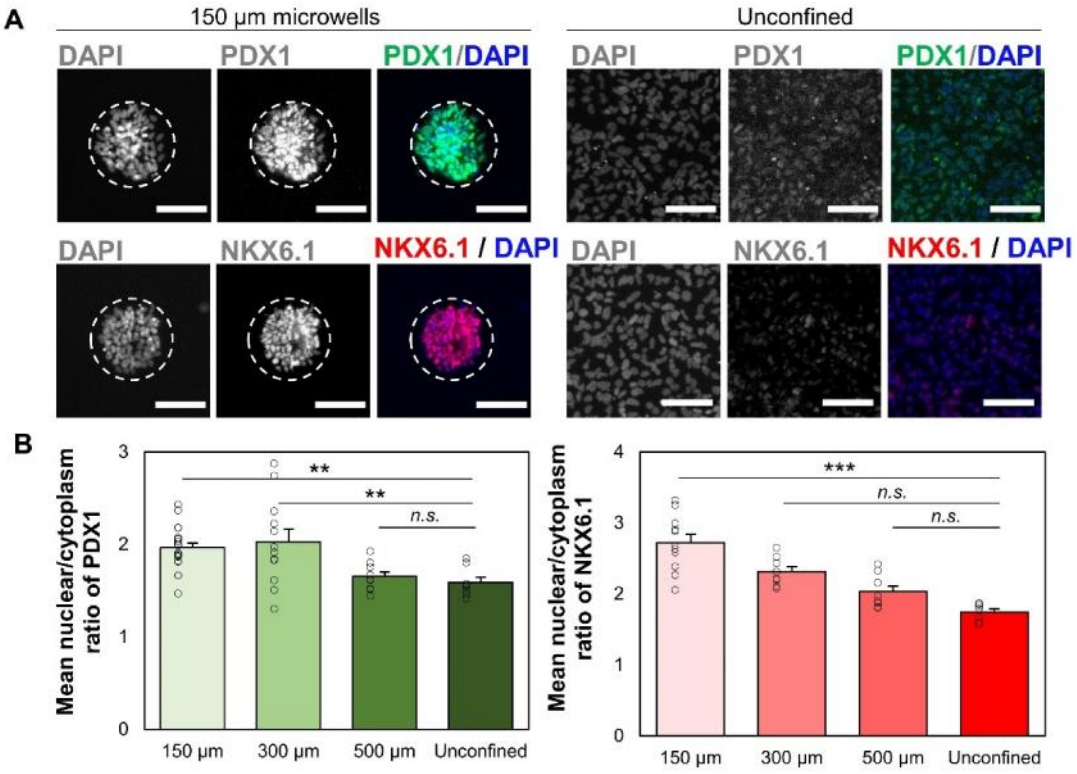

Figure 3-3*: Spatially confined differentiation of PF cells promotes the expression of PE markers. (A) Confined culture of iPSC-derived PF cells increases N:C staining intensity of PDX1 and NKX6.1 shown by immunocytochemistry. Displayed intensity ranges have been matched between confined and unconfined samples to illustrate increased staining intensity (B) N:C ratio in PDX1 (n = 21, 13, 9 for 150, 300, and 500 µm microwells) and NKX6.1 (n = 12, 8, 8 for 150, 300, and 500 µm microwells) immunofluorescence increased when presented with sufficient geometric confinement. Each point represents a data point from a single microwell. n.s = p>0.05, **=p<0.01, ***=p<0.005 for a one-way ANOVA with Tukey post-hoc multiple comparisons. Scale bars: 100 µm.*

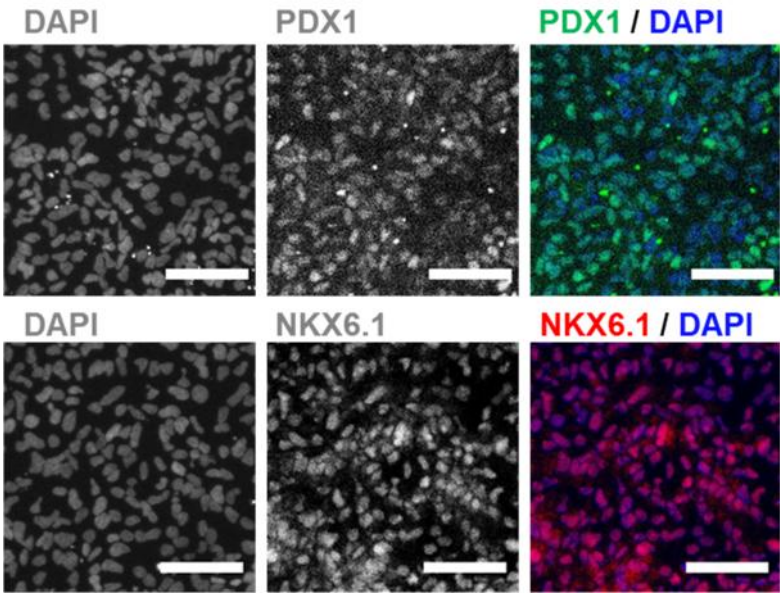

Figure S3-2: *Unconfined pancreatic endoderm cultures show positive staining for pancreatic transcription factors PDX1 and NKX6.1. Brightness and contrast have been increased to show positive staining. Scale bars: 100 µm.*

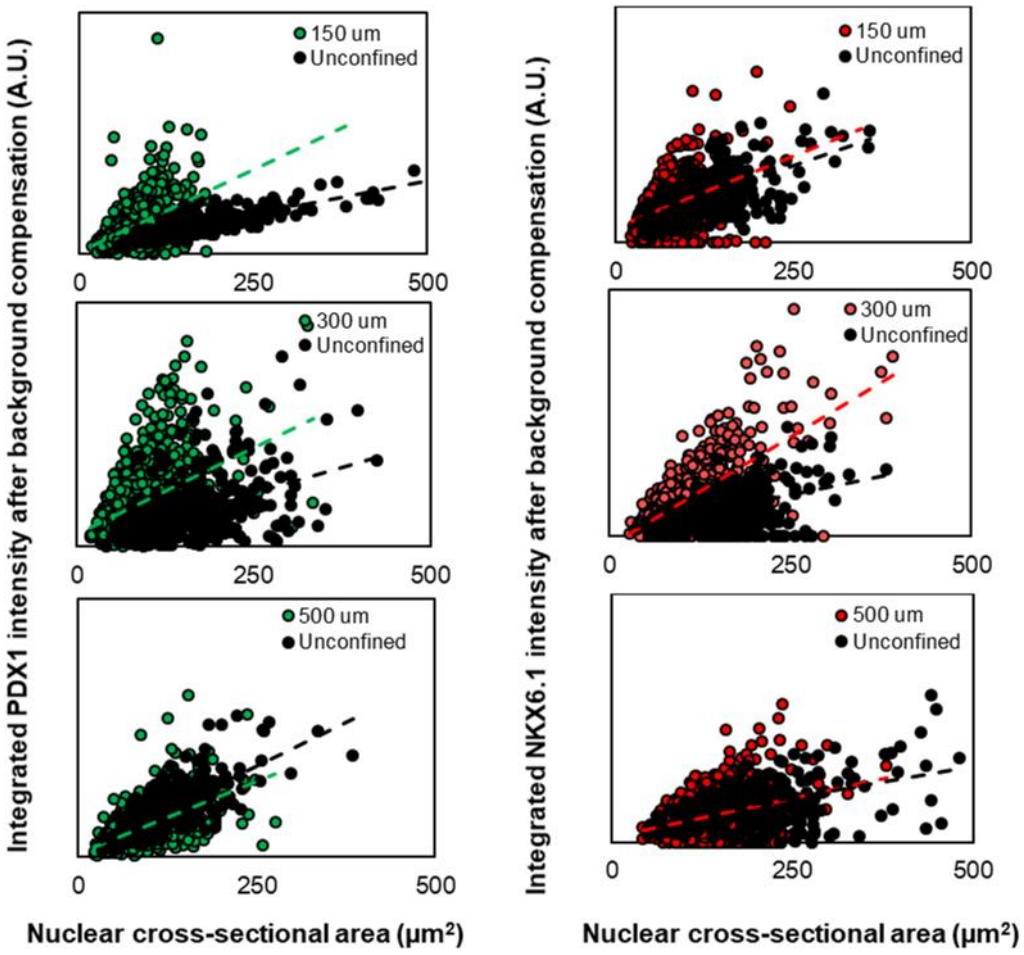

***Figure S3-3**: Representative plots of total nuclear fluorescence intensity. Each point represents a single nucleus within each culture condition. The effects of nuclear area and confined culture were determined by applying the following linear model: $y = \beta_0 + \beta_1 x_1 + \beta_2 x_2$, where y is the total nuclear fluorescence intensity, x_1 is the culture system and x_2 is the nuclear cross-sectional area. The nuclear area had a statistically significant positive correlation with the integrated fluorescence intensity of PDX1 or NKX6.1 staining in all conditions ($p<0.0001$). Confined culture had a significant positive effect on PDX1 and NKX6.1 integrated intensity in the 150 μm and the 300 μm diameter microwells, while a small but significant ($p<0.02$) negative effect was observed for 500 μm microwell confined culture compared to unconfined controls.*

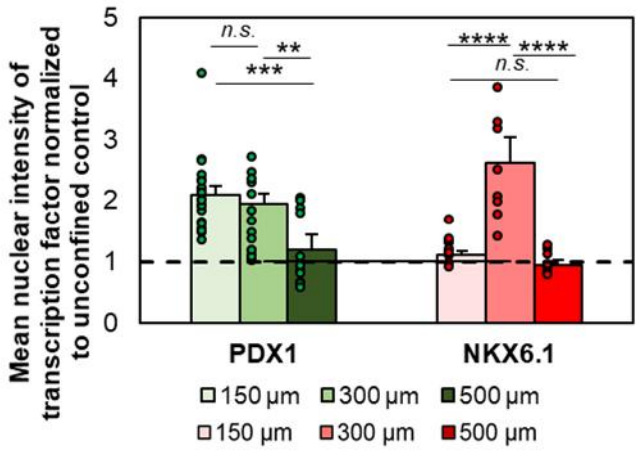

Figure S3-4: *PDX1 (n = 21, 13, 9 for 150, 300, and 500 µm microwells) and NKX6.1 (n = 12, 8, 8 for 150, 300, and 500 µm microwells) nuclear intensity is increased when presented with sufficient geometric confinement. Each point represents a data point from a single microwell. n.s = p>0.05, **=p<0.01, ***=p<0.005, ****=p<0.001.*

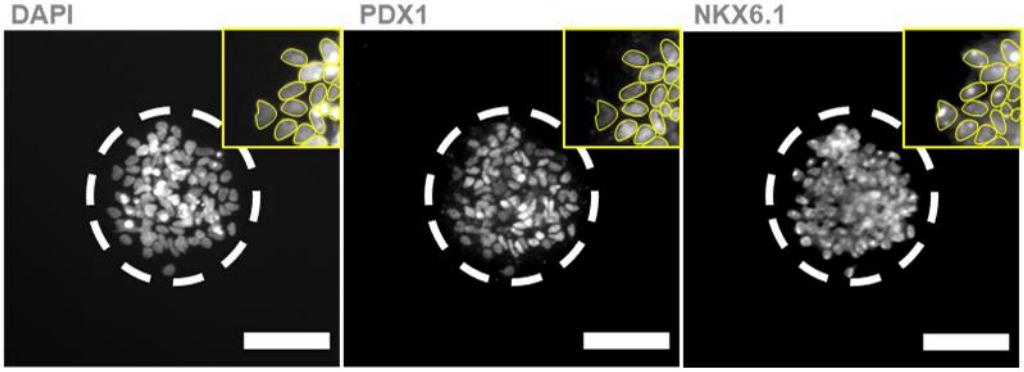

Figure S3-5: *Double stained 150 µm microwells show nuclear colocalization of PDX1 and NKX6.1. Scale bars: 100 µm.*

Since cell density affects differentiation outcomes in standard unconfined monolayer cultures, we asked whether local cell density within the clusters correlates with these improved differentiaton profiles. As we have determined the overall trends for nuclear/cytosolic ratios of PDX1 and NKX6.1, we studied the nuclear PDX1 and NKX6.1 intensity in 4 concentric regions as defined earlier (Figure 3-2D, Figure 3-4A) within each microwell and found that increased cell density in the center of each individual microwell correlated strongly with increased nuclear PDX1 and NKX6.1 expression. On a single cell basis, the majority of cells cultured within the microwell had increased expression of PDX1 or NKX6.1 (Figure 3-4B) with increasing expression towards the centers of the well for NKX6.1. Cells located at the periphery of 150 µm microwells have much lower NKX6.1 fluorescent intensity than the unconfined control. This could be due to the clustering as a result from confined culture, thus resulting in self-organization within the micropatterns. Another potential explanation could be that the decreased cell densities at the periphery inhibit pancreatic differentiation. Furthermore, nuclear NKX6.1 expression was greater in 300 µm microwells than in 150 µm which suggests an ideal microwell size exists maximizes nuclear accumulation of both PDX1 and NKX6.1. Altogether, these data suggest that controlled clustering into appropriately-sized adherent, multilayered microtissues can significantly impact nuclear expression of transcription factors such as PDX1 and NKX6.1, which are crucial to beta cell commitment.

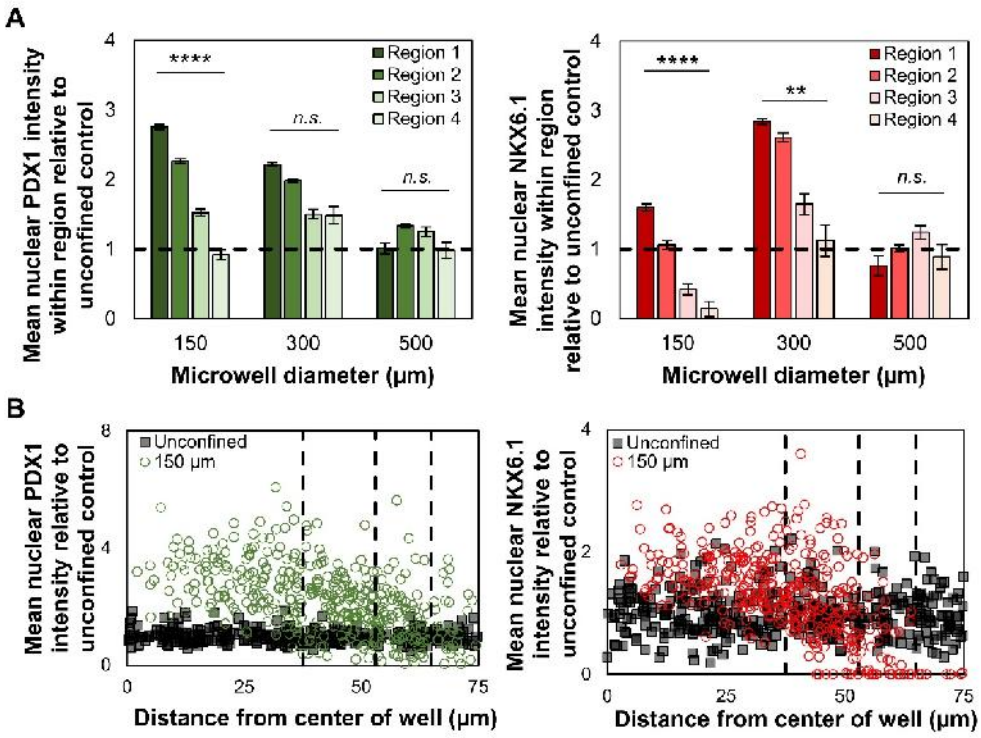

Figure 3-4*: Controlled cluster culture drives spatially dependent patterns of PDX1 and NKX6.1 within the cluster. (A) Mean nuclear PDX1 (n = 21, 13, 9 for 150, 300, and 500 μm microwells) and NKX6.1 (n = 12, 8, 8 for 150, 300, and 500 μm microwells) intensity varies region-to-region and shows correlation to local cell densities. (B) Confined PF cells show increased PDX1 and NKX6.1 intensity on a single cell level. Dashed lines represent limits of regions defined in Figure 2D. n.s. = p>0.05, ** = p<0.01, **** = p<0.001 for a one-way ANOVA between different regions.*

3.4.4. *Cell clustering and differentiation efficiency is associated with actin-driven morphogenesis*

Although confined culture in 150 µm microwells consistently increased PDX1 and NKX6.1 nuclear expression compared to unconfined cultures (Figure 3-3B), some heterogeneity in actin filament distribution and expression levels were still observed between microwells. We reasoned that this may be due to differences in clustering dynamics between wells. Therefore, we investiated the temporal evolution of the actin cytoskeletal structures associated with formation of these adherent, multilayered microtissues in 150 µm diameter microwells. A correlation was observed between microwells with low mean PDX1 expression and a distinctive actin cytoskeletal architecture where the stain was most intense at the microtissue periphery (Figure 3-5A). Conversely, microwells with high mean PDX1 expression showed intense actin staining near the well center and a more aggregated morphology, suggesting that the evolving microtissue architecture changes during differentiation.

To determine how such actin patterns arise during the clustering process, we looked at population-based temporal evolution of actin cytoskeletal structures in 150 µm diameter microwells. We observed characteristic actin architectures at 24, 48, and 72 hours of confined differentiation and classified them as either uniform, peripheral, or central based on the predominant actin morphology observed within the microwell (Figure 3-5B). Uniform actin filament distribution was observed 24 hours after seeding and culture in the 150 µm microwells. After 48 hours, some microwells developed well-defined F-actin structures concentrated at the microwell periphery. At 72 hours, a large proportion of the microwells had high intensity actin cytoskeletal structures develop in the center of the microwell (Figure 3-5C). The progression from ‘uniform’ to ‘peripheral’ to ‘central’ actin architectures suggests that the peripheral actin ring first forms around the colony, and then acts to contract the colony inwards to the microwell center. Furthermore, the large proportion of microwells with ‘central’ actin architectures suggests controlled clustering could be used to significantly reduce variability in otherwise stochastic cultures. We therefore hypothesize that centralized actin architectures are characteristic of wells that have undergone clustering morphogenesis to form multilayered microtissues, while other actin architectures represent earlier stages in the clustering process.

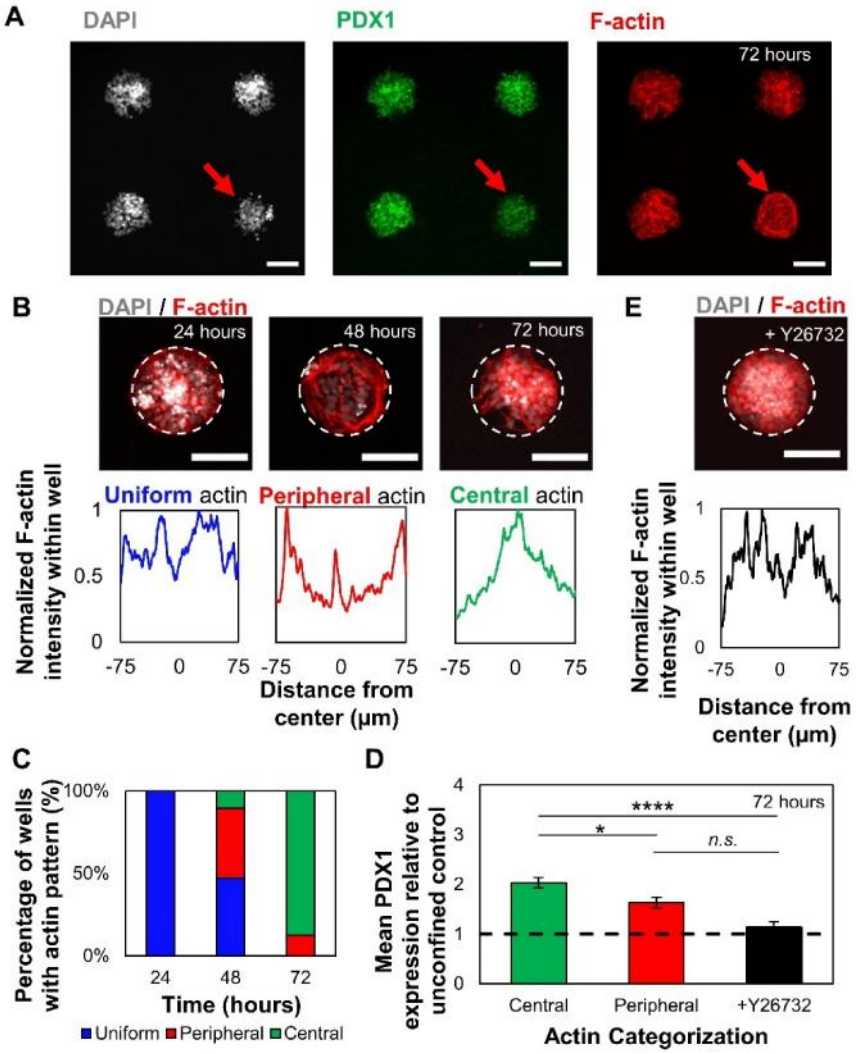

Figure 3-5*: Confined culture promotes temporal changes in F-actin organization during differentiation. (A) Micropatterned iPSC-derived PF cell colonies that show visibly lower PDX1 intensity (red arrows) are correlated with distinct actin cytoskeleton structures concentrated at the microwell periphery. (B) Characteristic actin structures found throughout 72 hours of differentiation in 150 μm microwells. These structures are grouped based on actin intensity analysis (bottom). The reported intensity profile is obtained from an average of 8 intersecting lines (Figure S6). (C) Proportion of wells with actin structure (classified in (B) at 24 (n = 10), 48 (n = 19), and 72 (n = 32) hours. Distribution of actin structures changes throughout differentiation and aggregates towards the center in 150 μm microwells. (D) Addition of Y-26732 ROCK inhibitor 24 hours after seeding prevents actin structural reorganization. (E) PF colonies in 150 μm microwells with central actin distribution (n = 16) showed increased nuclear PDX1 expression compared to those with peripheral actin distribution (n = 5). Addition of Y-26732 abrogated any increase in nuclear PDX1 expression compared to the unconfined control (n = 12). *=$p<0.05$ for the student's t-test. Scale bars: 100 μm.*

To determine whether the clustering is caused by pancreatic differentiation or a natural consequence of microwell geometry, confined culture was performed in basal medium without added PE differentiation factors. As expected, removing the differentiation factors abrogated the increases in PDX1 expression in both confined and unconfined monolayer culture (Figure S6A, B). It is important to note that reduced cell density was observed in the unconfined monolayer culture in the absence of differentiation factors (Figure S6C), suggesting that population-growth driven changes in density may play a role in nuclear PDX1 concentration. Without S4 differentiation factors, most microwells were filled with cells, and exhibited uniformly distributed actin architectures after 72 hours (Figure S6A, B), suggesting that the process of inducing differentiation itself is required for F-actin peripherally focused structures to drive cell clustering.

We then hypothesized that variations in PDX1 expression across our microwell cultures correlated with the observed characteristic actin cytoskeletal architectures. Microwells with actin filaments concentrated at the center had significantly higher average PDX1 nuclear intensity (Figure 3-5D) and PDX1 N:C ratio (not shown) than microwells with actin filaments concentrated at the periphery. This correlation suggests that cytoskeletal rearrangement of the micropatterned colonies is closely linked to the differentiation state of the cultures. Microwells hence bias cytoskeletal remodelling towards a clustered morphology, thereby improving differentiation efficiency as well as reducing differentiation variability.

To isolate the effect of cytoskeletal remodelling on confined, pancreatic differentiation, we added Y-26732, a selective inhibitor of ROCK(Katoh et al., 2001). Inhibition of the ROCK pathway in PF cells cultured in 150 μm microwells prevented actin reorganization and clustering (Figure 3-5E). This also abrogated previously observed increases in average PDX1 nuclear intensity compared to the surrounding unconfined PE cells. The Y-26732 treated microwells had similar cell numbers and densities to the untreated conditions, further suggesting that increases in PDX1 are dependent on cytoskeletal remodeling.

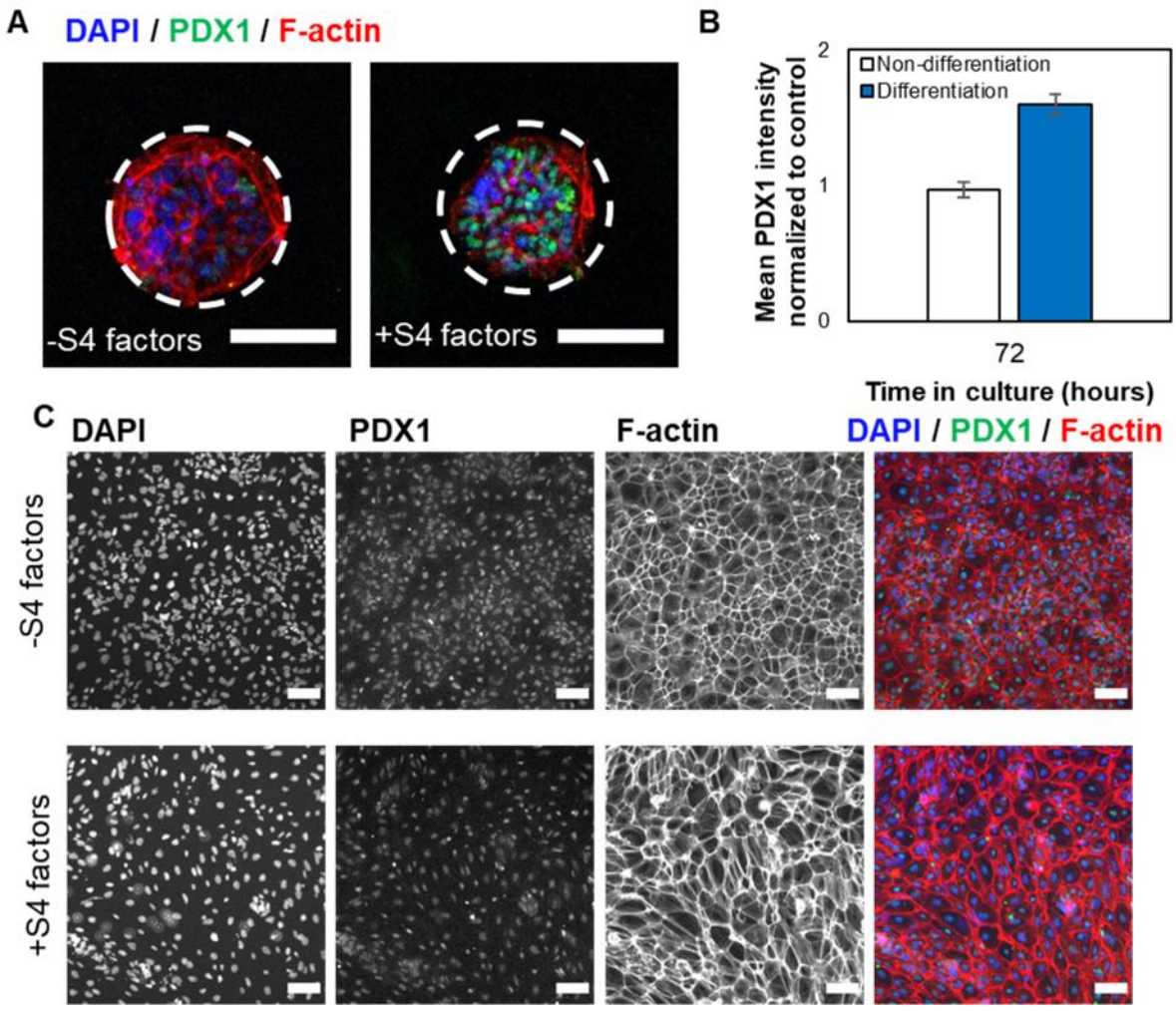

***Figure S3-6**: Culture in absence of differentiation inducing factors abrogates increased PDX1 expression, reduces cell density, and disrupts benefits of microwell culture. (A) Removal of S4 differentiation factors halts cytoskeletal reorganization and abrogates any improvements in pancreatic differentiation from microwell culture shown by immunocytochemistry of PF cells confined within 150 μm wells. (B) Confined culture in absence of soluble factors does not upregulate PDX1 expression over the unconfined control. (C) Decreased cell density is observed in unconfined controls when PE inducing differentiation factors are removed. Scale bars: 100 μm.*

3.5 Discussion

This work demonstrates that controlled clustering in adhesive microwells increases nuclear concentration of PDX1 and NKX6.1, two key transcription factors in beta cell development, in pancreatic endoderm (PE) cells. Inspired by spontaneous aggregation observed in standard unconfined monolayer cultures, we developed a simple, easy to handle 2D system that enabled the reproducible generation of multicellular pancreatic clusters. The effect of confined culture was dependent on microwell size as well as the presence of soluble factors known to drive posterior foregut (PF) cells towards PE phenotypes. Confined culture was also correlated with distinct organizing behaviour of filamentous actin and clustering of cells within each microwell towards a multilayered 3D adherent microtissue phenotype. Although microwell-to-microwell variations exist, we observed a significant and robust increase in nuclear concentration of PDX1 and NKX6.1 in 150 ⇑m diameter microwells compared to unconfined monolayer cultures.

The microwell-driven clustering method overcomes several key challenges in improving PSC differentiation towards mature pancreatic endocrine lineages. First, microwell cultures bias the stochastic formation of aggregates towards increased percentages of $PDX1^{high}$ cells, compared to spontaneous aggregation in unconfined monolayer culture(Nostro et al., 2015; Toyoda et al., 2015). In 150 µm and 300 µm but not 500 µm microwells, increased N:C ratio of PDX1 was observed as well as clustering towards the center of the microwell; consistent with the approximate sizes of cell-assembled aggregates that occur in monolayer differentiation experiments. Our studies demonstrate that culturing differentiating cells in these patterns and at these length scales promotes the formation of actin architectures that encourage colonies to adopt a multilayered clustered morphology. The majority of microwell colonies that adopted this clustered phenotype were $PDX1^{high}$ and also expressed higher levels of NKX6.1. Producing clusters of a defined size improves upon uncontrolled approaches such as coalescence in spinner flasks which results in aggregates with high size polydispersity. Since microenvironmental cues associated with aggregate size and density significantly impacts pancreatic differentiation(Gage et al., 2013; Takizawa-Shirasawa et al., 2013), the heterogeneity introduced during this aggregate formation step may explain the batch variability observed in beta cell yields, maturity and purity between research groups.

Second, microwell cultures ensure highly repeatable cell densities across the substrates, which may significantly influence lineage specification, and is challenging to achieve with other

aggregate-forming techniques that are amenable to culture for several days. This is particularly important to ensure uniform cell behaviour, which might be affected in complex ways. Compared to unconfined controls, increased PDX1 expression was observed in the 150 µm and 300 µm microwells, while a significant increase in NKX6.1 expression was only observed in the 150 µm microwells. This suggests that optimizing these processes for future production of PSC-derived beta cells will require consideration of a multiplexed panel of pancreatic biomarkers. The underlying reasons for these differences could be differences in cell density patterns between the microwell diameters that is known to influence PDX1 nuclear accumulation(Toyoda et al., 2015), but also alters paracrine signalling gradients that are known to affect NKX6.1 expression, which requires a certain threshold of soluble factor stimulation(Nostro et al., 2015). Furthermore, the effect of microwell size on PDX1 and NKX6.1 expression suggests that random aggregation in unconfined monolayer cultures presents significant variability in endocrine differentiation. Since the microwell system produced $PDX1^{+}/NKX6.1^{+}$ co-positive clusters in a more controlled manner compared to those that formed randomly in conventional unconfined culture, microwell-based studies may ultimately provide fundamental insight into the driving factors behind lineage commitment.

Third, although the benefits of aggregation on pancreatic differentiation are well-established, conventional methods to form aggregates present handling challenges and require “forced” aggregation rather than spontaneous self-organized cluster formation as shown here. The throughput of the presented 2D micropatterning method is on a similar order as state-of-the art commercial aggregation methods. We estimate that around 1000 self-assembled, uniform, clusters could be produced per square centimeter of culture area, thus requiring roughly 600 cm^2 to produce a therapeutic dose of √600,000 islet-like cell clusters per patient. Similarly, commercially available non-adhesive pyramidal microwells can produce roughly 700 similar sized clusters per square centimeter of culture area. However, harvesting requires repeated washing steps and aggregate recovery can vary from operator-to-operator(M. D. Ungrin et al., 2008). Moreover, the commercially available pyramidal microwells as well as other controlled suspension cell aggregation systems do not allow self-organization of adherent cultures into multilayered microtissues as shown with the adhesive microwell system.

In this work we showed robust expression of elevated PDX1 and NKX6.1 nuclear accumulation in microwells at the PE stage of culture. Although other studies do report numerically higher frequencies of PDX1+ cells as early as the PF stage, we were unable to replicate these differentiation levels in unconfined cultures, perhaps due to others' use of a lower threshold of PDX1 nuclear accumulation to define a positive cell(Nostro et al., 2015; Pagliuca et al., 2014; Rezania et al., 2013; Schulz et al., 2012). Since our results demonstrate that levels of nuclear concentration of both PDX1 and NKX6.1 can be controlled based on the culture environment, and others have shown that levels of transcription factor expression can be important to improve downstream differentiation and function(Fujitani et al., 2006; Gannon et al., 2008; H. Wang et al., 2001), optimizing for the nuclear amount of these transcription factors may be a fruitful strategy, rather than optimizing for the number of positive or negative cells based on an arbitrarily defined threshold.

These findings do raise several questions about the stem cell differentiation process, particularly regarding the specific microenvironmental cues that drive enhanced lineage commitment at this stage in differentiation. Enhanced differentiation could be driven by many factor that arise in this culture model, including increased cell-to-cell contact, distinct soluble signal gradients within the microwell, mechanical stress gradients across the culture(C. M. Nelson et al., 2005), the rearrangement dynamics of the actin cytoskeleton during aggregation, or simply allowing the microtissue to follow through on an intrinsic propensity to aggregate during differentiation[31,32]. Although the specific details of this transition remain open for investigation, our observations allow us to propose a putative model for enhanced pancreatic differentiation. Based on the progressive transition of F-actin patterning from uniform distribution to peripheral expression to concentration at the microwell center during the aggregation process, we believe that a ring of contractile actin drives "purse-string" morphogenesis(Rodriguez-Diaz et al., 2008) to compact the aggregate structures (***Figure 3-6***). The progressive contraction of the actin filaments from the microwell periphery correlates with higher levels of PDX1, suggesting that a dynamic culture process may prove to be an effective strategy to enhance differentiation during bioprocessing. While we hypothesize that clustering causes increased PDX1 expression, it is difficult to determine whether morphogenic changes lead to increased PDX1 expression or vice versa. Introducing approaches to downregulate PDX1 expression, such as siRNA, as well as time-lapse imaging studies with reporter PSC lines(Gupta et al., 2018; Micallef et al., 2012; Nostro et

al., 2015) may help to understand the interplay between pancreatic differentiation and clustering. Further investigation into the dynamic relationship between NKX6.1 expression, actin reorganization, and further downstream beta cell development could inform bioprocessing strategies. Going further to develop this into a feasible bioprocessing strategy would require systematic optimization of microwell diameter, demonstration of scalability, and validation of beta cell functionality.

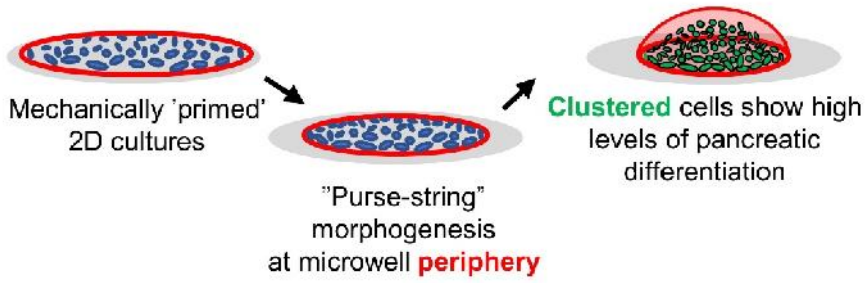

Figure 3-6*: Proposed mechanism of action for increased PDX1 expression via collective actin "purse-string" contraction.*

Overall, the presented microwell system is a simple, scalable and efficient method to produce pancreatic self-organized clusters in adherent cultures that could be used for patient-specific therapies or drug testing with cells that typically have poor pancreatic differentiation outcomes. Compared to unconfined adherent culture, the microwell system led to robust and consistent production of PDX1+/NKX6.1+ multilayered microtissues. Due to the increased accessibility of microfabrication techniques, fabrication of cell-adhesive microwells could be easily adapted into pancreatic differentiation protocols of other labs. The results from this work could inform the design and operation of new vessels for the scalable production of PE organoids by promoting cell-driven morphogenetic programs. By understanding cell behaviour during differentiation, novel substrates could be engineered to drive a larger percentage of cells towards pancreatic endocrine differentiation.

3.6 Materials and Methods

3.6.1. Cell culture and differentiation

Episomal iPSCs derived from CD34+ cord blood (Gibco, Cat # A18945) were maintained on Matrigel (Corning) coated plates in TeSR-E8 media (STEMCELL Technologies). For Matrigel coating, tissue culture treated 6-well plates were incubated with a Matrigel solution, diluted 1:25 in DMEM/F-12 medium (Fisher) for 1 h at room temperature. Media changes were performed every 24 h. Cells were passaged (1:6 dilution) with 0.5 mM EDTA in phosphate buffered saline solution (PBS) (Life Technologies) when reaching 70% confluency.

Prior to initiating differentiation, cells were cultured in mTeSR medium (STEMCELL Technologies) for 1 passage. To initiate differentiation, the iPSC cultures were dissociated with TrypLE Express (Life Technologies) and resuspended in mTeSR supplemented with 10 µM Y-26732 (ROCK inhibitor) (Sigma). The iPSCs were plated at a density of 200,000 cells/cm^2 on Matrigel-coated plates. After 24 h, the adherent cells were rinsed with PBS and differentiation was initiated by the addition of differentiation medium. The differentiation medium was changed every 24 h according to the schedule shown in Table S3 which was based on a published protocol(Rezania et al., 2014). At the end of PF induction, the differentiated PF cells were frozen at a concentration of 1 million cells/mL in S3 media supplemented with 10% DMSO and frozen at a controlled -1 ^{o}C/min until -80^{o}C and then transferred to liquid nitrogen storage until required for confined culture experiments. Between each stage of differentiation, cells were washed with PBS.

3.6.2. Quantitative polymerase chain reaction (qPCR)

Cell samples were collected as pellets (<5 million cells) and frozen at -20 ^{o}C for up to 2 weeks before RNA extraction. Extraction was performed using the QIAGEN RNeasy Mini kit according to the manufacturer's protocol. Complementary DNA (cDNA) was produced with the High Capacity cDNA Reverse Transcription kit (Applied Biosystems) according to the manufacturer's protocol. Next, qPCR was performed using the primers listed in Table S4 and Power SYBR Green Master Mix (Applied Biosystems). The samples were analyzed on an Applied Biosystems 7900HT Fast Real-Time PCR System. The thermal cycle used was: 50 for 2 min, 95 for 2 min, 40 cycles going from 94 for 30 s to 58 for 30 s to 72 for 30 s, 95 for 15 s, 60 for 15 s, 95 for 15 s, and 40 for 2 min.

Table S3-3: *Detailed composition of differentiation medium used in each stage to produce PF cells.*

Days	Medium	Basal Medium	Soluble Factors
1	S1A	MCDB131 + 10mM glucose + 1.5 g/L $NaHCO_3$ + 0.5% fatty acid free bovine serum albumin (FAF-BSA) + 1x GlutaMAX + 1% Pen/Strep	+100 ng/mL Activin A +3 µM CHIR99021
2-3	S1B		+100 ng/mL Activin A
4-5	S2		+0.25 mM ascorbic acid +50 ng/mL keratinocyte growth factor (KGF)
6-7	S3	MCDB131 + 10mM glucose + 2.5 g/L $NaHCO_3$ + 2% FAF-BSA + 1x GlutaMAX + 1% Pen/Strep	+0.25 mM ascorbic acid + 1:200 insulin-transferrin-selenium-ethanolamine (ITS-X) +50 ng/mL KGF + 0.25 µM SANT-1 + 1 µM retinoic acid + 100 nM LDN193189 + 200 nM TPB (PKC activator)
8-10	S4		+0.25 mM ascorbic acid + 1:200 ITS-X +2 ng/mL KGF + 0.25 µM SANT-1 + 0.1 µM retinoic acid + 200 nM LDN193189 + 100 nM TPB

***Table S3-4**: Primers used for qPCR*

Gene	**Forward / Reverse Primer**	**Sequence (5'-3')**
GAPDH	Forward	CCCATCACCATCTTCCAAGGAG
	Reverse	CTTCTCCATGGTGGTGAAGACG
OCT 3/4	Forward	TGGGCTCGAGAAGGATGTG
	Reverse	GCATAGTCGCTGCTTGATCG
SOX2	Forward	CACAACTCGGAGATCAGCAA
	Reverse	TCCGGGAAGCGTGTACTTA
SOX17	Forward	GGCGCAGCAGAATCCAGA
	Reverse	CCACGACTTGCCCAGCAT
FOXA2	Forward	GGGAGCGGTGAAGATGGA
	Reverse	TCATGTTGCTCACGGAGGAGTA
HNF1B	Forward	TCACAGATACCAGCAGCATCAGT
	Reverse	GGGCATCACCAGGCTTGTA
HNF4A	Forward	CATGGCCAAGATTGACAACCT
	Reverse	TTCCCATATGTTCCTGCATCAG
HNF6	Forward	CGCTCCGCTTAGCAGCAT
	Reverse	GTGTTGCCTCTATCCTTCCCAT
PDX1	Forward	AAGTCTACCAAAGCTCACGCG
	Reverse	GTAGGCGCCGCCTGC
NKX2.2	Forward	CCGAGGGCCTTCAGTACTCC
	Reverse	CGGGGTCTCCTTGTCATTGT
NKX6.1	Forward	TTCGCCCTGGAGAAGACTTT
	Reverse	GCGTGCTTCTTCCTCCACTT

3.6.3. *Immunocytochemistry (ICC)*

Cell samples were fixed in 4% paraformaldehyde for 20 min, washed with PBS three times, permeabilized with 0.1% Triton-X100 solution for 20 min then washed with PBS three times. Non-specific protein adsorption was blocked by applying DAKO Protein Block Solution (Agilent) for 1 h at room temperature. After washing with PBS, the primary antibodies were incubated at 4 ^{o}C overnight, washed three times with PBS and then incubated with the corresponding secondary antibodies for 1 h at room temperature, and washed three times with PBS. Finally, samples were incubated with DAPI counterstain diluted in PBS for 20 min at room temperature and washed three times with PBS. The antibodies and dilutions used are list in Table S5.

3.6.4. *2D geometric confinement using agarose microwells*

Circular pillars were fabricated using SU-8 photolithography. Briefly, a 15 µm layer of SU-8 5 (MicroChem) was spin-coated at 4000 rpm for 1 min onto a sonicated, acetone-cleaned 50 mm x 75 mm glass slide. The slide was soft baked at 70 ^{o}C for 2 min and then hard baked at 100 ^{o}C for 5 min. The SU-8 was covered with the mask (CAD/ART Services, containing circular features as small as 50 µm) and exposed to UV light for 30 s in 5 s intervals to create a pattern of photo-crosslinked surfaces. The microfeatures were developed by gentle agitation in SU-8 developer. The resultant mold was baked at 100^{o}C for 5 min then flood exposed under UV for another 10 min.

These features were replicated using polydimethylsiloxane (PDMS) soft lithography to produce an inverse mold. An additional replication step was done in PDMS to produce stamps with pillars ranging from 150 µm to 500 µm in diameter. The PDMS stamps were plasma oxidized with atmospheric air for 2 min to create a hydrophilic surface and placed feature-side down on a glass slide. A hot solution of agarose and ethanol (3:2) was perfused through the pillars by capillary action by pipetting a small drop on the side of the stamp. The slides were then placed under vacuum for 1 h to allow gelation, after which the stamps were removed in a vertical motion using tweezers. Before seeding cells onto the substrate, the surface was coated with a layer of fibronectin by incubating in a 25 µg/mL solution for 1 to 2 h at room temperature. Frozen PF cells were seeded at 5.0 x 10^5 cells/cm^2 at day 7 out of 10 in the differentiation protocol to ensure confluency and to prevent tissue formation between micropatterns as the cells adhere. Cytoskeletal inhibition experiments were performed by adding 10 µM Y-26732 (ROCK inhibitor) for 48 hours starting from day 8 out of 10.

Table S3-5*: Antibodies and reagents used for immunocytochemistry*

Antibody	**Supplier**	**Catalog #**	**Dilution**
Rabbit anti-human mAb HNF4α	Abcam	ab92378	1:400
Mouse anti-human mAb PDX1	BD Pharmigen	562160	1:200
Rabbit anti-human pAb NKX6.1	Novus Biologicals	NBP149672	1:200
Goat anti-mouse AlexaFluor 488	Life Technologies	A11001	Primary
Goat anti-rabbit AlexaFluor 568	Life Technologies	A11011	Primary
4′,6-Diamidino-2-phenylindole dihydrochloride (DAPI)	Life Technologies	D9542	1:1000
TRITC-conjugated phalloidin	Life Technologies	P1951	1:200

3.6.5. Image analysis

The nuclear levels of transcription factors (PDX1 and NKX6.1) was quantified by image analysis using Fiji(Schindelin et al., 2012). Nuclei were identified using the DAPI counterstain. Regions of interest were manually selected to encompass the nucleus (Figure S7). The mean fluorescent intensity within the regions of interest was obtained as a measure of nuclear transcription factor concentration. Here, the nuclear cross-sectional area was assumed to be an adequate measure of nuclear volume due to the homogenous nuclei height across samples. To determine the nuclear-cytosolic ratio of PDX1 and NKX6.1 fluorescent intensity, the total cytosolic intensity of PDX1 and NKX6.1 was calculated by measuring the total transcription factor intensity encompassed by the tissue actin cytoskeleton (marked with fluorescent phalloidin staining) and subtracting the total nuclear fluorescent intensity. In unconfined samples, nuclei were chosen indiscriminately in both clustered and non-clustered areas. The surrounding cytoskeletal area of the confluent monolayer was selected to just encompass the nuclei selected for analysis. The nucleus-cytoplasmic (NC) ratio was then calculated as the mean nuclear fluorescent intensity divided by the mean cytoplasmic intensity.

The mean nuclear intensity of all cells measured within a microwell was then normalized to the intensity in the surrounding unconfined control (Figure S8). This was done after background subtraction where the average background fluorescence of each image was obtained using the 'Subtract Background' algorithm in Fiji and subtracted from the raw fluorescent intensity measured. The radial position of a cell within the microwell was determined using x and y center of mass of the selected nuclei.

To confirm whether nuclear PDX1 fluorescent intensity of clustered cells is independent of any optical effects, we compared the fluorescent intensity of individual cells (n=150) between: 1) spinning disc confocal microscopy and, 2) epifluorescent microscopy with a large depth of field. A constant ratio between the two imaging techniques in both clustered and non-clustered cells suggested changes in nuclear PDX1 fluorescent intensity was independent of optical effects.

Classification of actin morphology was done by qualitatively assessing the intensity profile of the phalloidin stain. The intensity profile was obtained by taking an average of the intensity profile across 8 lines, intersecting at the microwell center (Figure S9). Microwells were classified as having an "peripheral" actin profile when the stain intensity was highest at the edge of the

microwells and a “central” actin profile when the stain intensity was highest at the center of the microwell. The “uniform” morphology was determined when the actin stain covered the entire microwell and had a flat intensity profile.

3.6.6. *Statistical Analysis*

Statistical analysis was performed using JMP 14. Multiple comparisons were analysed using one-way ANOVA followed by Tukey multiple comparisons test while two-way comparisons were analysed using the Student’s t-test. In all analyses, p-values < 0.05 denote a statistically significant result. Three experimental replicates were performed for each experiment unless otherwise indicated in the figure captions.

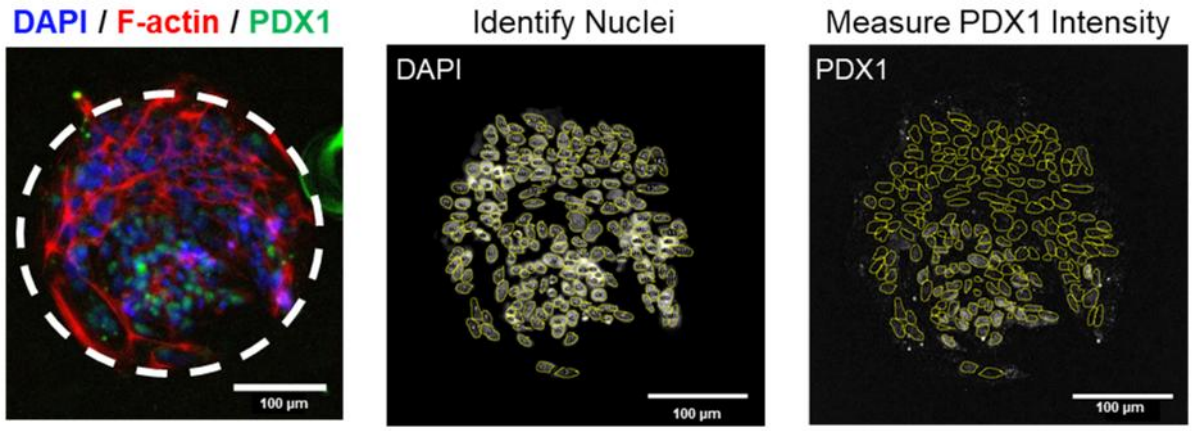

Figure S3-7*: Image analysis work flow. First nuclei were manually selected as regions of interest using the DAPI counterstain. Next, the intensity of the PDX1 stain was measured within the selected regions of interest.*

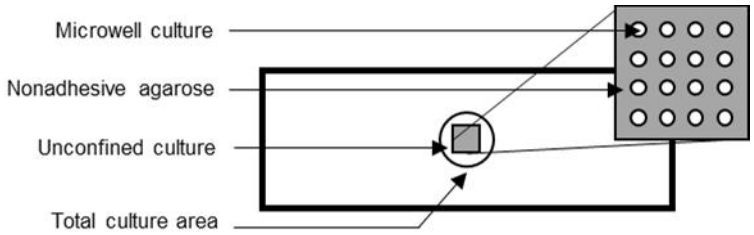

Figure S3-8: *Layout of slide containing microwell cultures.*

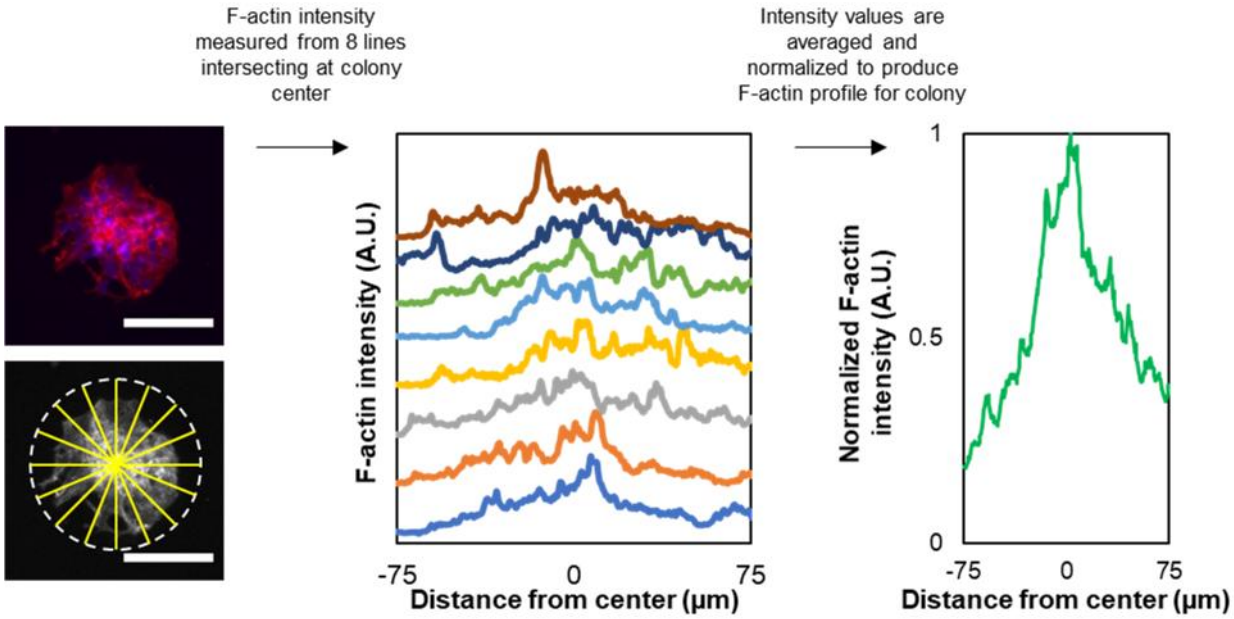

Figure S3-9*: Process flow to obtain actin intensity profile shown in Figure 5B. The reported actin intensity profiles are the average of 8 actin profiles which intersect at the microwell colony center.*

3.7 Acknowledgements

This study was supported by Canada's National Sciences and Engineering Research Council (NSERC, RGPIN-2015-05512 and RGPIN-2015-06271). The development of pancreatic differentiation protocols was supported by a JDRF Transition Award (3-APF-2014-145-A-N). RT and CH are members of the Quebec Network for Cell, Tissue and Gene Therapy – ThéCell (a thematic network supported by the Fonds de recherche du Québec–Santé), of the Québec Center for Advanced Materials (CQMF), of PROTEO (The Quebec *Network* for Research on Protein Function, Engineering, and Applications) and of the Montreal Diabetes Research Center (MDRC). This research was undertaken, in part, thanks to funding from the Canada Research Chairs program (CH and CM). RT received a PGS-D award from NSERC.

3.8 Conflicts of Interest

The authors declare no conflict of interest.

3.9 Data Availability

The data supporting the findings of this study are available within the paper and its Supplementary Information.

3.10 Ethics

Episomal iPSCs derived from CD34+ cord blood (Gibco, Cat # A18945) were maintained on Matrigel (Corning) coated plates in TeSR-E8 media (STEMCELL Technologies). All experiments conducted with pluripotent stem cell lines were approved by the Canadian Stem Cell Oversight Committee.

Chapter 4

Since multicellular tissue geometry can guide cell differentiation (Ruiz & Chen, 2008), I reasoned that micropatterned tissues with more complex geometries would better recapitulate the morphogenesis seen *in utero* than the circular micropatterns shown in Chapter 3. However, conventional high-resolution micropatterning techniques are expensive, time consuming, involve specialized equipment, and require rigorous operator training to create new geometries and molds. To address this technological need, I developed an easy-to-use, reproducible method, termed subtractive bioscribing (SuBScribing), to quickly prototype new micropatterned shapes down to ~600 µm in less than 90 minutes. Here I demonstrate a novel, accessible technique to generate micropatterned cultures which provides additional throughput, consistency, and versatility over other conventional techniques. Using this technique, I reveal that differences in endothelial cell migration depend on geometry as well as effects of ECM removal during scratch-based wounding assays, which together have implications on conventional tissue wounding and healing models. This then gave me the foundation to generate micropattern geometries mimicking the sagittal section of the developing pancreas later shown in Chapter 5, that would otherwise be difficult with conventional micropatterning techniques. This work was published in *Biofabrication* in March 2021 by IOP Publishing.

4.1 Accessible dynamic micropatterns in monolayer cultures via modified desktop xurography

Raymond Tran[1], Corinne A. Hoesli[1,2]*, Christopher Moraes[1,2,3]*

[1] Department of Chemical Engineering, McGill University, 3610 rue University, Montreal, QC, Canada
[2] Department of Biomedical Engineering, McGill University, 3775 rue University, Montreal, QC, Canada
[3] Rosalind and Morris Goodman Cancer Research Center, McGill University, Montreal, QC, Canada

* co-corresponding authors

E-mail: chris.moraes@mcgill.ca ; corinne.hoesli@mcgill.ca

Keywords: wound healing assay, scratch assay, epithelial monolayer, micropatterning

4.2 Abstract

Micropatterned cell cultures provide an important tool to understand dynamic biological processes, but often require specialized equipment and expertise. Here we present subtractive bioscribing (SuBscribe), a readily accessible and inexpensive technique to generate dynamic micropatterns in biomaterial monolayers on-the-fly. We first describe our modifications to a commercially available desktop xurographer and demonstrate the utility and limits of this system in creating micropatterned cultures by mechanically scribing patterns into a brittle, non-adhesive biomaterial layer. Patterns are sufficiently small to influence cell morphology and orientation and can be extended to pattern large areas with complex reproducible shapes. We also demonstrate the use of this system as a dynamic patterning tool for cocultures. Finally, we use this technique to explore and improve upon the well-established epithelial scratch assay, and demonstrate that robotic control of the scratching tool can be used to create custom-shaped wounds in epithelial monolayers, and that the scribing direction leaves trace remnants of matrix molecules that may significantly affect conventional implementations of this common assay.

4.3 Introduction

Cell and tissue geometry are well-established to regulate cell functions such proliferation(C. M. Nelson et al., 2005), migration(Nam et al., 2016), signaling(Etoc et al., 2016; W. Lee et al., 2019), and differentiation(Tran, Moraes, et al., 2020b). Hence, controlling tissue shape is an important strategy in tissue engineering and regenerative medicine, but generally accessible technologies such as additive three-dimensional (3D) bioprinting are severely limited in resolution of fabricated features(Miri et al., 2019), which limits broad experimentation with this critically important parameter. Alternatively, several studies have demonstrated that patterning cells and tissues into defined shapes on two-dimensional surfaces is effective at predicting cell behaviour in three-dimensional tissues(Gjorevski & Nelson, 2010; J. Lee et al., 2016; C. M. Nelson et al., 2005, 2006). Therefore, using such 2D techniques can be an important first step in establishing cell-geometry interactions for the custom design of novel biomaterials and tissue engineering strategies.

High resolution micropatterning technologies such as microcontact printing(C. S. Chen et al., 1997; Khadpekar et al., 2019; Ruiz & Chen, 2008), patterned surface blocking (Ma et al., 2019; C. M. Nelson et al., 2003; Tran, Moraes, et al., 2020b), or laser patterning (Doyle et al., 2009; Vignaud et al., 2012) of two-dimensional surfaces can achieve precise control of cell size, shape, and colony geometry. Unfortunately, these methods frequently require expensive specialized equipment, reagents, and technical expertise. Although some commercial alternatives now exist (Bosch-Fortea et al., 2019; Monjaret et al., 2015; Young et al., 2018), customization for specific applications remains a challenge in standard wet labs. Furthermore, dynamically-adhesive patterns(Raghavan et al., 2010; N. M. Rodriguez et al., 2014) can provide insight into developmental and homeostatic mechanisms such as wound closure(Almeida et al., 2019; Raghavan et al., 2010; van Dongen et al., 2013) . To resolve these issues and broadly improve accessibility to customized 2D patterning technologies, here we develop a versatile, inexpensive, and easy-to-use technique, that can create dynamic geometric cues on 2D patterned surfaces, for broad deployment in standard wet labs.

Our strategy, termed subtractive bioscribing (SuBscribe), is based on patterned removal of cells or biomaterials at any experimental time point. For example, a non-adhesive film can be mechanically removed prior to cell seeding; or the cells themselves can be mechanically removed during culture. While similar in concept to UV-based photodegradation patterning methods(Strale

et al., 2016; Vignaud et al., 2012) or photothermal degradation(Moriguchi & Yasuda, 2006), this mechanical process does not require specialized equipment, and can be applied on existing live patterned cultures without exposing them to potentially cytotoxic compounds(Brandenberg & Lutolf, 2016) or thermal shock(Moriguchi & Yasuda, 2006) during the process.

Ordinarily, mechanically subtractive biopatterning approaches such as the monolayer cell scratch assay (Jonkman et al., 2014; Liang et al., 2007; L. G. Rodriguez et al., 2005), are limited in positional resolution and pattern shape(Liang et al., 2007; Javaherian et al., 2011; Khadpekar et al., 2019; Wright et al., 2008; Dubois et al., 2019). Computerized robotic controls could overcome these handling limitations to precisely damage(Sakar et al., 2016) or pattern tissues by improving precision, consistency, and reducing operator errors(Simpson et al., 2008). These micromanipulation technologies previously required considerable expertise and specialized equipment, but simple modifications to commercially-available and inexpensive hobby crafting tools, such as desktop craft cutters or xurographers(Álvarez-García et al., 2018; D. A. Bartholomeusz et al., 2005; Speller et al., 2019; Stallcop et al., 2018, 2018) are easy pathways towards automation. We and others have previously used such modified tools to etch microfluidic channels in plastic(Chandrasekaran et al., 2017; Guckenberger et al., 2015), and here we modify the craft cutter to mechanically ‘scratch’ biomaterials and cell layers, using scribes selected to control the size of the desired patterns. In this way, we robustly produce features smaller than the positional resolution of the craft cutter over large culture areas. We demonstrate the utility of this technique to control the shape of multicellular clusters; and use this system to investigate the role of wound geometry on closure rates of established cultures.

4.4 Results

4.4.1. Optimization of agarose film thickness for scratch-based micropatterns

The blade of an inexpensive, electronically controlled desktop craft cutter (KNK Zing Air; ~$800) was replaced with a metal needle to precisely scratch preprogrammed shapes into the surface. Thin agarose films are cell-repellent due to their characteristically low protein adsorption and are sufficiently brittle to be mechanically patterned with high fidelity(C. M. Nelson et al., 2007). To create the initial patterns of cells, the SuBscribe system was used to physically scratch patterns into dehydrated agarose films (Figure 4-1A). The agarose concentration and spin coating parameters were used to tune film thickness.

Thinner agarose films, (approximately 40 nm, measured via 3D laser confocal scanning microscopy; Figure S4-1) yielded the best SuBscribe pattern fidelity (Figure 4-1B). Furthermore, scribing of the agarose film layer did not result in any observable physical damage to the underlying glass surface (Figure S4-1). Thicker layers produced with a 1% agarose solution resulted in film delamination from the underlying glass substrate, likely due to poor adhesion[21]. Thicker layers were also subjected to more cracking and delamination during scribing, as the critical delamination(Beake et al., 2006; Kang & Huang, 2017; Roy et al., 2010) is proportional to the film thickness and needle penetration depth, which resulted in poor pattern quality. We experimentally determined that such thin films could be formed by decreasing agarose content to 0.5% and spin coating at 1500 RPM; or dip-coating glass slides in a 0.25% agarose solution (Figure S4-2). While dip-coating is readily accessible to all labs and can be used to create large films, it can also result in non-uniform film thickness at the glass slide edge. For these proof of concept experiments, we therefore spin-coated our films in all subsequent experiments but note that dip-coating concentrations and surface tensions can be optimized as needed to make this technique accessible without spin-coating equipment.

4.4.2. Characterized limits of scratch-based micropatterning

The smallest spacing between patterns allowable was ~35 µm, which was slightly above the advertised x-y resolution limits (25 µm) of the craft cutter (Figure 4-1B, Figure S4-3A). This allowed us to increase pattern line width by strategically programming micropattern designs (Figure S4-3B). The feature sizes were defined by selecting needles of different dimensions, and when scratched across a surface, the needle diameter dictates the width of the micropatterned lines (Figure 4-1C). Sometimes larger needles produced feature sizes smaller than expected from the

needle geometry, and this could be attributed to incomplete contact between the needle and surface. The line widths created from our batch of sewing needles was 38.6 ± 5.4 µm (n = 15 needles). Micropatterns down to 10 ⇑m wide could be produced using a microdissection needle while larger patterns could be produced with a blunt sewing needle. Due to the repetitive strikes made by our relatively malleable needles against a hard glass substrate, we wondered whether needle tip diameter would change with repeated use, thereby changing pattern dimensions with usage. Repeated load testing of the SuBscribe system with sewing needles demonstrated that some tip dulling occurred between 1000 patterns and 2000 micropatterns but was stable before and after these points (Figure 4-1D, E). Tip dulling was independent of pattern length or geometry (Figure S4-4). Optimization of scribing tip hardness through selection of needle material could reduce the dulling effect; harder scribing needles would reduce tip dulling but could damage the underlying glass substrate while extremely soft needles would preserve the glass substrate but may not consistently generate micropatterned surfaces. In addition, optimization of scribing force or calibration of the needle distance to the surface can also reduce the change in line width but should be optimized for different machines (Figure S4-5,Figure S4-6). These results demonstrate that this approach can consistently make well-defined and predictable patterns, suitable for high-throughput micropatterned cell culture arrays. Should even greater consistency be required, alternative scribing needles of harder materials and coatings may be used.

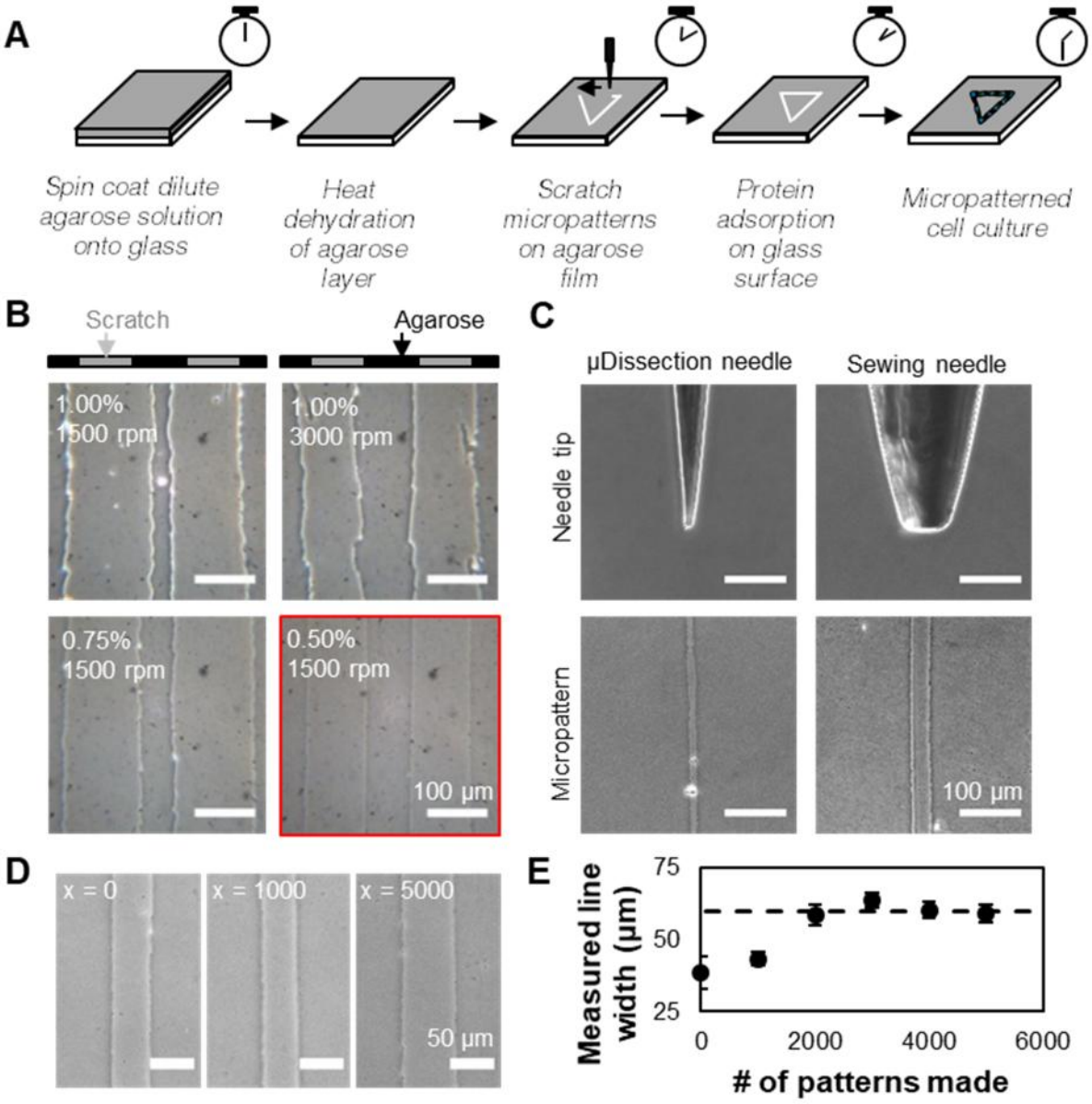

Figure 4-1: *Production of micropatterned cell cultures via subtractive bioscribing (SuBscribing) of cell-repellant agarose layers. (A) Process flow requires less than 90 minutes to prototype slide designs. Patterns can be scribed at a speed of 2-3 mm/s allowing scribing of the patterns over a total surface area of 10 cm^2 within 10 minutes. (B) Dilute solutions of agarose reduce tearing and result in precise micropatterned substrates. Red outline denotes optimal conditions used for remaining studies. (C) Micropattern width can be varied by changing needle tip diameter. (D) Micropattern width shows insignificant degradation of a sewing needle tip over time. x represents the cumulative number of line micropatterns produced with tip. (E) Pattern width stays consistent over time. Error bars represent standard deviation over at least 15 measurements. Dashed line represents average line width after 2000 patterns scratched. Scale bars: 100 µm (B, C), 50 µm (D).*

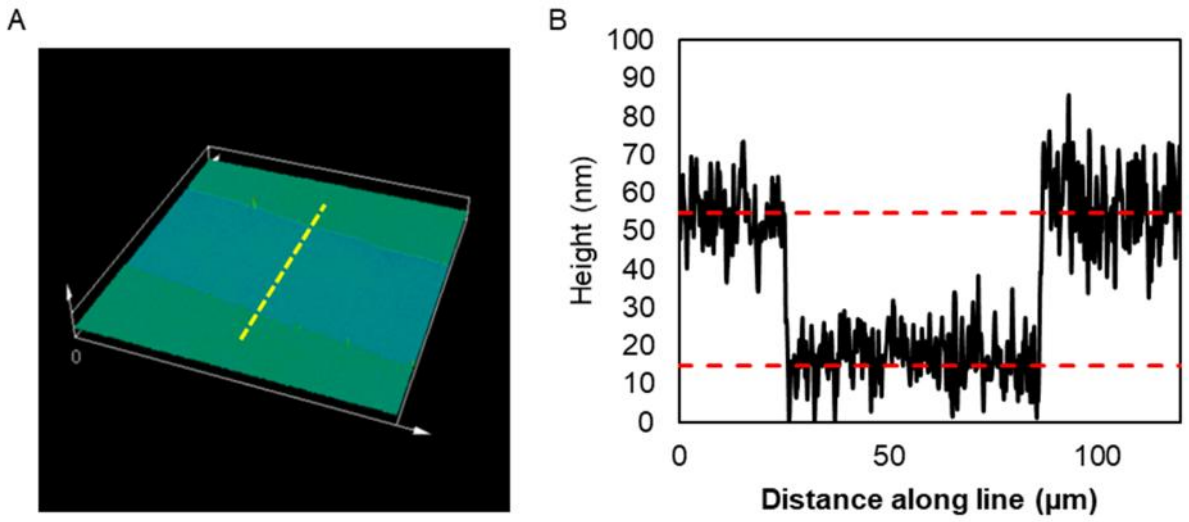

Figure S4-1*: Agarose film layer height is roughly 40 nm thick*

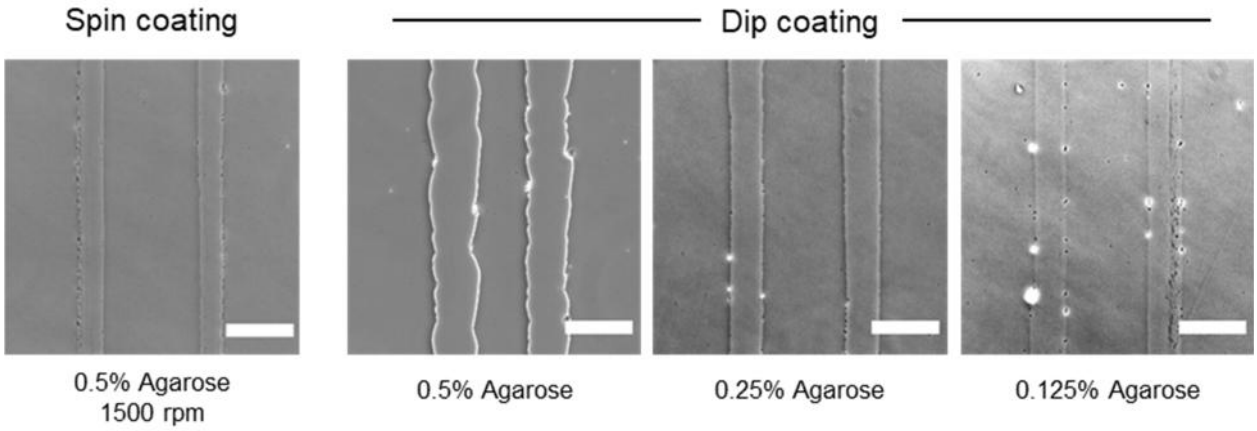

Figure S4-2: *High precision, tear free RMS patterning can also be achieved with a dip coating technique to create agarose film with optimal scribing characteristics. Optimal coating parameters can be determined visually. SuBscribed patterns should have little roughness (<5 µm bumps) and should not have bright outlines when visualized with phase contrast microscopy. Scale bars represent 100 µm.*

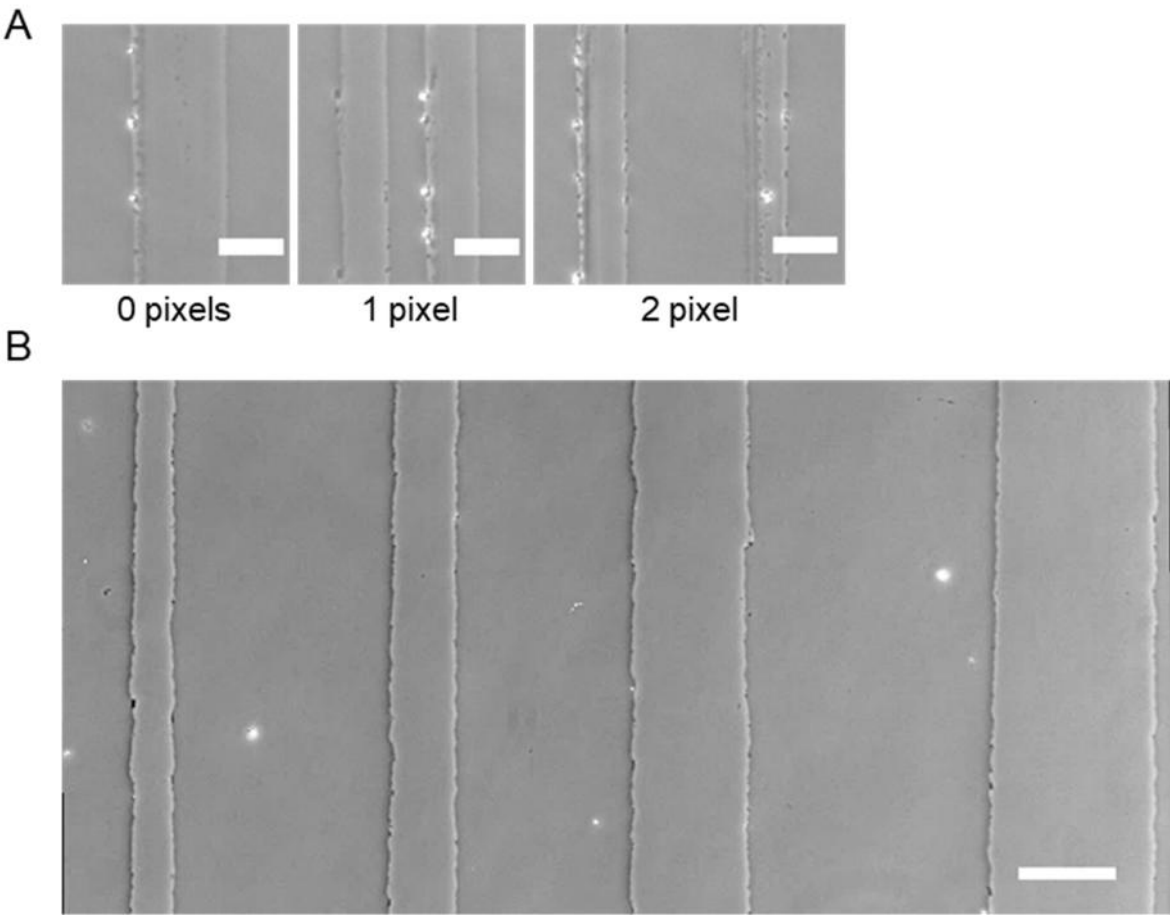

Figure S4-3: *SuBscribing technique allows for precise control of micropattern pitch. (A) High resolution of craft cutter allows for micropattern pitch down to 70 µm. (B) Programming of micropattern design allows for different micropattern dimensions with the same tip. Scale bars: (A) 50 µm, (B) 100 µm.*

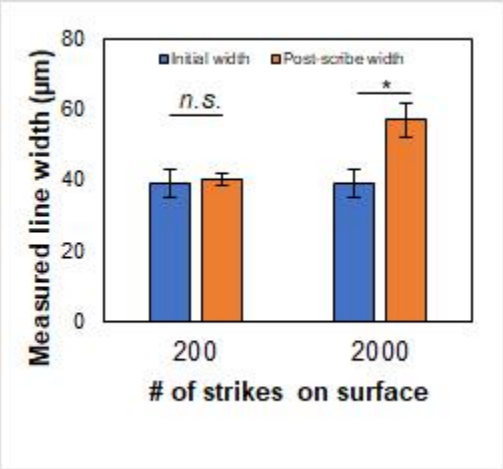

Figure S4-4: *Number of strikes against surface is responsible for tip dulling, not pattern length or geometry. Change in pattern width was characterized by varying the number of impacts for a set scribing length (800 mm). N = 3 needles for each condition, error bars represent standard error on the mean. * represents $p<0.05$ for a Two-way matched ANOVA with Sidak's post-hoc multiple comparisons test.*

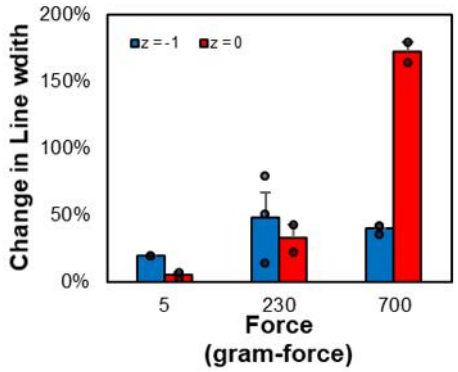

Figure S4-5*: Change in line width can be reduced by lowering the 'force' setting used to scribe micropatterns. Data represents average line width after 2000 scribes at the specified force. Initial line width was 38.6 ± 5.4 µm (n = 15 needles).*

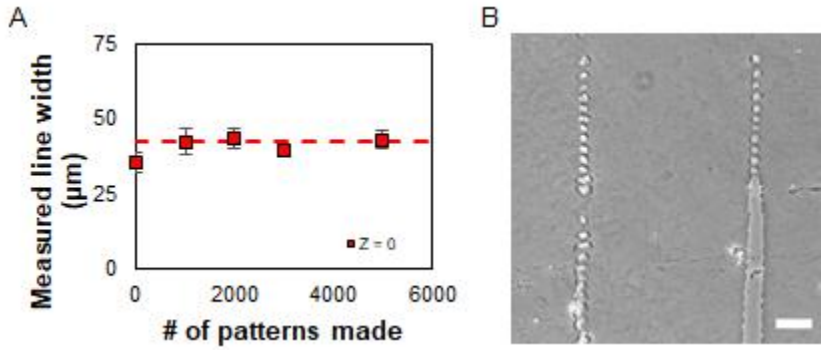

Figure S4-6*: Change in line width can be reduced by calibrating needle tip closer to the glass surface. (A) Measured line width does not significantly change when needle is calibrated at substrate surface. Error bars represent standard deviation of line width. (B) Calibration of the scribing tip at the surface can lead to the tip missing the surface, resulting in incomplete pattern generation. Incomplete patterns were excluded from analysis. Scale bar represents 50 µm.*

4.4.3. Cells confined within scratch-based micropatterns align along direction of pattern

Next, we confirmed that SuBscribed micropatterns could successfully confine cells within the desired geometries. Our patterned surfaces were first incubated with fibronectin to promote attachment in the scribed regions and seeded with human umbilical vein endothelial cells (HUVECs). Cells were confined to micropatterned lines, which limited cell attachment to the pattern widths (Figure 4-2). Patterns down to the width of a single cell were successfully fabricated. (Figure 4-2A). Furthermore, patterns made with 0.5% and 1.0% agarose solutions showed no observable difference in ability to confine cells within micropatterns (data not shown). To determine whether patterns of these dimensions were small enough to influence cell behaviour, we analysed the nuclear alignment within our scratch-based micropatterns. Confined HUVECs showed increased nuclear alignment with decreasing line width (Figure 4-2B), consistent with findings in HUVECs cultured on micropatterns produced with other techniques (Versaevel et al., 2012). At larger pattern widths, preferential alignment direction became substantially less prominent, approaching non-patterned culture conditions. Together, these results demonstrate that cells cultured in SuBscribed micropatterns are consistent with other existing micropatterning technologies.

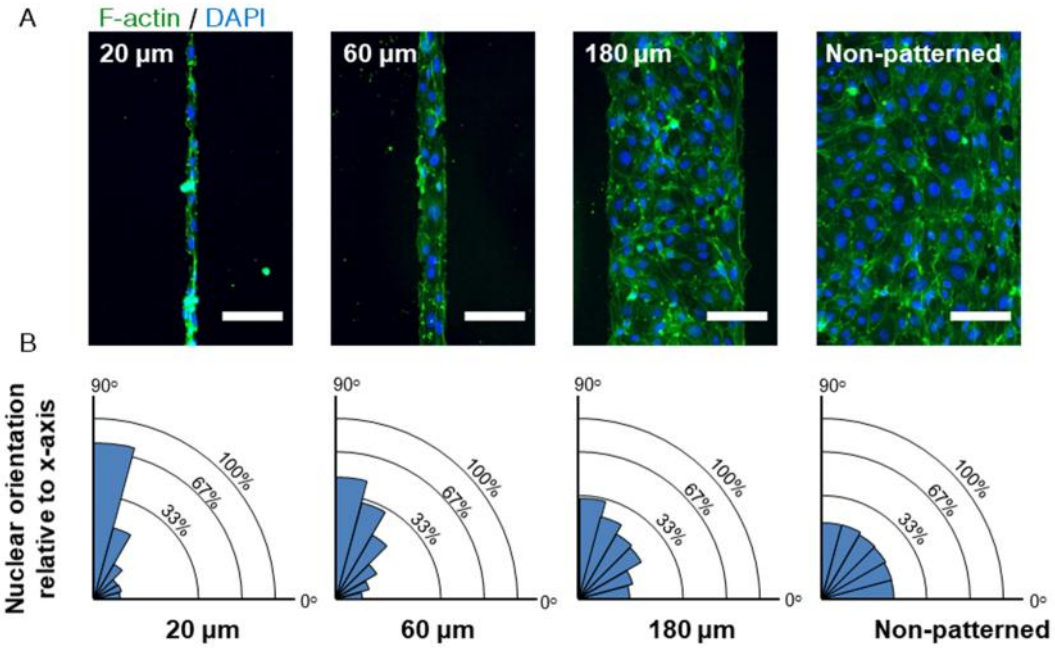

Figure 4-2: *Scratch-based micropatterned cell cultures reproduce previously reported cell alignment. (A) Micropatterned cultures are robust and can be stained for immunofluorescent analysis. (B) Nuclei alignment correlates with decreasing line width as seen by radial histograms. Scale bars: 100 µm.*

4.4.4. *Reproducible formation of more complex micron-scale patterns*

The width of the 1D patterns produced by the SuBscribe technique in the previous experiments are solely based on the needle dimensions. When creating 2D patterns, x-y "step" resolution limitations (previously shown to be ~35 µm (Figure S4-3)) become more important. We therefore tested the minimum feature size limits possible when producing 2D, rounded features. The desktop craft cutter was programmed to produce circles with diameters of 2 mm down to 250 µm (Figure 4-3A). Circles could be fabricated reliably down to ~600 µm in diameter with less than 10% deviation from the programmed shape (Figure 4-3B). Smaller patterns did not retain circularity or projected size. Furthermore, small shapes were occasionally discontinuous and open, likely due to accumulated positioning errors over multiple steps. For subsequent experiments, programmed geometries were hence limited to minimum diameters of 600 µm. We confirmed that at these sizes, other basic shapes could be consistently produced while retaining sharp features (Figure 4-3C). We also tested our capacity to consistently pattern features over a large area with the SuBscribe technique (Figure 4-3D). With conventional microcontact printing approaches, multiple stamps and patterning steps would be required since it is difficult to consistently stamp a single pattern stamp over large areas, as stamps are prone to mechanical collapse and smearing of transferred proteins(Hui et al., 2002). Patterning agarose cell-repellent surfaces using PDMS microfluidic channels directly is limited by capillary-driven flow of agarose solutions(C. M. Nelson et al., 2007). By precoating the glass substrates with the cell-repellent agarose layer, the SuBscribe system provides an alternative and less labour-intensive solution to these issues. The consistent and reproducible patterns formed 'on-the-fly' here facilitates reliable fabrication of multiple, cell-adhesive geometries over a full microscope slide (~10cm^2) in around 10 minutes, demonstrating the versatility and broad applicability of the current technique.

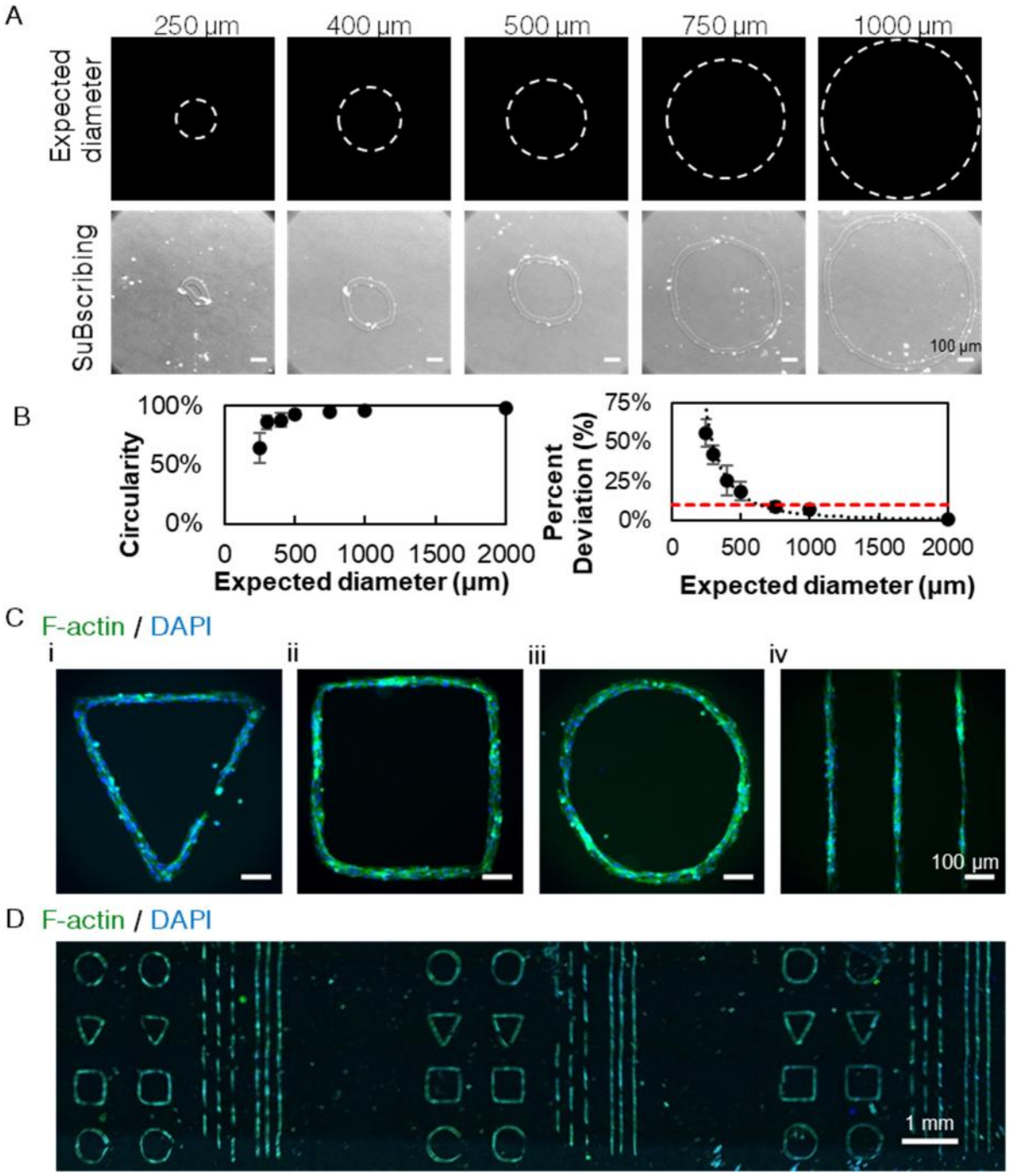

Figure 4-3: *Scratch-based patterning technique produces consistent, micron-scale resolution patterns and allows for high-throughput screening of various geometries. (A) Annuli features can be fabricated down to 500 µm diameter with (B) high circularity and pattern fidelity. n = 20 samples were analyzed. Error bars represent standard deviation. Red dashed line represents 10% deviation from programmed patterns. (C) Magnified view of cell-laden micropatterns (i) triangle, (ii) square, (iii) circle, (iv) lines. (D) Stitched image of multiple fluorescently labelled cell micropatterns. Scale bar: 100 µm (A, C), 1 mm (D).*

4.4.5. *Dynamic modifications to agarose surface enables micropatterned co-culture*

A unique feature of the SuBscribe patterning technique is that micropatterns are produced in a pre-formed non-adhesive layer, and hence requires no subsequent blocking steps that are often the cause of experimental failure in other techniques(Dixon et al., 2014). Since the entire surface is initially blocked, this technique therefore allows dynamic additions to patterns of living cultures. To demonstrate proof of principle of this concept, the SuBscribe system was used to create line-patterns, coated with fibronectin, and seeded with HUVECs (live labelled with CellTracker™ Green CMFDA) as in the previous experiment. Once cultures were established, the samples were returned to the craft cutter, and new micropatterns were formed adjacent to the living cells. After a brief incubation with fibronectin to provide attachment sites on the newly exposed glass surfaces, a 2nd population of HUVECs (live labelled with CellTracker™ Red CMTPX) were seeded on the micropatterned co-surfaces (Figure 4-4A). These results confirm that the co-cultured cells were well segregated between the initial and secondary micropatterns, but some cells from the second round of seeding (red) did layer themselves on top of the existing patterns of green cells. No tearing was evident in the secondary SuBscribed micropatterned lines, suggesting that hydration of the agarose film did not negatively affect pattern fidelity within the ~4 hours between initial seeding and secondary patterning.

4.4.6. *Precise, geometrically controlled wounding of live cell cultures*

Since the SuBscribe technique can add new micropatterns dynamically in live cultures, scratch-based wounding can also be performed directly on a live cell monolayer. Typically, such wounding assays are performed manually with pipette tips or razor blades, with relatively poor control over wound size and shape. While specialized inserts can be custom-designed to create desired wound sizes, this requires the technological capability to produce custom devices(Dubois et al., 2019; Jonkman et al., 2014; Nyegaard et al., 2016), and do not recreate features of damage associated with conventional wounding strategies(Murrell et al., 2011). Typical wounds are made in a straight line, and these assays implicitly assume that the short wound edges do not contribute significantly to migration within the field of view, and that the direction of wounding does not influence closure. Using SuBscribing, a confluent monolayer of HUVEC cells cultured on a glass slide was wounded (Figure 4-5A, B) and closure was observed for various wound patterns and directions.

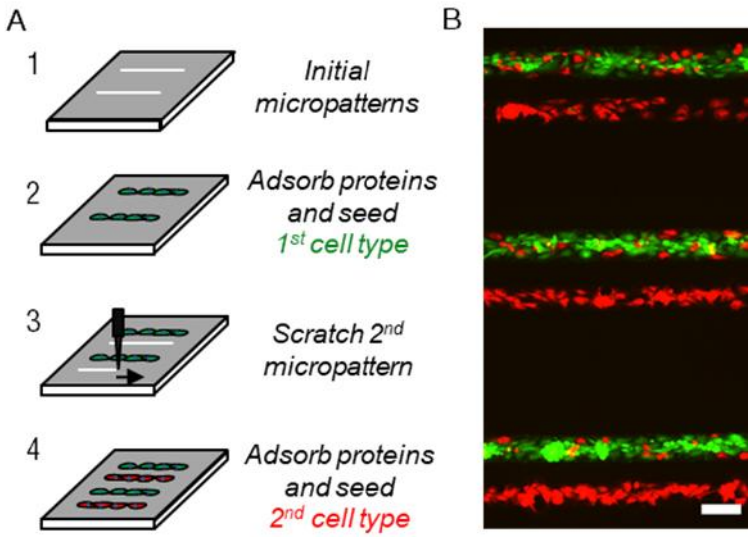

Figure 4-4: *Technique allows for dynamic, modifiable, micropatterned cell cultures. (A) Step-by-step process to create co-cultures with multiple cell types. (B) Different HUVEC populations, stained with CellTracker™ show distinct segregation via fluorescent microscopy. Scale bar: 100 µm.*

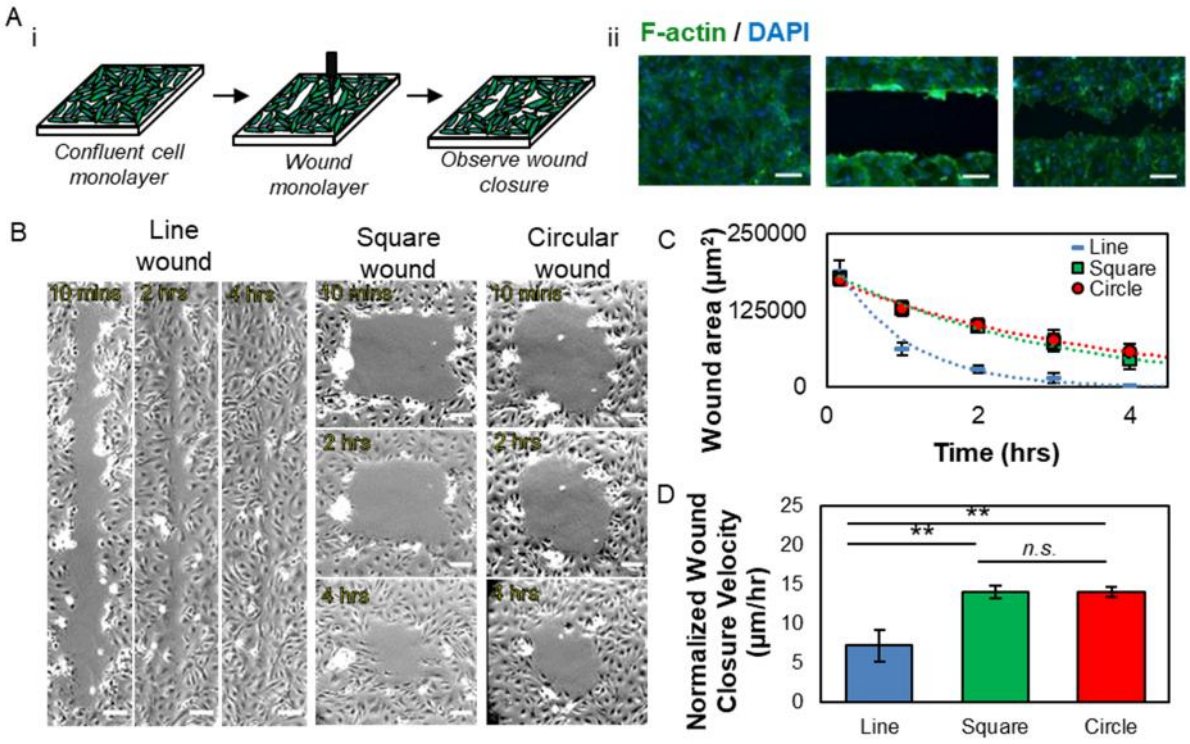

Figure 4-5: *SuBscribe technique can be adapted to wound healing assays to test various wound lengths. (A) i) Process flow to create wounded tissues with SuBscribe. ii) Wound closure can be visualized over time with fluorescent staining. (B) Wounds with defined geometry were created using SuBscribe wounding approach and visualized over time. (C) Line-shaped wounds close fastest as shown by wound area over time. (D) Wound closure velocity normalized to wound perimeter quantified from phase contrast images during live cell imaging (n=3 for each wound type). Velocity was obtained from linear regression. * represents $p<0.05$ for a one way ANOVA with Tukey post-hoc multiple comparisons test. Scale bars: 100 µm.*

To evaluate the contributions of wound geometry towards endothelial closure time, wounds with equal areas but of varying aspect ratio (lines vs. squares) and geometry (squares vs. circles) were formed, and their closure rates were visualized over 4.5 hours with live cell imaging (Figure 4-5C, Figure S4-7). All wounds closed over time, with wound closure velocities similar to those previously reported in in vivo animal studies(McGrath & Simon, 1983). Individual cells in wound with unity aspect ratio shapes must travel further to close, and hence we expected and confirmed that thin, line-shaped wound areas close significantly faster compared to circular and rectangular wound, with significantly faster areal closure rates in the first hour (Figure 4-5C, Figure S4-7). These findings are consistent with delayed exponential models commonly used to describe wound closure rates(Cukjati et al., 2000; Du Noüy, 1916; Dubois et al., 2019). In order to compare wounds of different geometry, we normalized the wound closure rate to wound perimeter(Arciero et al., 2013; Cukjati et al., 2000; Gorin et al., 1996). This yields a linear healing parameter which represents the migration speed of the wound edge(Gilman, 1990, 2004). Line shape wounds had lower normalized migration speeds compared to square and circular geometries (Figure 4-5D), suggesting that thin line-shaped wounds only appear to close faster because of the aspect ratio of the wound. Tracking the cells at the wound edge also show significantly slower migration speeds in line-shaped patterns but also in circular patterns (Figure S4-8) further suggesting geometric dependence of cell migration during wounding. These differences between geometries may be due to differences in migration mechanism, for example purse-string closure mechanisms(Kiehart, 1999) versus lamellipodia-protrusion based migration (Vedula et al., 2015), which may each dominate wound closure depending on local geometry.

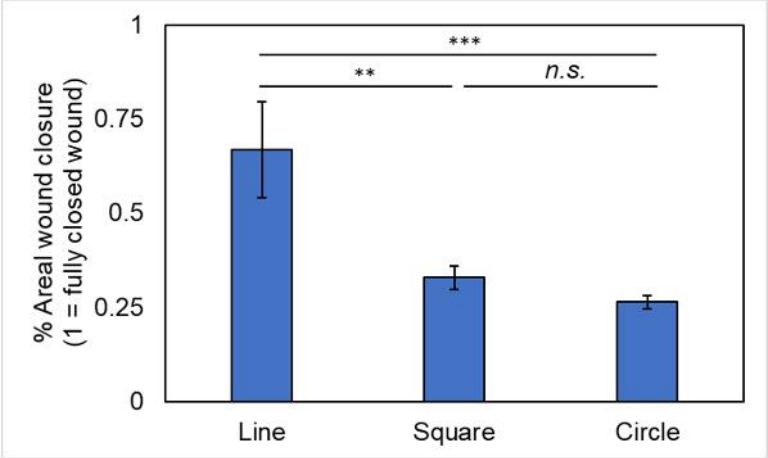

***Figure S4-7**: Percent wound closure by area after 1 hour of wounding. ** represents p<0.01, *** represents p<0.005 for a one way ANOVA with Tukey post-hoc multiple comparisons test.*

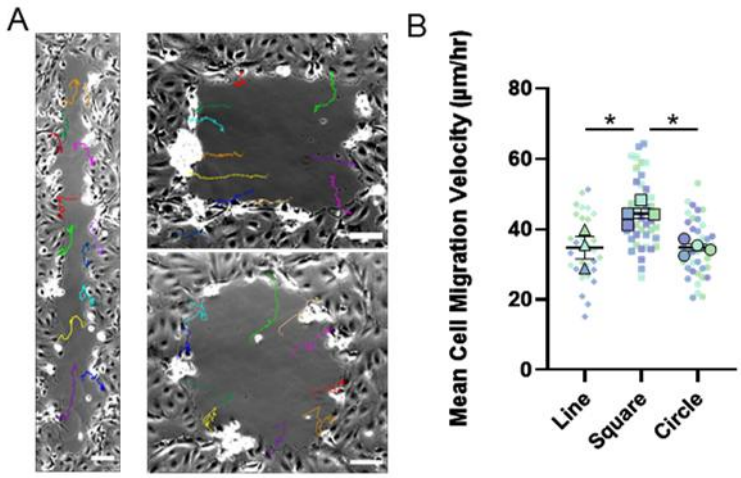

***Figure S4-8**: Single cell migration speed reveals cells at wound borders of lines and circles migrate slower than in square geometries. (A) Single cell tracking was performed manually using MTrackJ plugin. (B) Mean cell migration of cells at wound edge for line (n = 3), square (n 4), and circular (n = 4) wounds. Each data point represents the average migration velocity of 10 cell nuclei at the wound edge. Error bars represent standard error. * represents p<0.05 for a one way ANOVA with Tukey post-hoc multiple comparisons test. Scale bar represents 100 µm.*

A potential confounding factor in conventional scratch-based assays is the presence or absence of ECM on the denuded surface(Vedula et al., 2015). If ECM is left intact, cells can close the gap via lamellipodia-mediated adhesive migration, while ECM removal prevents lamellipodial crawling to close the wound(Grasso et al., 2007; Vedula et al., 2015). In our straight-line wounds, we observe rapid migration in the first hour after wounding, accompanied by large lamellipodial extensions for cells at the leading edge. As the wound closes, these lamellipodia become smaller and fewer (Supplementary Video 1). We reasoned that the central area of the wound has greater ECM removal because of the needle profile, while the edges may retain some ECM that supports lamellipodial-assisted crawling migration. Designing needle profiles and tuning the applied loading force exerted by the craft cutter may hence provide additional control over wound quality and closure rates in subsequent studies.

We then reasoned that if remaining ECM plays a role in wound closure, then the scratching paths may leave traces of oriented ECM that guide wound closure. We are uniquely able to test this parameter by programming distinct scratching paths that wound not be possible with conventional scratching tools. To test this idea, we created a square wound using a side-to-side scratching motion (Figure 4-6A). We confirmed that trace nanoscale ECM cues remain in linear patterns oriented along the scratch path by staining adsorbed fibronectin on cell-free controls (Figure 4-6B, Figure S4-9). Square-shaped wounds in cell monolayers rapidly become rectangular and closed consistently along the longitudinal scribing direction (Figure 4-6C, D).

We then compared the average migration velocities of HUVEC edges both parallel and perpendicular to the scratching direction (Figure 4-6E). The migration of cells into a circular wound, created by repeated scratching of concentric circles, was also measured and the direction of wound closure was considered perpendicular to the scratch direction. The migration velocity of HUVECs parallel to the scratch direction was significantly greater than perpendicular to the scratch direction, suggesting cues that arise from the scratching direction itself could act to guide migration. Since topographic direction of 1-D patterns of ECM is well-established to guide and enhance migration rates (Doyle et al., 2009), these findings suggest an additional parameter present in conventional wound assays that may affect results, and that can be controlled for using robotically-controlled scribing assays.

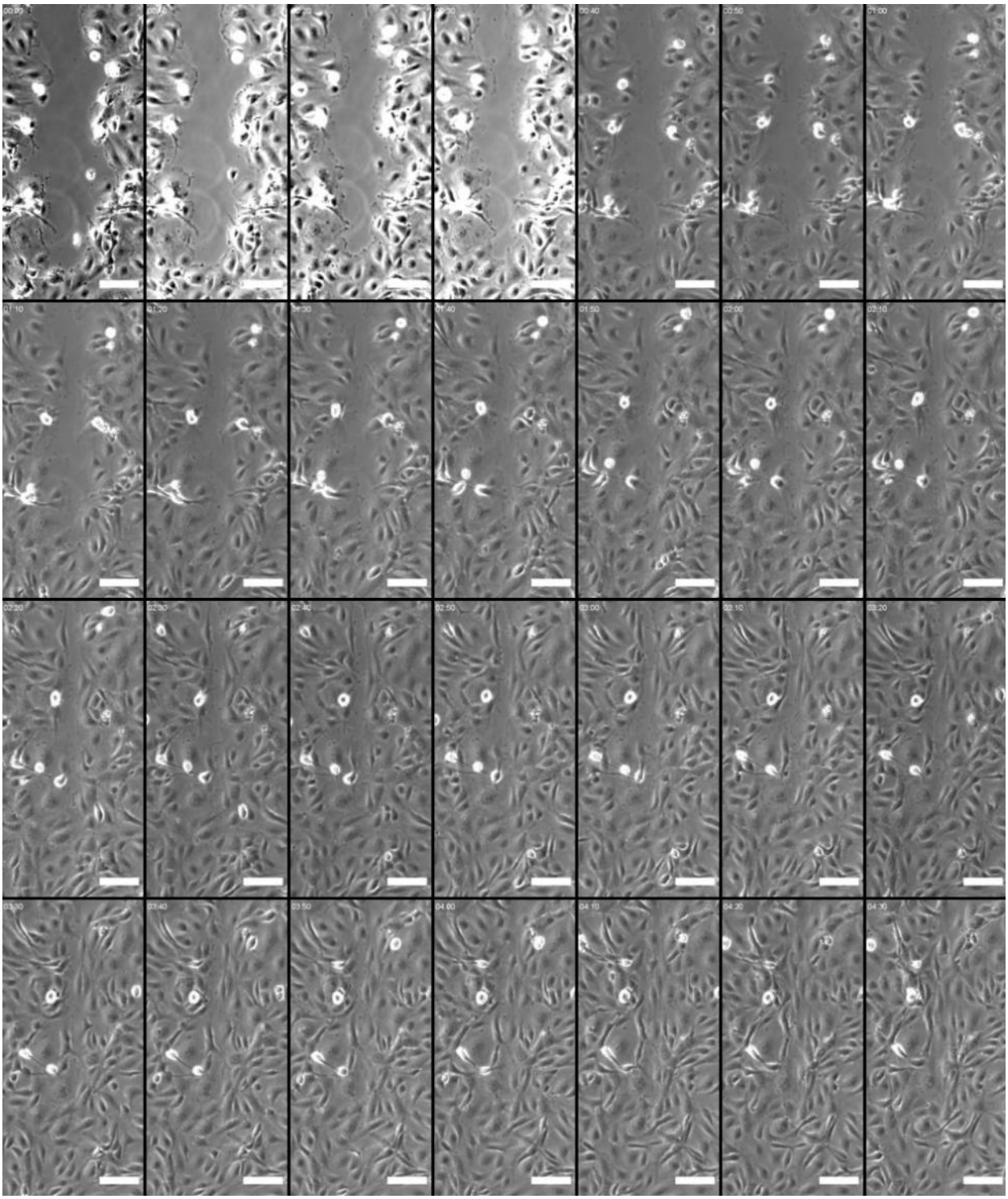

Supplemental Video 1. *Wound closure of epithelial monolayer showing distinct lamellipodal behaviour in different wound regions.*

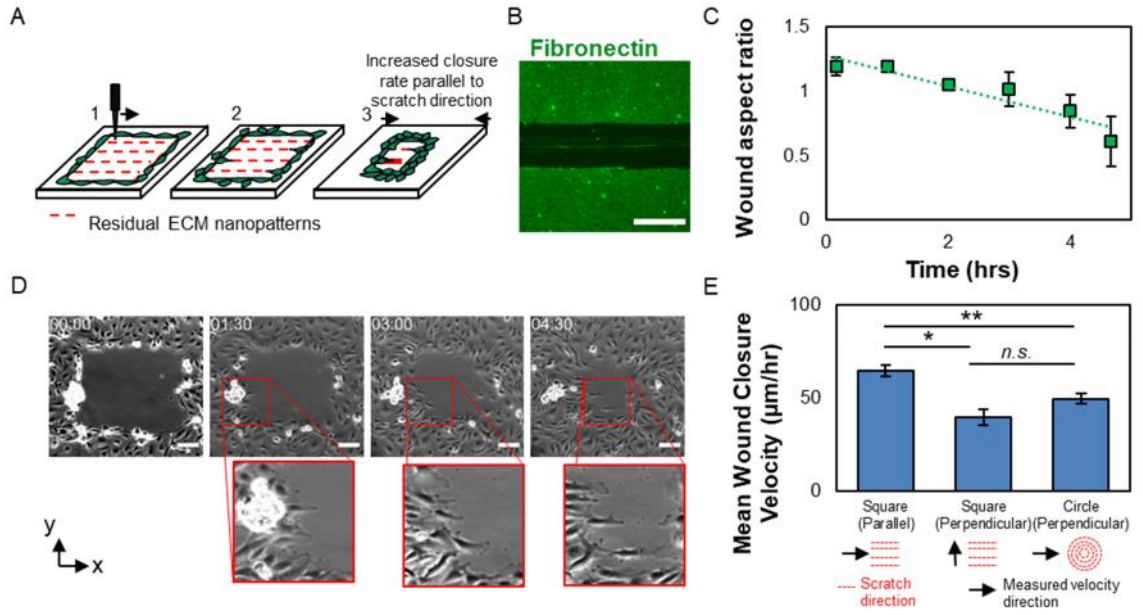

***Figure 4-6**: Nanotopographic ECM cues produced from SuBscribe technique increases migration velocity parallel to scratch direction. (A) Proposed model for increased directional migration velocity action due to remaining ECM cues after scratch patterning. (B) SuBscribe technique physically removes ECM but also leaves trails of fibronectin in direction of scribe path. (C) Asymmetric wound closure of square wounds over time results in rectangular wounds with aspect ratio < 1. (D) Representative wound closure over time in square wounds. Inset shows increased directional migration along scratch direction. Time stamps in HH:MM format. (E) Mean wound closure velocity with respect to scratch direction in different shapes. Error bars represent standard error. * represents $p<0.05$ for a one-way ANOVA with Tukey post-hoc multiple comparisons test. Scale bars: (B) 50 µm, (D) 100 µm.*

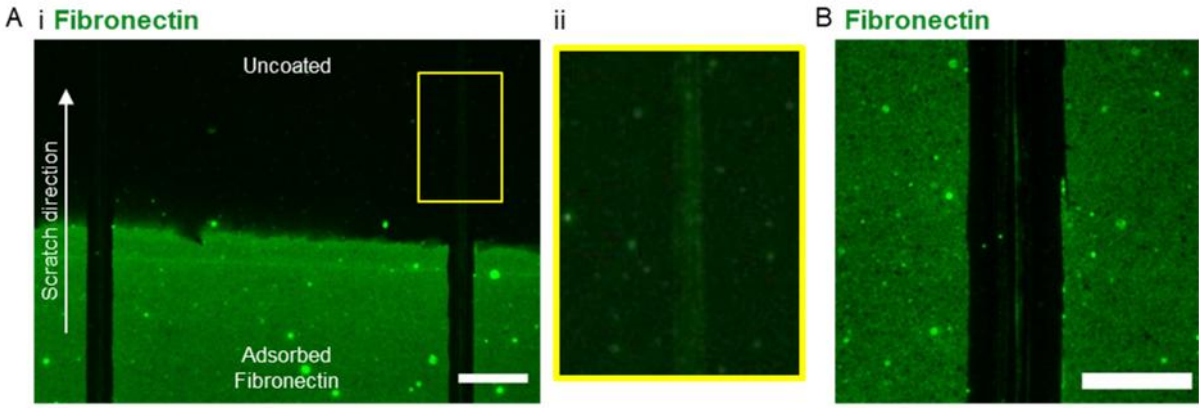

Figure S4-9: *Residual fibronectin is deposited from scratching a fibronectin-coated glass layer. (A) (i) Fibronectin trails are deposited by scratching needle shown by indirect immunostaining of scratched, adsorbed fibronectin. Trails are present in both areas with adsorbed fibronectin and uncoated areas. (ii) Brightness-amplified, magnified image shows fibronectin deposition in uncoated areas. (B) Deposited fibronectin is located at center of scratch pattern as shown by high magnification image. Scale bars: (A) 100 µm, (B) 50 µm.*

4.5 Discussion

This work demonstrates a novel micropatterning strategy where thin layers of cell-repellent agarose are mechanically removed with a pointed needle, controlled by an inexpensive and readily available hobby craft cutter. Removal of agarose can produce confined cell cultures like those produced in other, more laborious micropatterning techniques. Circular micropatterns down to 600 µm can be reproducibly created in both biomaterial films and on-the-fly in live cultures, allowing subsequent patterning and seeding steps. Using this platform, we were then able to investigate the effect of precisely defined wound geometry and scribing direction on closure rate, revealing an intriguing role for nanotopographic remnant ECM in influencing wound closure rates in conventional assays. Overall, the presented SuBscribe technique provides additional consistency, throughput, capabilities and accessibility over other microengineered techniques and assays.

In this proof-of-concept work, we used a relatively inexpensive hobby craft cutter to achieve these patterns. This $800 system had an advertised positioning resolution of 25 µm, which does present some limitations on the resolution of rounded features. Micropattern resolution may be improved by hacking an inexpensive 3D printer to achieve x-y stepping resolutions down to 5 µm or using alternative vector-based craft cutters to implement the SuBscribe technique. Currently, our technique is limited in the choice of substrates; patterns cannot be generated on substrates with nanoscale features as they may be damaged during the SuBscribing process. We also limited our studies to off-the-shelf needles, which do have some limitations in available geometry and relevant material properties such as hardness. Custom-cut needles with non-standard profiles may also further improve the resolution of this technique, and the applied loading force profile may also be tuned to eliminate or retain nanotopographic ECM cues without damaging the underlying surface. Alternatively, soft silicone tips may allow further fine-tuning of these removal processes(Ammann et al., 2015; Kam et al., 2008). We also observed that different degrees of ECM cue removal can be controlled by tuning the force and calibration of the craft cutter (Figure S4-10). Finally, the capacity of this technique to pattern relatively large surface areas could allow for systematic investigation of the effect of geometrically defined multicellular islands on cell function.

There may also be considerable room for expanding this technique by carefully selecting alternative biomaterial films for scribing. In our experience, SuBscribe-produced agarose micropatterns could be maintained in culture for at least 3 days, but can fail after this timepoint

due to poor physical adsorption of the agarose to the underlying glass substrate(C. M. Nelson et al., 2003). Longer duration experiments would require an alternative material that is sufficiently cell-repellent and brittle and may require advanced deposition techniques to process. Our SuBscribe technique is particularly useful for prototyping new micropatterned cultures in lines or non-filled shapes with radii of curvatures greater than 600 µm. Patterns of this scale have previously been shown to pattern pluripotent(Tewary et al., 2017) and mesenchymal(Ruiz & Chen, 2008) stem cell differentiation and are important to establish soluble factor gradients within micropatterned culture. Filled-in shapes can be created by the repeated etching of concentric patterns which decrease in size, similar to the methods presented to create square or circular wounds. Increasingly complex geometries are also theoretically possible but require fine craft cutter calibration to ensure scribing errors do not propagate during patterning. With some optimization, this technique could be employed to generate numerous novel patterns to perform high-throughput screens on novel geometries. Given the demonstrated capacity of this technique to handle live cultures, we envision a dynamically tunable surface able to generate dynamic adhesive sites on demand and at selected locations, opening new avenues for investigation into responsive morphodynamic cell culture systems.

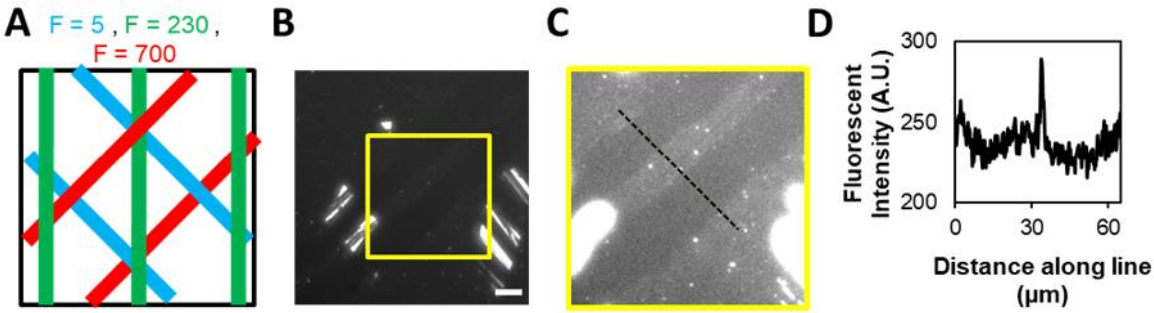

***Figure S4-10**: SuBscribing with different force settings can produce varying amounts of fibronectin removal. (A) Map of different scribing forces applied in B and C. (B) Multiple scratch directions were implemented at different forces. (C) Magnified area (yellow box in A) with enhanced brightness and contrast to demonstrate increased fibronectin removal. (D) Fluorescent intensity profile across the dashed black line in C) of adsorbed fibronectin on the surface. Scale bars represent 50 µm.*

This work also builds upon conventional scratch-based wounding techniques by allowing precise control of wound geometry which has not been possible previously due to operator handling limitations(Riahi et al., 2012). Robotically-aided wounding has previously been reported but were limited to large, straight wounds(Simpson et al., 2008). Wound geometry can also be controlled using silicone-based culture inserts during cell seeding but, this approach does not allow mechanical retraction of cells on wounding, which has been shown to be important in initiating wound closure mechanisms in 2D(Murrell et al., 2011) and 3D cultures(Dubois et al., 2019). Furthermore, this work demonstrates that the process of scratching may itself leave nanotopographic cues that affect observed wound closure, further emphasizing the need for an active wounding process, and precise control over wounding conditions. Interestingly, cells at the wound edge in line and circular wounds migrated slower than those in square wounds (Figure S4-8). This could be due to the nanotopographic cues left from scratching, where in line and circular wounds most cells are migrating perpendicular to the wounding direction. Conversely, in square wounds ~50% of cells are migrating parallel to the wounding direction. Finally, future studies using this system could be integrated into existing platforms to investigate the role of gap closure in the a more realistic environment by better recapitulating ECM protein interactions, co-culture, or in the presence of in vivo flow dynamics(Hoesli et al., 2018).

4.6 Conclusions

Using a robotically-controlled mechanical micropatterning technique raises the possibility for dynamic micropatterning systems that would be otherwise difficult with chemical approaches. Such a system could allow for novel confined migration assays, wounding assays, or micropatterned co-cultures with greater than 2 cell types. Here, we demonstrate an approach that allows us to precisely define geometry in our wounding assay and we show the importance in considering the presence of ECM in such studies. Overall, the described SuBscribe technique provides an inexpensive, novel, and accessible route towards surface micropatterning, which will ultimately lead to improved collaborative opportunities between biomaterials scientists, engineers and fundamental biologists.

4.7 Methods

4.7.1. Micropatterned agarose layer preparation

A dilute stock solution of agarose in water was heated to 80 ^{o}C until completely liquid. Thin films of cell repellent agarose surfaces were fabricated by spin coating the 0.5 % UltraPure^{TM} Agarose (Invitrogen) solution at 1500 rpm for 30 seconds onto standard 25 mm x 75 mm glass slides. The slides were then placed on a hot plate set at 100 ^{o}C for 5 minutes to dehydrate the glass slide.

Microscale patterns were mechanically scratched into the dehydrated agarose film atop a glass slide using an electronically-controlled, inexpensive desktop craft cutter (KLIK-N-CUT Zing Air, KNKUSA). Sewing needles and microdissection needles were fitted into an 18-gauge needle, immobilized with epoxy, and attached to a syringe which was mounted onto the desktop craft cutter. Calibration of the z-axis was done by manually by adjusting the position of the needle holder. To ensure the cuts always contacted the substrate throughout the programmed pattern, the needle position was calibrated to cut below the glass surface (i.e. 1mm below the glass surface). Designs were created in the Make-the-Cut! software provided by the manufacturer. In this software, the cutting parameters were adjusted in the following ranges; Cutting speed: 1-10, Travel speed: 1-10, Cutting force: 50, Multi-cut: 1. The patterned substrates were coated with 25 ⇑g/mL fibronectin (Millipore) diluted in phosphate buffered saline (PBS) for 1-2 hours and then rinsed once with PBS before cell seeding.

4.7.2. Cell culture

Human umbilical vein endothelial cells (HUVECs) up to passage 6 were used in RMS patterning experiments. HUVECs were cultured on 25 ⇑g/mL fibronectin-coated tissue culture polystyrene in Medium 200 supplemented with low serum growth supplement (LSGS) (Thermo Fisher Scientific) and 1% antibiotic-antimycotic (Gibco). Medium changes were performed every 2-3 days and cells were passaged at 90% confluency. Patterned substrates were seeded with at least 50,000 cells/cm^2 to ensure confluency of patterns. Patterns were then rinsed with PBS after 2 hours to remove cells that did not adhere.

4.7.3. Co-culture experiments

HUVECs were fluorescently labelled with CellTracker^{TM} Red CMTPX (Life Technologies) and CellTracker^{TM} Green CMFDA (Life Technologies) as per manufacturer's instruction. Patterned co-culture was accomplished by sequential seeding of the two cell populations. The first cell population was treated as before, allowed 2 hours to adhere, and then rinsed once with PBS. The

second patterns were immediately scribed while still in solution. Afterwards, the culture was soaked in Medium 200 supplemented with LSGS, 1% antibiotic-antimycotic, and 25 µg/mL of fibronectin to coat the new micropatterns for 1 hour. The second cell population was then seeded at 50,000 cells/cm^2, allowed 2 hours to adhere, and then rinsed of excess cells.

4.7.4. Immunofluorescent staining

Cell micropatterning samples were fixed with 4% paraformaldehyde for 20 minutes, washed with PBS three times, permeabilized with 0.1% Triton-X100 solution for 20 minutes, then washed with PBS three times. A cocktail of FITC-phalloidin (1:200 dilution) and the DAPI counterstain (1:1000) were diluted in PBS, incubated with the sample for 20 minutes at room temperature, then washed three times with PBS. Images were obtained on an Olympus IX73 microscope.

Fibronectin patterns were visualized with an indirect immunostaining approach. First, non-specific binding was blocked by a 30 minute incubation at room temperature with DAKO Protein Block (X0909, Agilent) and then rinsed once with PBS. The primary antibody, mouse anti-human fibronectin (SAB4200760, 1:400 dilution, Sigma) was incubated at 4 ºC overnight then washed three times with PBS. Afterwards, the corresponding secondary antibody, goat anti-mouse AlexaFluor 488 (A11001, 1:400 dilution, Life Technologies) was incubated at room temperature for 1 hour, washed three times in PBS and then visualized.

4.7.5. Data Analysis

All images obtained were analysed using the open-source software, Fiji.(Schindelin et al., 2012) The nuclear alignment of micropatterned cells was measured by approximating each nucleus as an ellipse. The angles reported represent the angle between the primary axis of the nucleus and the x-axis. Circularity of the patterns presented in Figure 3 was obtained by manually tracing the resultant micropatterns and reporting the circularity outputted by Fiji. Deviation of the micropatterns was computed as the percent difference between the expected diameter and the actual diameter of the resultant micropatterned circle. The calculated diameter was approximated with the traced perimeter of the micropatterned circle. Stitched images of the line-shaped wounds were created using the Fiji Pairwise stitching plugin(Preibisch et al., 2009). Single cell tracking was performed using the MTrackJ plugin for Fiji (Meijering et al., 2012). Statistics were calculated using GraphPad Prism 8.

4.8 Acknowledgements

The authors received funding from Canada's National Sciences and Engineering Research Council (NSERC, PGS-D award for RT, RGPIN-2015-05512 to CM and RGPIN-2015-05877 to CH) which supported this work. This work was undertaken, in part, thanks to funding from the Canada Research Chairs program (CH and CM) and the 'Funding Biotechnology Partnerships' program from the Stem Cell Network. RT and CH are members of the Quebec Network for Cell, Tissue and Gene Therapy – ThéCell (a thematic network supported by the Fonds de recherche du Québec–Santé), of the Québec Center for Advanced Materials (CQMF), of PROTEO (The Quebec *Network* for Research on Protein Function, Engineering, and Applications), of the Cardiometabolic Health, Diabetes and Obesity Research Network (CMDO), and of the Montreal Diabetes Research Center (MDRC).

Chapter 5

The developing pancreas undergoes complex morphological changes during primary and secondary transition, which are correlated with key cell fate decisions. In Chapter 3, I discovered that confinement of posterior foregut (PF, Stage 3) cells in circular micropatterns mechanically primed cytoskeletal rearrangement, which increased nuclear PDX1 levels. Finite element models predicted that microtissues confined in circular micropatterns are subjected to gradients of stress due to non-uniform cell contraction (Ma et al., 2019; McBeath et al., 2004). This suggested to me that biomechanical stimuli can guide pancreatic lineage decisions, but this finding was convoluted with other effects such as cell density and soluble signalling gradients. To address these limitations, I aimed to specifically test the effect of biomechanical stresses on pancreatic differentiation by 1) creating more complex micropatterned geometries, using the SuBScribing technique described in Chapter 4, to keep paracrine signalling gradients constant while varying the effect of curvature; and 2) applying an active biomechanical stress in the form of stretching onto a cell monolayer. To accomplish this, I first predicted the forces present during pancreas morphogenesis due to shape changes using a finite element modelling approach. I then leveraged this knowledge to apply physiological stress gradients during directed differentiation protocols using a microfabricated device capable of applying timed, equibiaxial strain to a monolayer of PSC-derived PF cells while maintaining constant cell density.

5.1 Biomechanical forces enhance PDX1 expression during pancreatic differentiation of pluripotent stem cells

Raymond Tran[1], Yanqing Liu[1], Adele Khavari[2], Allen J. Ehrlicher[2], Corinne A. Hoesli[1,3]*, Christopher Moraes[1,2,4]*

[1] Department of Chemical Engineering, McGill University, Montreal, QC, Canada

[2] Department of Bioengineering, McGill University, Montreal, QC, Canada

[3] Department of Biomedical Engineering, McGill University, Montreal, QC, Canada

[4] Goodman Cancer Research Center, McGill University, Montreal, QC, Canada

[5] Department of Experimental Medicine, McGill University, Montreal, QC, Canada

* indicates co-corresponding authors

chris.moraes@mcgill.ca; corinne.hoesli@mcgill.ca;

5.2 Abstract

Tissue geometries which arise during organogenesis impart biomechanical forces onto the developing cells. In the pancreas, we hypothesized that the forces which arise in developmental tissue geometry regulate differentiation towards endocrine lineage by mechanically activating cells through the mechanosensitive YAP/Hippo signaling pathway. Finite element models were generated to recreate these developmental geometries and demonstrate areas of high stress are found at concave regions of protruding, proliferative structures. During *in vitro* directed differentiation protocols, PDX1^{high} cells spontaneously appear in cell-dense clusters. These PDX1^{high} clusters were more contractile based on traction force microscopy and displayed low YAP expression. Pancreatic endoderm cells cultured on adhesive micropatterns showed increased PDX1 expression in curved, mechanically primed regions. External biomechanical stimuli from a dynamic, deformable silicone substrate also increased local PDX1 expression. Altogether, these results suggest that biomechanical force sensing mechanisms can be leveraged to increase nuclear levels of key pancreatic transcription factors such as PDX1.

5.3 Introduction

During early embryogenesis, mechanical forces play a critical role in instructing cell differentiation (Herrera-Perez & Kasza, 2019). In particular, the pancreas undergoes multiple morphological changes during tissue growth which impart time-dependent biomechanical stimuli onto the developing cells. Much of the current art focuses on manipulating biochemical signalling pathways involved in pancreatic development, which have to date produced several directed differentiation protocols to generate insulin-producing beta cells from pluripotent stem cells (PSCs) (H. Liu et al., 2021; Millman et al., 2016; Nair et al., 2019; Pagliuca et al., 2014; Rezania et al., 2014; Russ et al., 2015). However, the cost and relatively low efficiency of current directed protocols severely limit the accessibility of potential treatment. Insulin-producing cells approaching the functionality of human islets can be generated without aggregation by precisely timed cytoskeletal depolymerization during endocrine induction (Hogrebe et al., 2020). The cytoskeleton is heavily involved in biomechanical sensing, suggesting a role in the biomechanics of the surrounding microenvironment (Fletcher & Mullins, 2010). Therefore, mechanically priming endocrine precursors with developmentally-relevant biomechanical forces could improve downstream beta cell commitment, reduce batch-to-batch variability, and potentially lead to novel innovations to generating insulin-secreting beta cells from direct differentiations protocols for type 1 diabetes treatment.

Tissue-scale forces transduce through the extracellular matrix (ECM) and impart biomechanical stresses onto developing cells, causing cell-scale specification and patterning (Vijayraghavan & Davidson, 2017). Mechanical forces are translated into biochemical signals in a process called mechanotransduction, which can control cell responses through the Hippo pathway via YAP/TAZ regulation (Dasgupta & McCollum, 2019; Heng et al., 2020). YAP acts as a core mechanotransducer which will translocate into the nucleus upon activation, in response to external mechanical force transduced from cell focal adhesions (Lachowski et al., 2018) or cadherins (Huveneers & de Rooij, 2013; Zaidel-Bar, 2013). Several studies suggest that pancreatic differentiation of PSCs is controlled by cytoskeletal tension and extracellular matrix interactions (Hogrebe et al., 2020; Mamidi et al., 2018b), further suggesting that biomechanical stimuli may play a role in endocrine specification.

Pancreatic duodenal homeobox 1 (PDX1) is a key player in pancreatic specification and is necessary for beta cell maturation, maintenance, survival, and function (Babu et al., 2007;

Fujimoto & Polonsky, 2009; Spaeth et al., 2017, p. 1). The co-expression of PDX1 with other transcription factors such as NKX6.1 (J. K. Pedersen et al., 2005; Russ et al., 2015; Schaffer et al., 2013, p. 1; Taylor et al., 2013b) and NGN3 (Burlison et al., 2008; Johansson et al., 2007; Xu et al., 2013; Y. Zhu et al., 2017) is important for differentiation downstream to insulin-secreting beta cells. During secondary transition, high levels of PDX1 expression, denoted as $PDX1^{high}$, have been correlated with downstream beta cell differentiation (L.-C. Li et al., 2018; H. Wang et al., 2001; Willmann et al., 2016). Overexpression of PDX1 in the differentiation of pluripotent stem cells *in vitro* promotes downstream differentiation towards insulin-expressing beta cells (Kubo et al., 2011; Lavon et al., 2006). Endocrine differentiation of pancreatic progenitors is correlated with increased PDX1 expression and the loss of YAP *in vivo* (George et al., 2012; Mamidi et al., 2018b).

We propose that presenting biomechanical stimuli to differentiating PSC-derived posterior foregut cells can promote endocrine differentiation downstream. In mesenchymal stem/stromal cells, the transfer of mechanical strain to the cytoskeleton regulates YAP (Driscoll et al., 2015) which controls focal adhesion assembly (Nardone et al., 2017), and downstream lineage specification (Heng et al., 2020; Kearney et al., 2010; Killaars et al., 2020; Kurpinski et al., 2006; McMahon et al., 2008; Oliver-De La Cruz et al., 2019). Mechanical stimuli plays a role in regulating lineage decisions in the early fate decisions of PSCs (Xue et al., 2018) which may suggest mechanical forces play a role later downstream in the differentiation process (Gwak et al., 2008; Mihic et al., 2014; Ravichandran et al., 2017). Recent evidence suggests the cell niche is responsible for downstream acinar and endocrine lineage specification in tip-trunk patterning as opposed to being predisposed to their final fate (Nyeng et al., 2019), suggesting a role of surrounding mechanics. In this work, we modelled pancreatic morphogenesis and demonstrate that changes in geometry produce areas of tension, which may affect differentiation downstream. We also confirm that the differentiation of $PDX1^{high}$ cells is correlated with low levels of nuclear YAP, as well as increased cell-generated contractile forces, suggesting a role of mechanical stimuli on pancreatic endocrine differentiation. Finally, we demonstrate that externally applying mechanical strain, in tandem with biochemical-focused directed differentiation protocols can promote the differentiation into $PDX1^{high}$ cells which may lead to enhanced endocrine differentiation downstream.

5.4 Results

5.4.1. Pancreatic budding and branching is dependent on geometry, proliferation, and stiffness

During pancreas development, various morphological changes occur during primary and secondary transition, which both involve the formation of bud and branched structures (Figure 5-1A). The formation of these curved geometries produces mechanical stress within the developing tissue. To understand the stress profiles that arise within the developing pancreatic epithelia, we created a general model, simulating tissue outgrowth from a tube, *in silico* using finite element modeling (FEM). During development, the pancreatic branches (with diameters varying between 50 – 150 µm (Villasenor et al., 2010)) develop from the initial pancreatic bud (starting ~100 µm diameter (Jennings et al., 2013; Piper et al., 2004)), and eventually give rise to the complex branched ductal structure of the pancreas. In our general model, we varied the diameters of the parent pancreatic duct to be 2.5 – 10 times larger than the developing branch and assumed that the formation of a pancreatic branch was due to regions of differential growth, which could arise *in vivo* due to cell stratification (Villasenor et al., 2010). Differential rates of tissue growth likely occur during pancreatic development due to changes in cell shape and tissue remodelling (Pan & Wright, 2011), or proliferation differences between different cell types (Chiang & Melton, 2003; Horb & Slack, 2004), also seen during differentiation protocols *in vitro* (Figure S5-1). Finite element models were therefore developed to capture cell growth and simulate circular areas of increased tissue growth in a tube.

Recreating the cylindrical, tube-like geometry was sufficient to recreate morphogenesis resembling the beginning morphogenesis of a pancreatic branch (Figure 5-1Bi, Ci). Conversely, models built using a flat disc geometry resulted in tissue thickening on both the simulated apical and basal surfaces (Figure S5-2). The ratio of tube curvature to the size of the proliferative zone was correlated to the relative displacement of the simulated branch, where a smaller curvature resulted in larger relative displacement (Figure 5-1Bi,ii). This suggests that the presence of curvature in the initial tube geometry dictates the direction and displacement during bud development compared to equal thickening of a cell sheet.

As the pancreas develops, architectural variations arise in cell organization, morphology, and matrix composition and these differences could result in perceived stiffness changes (A. J. Thompson et al., 2019; M. Zhu et al., 2020). We therefore performed a parametric sweep to test

the effect of stiffness gradients surrounding the proliferative zone. To simulate this, we varied the stiffness differences between the two simulated tissue zones. Increasing the surrounding tube stiffness resulted in greater bud deformation (Figure 5-1Ci,ii) and increased the magnitude of stresses around the growing region. From these experiments, we can recreate curvatures similar to those seen *in vivo* ($6.7 \times 10^{-3}\ \mu m^{-1} < \kappa < 2.0 \times 10^{-2}\ \mu m^{-1}$) (Villasenor et al., 2010), allowing us to infer the associated stress patterns that may be acting on developing pancreatic cells. In both our models, the development of a protruding bud resulted in high tensile forces at the edge of the area of increased tissue growth (Figure 1Biii,iv & 1Ciii,iv). This suggests that during pancreas development, mechanical forces are present and act upon growing tissues, which may play a role in differentiation.

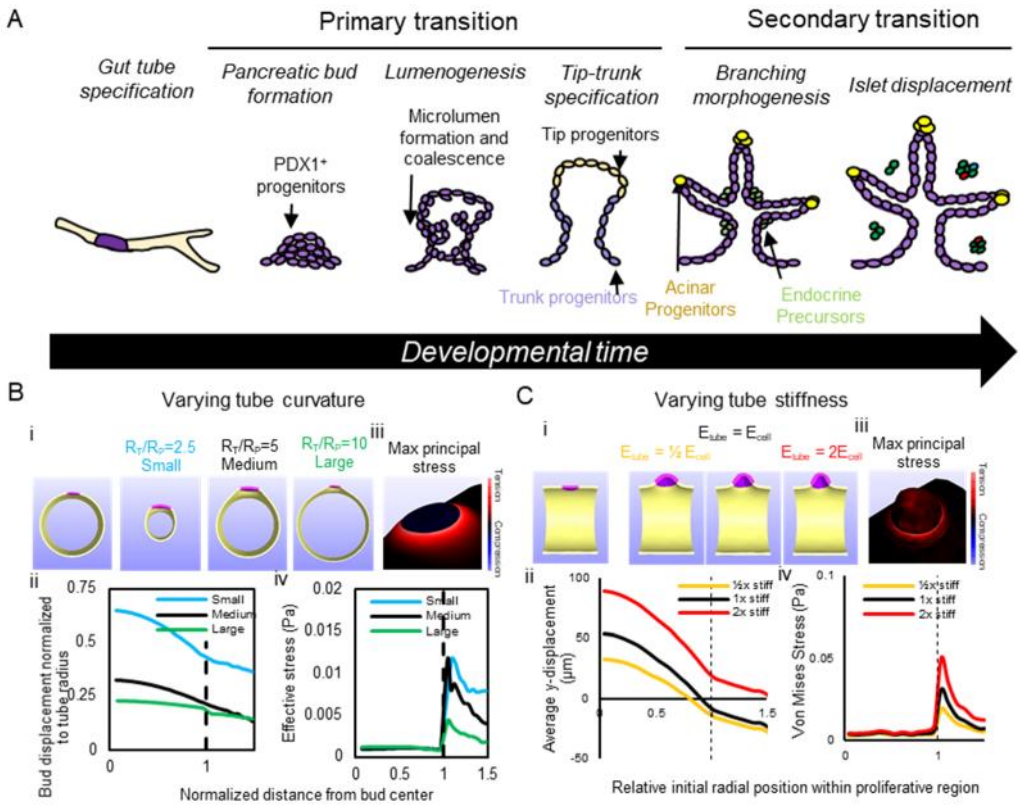

Figure 5-1*: Shape changes during development impart tensile forces at tissue boundaries. (A) Classical model of early pancreatic development and cell specification. (B) (i) Increasing the initial tube radius relative to the size of the proliferative region (ii) decreases the relative bud displacement and (iii,iv) generates tensile stresses surrounding the proliferative region. (C) (i) Increasing the surrounding tube stiffness (ii) increases the displacement of the proliferative bud and similar (iii,iv) tensile stresses are generated surrounding the proliferative region. Purple region of model represents areas with increased tissue growth. Yellow region represents surrounding epithelial tube.* R_T *represents the radius of the tube and* R_P *represents the radius of the circular proliferative zone.* E_{tube} *represents the Young's modulus of the tube and* E_{cell} *represents the Young's modulus of the proliferative zone.*

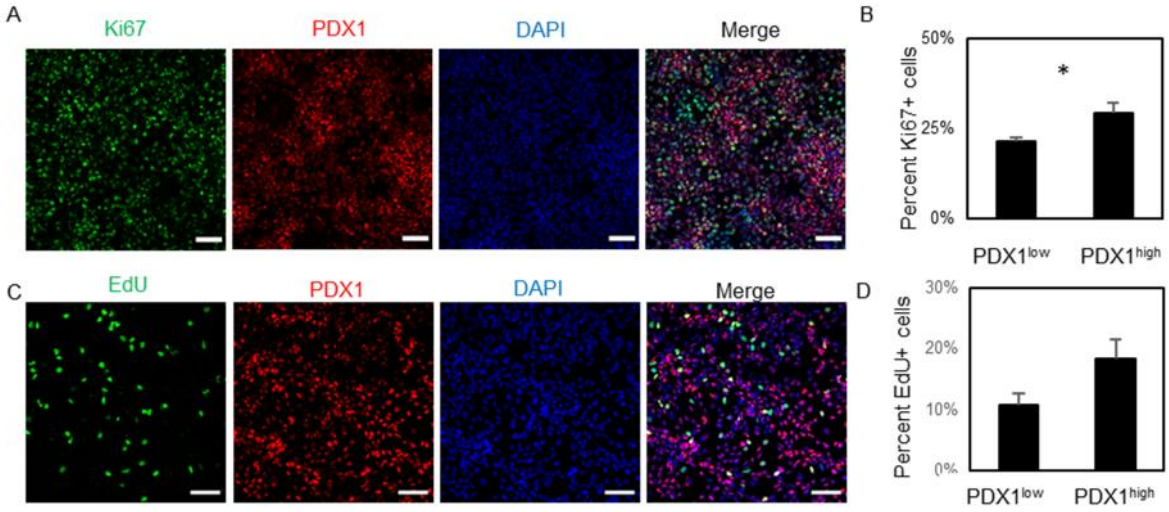

***Figure S5-1**: PDX1^{high}cells are more proliferative than PDX1^{low} cells during differentiation. (A) Cells are highly proliferative during differentiation and Ki67 expression is scattered throughout culture. (B) PDX1^{high} cells are more proliferative than PDX1^{low} cells. (N = 3 experimental replicates of different differentiations). Similar trends were seen between replicates. (C,D) EdU assay confirms proliferation differences at the end of stage 4. EdU was incubated for 3 hours before the end of differentiation where cells were then fixed, permeabilized, and immunostained. (N = 2 technical replicates) * represents p<0.05 for a two-sided Student's t-test. Scale bars: 100 µm.*

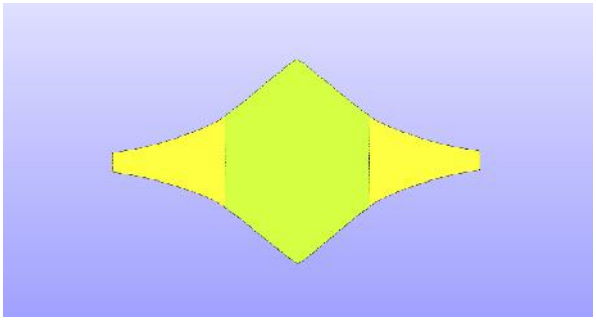

***Figure S5-2**: FEMs reveal that proliferative regions in a plane-geometry results in two-sided tissue growth. Green represents a tissue region with 2 times faster growth than yellow regions.*

5.4.2. *Directed pancreatic differentiation produces highly proliferative, PDX1$^+$/NKX6.1$^+$ clusters*

We produced PDX1$^+$ pancreatic endoderm (PE) cells from pluripotent stem cells (PSCs) using a previously established 10 day directed differentiation protocol (Figure 5-2A) (Rezania et al., 2014; Tran, Moraes, et al., 2020b). Large clusters of cells with high PDX1 expression (denoted as PDX1^{high} cells) were scattered randomly throughout the culture (Figure 5-2B). Further differentiation into endocrine precursor (EP) cells *in vitro* produced PDX1^{high} cells which also expressed the markers NKX6.1 and NGN3 (Figure 5-2C), suggesting the PDX1^{high} cells are primed towards beta cell lineage, as previously shown (Mamidi et al., 2018b; Ohlsson et al., 1993).

To determine if mechanical stimuli might influence pancreatic differentiation, we next looked at the mechanosensitive Hippo pathway which has previously been connected with mechanosensitivity (Tran, Moraes, et al., 2020b). In particular, we looked at the expression of YAP which is a key regulator of tissue growth (Piccolo et al., 2013) and has previously been shown to be deactivated through the course of endocrine differentiation (Rosado-Olivieri et al., 2019). PDX1^{low} pancreatic progenitors expressed higher amounts of active, nuclear YAP than PDX1^{high} cells (Figure 5-2D,E). The inhibition of YAP by the addition of verteporfin during Stage 4 of differentiation resulted in an increased amount of PDX1^{high} cells expressing cytosolic YAP, further confirming a previously shown role of YAP in pancreatic differentiation (Mamidi et al., 2018b; Rosado-Olivieri et al., 2019) (Figure S5-3A). Interestingly, the inhibition of YAP did not increase the incidence of PDX1^{high} cells in our cultures, suggesting changes in YAP occur downstream of changes in PDX1 expression (Figure S5-3B).

Force mechanotransduction occurs through the actin cytoskeleton. PDX1 expression levels correlated with increased staining intensity of E-cadherin, active vinculin, and beta-catenin (Figure S5-4), all of which bind to the cytoskeleton to transmit external forces, suggesting an increased ability of the PDX1^{high} cell population for mechanosensing (Zaidel-Bar, 2013) compared to cells with lower PDX1 levels. The influencing forces could arise in culture due to stochastic changes in cellular contractility, which is regulated by phosphorylation of myosin. Phosphorylation of myosin light chain 2 is correlated with myosin activity and thus cellular contraction. Previously, we observed PE cell clustering when confined to circular micropatterns, suggesting these cells have a contractile phenotype (Tran, Moraes, et al., 2020b). We saw that PDX1^{high} and the surrounding PDX1^{low} cells had increased staining intensity of phosphorylated myosin light chain 2 co-localized

with F-actin, suggesting increased contractile activity and cytoskeletal tension may be involved in generating these multicellular clusters (Figure 5-2F) (Fernandez-Gonzalez et al., 2009).

Reducing the cell-generated contractile activity during Stage 4 by the addition of Y-26732 or blebbistatin (Z. Liu et al., 2010), which inhibits ROCK and myosin II ATPase respectively, increased the fraction of $PDX1^{high}$ cells expressing cytosolic YAP, contrary to our initial hypothesis (Figure S5-5A). However, adding these factors also disrupts cytoskeletal tension which could in itself promote cytosolic YAP expression. This could imply that cell mechanosensing and cytoskeletal tension is required for increases in PDX1 expression and the formation of $PDX1^{high}$ cells (Figure S5-5B). Since YAP is regulated by cytoskeletal tension (Totaro et al., 2018), this may further suggest upstream mechanosensing by posterior foregut (PF) cells under high cytoskeletal tension is involved in downstream lineage specification.

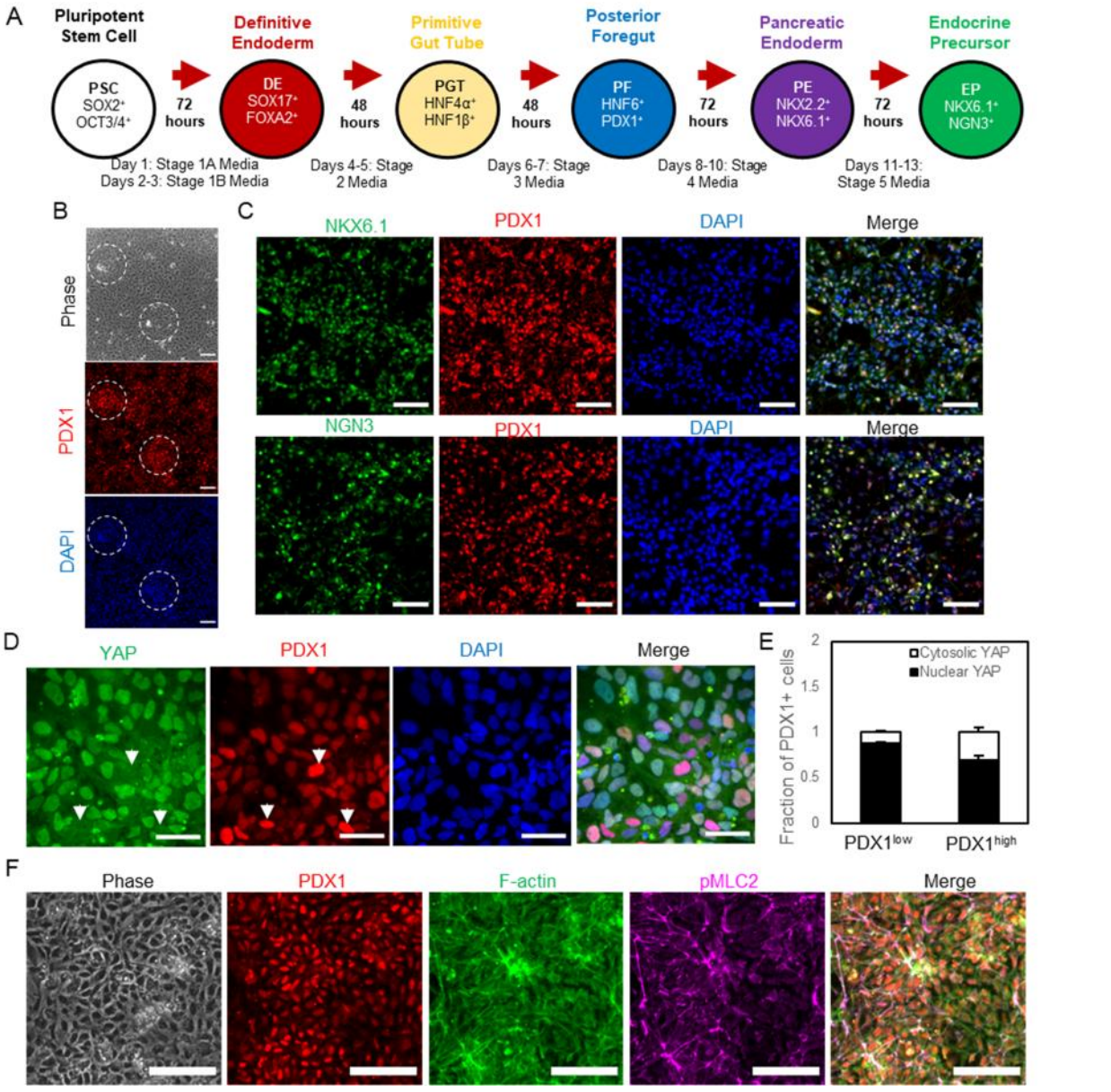

Figure 5-2: *Pancreatic differentiation is correlated with changes in YAP expression and cytoskeletal mechanics. (A) Directed differentiation protocol scheme towards endocrine precursor (EP) cells (adapted from Rezania et al. 2014). (B) Clusters of cells expressing high levels of PDX1 (PDX1^{high}) are found sporadically throughout culture surface. (C) Upon further differentiation towards EP cells, high PDX1 expression was correlated with high expression of endocrine markers NKX6.1 and NGN3. (D) PDX1^{high} pancreatic endoderm (PE) cells are associated with cytosolic expression of YAP. White arrows indicate PDX1^{high} cells which express cytosolic YAP. (E) PDX1^{low} cells predominantly express nuclear YAP. (F) Expression of phospho-myosin light chain 2 (pMLC2) co-localized with areas of intense F-actin staining in PDX1^{high} cells, suggesting a contractile phenotype. Scale bar: (B,C,F) 100 µm, (D) 50 µm.*

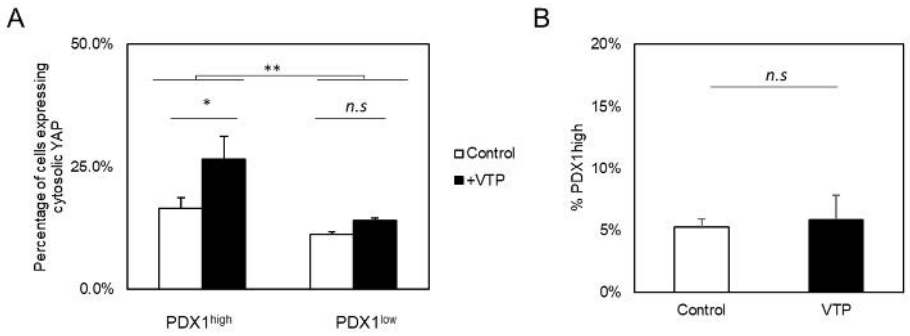

***Figure S5-3**: Addition of 0.3 µM verteporfin for 48 hours during Stage 4 of differentiation (A) increases fraction of PDX1^{high} cells expressing cytosolic YAP while (B) not significantly increasing fraction of PDX1^{high} cells. * represents p<0.05, ** represents p<0.01. N=1, n=10 images analyzed. Error bars represent standard error.*

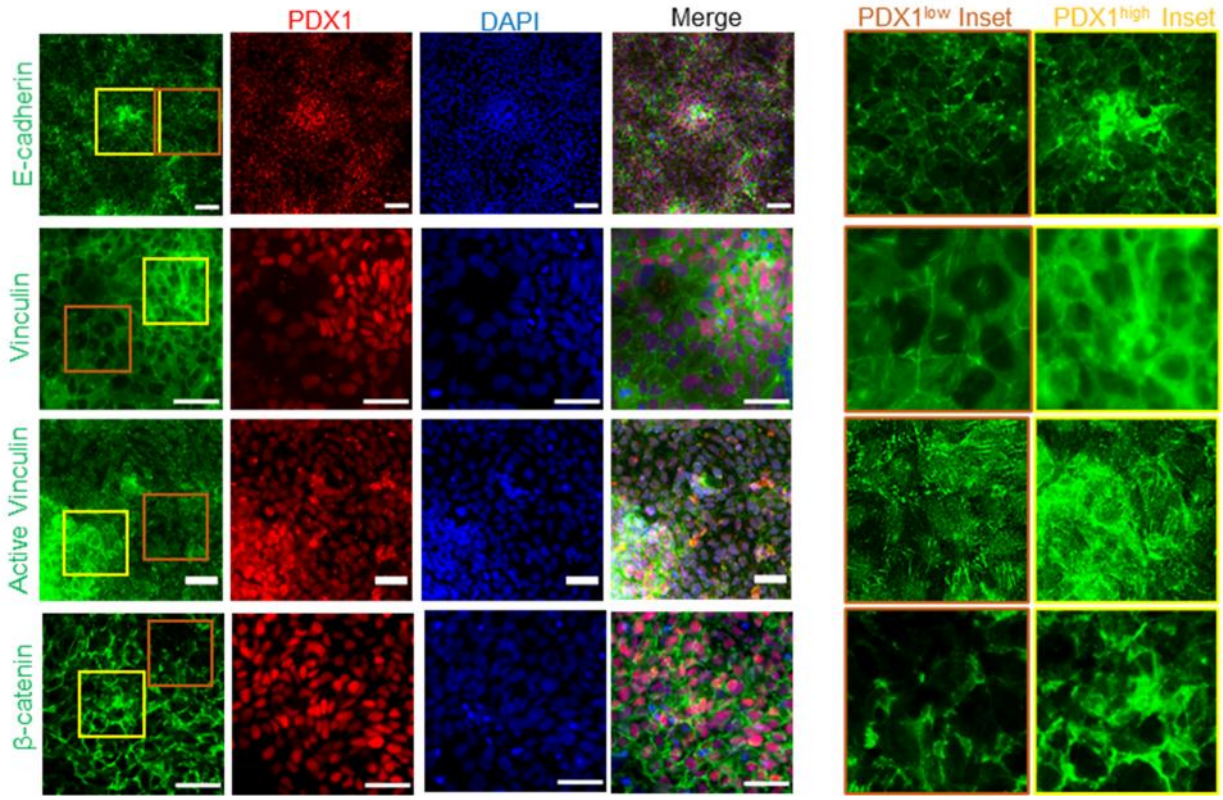

***Figure S5-4:** Increased expression of proteins responsible for tethering F-actin to external stimuli for mechanosensing in PDX1^{high} cells. Orange and yellow border insets represent high magnification views of PDX1^{low} and PDX1^{high} cells respectively. Scale bar: 100 µm.*

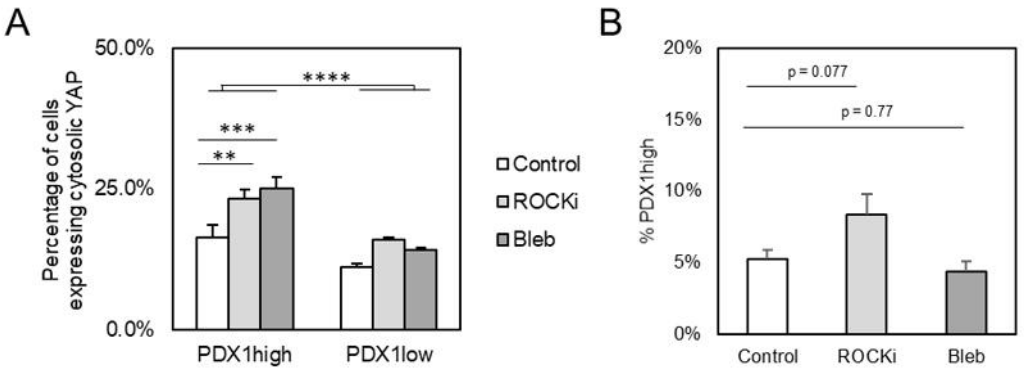

Figure S5-5*: The addition of cytoskeletal modulators for 48 hours during Stage 4 of differentiation (A) increases fraction of PDX1^{high} cells with cytosolic YAP expression while (B) the overall fraction of PDX1^{high} cells remains constant. ** represents p <0.01, *** represents p<0.005, and **** represents p<0.001.*

5.4.3. *Pancreatic clustering in vitro is correlated with formation of mechanical architecture and dynamic force generation*

To determine whether the surrounding cell-generated mechanical stimuli could be associated with generating PDX1^{high} clusters, we measured the nearby cell contractility present during the differentiation of PF cells to PE cells. Traction force microscopy was used to determine the average stresses involved during cluster formation. The differentiation into PDX1^{+} PE cells was efficient but the appearance of PDX1^{high} cells was spatially stochastic (Figure 5-3A). During secondary transition, endocrine cells originate from the trunks of the branched pancreas while exocrine cells are found at the tips (Nyeng et al., 2019; Sharon, Chawla, et al., 2019; Q. Zhou et al., 2007). The cells that generate endocrine and ductal cells are thought to be PDX1^{high} and PDX1^{low} cells respectively (Mamidi et al., 2018b; Piccand et al., 2014). To recreate this patterned differentiation, we co-cultured PDX1^{high} PE cells with less differentiated, PDX1^{low} PF cells in a 1:3 ratio respectively. This resulted in the formation of well-segregated PDX1^{high} clusters (Figure 5-3B) that were brightly stained for E-cadherin compared to the surrounding PDX1^{low} cells (Figure 5-3C). Nuclear YAP levels were low in PDX1^{high} cells (Figure S5-6) similar to previous observations with pure PE cultures (Figure 5-2D).

Traction stresses were calculated from the displacement fields of fluorescent tracking beads (Figure 5-3D) and then projected onto vectors towards the center of E-cadherin^{high}/PDX1^{high} clusters. Within PDX1^{high} clusters, traction stresses projected towards the center of the clusters were significantly higher than traction stresses towards the center of random surrounding areas (control) (Figure 5-3G). The contraction of PDX1^{high} cells suggests that a tensile stress is being applied to the surrounding PDX1^{low} cells, which may affect the differentiation of these cells downstream. Post-hoc analysis of cell migration within our cultures shows that surrounding cells migrate into these clusters (Figure S5-7, Supplementary Video 2), suggesting mechanical forces are exerted on the surrounding cells. This further suggests that endocrine differentiation *in vitro* is influenced by the presence of mechanical stimuli from neighbouring cells.

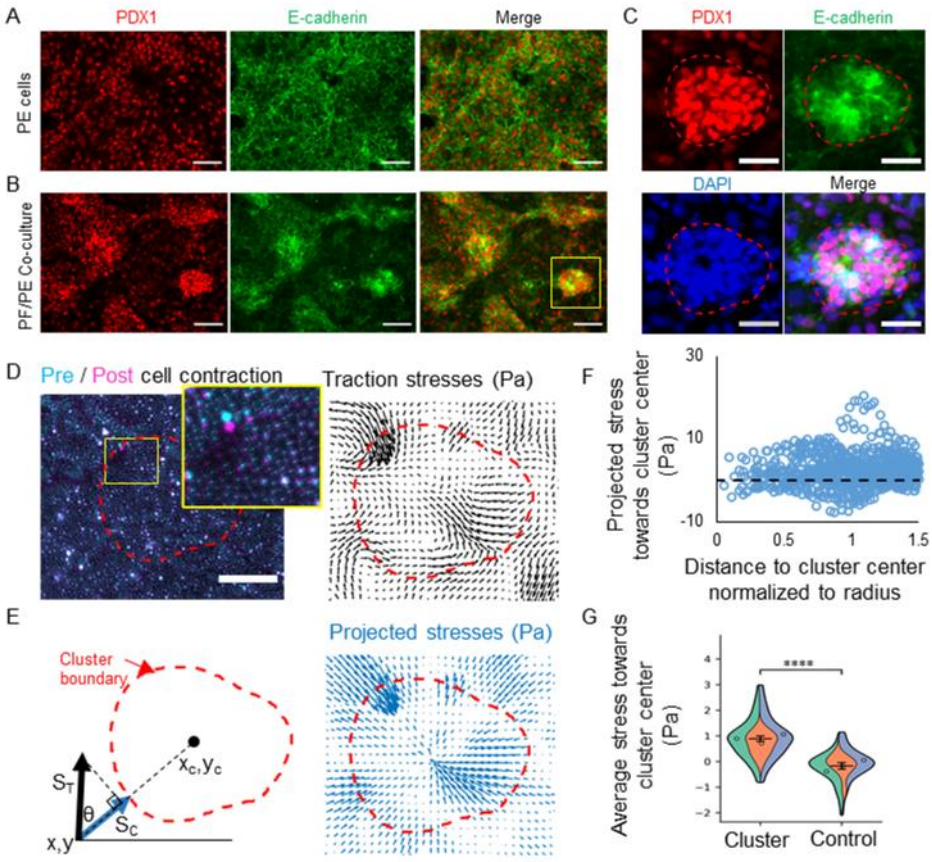

Figure 5-3: *Appearance of PDX1^{high} pancreatic clusters is correlated with compressive/contractile traction forces. (A) PE cells stochastically form PDX1^{high} cells throughout culture which cluster together to form 'islands' surrounded by PDX1^{low} cells. (B) Co-culture of S3 and S4 cells results in well-defined clusters of PDX1^{high} cells which displace fluorescent beads on substrate surfaces. Yellow box indicates magnified area shown in (C). Red dashed line represents the boundary of the PDX1^{high} cluster. (D) Traction stresses within cell cluster (identified in (C)) are calculated from displacement of fluorescent tracking beads. (E) Traction stresses are projected towards the center of each cluster to measure contractility of the cluster. (F) Traction stresses are positive on average, and peak near the cluster boundary. (G) Average traction stresses toward cluster centers are significantly greater than random regions in the surrounding areas (control). N = 3 experimental replicates. Each point represents the average stress for that replicate. Scale bars: (A,B) 100 µm, (C,D) 50 µm. ****, represents p<0.001 for an unpaired t-test.*

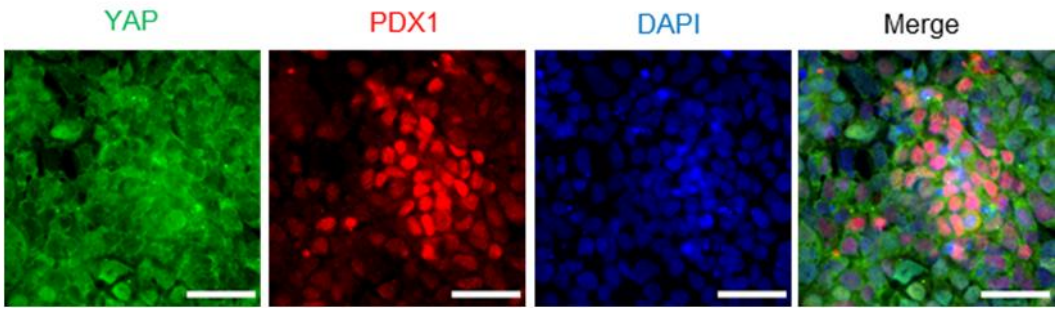

Figure S5-6: *PDX1^{high} clusters in PF/PE co-culture model expressed cytosolic YAP.*

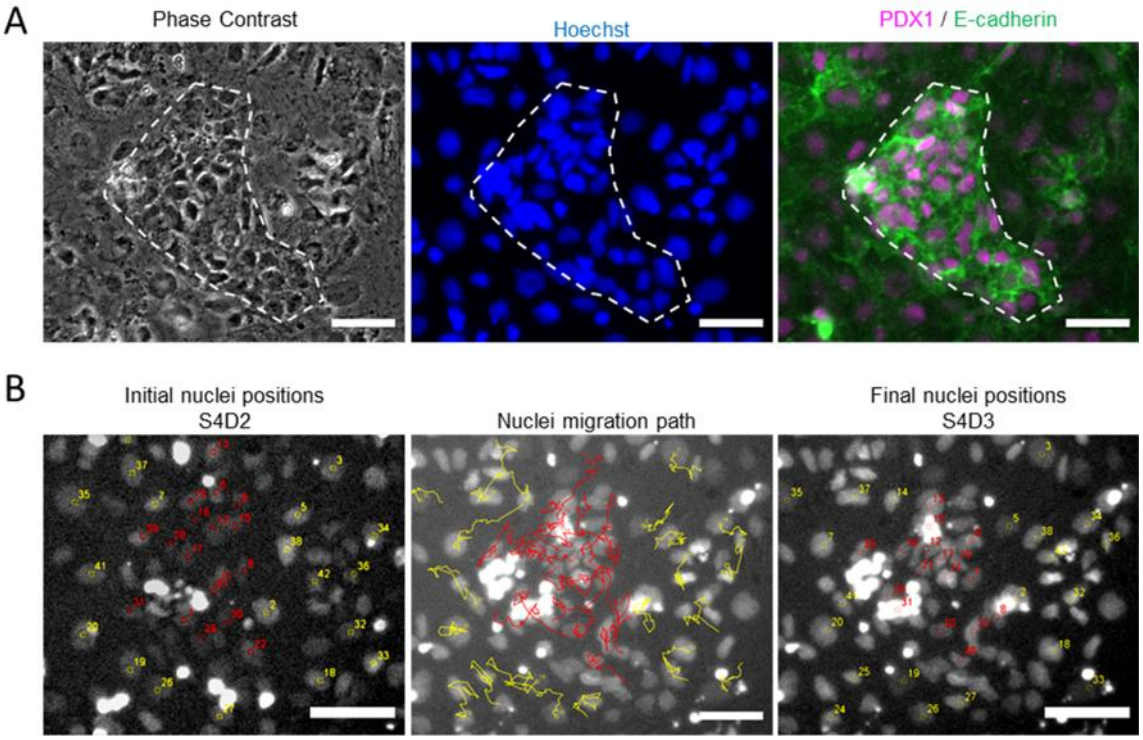

Figure S5-7: *Cells migrate into the eventual PDX1^{high} clusters. (A) Immunostaining of S3/S4 co-culture shows PDX1^{high} clusters are demarcated by high expression of E-cadherin. (B) Live nuclei tracking with live Hoechst shows that cells contract and migrate together to form a cluster. Red tracks indicate a cell with a final position within the PDX1^{high} cluster. Yellow tracks indicate a cell with a final position outside the cluster. Scale bars: 50μm*

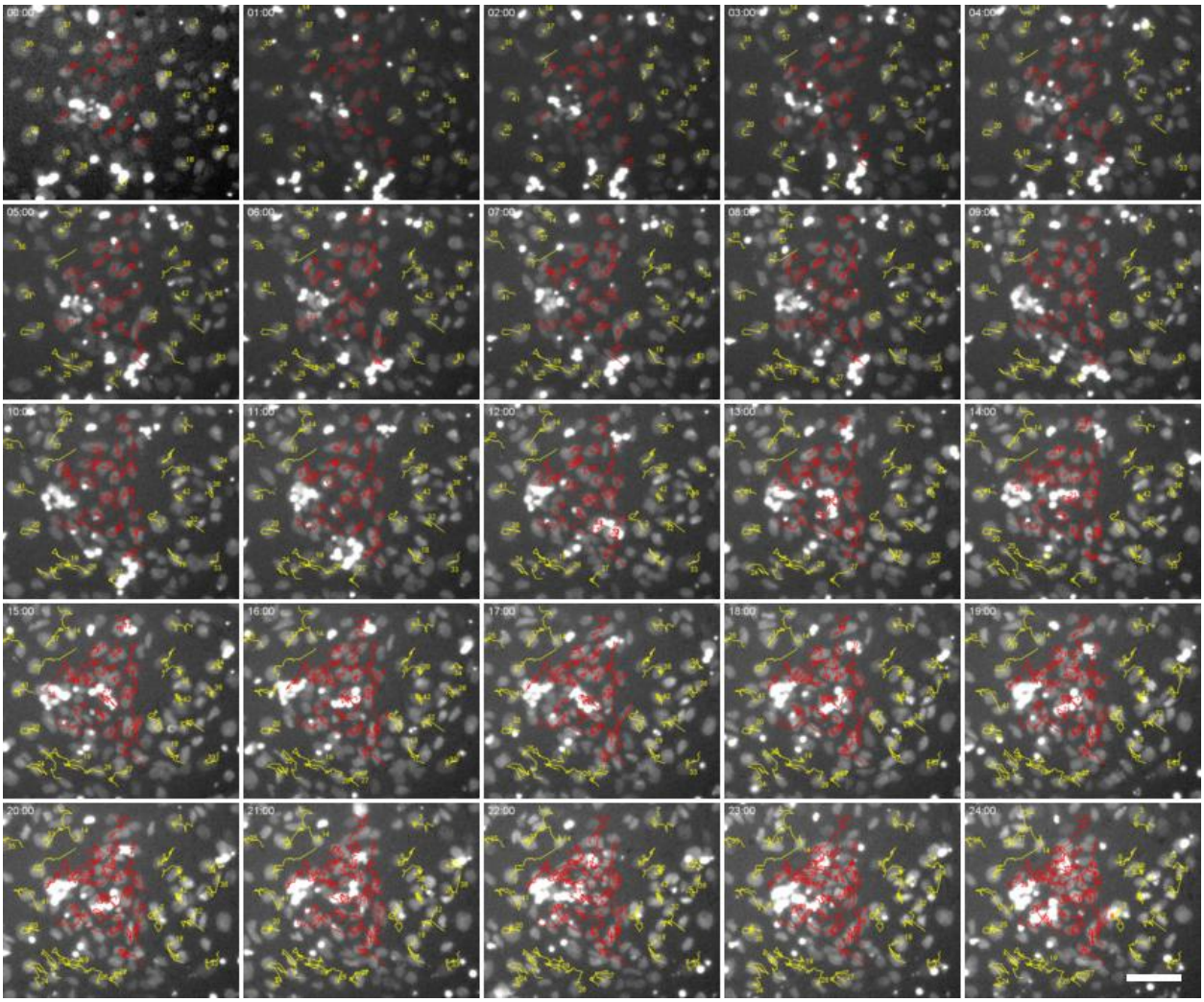

Supplementary Video 2*: Tracking of Hoecsht-labelled nuclei shows that PDX1^{high} cells (identified in Figure S5-7) cluster together while PDX1^{low} cells do not undergo large migration. Red tracks indicate a cell with a final position within the PDX1^{high} cluster. Yellow tracks indicate a cell with a final position outside the cluster. Each frame, starting from the top left, represents 1 hour starting where time 0 is Stage 4 day 2. Scale bars: 50µm*

5.4.4. *Biomimicry of force profiles is correlated with enhanced PDX1 expression*

Given the uncovered correlation between cell clustering, traction forces and PDX1 expression, we reasoned that confining cells within a curved geometry which mimicked that of a developing pancreatic branch could improve pancreatic differentiation. Since we observed a highly contractile phenotype associated with PDX1^{high} cells in PF/PE co-cultures, applying local stress gradients during PE differentiation may lead to related patterns in PDX1 expression. Previously, we had demonstrated that PE cells confined within circular micropatterns displayed increased PDX1 and NKX6.1 expression, while inhibition of actin remodelling with ROCK inhibitor abrogated the effects of confinement (Tran, Moraes, et al., 2020b). However, those experiments did not capture the changing transverse stresses along the pancreatic branch structure and are confounded with paracrine signalling gradients within the micropatterns (Tewary et al., 2017).

To this end, we generated S-curve micropatterns to mimic the sagittal cross-section of a developing pancreatic branch using our previously demonstrated xurography technique (Figure 5-4A) (Tran, Hoesli, et al., 2020). These patterns enabled us to simulate stresses in the transverse plane and keep consistent local cell density across the length of the pattern allowing consistent paracrine signalling. FEM simulations predict the micropattern edges to be under tensile stress due to confined cell contractility (Figure 5-4B).

PE cells confined within these S-curves contracted non-uniformly, creating local concentrations of F-actin filaments in concave regions of micropatterns, suggesting increased cellular tension, which matched the trends predicted in our FEM simulations (Figure 5-4C). To determine if the tension caused by micropattern curvature can guide the formation of PDX1^{high} cells, we segmented our curve into the straight portion and curved portions (Figure 5-4E). Within the curved sections, the normalized PDX1 expression was higher than in the straight areas, which may suggest a higher incidence of PDX1^{high} cells with similar cell density.

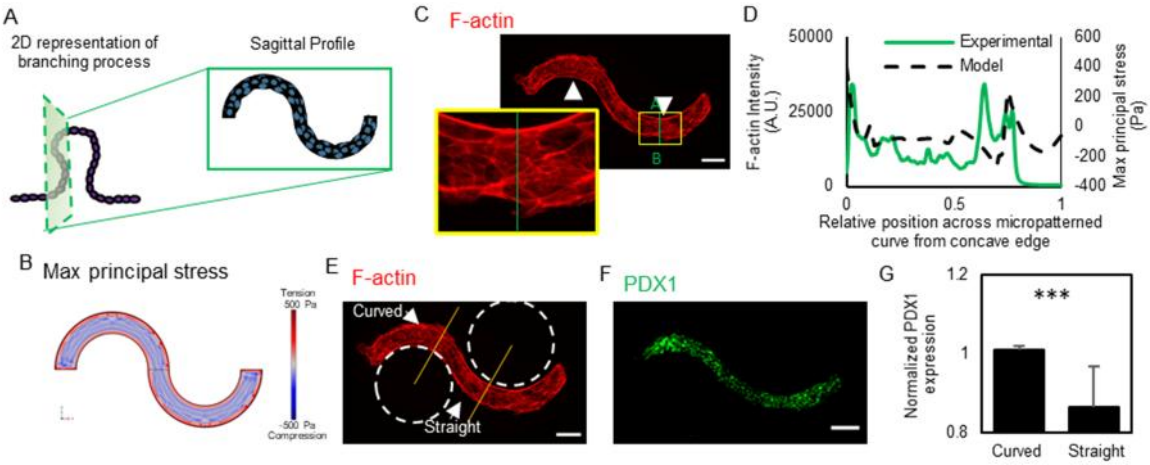

Figure 5-4: *Confined, micropatterned culture of PE cells produces cell-generated stress gradients within culture. (A) Proposed sagittal section of a developing pancreatic branch. Green box represents the section mimicked by the micropattern. (B) Tensile stresses are predicted along edges of the micropattern. (C) F-actin is highly concentrated in concave regions of the S-curve. (D) Increases in F-actin intensity correlate with max principal stress predicted in FEM. (E) Sectioning of cells cultured within S-curve patterns. Dashed white line represents curved perimeter of micropattern segment. Yellow lines segment the "curved" regions from the "straight" center region. (F) PDX1^{high} cells cluster within curved micropatterns. PDX1 expression normalized to average expression within micropattern is higher in curved regions compared to the straight region. (N=1, n=14 micropatterns analyzed) Error bars represent standard deviation. PDX1 expression was normalized to the average PDX1 expression of all cells within each image. *** represents $p<0.005$ for an unpaired t-test. Scale bars: 100 µm.*

5.4.5. *Dynamic application of external force differentially guides pancreatic and beta cell differentiation*

To specifically test the effect of external mechanics on pancreatic differentiation, we constructed a pressure-actuated, deformable membrane using polydimethylsiloxane (PDMS) which allowed us to strain cells in a geometry which mimicked that seen during pancreatic branching (Figure 5-5A). The externally applied stresses acting upon the PF (Stage 3) cell layer were predicted by FEM. When operating with positive pressures, cells at the center of the strained area was subject to tensional forces (red) while compressive forces (blue) were dominant at the edge of the interface. When a vacuum was applied, these stress profiles reversed (Figure 5-5B,C).

Three subsections within images were classified based on the differing stress profiles observed and denoted as: the strained area, the interface, and the outer area (Figure 5-5D). In this analysis, the boundaries of these regions were determined with phase contrast images, which show clear demarcation of the edge of the strained region (Figure 5-5E). A confluent layer of PF cells was seeded on day 7 of the differentiation protocol, allowed 24 hours to adhere, and then strained for 48 hours. At the end of our experiments, we didn't observe any ordered spatial patterning of PDX1 in the strained regions. When a tensile load was applied to PE cells, the average normalized PDX1 expression (Figure 5-5F) was significantly increased compared to unactuated regions and separate unactuated samples. Conversely, when a compressive load was applied, the average normalized PDX1 expression was decreased (Figure 5-5G). These changes in normalized, regional PDX1 expression could be due to changing numbers of $PDX1^{high}$ cells, suggesting that culture in the presence of external forces could help specify endocrine differentiation.

We next asked if this mechanical activity was regulating the Hippo signalling pathway by activating YAP expression. An increased percentage of PE cells located within the strained regions contained cytosolic YAP (Figure 5-5H), which was previously associated with $PDX1^{high}$ cells and increased endocrine differentiation. Since our control samples had a larger fraction of cells expressing nuclear YAP, this suggests mechanical strain caused phenotypic changes which resulted in endocrine-primed differentiation and thus deactivation of YAP. Overall, this suggests that mechanical priming with biomechanical stress plays a role in regulating PDX1 expression.

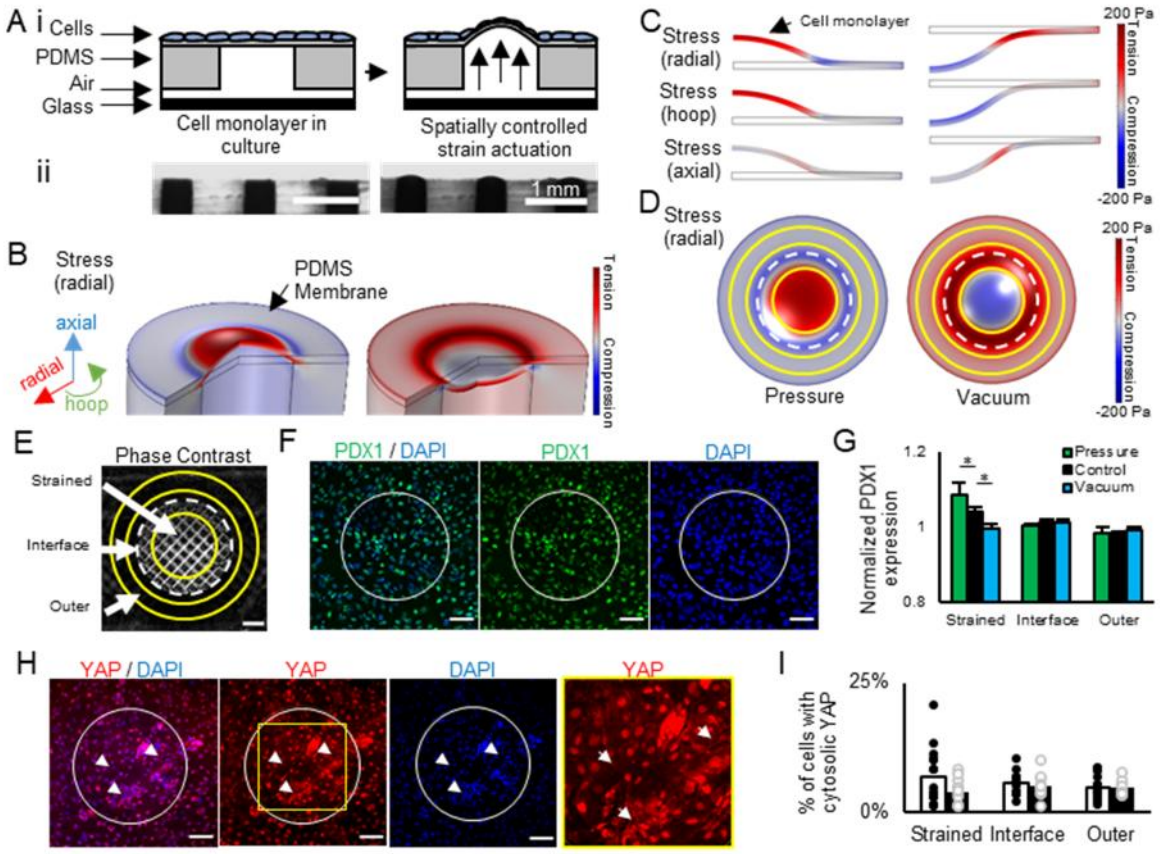

Figure 5-5*: Externally applied stress applied to PF cells during PE (Stage 4) differentiation alters spatial differentiation profile. (A,i) Schematic of pressure-actuated strain device to apply stress onto cultured cells. (ii) Profile view of membrane during actuated straining. (B) Finite element models predict tensile stress in the strained area of the PDMS membrane when a positive pressure is applied and slight compressive stress when a negative pressure is applied. (C) Stress profiles in cylindrical coordinates show mainly radial and hoop (circumferential) stresses act on cells with relatively low amounts of axial stress. (D)Three regions were created based on overall stress profile within strained area. (E) Phase contrast images were used to identify the strained area and segmented based on (D). (F) PDX1 expression was sporadic on our actuated culture surface. (G) PDX1 expression normalized to expression throughout image is increased when exposed to tensile stress and decreased when exposed to compressive stresses. N= 3 (pressure or vacuum) or 6 (control) experimental replicates, with n>10 membrane regions analyzed per replicate, error bars represent S.E.M. PDX1 expression levels were determined by taking the average fluorescence intensity in the green channel in nuclear regions defined through DAPI staining. The normalized PDX1 expression was taken as the value for a given cell or cells in a region of interest, divided by all cells within each image. (H,I) A larger proportion of PE cells cultured within the strained area express cytosolic YAP. Yellow box represents magnified image shown. White arrows indicate example cells expressing cytosolic YAP. Each point represents the percent of cells with nuclear-cytosolic ratio <1.0 in the region of interest (N=1, n>10 regions analyzed). Scale bar: (A)1 mm, (E,F,H) 100 μm.*

5.5 Discussion

This work demonstrated that biomechanical stimuli, applied to posterior foregut (PF) cells during Stage 4 of pancreatic differentiation, increased PDX1 expression of the resultant pancreatic endoderm (PE) cells and this was correlated with downstream endocrine commitment. To recreate the tissue patterning observed *in vivo*, we developed a PF/PE co-culture system where we observed consistent formation of PDX1^{high} PE clusters, which generate high contractile stresses as seen with traction force microscopy. A marked decrease in nuclear YAP levels was observed in PDX1^{high} cells, pointing towards of role of the mechanosensing YAP pathway in PE differentiation. After trunk specification *in vivo*, high PDX1 expression becomes restricted to endocrine-fated trunk cells while PDX1 levels are diminished in nearby exocrine and ductal-fated cells (Dassaye et al., 2016; Mamidi et al., 2018b). We showed that PDX1^{high} cells coordinate to cluster and generate traction forces *in vitro* which may prompt surrounding cells to specify tip or trunk lineage. Inspired by the bud-like geometries observed during pancreatic development, we developed a pressure-actuated platform to provide equibiaxial strain onto cells, similar to previously described systems (Moraes et al., 2010; Xue et al., 2018). Together with observations of PDX1 patterning in S-shape adhesive micropatterns, our results suggested a close relationship between PDX1 expression levels and culture areas under higher tension.

We confirmed reports that the appearance of PDX1^{high} cells and downstream endocrine differentiation was correlated with cytosolic YAP expression (Mamidi et al., 2018b; Rosado-Olivieri et al., 2019), suggesting changes in cell phenotype involved the mechanosensitive Hippo signalling pathway (George et al., 2012; Y. Wu et al., 2021). YAP inactivation is dependent on cell shape and cytoskeletal tension (Wada et al., 2011) and focal adhesion assembly (Kuroda et al., 2017; Nardone et al., 2017) which is altered in confinement (J. Gao et al., 2017), high densities (Gumbiner & Kim, 2014; Hsiao et al., 2016), or during detachment from extracellular matrix (B. Zhao et al., 2012). Well spread cells, associated with high cytoskeletal tension, were correlated with low levels of PDX1 expression, nuclear YAP, and ductal specification (Mamidi et al., 2018b). In general, it is difficult to decouple YAP expression, differentiation-associated changes in cell phenotype, and changes in the cell microenvironment, which may together lead to islet delamination. In the future, live tracking of YAP translocation during pancreatic differentiation and the clustering process could help determine if cell differentiation leads to YAP inactivation or vice-versa.

In this work, we suggested that biomechanical stimuli acting on the force-sensing cytoskeleton at earlier stages in pancreatic differentiation could prime downstream endocrine differentiation. Specifically, we strained PF cells and found that the response was also dependent on the direction of strain which may play a part in how mechanosensing occurs, perhaps due to how the cytoskeletal structure adapts to strain. Mechanosensing of positive substrate strain promotes more robust cytoskeleton assembly (Panzetta et al., 2019), which may lead to downstream changes in cell phenotype. Mechanically-primed cells with a robust cytoskeleton and high tension could be more mechanosensitive. Due to the adaptable nature of the equibiaxial strain platform, it would be interesting to apply strain in different programmes (i.e. cyclically or incrementally) which could result in more distinct differentiation patterning (Xue et al., 2018) if stress dissipation plays a role in pancreatic differentiation. Overall, determining the optimal parameters to strain differentiating cells including magnitude, stage of differentiation, length of time, and strain programme could lead to more efficient, cost effective differentiation protocols in the future.

Throughout pancreatic differentiation, cells undergo changes in phenotype, such as during secondary transition, where EP cells undergo epithelial-mesenchymal transition (EMT), delaminate from the epithelium, and migrate through the surrounding mesenchyme to eventually form the islets of Langerhans (Sharon, Chawla, et al., 2019; Willmann et al., 2016). Changes in cell phenotype could alter mechano-sensitivity and response to biomechanics, in part due to changes in cell-cell E-cadherin contacts and cytoskeletal organization (D.-H. Kim et al., 2009; Park et al., 2019; Schneider et al., 2013). We observed that $PDX1^{high}$ cells in our culture had increased staining intensity of F-actin, E-cadherin, beta-catenin, vinculin, all of which are associated with mechanosensing (Bays & DeMali, 2017; Huveneers & de Rooij, 2013; le Duc et al., 2010) compared to $PDX1^{low}$ cells, suggesting different cell phenotypes with varying degrees of mechano-sensitivity arise during pancreatic development. Previously, $PDX1^{high}$ and $PDX1^{low}$ cells have been reported to be primed to endocrine or ductal lineages respectively (Mamidi et al., 2018b). Interestingly, we observed that $PDX1^{high}$ cells typically had high levels of vinculin at cell-cell interfaces, while substrate-bounded vinculin focal adhesions were found predominantly in $PDX1^{low}$ cells, which may suggest a switch from substrate-bound to intercellular force sensing (*Figure S5-4*). This is consistent with evidence suggesting secondary transition of endocrine precursors occurs as delamination of whole cell clusters (Sharon, Chawla, et al., 2019). During

differentiation, PDX1^{high} cells are potentially more mechanosensitive but it was unclear whether increased mechanosensitivity leads to PDX1^{high} cells or vice versa. Overall, these data suggests that changes in the mechanosensing machinery during pancreatic differentiation primes subsets of PE cells for endocrine specification.

Recent evidence suggests tip-trunk patterning is due to migration to the "tip" niche and that cells are not pre-disposed to acinar or endocrine lineage earlier in differentiation (Nyeng et al., 2019), further suggesting a role of the surrounding mechanical microenvironment. Although we did not observe significant cell-patterning when PF cells were strained, our results show that cell strain increases average PDX1 expression which may promote downstream endocrine differentiation. Other mechanical aspects of the surrounding cell microenvironment such as extracellular matrix or substrate stiffness could affect differentiation outcomes. PDX1^{high} cells seeded on fibronectin tended to adopt a more spread phenotype and downregulated endocrine differentiation while laminin promoted endocrine differentiation (Mamidi et al., 2018b). In our experiments, we mainly used fibronectin which may have decreased the clustering capability of our cells. Increased clustering could potentially be seen by using laminin or physiologically relevant mixtures like decellularized fetal pancreas extracellular matrix. In general, softer substrates reportedly promote cell architectures associated with improved pancreatic differentiation (Tran, Moraes, et al., 2020a). In our experiments, we cultured cells on tissue culture plastic, PDMS, and soft PDMS, which have large differences in substrate stiffness. Across the substrates, we observed no noticeable difference in cell morphology between soft and stiff substrates (comparing Figure 5-2 (tissue culture plastic), Figure 5-3 (Sylgard 527, soft), Figure 5-5 (Sylgard 184, stiff)) suggesting similar levels of cytoskeletal tension. Further optimization of the cell microenvironment and potential synergistic effects between biomechanical and biochemical signalling could be key to obtaining optimal, efficient differentiation protocols.

In our experiments, we introduced mechanical stimuli during the transition from PF cells to PE cells for 48 hours. Beyond that, the time frame in which mechanics plays a role in specifying pancreatic lineage is unclear. Others have found that adding cytoskeletal inhibitors (Hogrebe et al., 2020; Rosado-Olivieri et al., 2019; Toyoda et al., 2017) or biomechanical cues (Legøy et al., 2020; Maldonado et al., 2017; Rasmussen, Reynolds, et al., 2016b) have stage-specific results, suggesting that further stage-by-stage optimization is required. Previously, mechanics have been

shown to guide differentiation early in development (Galea et al., 2017; Keller et al., 2003; Poh et al., 2014) however this is relatively unstudied in pancreas development. Since different cell subsets may have varying degrees of mechano-sensitivity, applying biomechanics at earlier stages of differentiation where cells are mechanically primed may have more significant effects. Different methods of definitive endoderm induction via biochemical signalling have been shown to affect downstream differentiation outcomes (Jaramillo et al., 2014), which suggests that utilizing biomechanical signalling pathways earlier during differentiation could improve downstream beta cell maturation.

Overall, our evidence suggests that the geometry changes associated with pancreas morphogenesis may provide biomechanical cues, potentially influencing differentiation outcomes. This could result in more efficient protocols which do not rely as heavily on high concentrations of growth factors to activate specific signalling pathways. This knowledge may lead to the development of next generation directed differentiation protocols, which involve biochemical stimuli as well as mechanical stimuli.

5.6 Materials and Methods

5.6.1. Finite Element Modelling

Finite element modelling of the developing pancreatic bud/branch was performed using the FEBio software package (PreView, FEBio, and PostView) (Maas et al., 2012) with the cell growth model, which models growth by volume change due to osmotic effects (Ateshian et al., 2009; Maas et al., 2018). Briefly, tissue growth was modelled by increasing the number of membrane-impermeant intracellular solutes, cr, and the normalized volume of intracellular solid matrix, phir, to generate osmotic effects and tissue growth (Ateshian et al., 2012). The tube geometries and meshes used were created using GMsh, an open-source, 3D finite element mesh generator (Geuzaine & Remacle, 2009). The following material properties were used for our simulations (Table S5-1).

Finite element models were generated to predict the stresses acting upon cell monolayers in both micropatterned culture experiments and in the equibiaxial strain system using COMSOL 5.3. Stresses in our micropatterned culture model were generated as previously described (Ma et al., 2019). Briefly, a cell layer was simulated as a two-layer system consisting of a 20 µm thick active layer isotropic elastic modulus: 500 Pa; Poisson's ratio: 0.499; thermal conductivity: 10 W m^{-1} K^{-1}; coefficient of expansion: 0.05 K^{-1}) and a 4 µm passive layer (isotropic elastic modulus: 100 Pa; Poisson's ratio: 0.499). Cell contraction was simulated using thermal contraction where an isothermal 5 K temperature drop was applied to the active layer while a fixed displacement boundary condition was applied to the bottom surface of the passive layer. Max principal stress is reported and similar trends were observed with von Mises stress. The equibiaxial strain system was simulated with a 25 µm PDMS membrane (density = 965 kg/m^3, Young's modulus = 0.98 MPa, Poisson's Ratio = 0.495). A +/- 50000 Pa pressure boundary condition was applied to the inner surfaces of the device.

Table S5-1*: Simulation properties for FEBio simulations of branching morphogenesis*

Material property	
Density	1.00 kg/m^3
Young's modulus	0.019 Pa
Poisson's ratio	0.48
Cell growth model parameters	
cr (concentration of membrane-impermeant intracellular solutes)	210 mM
phir (normalized volume of intracellular solid matrix)	0.3
ce (osmolarity of extracellular environment)	300 mM

5.6.2. *Human pluripotent stem cell culture*

The pluripotent stem cell line used in this study was mainly the Episomal hiPSC line (Gibco, Cat # A18945) and was maintained as described previously (Tran, Moraes, et al., 2020b). Additional experiments were also performed with hESCs (WA01, WiCell) and the NKX6.1-GFP HES3 line (donated from the lab of Prof. C. Nostro and A.G. Elefanty). Briefly, hPSCs were cultured on Matrigel (Corning, Cat # 354277) coated plated with TeSR-E8 media (STEMCELL Technologies). For Matrigel coating, tissue culture 6-well plates were incubated with a Matrigel solution, diluted 1:25 in cold DMEM/F-12 medium (Gibco, 21331020) for 1-2 h at room temperature. Media changes were performed every 24 h. Cells were passaged (1:6 dilution) with 0.5 mM EDTA in phosphate buffered saline solution (PBS) (Life Technologies) at roughly 70% confluency.

5.6.3. *Pancreatic endoderm cell directed differentiation*

Prior to differentiation, cells were cultured in mTeSR medium (STEMCELL Technologies) for 1 passage. To initiate differentiation, the PSC cultures were dissociated with TrypLE Express (Life Technologies) and resuspended in mTeSR supplemented with 10 µM Y-26732 (ROCK inhibitor) (Sigma). The PSCs were plated at a density of 200,000 cells/cm^2 on Matrigel-coated plates. After 24 h, the adherent cells were rinsed with PBS and differentiation was initiated by the addition of differentiation medium. The differentiation medium was changed every 24 h according to the schedule shown in Table S3 which was based on a published protocol (Rezania et al., 2014). Between each stage of differentiation, cells were washed with PBS.

For our micropattern or equibiaxial strain experiments, frozen PF cells were thawed directly onto our culture systems. The differentiated PF cells were frozen at a concentration of 1 million cells/mL in S3 media supplemented with 10% DMSO and frozen in a CoolCell® freezing container (Corning) until -80^{o}C and then transferred to liquid nitrogen storage until required for experiments.

Table S5-2: *Detailed composition of differentiation medium used in each stage to produce PF cells.*

Days	Medium	Basal Medium	Soluble Factors
0-1	S1A	MCDB131 + 10mM glucose + 1.5 g/L $NaHCO_3$ + 0.5% fatty acid free bovine serum albumin (FAF-BSA) + 1x GlutaMAX + 1% Pen/Strep	+100 ng/mL Activin A +3 µM CHIR99021
1-3	S1B		+100 ng/mL Activin A
3-5	S2		+0.25 mM ascorbic acid +50 ng/mL keratinocyte growth factor (KGF)
5-7	S3	MCDB131 + 10mM glucose + 2.5 g/L $NaHCO_3$ + 2% FAF-BSA + 1x GlutaMAX + 1% Pen/Strep	+0.25 mM ascorbic acid + 1:200 insulin-transferrin-selenium-ethanolamine (ITS-X) +50 ng/mL KGF + 0.25 µM SANT-1 + 1 µM retinoic acid + 100 nM LDN193189 + 200 nM TPB (PKC activator)
7-10	S4		+0.25 mM ascorbic acid + 1:200 ITS-X +2 ng/mL KGF + 0.25 µM SANT-1 + 0.1 µM retinoic acid + 200 nM LDN193189 + 100 nM TPB
10-13	S5	MCDB131 + 20mM glucose + 1.5 g/L $NaHCO_3$ + 2% FAF-BSA + 1x GlutaMAX + 1% Pen/Strep	+ 1:200 ITS-X + 10 µM zinc sulfate + 10 µg/mL heparin + 0.25 µM SANT-1 + 1 µM T3 + 10 µM ALK5 inhibitor II + 0.05 µM retinoic acid + 100 nM LDN193189

5.6.4. *Immunocytochemistry and image collection*

Cell samples were stained and fixed as described previously (Tran, Moraes, et al., 2020b). Cells were fixed in 4% paraformaldehyde for 20 min, washed with PBS three times, permeabilized with 0.1% Triton-X100 solution for 20 min then washed with PBS three times. Non-specific protein adsorption was blocked by applying DAKO Protein Block Solution (Agilent) for 1 h at room temperature. After washing with PBS, the primary antibodies were incubated at 4 ^{o}C overnight, washed three times with PBS and then incubated with the corresponding secondary antibodies for 1 h at room temperature, and washed three times with PBS. Finally, samples were incubated with DAPI counterstain diluted in PBS for 20 min at room temperature and washed three times with PBS. The antibodies and dilutions used are list in Table S5-3.

5.6.5. *Traction force microscopy*

Traction force microscopy was performed by tracking the movement of custom synthesis fluorescent beads (gift from the lab of Allen Ehrlicher) dispersed on the surface of soft silicone, polydimethylsiloxane (PDMS) gels (Sylgard 527, mixed in a 1:1 ratio) similar to that previously described (Yoshie et al., 2018). Briefly, an initial layer of freshly mixed Sylgard 527 was spin-coated onto an 18 mm glass coverslip (1. 200 rpm 1min, acceleration 50rpm/s; 2. 300 rpm for 1 min, acceleration 200 rpm/s; 3. deceleration to stop 50 rpm/s) to form a roughly 100 µm thick layer and then incubated at 40 ^{o}C overnight to cure.

The next day, the fluorescent tracking beads were placed in a sonicator for 5 minutes, dispersed into a fresh Sylgard 527 mixture to make a ~10% w/w solution of fluorescent tracking beads, and spincoated onto the previous ~100 µm thick layer of Sylgard 527 (1. 500 rpm for 1 minute, acceleration 100rpm/s; 2. 5000 rpm for 20 sec, acceleration 200 rpm/s; 3. Deceleration to stop at 100 rpm/s). These gels were cured overnight at 40 ^{o}C on a level surface, then adhered onto the bottom of a 12-well plate using a 10:1 ratio of Sylgard 184, then cured overnight at 70 ^{o}C. The gels were then placed in a UV chamber for at least 2 hours and then coated with a 25 ug/mL solution of fibronectin for 2 hours at 37 ^{o}C.

***Table S5-3**: Antibodies and reagents used for immunocytochemistry*

Antibody	**Supplier**	**Catalog #**	**Dilution**
Mouse anti-human mAb PDX1	BD Pharmigen	562160	1:200
Rabbit anti-human mAb PDX1	Abcam	ab219207	1:200
Rabbit anti-human pAb NKX6.1	Novus Biologicals	NBP149672	1:200
Mouse anti-human mAb NKX6.1	DSHB	F55A12	1:50
Rabbit anti-human mAb E-cadherin	Abcam	ab40772	1:500
Rabbit anti-beta catenin mAb	Cell Signalling Technology	8480	1:100
Rabbit anti-human mAb Ki67	Abcam	ab92742	1:200
Rabbit anti-human pAb phosphorylated myosin light chain 2	Cell Signaling Technology	3671	1:50
Rabbit anti-human mAb vinculin	Abcam	ab129002	1:200
Rabbit anti-human mAb YAP	Cell Signaling Technology	8418	1:200
Goat anti-mouse AlexaFluor 488	Life Technologies	A11001	1:200
Goat anti-rabbit AlexaFluor 568	Life Technologies	A11011	1:200
Goat anti-rabbit AlexaFluor 594	Abcam	ab150116	1:200
4′,6-Diamidino-2-phenylindole dihydrochloride (DAPI)	Life Technologies	D9542	1:1000
Hoecsht 33342	Invitrogen	H3570	0.1 µg/mL
AF488-conjugated phalloidin	Sigma	P5282	1:200
AF555-conjugated phalloidin	Life Technologies	A34055	1:200
AF350-conjugated phalloidin	Life Technologies	A22281	1:400

Reference images of the unstrained TFM beads were obtained at 20x magnification immediately before cell seeding, where posterior foregut (PF or S3) and pancreatic endoderm (PE or S4) cells were seeded in a 3:1 ratio respectively at 200,000 cells/cm^2 onto the TFM substrates. After 72 hours, cells were fixed, permeabilized, and stained as previously described, then images were acquired, including the strained TFM beads.

5.6.6. Sagittal section micropattern fabrication

To confine PP cells in non-circular geometries, we used a modified desktop craft cutter to physically scribe patterns in an agarose layer as described previously (Tran, Hoesli, et al., 2020). Briefly, a 0.5% w/w solution of agarose was heated to 80^{o}C, spincoated onto a glass slide (1500 rpm for 30 seconds), and heated at 100^{o}C for 5 minutes, resulting in a brittle, nanometer-thin film of agarose. The slide was mounted onto a hobby crafter cutter (Zyng Air, KNK), custom fit with a needle-tip where micron-scale patterns, designed in the 'Make the Cut!^{TM}' software could be robotically scribed. The patterns were coated with 25 µg/mL fibronectin (Millopore) diluted in PBS for 1-2 hours then rinsed once with PBS before seeding.

5.6.7. Silicone equibiaxial strain system fabrication

Briefly, the DPAM system was fabricated by soft lithography using 3D printed negative molds. Negative molds were fabricated using SLA 3D printer (Ember, Autodesk), cured with UV overnight, and coated with Ease Release^{TM} (Mann). Sylgard 184 (Paisley), mixed in a 10:1 ratio by weight, was poured into the negative molds, sandwiched against an acetate sheet to prevent adhesion, and cured at 70 ^{o}C overnight. This sandwich technique resulted in a membrane thickness of roughly 25 µm once peeled. The DPAM channels were then adhered onto a glass slide by stamping the underside on a thin layer of spincoated Sylgard 184.

All devices were then leak-tested and confirmed to strain when pressure is applied. The DPAM system was pressurized using a miniature eccentric diaphragm air pump (SP 100 EC, Schwarzer Precision) capable of achieving a max pressure of 600 mbar and max vacuum of -500 mbar when powered by +5V DC. The pump was powered (+5V) and controlled by an Arduino Uno. A media reservoir was fabricated out of PDMS and glued to the DPAM channels, where connections were made using blunted 90^o bent needles (Jensen), Luer-lock fittings, and flexible tubing. Cells were fixed in an unstrained state and then immunostained to visualize PDX1 and YAP expression.

5.6.8. *Data Analysis*

For the traction force microscopy experiments, particle tracking and traction stress calculations of the fluorescent beads was done using the Fiji plugin as previously described (Tseng et al., 2012). Cluster boundaries were manually drawn based on high fluorescent staining intensity of E-cadherin and PDX1 to create regions of interest (ROI) of these clusters. A custom MATLAB script was used to project the traction stresses towards the center of the clusters, defined as the ROI center of mass in ImageJ, and to calculate the average stresses within the cluster ROIs.

For the strained PDMS membrane devices, image processing and analysis was performed on Fiji. Briefly, the 'Subtract Background' function was used to correct for non-uniform background fluorescence due to different layer thicknesses of the autofluorescent PDMS device. The 'Analyze Particles' function (set to include particles from 25 – 500 μm^2) was used to obtain regions of interest for all nuclei using a watershed, thresholded DAPI image, from which the positions and fluorescent intensities of each nuclei were measured. The center and diameter of the strained region was obtained using phase contrast images and the position of all nuclei analyzed was mapped to the center of the strained region. The normalized radial position was calculated and the strained, interface, and outer regions was classified for nuclei falling within normalized radial positions of $r < 0.6$, $r < 1.2$, and $r < 1.8$ respectively, where r is the measured radius of the strained region.

5.6.9. *Statistical analysis*

Statistical analysis was performed using GraphPad 8. For two-way comparisons, the two-sided student's T-test were performed (Figure 5-3G, Figure 5-4G). For the strain experiments shown in Figure 5-5G, a two-way ANOVA was performed followed by Tukey multiple comparisons test. In all analysis, p-values < 0.05 denote a statistically significate result. Three experimental replicates were performed for each experiment unless otherwise indicated in the figure captions.

5.7 Acknowledgements

We would like to thank Dr. Andrew Elefanty for the NKX6.1-GFP HES3 reporter line which was used in this work and Dr. Cristina Nostro for helping to facilitate the transfer of the cells. The authors received funding from Canada's National Sciences and Engineering Research Council (NSERC, PGS-D award for RT, RGPIN-2015-05512 to CM and RGPIN-2015-05877 to CH) which supported this work. This work was undertaken, in part, thanks to funding from the Canada Research Chairs program (CH and CM) and the 'Funding Biotechnology Partnerships' program from the Stem Cell Network. RT and CH are members of the Quebec Network for Cell, Tissue and Gene Therapy – ThéCell (a thematic network supported by the Fonds de recherche du Québec–Santé), of the Québec Center for Advanced Materials (CQMF), of PROTEO (The Quebec *Network* for Research on Protein Function, Engineering, and Applications), of the Cardiometabolic Health, Diabetes and Obesity Research Network (CMDO), and of the Montreal Diabetes Research Center (MDRC).

Chapter 6

6.1 Final Remarks

6.2 Comprehensive Discussion

The overall goal of this work was to test the effect of mechanics during pancreatic differentiation by taking a biomimetic approach to emulate the developing cellular microenvironment. In Chapter 2, I presented a comprehensive overview of innovations in pancreatic directed differentiation protocols where biomimetic strategies are used to manipulate mechanical cell interactions along with the conventional timed soluble factor addition. Although these works have effectively improved the resultant cell functionality (Nair et al., 2019; Velazco-Cruz et al., 2019) and efficiency (Hogrebe et al., 2020; H. Liu et al., 2017, 2021) in the pancreatic differentiation workflow, none of the works have directly addressed the geometric and mechanical cues presented by the changing form of the developing pancreas (Jennings et al., 2015; D. W. Thompson, 1942). Tissue growth and remodelling in development results in complex geometries with curvature-driven and mechanical effects on cell behaviour (Alias & Buenzli, 2017; Callens et al., 2020). Curved geometries directly affect cytoskeletal tension of cultured cells (Callens et al., 2020; Lou et al., 2019) which prime lineage decisions during differentiation (McBeath et al., 2004; Ruiz & Chen, 2008; Werner et al., 2017). Recognizing the need to investigate various mechanical influences during pancreatic differentiation, I developed approaches to: 1) recreate cell clustering in a 2D platform, 2) recreate tissue geometry, and 3) apply dynamic mechanical forces during directed differentiation protocols. By incorporating biomimetic cues inspired by pancreas development, this body of work takes a mechanical approach to directed differentiation protocols to better guide the generation of insulin-producing beta cells.

Identifying the mechanical stresses present during development and then applying similar stresses during directed differentiation can promote pancreatic differentiation towards the endocrine lineage. In Chapters 3 and 5, I explored the relationship between pancreatic differentiation and the actin cytoskeleton. Specifically, in Chapter 3, I showed that when confined in agarose micropatterns, PF cells clustered and simultaneously underwent coordinated supracellular cytoskeletal reorganizations which were associated with increased PDX1 expression, suggesting a role of cell shape and the actin cytoskeleton in pancreatic differentiation. Micropatterned culture has previously been associated with patterns of stress generation (Ma et al., 2019; C. M. Nelson et al., 2005; Ruiz & Chen, 2008), suggesting the agarose micropatterns

mechanically primed the confined cells during differentiation. Then in Chapter 5, I show that there is heterogeneity in cell-generated traction stresses of pancreatic endoderm cells, with high stresses surrounding PDX1^{high} clusters, suggesting a role of mechanical force in differentiation. With this information, I then engineered a micro-scale device to mechanically stretch differentiating PF cells and showed that strain promotes PDX1 expression. These results together highlight a role for mechanical priming during pancreatic differentiation and support the observations that pancreatic fate decisions are mediated by mechanosignalling (Hogrebe et al., 2020; Mamidi et al., 2018a). However, the addition of guiding cues in directed differentiation is time-dependent (Hogrebe et al., 2020; Rasmussen, Reynolds, et al., 2016a) and may only act as initial guiding cues due to tissue homeostasis (Youngblood et al., 2019), suggesting the need for additional future optimization.

The evidence presented in this thesis suggests that *in vitro* PE differentiation involves a change in mechanical cell phenotype to become more contractile. During the transition from PF cells to PE cells, we observed distinct changes in cell architecture from smaller, rounded cells to more elongated cells, which may suggest changes in cytoskeletal tension and thus mechanosensing ability, that could play a role in differentiation (McBeath et al., 2004). During *in vitro* culture, point spots of high cell contractility could prime differentiation into PDX1^{high} cells, which then cascade contraction and differentiation to other nearby cells. In Chapter 3, we observed the formation of spontaneous, self-aggregating, contractile pancreatic cell clusters during differentiation and were able to mimic this behaviour in a 2D micropatterning platform. Self-clustering aggregates could have phenotypic differences from manual, user-aggregated clusters due to the cell enrichment and the harsh forces associated with dissociation (Docherty et al., 2021). Downstream this may lead to functional differences in maturation compared to heterogeneous PSC-derived clusters formed manually in other protocols. Further study of the self-clustering phenomena with a PDX1 reporter could give insight into how clusters and local cell densities self-assemble during pancreatic differentiation.

Throughout this thesis, pluripotent stem cell (PSC)-derived stem cells were used to model the developmental process. Although the efficiency of pancreatic progenitor generation varies between protocols and cell lines, a common transcriptomic and epigenomic signature is shared between protocols (Rostovskaya et al., 2015; Wesolowska-Andersen et al., 2020). Previously, single-cell transcriptomics show that *in vitro* pancreatic differentiation protocols generate a

mixture of hormonal cells which are immature (Hrvatin et al., 2014; Veres et al., 2019) compared to native human islets. However, maturation can occur *in vivo* through stimuli likely including both soluble factors, non-soluble matrix components and mechanical cues (Augsornworawat et al., 2020). The intermediate endocrine precursor cells obtained during differentiation have transcriptomes similar to those found during mouse development *in utero* and most hESC-derived endocrine cells were "fated" to the beta cell lineage (Krentz et al., 2018; Wesolowska-Andersen et al., 2020), suggesting PSC-derived cells are a good analogue for human pancreatic development. In this thesis, the PSC-derived cells (Rezania et al., 2014) expressed key markers of pancreatic and endocrine lineage such as PDX1, NKX6.1, and NGN3, suggesting a similar signature to previous works. However, the expression of NGN3 does not require earlier NKX6.1 expression, suggesting alternate pathways to become endocrine progenitors which could be important when classifying the cell types found earlier in differentiation (Petersen et al., 2017). Applying the appropriate biomechanical stimuli during differentiation could potentially guide differentiation through alternate pathways which may be more favourable towards beta cell lineage, but more in-depth study of the dynamic transcriptome and resultant functionality is required.

6.3 Future Directions

The developing cellular microenvironment is constantly changing and microenvironmental niche for one stage of differentiation may be completely different from the next (Hogrebe et al., 2020; Rasmussen, Reynolds, et al., 2016a). Designing novel, dynamic, user-controllable cell culture platforms which allow temporal control of the presented mechanical stimuli alongside biochemical cell signalling could better mimic stages of development, potentially improving differentiation outcomes downstream. The equibiaxial strain system presented in Chapter 5 as well as by others (Moraes et al., 2010; Xue et al., 2018), could allow for temporal control and therefore enabling stage-specific mechanical strain. Further optimization of the magnitude of strain and stress provided to differentiating cells could also improve protocols towards desired lineages. It would be interesting to test the platform with different modes of operation (e.g. cyclic strain, ramping strain, uniaxial stretch), which may be important to optimize for endocrine cell production. Expanding on this, multiplexing of this platform could allow for controlled, dynamic strain of multiple selected regions to get cell patterning. These strategies could lead to new paradigms which incorporate mechanical stresses at various stages of directed differentiation, potentially increasing differentiation uniformity or decreasing costs. These technologies would

require multi-stage optimization to determine the necessary, mechanosensitive stages of differentiation to control and the types of biomechanics required (e.g. different stiffnesses, stresses, topography, etc.). For example, removal of endogenous cytoskeletal tension through precisely timed actin depolymerization can improve differentiation into $NGN3^{+}$ endocrine precursors (Hogrebe et al., 2020). Alternatively, mechanical control of the substrate to provide compressive strains or to change differentiating cell shape could reduce cytoskeletal tension which may have similar effects on pancreatic differentiation. Further down the line, self-sustaining systems which combine user-actuatable culture substrates, feedback controllers, and reporter cell lines could reduce the labour and variability of differentiation protocols, thus increasing accessibility of cell therapies. Doing so could prime Stage 4 cells which could profoundly impact downstream differentiation events towards endocrine lineage, however this needs to be investigated further.

Almost all developmental systems undergo complex morphogenesis which impart mechanical forces onto differentiating cells (Heisenberg & Bellaïche, 2013). For example, smooth muscle differentiation and contraction is correlated with regions of epithelial shape change and is necessary for lung branching morphogenesis (H. Y. Kim et al., 2015). Providing physical boundary conditions with growth factor gradients to human intestinal stem cells is sufficient to form a polarized crypt-villus (Y. Wang et al., 2017). The mechanics associated with morphogenesis have been well studied but the systems available to apply these forces in a physiological way need to be developed (Herrera-Perez & Kasza, 2019). The strategy of identifying and integrating the relevant biomechanical forces during directed differentiation of PSCs could lead to breakthroughs in generating functional cells for other developmental systems (Hernández-Hernández et al., 2014; Vining & Mooney, 2017). For example, cyclical stretch can be applied to provide physiologically similar forces to processes such as heart beating (Mihic et al., 2014) or breathing (Huh et al., 2010). Therefore, identifying correlations between cell patterning and tissue morphogenesis could then lead to new strategies for directed differentiation in various fields.

In general, cell identification in early development is done with a panel of protein and gene expression due to lack of functional outputs. In Chapter 5, I mainly looked at the expression of PDX1 and confirmed downstream that $PDX1^{high}$ cells are correlated with downstream NKX6.1 and NGN3 expression. In the traction force experiments, the contractile strength of PE cells was

greater than PF cells, suggesting mechanical differences between cells could be a marker of differentiation and changing cell phenotypes. Therefore, studying the differentiation process with a panel of reporter markers, including potential mechanical markers (e.g. contractility, cell stiffness, cell shape), could improve our understanding of lineage decisions. It will be necessary to verify if mechanical strain can produce cells with more functional insulin secretion by continuing directed differentiation protocols long-term or through *in vivo* implantation studies. In future work, better understanding how mechanical strain affects cell phenotype during differentiation by single cell RNA sequencing could shed light on differentiation trajectory (Krentz et al., 2018; Veres et al., 2019) and other signalling pathways being affected (Sharon, Vanderhooft, et al., 2019), potentially resulting in more efficient biomanufacturing processes.

The ultimate goal of this research area would be to achieve therapeutic doses of islet-like clusters efficiently to improve accessibility of islet transplantation or other novel implantable biomedical devices targeting diabetes. To accomplish this, novel systems may be required to apply mechanical stimuli onto differentiating cells in a scalable manner. To meet the currently required ~8,000 islet equivalents/kg (~600,000 islet-like clusters per 75 kg patient) (Hering et al., 2016) required for islet transplantation, roughly 1 billion cells would be required, assuming 60% beta cell composition (Da Silva Xavier, 2018) and 1,000 cells per islet equivalent (in an average 150 µm islet) (Ramachandran et al., 2015). By some estimates in 2D cultures, this would require from 2,000 cm^2 (Hogrebe et al., 2021) – 6,000 cm^2 (Rezania et al., 2014) of initial cell culture surface area. This could potentially be reduced since we show that mechanical stimuli could further promote downstream beta cell differentiation. In Chapter 5, the equibiaxial strain system tested was designed to strain 70 circular regions (500 µm diameter, ~0.14 cm^2 strained area total in a 1.65 cm^2 device) but could be scaled linearly and further optimized to meet the surface area required. Other systems which apply force onto cell cultures, such as larger-scale uniaxial strain systems (Somers & Grayson, 2021) or low magnitudes of shear force (Yourek et al., 2010), could be more feasibly at larger scales. Likewise, other mechanical influences from ECM composition or stiffness could mimic the cell behaviour and shape produced in mechanically strained cell cultures. Simultaneously, once a reliable, accessible cell source is secured, other challenges such as immunoisolation (Hoesli et al., 2011; O'Sullivan et al., 2011) and oxygenation (Avgoustiniatos & Colton, 1997; Suszynski et al., 2014) of the implanted beta-like cells also need to be addressed.

6.4 Conclusions

In this thesis, I have taken a biomimetic approach to investigate the effect of various mechanical cues from the developing cellular microenvironment during pancreatic differentiation. Together, these works suggest that mechanical stimuli during pancreatic differentiation of pluripotent stem cells can positively regulate endocrine lineage specification when applied during the transition from posterior foregut to pancreatic endoderm cells. However, the developmental microenvironment is constantly changing and evolving suggesting that dynamic, stage-specific approaches may be required to further improve pancreatic differentiation. Although this thesis focuses within the context of pancreatic differentiation, this knowledge could be used to guide and optimize other lengthy, variable differentiation protocols which mimic other mechanically-influenced developmental phenomena (Strano et al., 2020; H. Wu et al., 2018). Further development of high throughput, bioprocessing strategies such as mechanically actuatable, high surface area platforms may improve throughput and scalability of these findings. A synergistic approach where protocols combine different aspects of microenvironment, such as ECM composition, stiffness, mechanical strain, and soluble signalling molecules could further improve differentiation and maturation. Overall, this body of work has found that utilizing a biomimetic approach to recreate pancreatic differentiation can improve differentiation outcomes for beta cell generation but further stage-specific optimization and scale-up is needed to efficiently obtain the therapeutic doses required for islet transplantation.

Chapter 7

7.1 Complete References

Aisenbrey, E. A., & Murphy, W. L. (2020). Synthetic alternatives to Matrigel. *Nature Reviews Materials*, *5*(7), 539–551. https://doi.org/10.1038/s41578-020-0199-8

Alberti, K., Davey, R. E., Onishi, K., George, S., Salchert, K., Seib, F. P., Bornhauser, M., Pompe, T., Nagy, A., Werner, C., & Zandstra, P. W. (2008). Functional immobilization of signaling proteins enables control of stem cell fate. *Nat Meth*, *5*(7), 645–650. https://doi.org/10.1038/nmeth.1222

Alias, M. A., & Buenzli, P. R. (2017). Modeling the Effect of Curvature on the Collective Behavior of Cells Growing New Tissue. *Biophysical Journal*, *112*(1), 193–204. PubMed. https://doi.org/10.1016/j.bpj.2016.11.3203

Almeida, F. V., Gammon, L., Laly, A. C., Pundel, O. J., Bishop, C. L., & Connelly, J. T. (2019). High-Content Analysis of Cell Migration Dynamics within a Micropatterned Screening Platform. *Advanced Biosystems*, *3*(8), 1900011. https://doi.org/10.1002/adbi.201900011

Álvarez-García, Y. R., Ramos-Cruz, K. P., Agostini-Infanzón, R. J., Stallcop, L. E., Beebe, D. J., Warrick, J. W., & Domenech, M. (2018). Open multi-culture platform for simple and flexible study of multi-cell type interactions. *Lab on a Chip*, *18*(20), 3184–3195. https://doi.org/10.1039/C8LC00560E

Amer, L. D., Holtzinger, A., Keller, G., Mahoney, M. J., & Bryant, S. J. (2015). Enzymatically degradable poly(ethylene glycol) hydrogels for the 3D culture and release of human embryonic stem cell derived pancreatic precursor cell aggregates. *Acta Biomaterialia*, *22*, 103–110. PubMed. https://doi.org/10.1016/j.actbio.2015.04.013

Amit, M., Shariki, C., Margulets, V., & Itskovitz-Eldor, J. (2004). Feeder Layer- and Serum-Free Culture of Human Embryonic Stem Cells1. *Biology of Reproduction*, *70*(3), 837–845. https://doi.org/10.1095/biolreprod.103.021147

Ammann, K. R., DeCook, K. J., Tran, P. L., Merkle, V. M., Wong, P. K., & Slepian, M. J. (2015). Collective cell migration of smooth muscle and endothelial cells: Impact of injury versus non-injury stimuli. *Journal of Biological Engineering*, *9*(1), 19. https://doi.org/10.1186/s13036-015-0015-y

Antoni, D., Burckel, H., Josset, E., & Noel, G. (2015). Three-Dimensional Cell Culture: A Breakthrough in Vivo. *International Journal of Molecular Sciences*, *16*(3), 5517–5527. PMC. https://doi.org/10.3390/ijms16035517

Arciero, J. C., Mi, Q., Branca, M., Hackam, D., & Swigon, D. (2013). Using a continuum model to predict closure time of gaps in intestinal epithelial cell layers. *Wound Repair and Regeneration : Official Publication of the Wound Healing Society [and] the European Tissue Repair Society*, *21*(2), 256–265. PubMed. https://doi.org/10.1111/j.1524-475X.2012.00865.x

Arous, C., & Wehrle-Haller, B. (2017). Role and impact of the extracellular matrix on integrin-mediated pancreatic β-cell functions. *Biology of the Cell*, *109*(6), 223–237. https://doi.org/10.1111/boc.201600076

Assady, S., Maor, G., Amit, M., Itskovitz-Eldor, J., Skorecki, K. L., & Tzukerman, M. (2001). Insulin Production by Human Embryonic Stem Cells. *Diabetes*, *50*(8), 1691. https://doi.org/10.2337/diabetes.50.8.1691

Ateshian, G. A., Costa, K. D., Azeloglu, E. U., Morrison, B., 3rd, & Hung, C. T. (2009). Continuum modeling of biological tissue growth by cell division, and alteration of

intracellular osmolytes and extracellular fixed charge density. *Journal of Biomechanical Engineering*, *131*(10), 101001–101001. PubMed. https://doi.org/10.1115/1.3192138

Ateshian, G. A., Morrison, B., Holmes, J. W., & Hung, C. T. (2012). Mechanics of cell growth. *Recent Advances in the Biomechanics of Growth and Remodeling*, *42*, 118–125. https://doi.org/10.1016/j.mechrescom.2012.01.010

Augsornworawat, P., Maxwell, K. G., Velazco-Cruz, L., & Millman, J. R. (2020). Single-Cell Transcriptome Profiling Reveals β Cell Maturation in Stem Cell-Derived Islets after Transplantation. *Cell Reports*, *32*(8). https://doi.org/10.1016/j.celrep.2020.108067

Augsornworawat, P., Velazco-Cruz, L., Song, J., & Millman, J. R. (2019). A hydrogel platform for in vitro three dimensional assembly of human stem cell-derived islet cells and endothelial cells. *Acta Biomaterialia*, *97*, 272–280. https://doi.org/10.1016/j.actbio.2019.08.031

Avgoustiniatos, E., & Colton, C. (1997). Effect of external oxygen mass transfer resistances on viability of immunoisolated tissue. *Annals of the New York Academy of Sciences*, *831*, 145–167. PubMed. https://doi.org/10.1111/j.1749-6632.1997.tb52192.x

Babu, D. A., Deering, T. G., & Mirmira, R. G. (2007). A Feat of Metabolic Proportions: Pdx1 Orchestrates Islet Development and Function in the Maintenance of Glucose Homeostasis. *Molecular Genetics and Metabolism*, *92*(1–2), 43–55. PMC. https://doi.org/10.1016/j.ymgme.2007.06.008

Basson, M. A. (2012). Signaling in cell differentiation and morphogenesis. *Cold Spring Harbor Perspectives in Biology*, *4*(6), a008151. PubMed. https://doi.org/10.1101/cshperspect.a008151

Bauwens, C. L., Peerani, R., Niebruegge, S., Woodhouse, K. A., Kumacheva, E., Husain, M., & Zandstra, P. W. (2008). Control of Human Embryonic Stem Cell Colony and Aggregate Size Heterogeneity Influences Differentiation Trajectories. *STEM CELLS*, *26*(9), 2300–2310. https://doi.org/10.1634/stemcells.2008-0183

Bays, J. L., & DeMali, K. A. (2017). Vinculin in cell–cell and cell–matrix adhesions. *Cellular and Molecular Life Sciences*, *74*(16), 2999–3009. https://doi.org/10.1007/s00018-017-2511-3

Beake, B. D., Ogwu, A. A., & Wagner, T. (2006). Influence of experimental factors and film thickness on the measured critical load in the nanoscratch test. *Mechanical Behaviour of Micro- and Nano-Scale Systems*, *423*(1), 70–73. https://doi.org/10.1016/j.msea.2005.09.121

Belair, D. G., Le, N. N., & Murphy, W. L. (2014). Design of growth factor sequestering biomaterials. *Chemical Communications (Cambridge, England)*, *50*(99), 15651–15668. PubMed. https://doi.org/10.1039/c4cc04317k

Bendayan, M. (1992). Association of secreted insulin with particular domains of the pancreatic B-cell plasma membrane: The actin-rich microvilli. *Journal of Histochemistry & Cytochemistry*, *40*(3), 327–331. https://doi.org/10.1177/40.3.1552173

Benitez, C. M., Goodyer, W. R., & Kim, S. K. (2012). Deconstructing Pancreas Developmental Biology. *Cold Spring Harbor Perspectives in Biology*, *4*(6). https://doi.org/10.1101/cshperspect.a012401

Berthiaume, F., & Frangos, J. A. (1995). Flow Effects on Endothelial Cell Signal Transduction, Function, and Mediator Release. In J. A. Bevan, G. Kaley, & G. M. Rubanyi (Eds.),

Flow-Dependent Regulation of Vascular Function (pp. 85–116). Springer New York. https://doi.org/10.1007/978-1-4614-7527-9_5

Bi, H., Ye, K., & Jin, S. (2020). Proteomic analysis of decellularized pancreatic matrix identifies collagen V as a critical regulator for islet organogenesis from human pluripotent stem cells. *Biomaterials*, *233*, 119673. https://doi.org/10.1016/j.biomaterials.2019.119673

Bonnans, C., Chou, J., & Werb, Z. (2014). Remodelling the extracellular matrix in development and disease. *Nature Reviews. Molecular Cell Biology*, *15*(12), 786–801. PubMed. https://doi.org/10.1038/nrm3904

Bosch-Fortea, M., Rodriguez-Fraticelli, A. E., Herranz, G., Hachimi, M., Barea, M. D., Young, J., Ladoux, B., & Martin-Belmonte, F. (2019). Micropattern-based platform as a physiologically relevant model to study epithelial morphogenesis and nephrotoxicity. *Biomaterials*, *218*, 119339. https://doi.org/10.1016/j.biomaterials.2019.119339

Brafman, D. A., Phung, C., Kumar, N., & Willert, K. (2013). Regulation of endodermal differentiation of human embryonic stem cells through integrin-ECM interactions. *Cell Death Differ*, *20*(3), 369–381.

Brandenberg, N., & Lutolf, M. P. (2016). In Situ Patterning of Microfluidic Networks in 3D Cell-Laden Hydrogels. *Advanced Materials*, *28*(34), 7450–7456. https://doi.org/10.1002/adma.201601099

Buchwald, P. (2009). FEM-based oxygen consumption and cell viability models for avascular pancreatic islets. *Theoretical Biology and Medical Modelling*, *6*(1), 5. https://doi.org/10.1186/1742-4682-6-5

Burghoff, S., & Schrader, J. (2011). Secretome of Human Endothelial Cells under Shear Stress. *Journal of Proteome Research*, *10*(3), 1160–1169. https://doi.org/10.1021/pr100937a

Burlison, J. S., Long, Q., Fujitani, Y., Wright, C. V. E., & Magnuson, M. A. (2008). Pdx-1 and Ptf1a concurrently determine fate specification of pancreatic multipotent progenitor cells. *Developmental Biology*, *316*(1), 74–86. PubMed. https://doi.org/10.1016/j.ydbio.2008.01.011

Caicedo, A. (2013). PARACRINE AND AUTOCRINE INTERACTIONS IN THE HUMAN ISLET: MORE THAN MEETS THE EYE. *Seminars in Cell & Developmental Biology*, *24*(1), 11–21. PMC. https://doi.org/10.1016/j.semcdb.2012.09.007

Callens, S. J. P., Uyttendaele, R. J. C., Fratila-Apachitei, L. E., & Zadpoor, A. A. (2020). Substrate curvature as a cue to guide spatiotemporal cell and tissue organization. *Biomaterials*, *232*, 119739. https://doi.org/10.1016/j.biomaterials.2019.119739

Carlsson, P. O., Liss, P., Andersson, A., & Jansson, L. (1998). Measurements of oxygen tension in native and transplanted rat pancreatic islets. *Diabetes*, *47*(7), 1027. https://doi.org/10.2337/diabetes.47.7.1027

Chandrasekaran, A., Kalashnikov, N., Rayes, R., Wang, C., Spicer, J., & Moraes, C. (2017). Thermal scribing to prototype plastic microfluidic devices, applied to study the formation of neutrophil extracellular traps. *Lab on a Chip*, *17*(11), 2003–2012. https://doi.org/10.1039/C7LC00356K

Chen, C. S. (2008). Mechanotransduction – a field pulling together? *Journal of Cell Science*, *121*(20), 3285. https://doi.org/10.1242/jcs.023507

Chen, C. S., Mrksich, M., Huang, S., Whitesides, G. M., & Ingber, D. E. (1997). Geometric Control of Cell Life and Death. *Science*, *276*(5317), 1425. https://doi.org/10.1126/science.276.5317.1425

Chen, G., Gulbranson, D. R., Hou, Z., Bolin, J. M., Ruotti, V., Probasco, M. D., Smuga-Otto, K., Howden, S. E., Diol, N. R., Propson, N. E., Wagner, R., Lee, G. O., Antosiewicz-Bourget, J., Teng, J. M. C., & Thomson, J. A. (2011). Chemically defined conditions for human iPSC derivation and culture. *Nature Methods*, *8*(5), 424–429. PubMed. https://doi.org/10.1038/nmeth.1593

Chiang, M.-K., & Melton, D. A. (2003). Single-Cell Transcript Analysis of Pancreas Development. *Developmental Cell*, *4*(3), 383–393. https://doi.org/10.1016/S1534-5807(03)00035-2

Chowdhury, A., Dyachok, O., Tengholm, A., Sandler, S., & Bergsten, P. (2013). Functional differences between aggregated and dispersed insulin-producing cells. *Diabetologia*, *56*(7), 1557–1568. PMC. https://doi.org/10.1007/s00125-013-2903-3

Clark, A. R., Petersen, H. V., Read, M. L., Scott, V., Michelsen, B. K., & Docherty, K. (1993). Human insulin gene enhancer-binding proteins in pancreatic α and β cell lines. *FEBS Letters*, *329*(1–2), 139–143. https://doi.org/10.1016/0014-5793(93)80210-L

Cukjati, D., Reberŝek, S., Karba, R., & Miklavĉiĉ, D. (2000). Modelling of chronic wound healing dynamics. *Medical and Biological Engineering and Computing*, *38*(3), 339–347. https://doi.org/10.1007/BF02347056

D. A. Bartholomeusz, R. W. Boutte, & J. D. Andrade. (2005). Xurography: Rapid prototyping of microstructures using a cutting plotter. *Journal of Microelectromechanical Systems*, *14*(6), 1364–1374. https://doi.org/10.1109/JMEMS.2005.859087

Da Silva Xavier, G. (2018). The Cells of the Islets of Langerhans. *Journal of Clinical Medicine*, *7*(3), 54. PubMed. https://doi.org/10.3390/jcm7030054

D’Amour, K. A., Agulnick, A. D., Eliazer, S., Kelly, O. G., Kroon, E., & Baetge, E. E. (2005). Efficient differentiation of human embryonic stem cells to definitive endoderm. *Nature Biotechnology*, *23*(12), 1534–1541. https://doi.org/10.1038/nbt1163

D’Amour, K. A., Bang, A. G., Eliazer, S., Kelly, O. G., Agulnick, A. D., Smart, N. G., Moorman, M. A., Kroon, E., Carpenter, M. K., & Baetge, E. E. (2006). Production of pancreatic hormone-expressing endocrine cells from human embryonic stem cells. *Nat Biotech*, *24*(11), 1392–1401.

D’Angelo, F., Tiribuzi, R., Armentano, I., Kenny, J. M., Martino, S., & Orlacchio, A. (2011). Mechanotransduction: Tuning Stem Cells Fate. *Journal of Functional Biomaterials*, *2*(2), 67–87. PMC. https://doi.org/10.3390/jfb2020067

Dasgupta, I., & McCollum, D. (2019). Control of cellular responses to mechanical cues through YAP/TAZ regulation. *Journal of Biological Chemistry*, *294*(46), 17693–17706. https://doi.org/10.1074/jbc.REV119.007963

Dassaye, R., Naidoo, S., & Cerf, M. E. (2016). Transcription factor regulation of pancreatic organogenesis, differentiation and maturation. *Islets*, *8*(1), 13–34. PubMed. https://doi.org/10.1080/19382014.2015.1075687

Davis, J. C., Alves, T. C., Helman, A., Chen, J. C., Kenty, J. H., Cardone, R. L., Liu, D. R., Kibbey, R. G., & Melton, D. A. (2020). Glucose Response by Stem Cell-Derived β Cells In Vitro Is Inhibited by a Bottleneck in Glycolysis. *Cell Reports*, *31*(6), 107623. https://doi.org/10.1016/j.celrep.2020.107623

de Back, W., Zhou, J. X., & Brusch, L. (2013). On the role of lateral stabilization during early patterning in the pancreas. *Journal of The Royal Society Interface*, *10*(79), 20120766. https://doi.org/10.1098/rsif.2012.0766

Discher, D. E., Mooney, D. J., & Zandstra, P. W. (2009). Growth Factors, Matrices, and Forces Combine and Control Stem Cells. *Science*, *324*(5935), 1673. https://doi.org/10.1126/science.1171643

Dixon, A. R., Moraes, C., Csete, M. E., Thouless, M. D., Philbert, M. A., & Takayama, S. (2014). One-dimensional patterning of cells in silicone wells via compression-induced fracture. *Journal of Biomedical Materials Research. Part A*, *102*(5), 1361–1369. PubMed. https://doi.org/10.1002/jbm.a.34814

Docherty, F. M., Riemondy, K. A., Castro-Gutierrez, R., Dwulet, J. M., Shilleh, A. H., Hansen, M. S., Williams, S. P. M., Armitage, L. H., Santostefano, K. E., Wallet, M. A., Mathews, C. E., Triolo, T. M., Benninger, R. K. P., & Russ, H. A. (2021). ENTPD3 Marks Mature Stem Cell Derived Beta Cells Formed by Self-Aggregation in Vitro. *Diabetes*, db200873. https://doi.org/10.2337/db20-0873

Doyle, A. D., Wang, F. W., Matsumoto, K., & Yamada, K. M. (2009). One-dimensional topography underlies three-dimensional fibrillar cell migration. *Journal of Cell Biology*, *184*(4), 481–490. https://doi.org/10.1083/jcb.200810041

Driscoll, T. P., Cosgrove, B. D., Heo, S.-J., Shurden, Z. E., & Mauck, R. L. (2015). Cytoskeletal to Nuclear Strain Transfer Regulates YAP Signaling in Mesenchymal Stem Cells. *Biophysical Journal*, *108*(12), 2783–2793. PubMed. https://doi.org/10.1016/j.bpj.2015.05.010

Du Noüy, P. L. (1916). CICATRIZATION OF WOUNDS : II. MATHEMATICAL EXPRESSION OF THE CURVE REPRESENTING CICATRIZATION. *Journal of Experimental Medicine*, *24*(5), 451–460. https://doi.org/10.1084/jem.24.5.451

Dubois, S. J., Kalashnikov, N., & Moraes, C. (2019). Robust and Precise Wounding and Analysis of Engineered Contractile Tissues. *Tissue Engineering Part C: Methods*, *25*(11), 677–686. https://doi.org/10.1089/ten.tec.2019.0123

Elrick, L. J., & Docherty, K. (2001). Phosphorylation-Dependent Nucleocytoplasmic Shuttling of Pancreatic Duodenal Homeobox-1. *Diabetes*, *50*(10), 2244. https://doi.org/10.2337/diabetes.50.10.2244

Engler, A. J., Sen, S., Sweeney, H. L., & Discher, D. E. (2006). Matrix Elasticity Directs Stem Cell Lineage Specification. *Cell*, *126*(4), 677–689. https://doi.org/10.1016/j.cell.2006.06.044

Etoc, F., Metzger, J., Ruzo, A., Kirst, C., Yoney, A., Ozair, M. Z., Brivanlou, A. H., & Siggia, E. D. (2016). A Balance between Secreted Inhibitors and Edge Sensing Controls Gastruloid Self-Organization. *Developmental Cell*, *39*(3), 302–315. https://doi.org/10.1016/j.devcel.2016.09.016

Eyckmans, J., Boudou, T., Yu, X., & Chen, C. S. (2011). A hitchhiker's guide to mechanobiology. *Developmental Cell*, *21*(1), 35–47. PubMed. https://doi.org/10.1016/j.devcel.2011.06.015

Fang, B., Liu, Y., Zheng, D., Shan, S., Wang, C., Gao, Y., Wang, J., Xie, Y., Zhang, Y., & Li, Q. (2019). The effects of mechanical stretch on the biological characteristics of human adipose-derived stem cells. *Journal of Cellular and Molecular Medicine*, *23*(6), 4244–4255. https://doi.org/10.1111/jcmm.14314

Fernandez-Gonzalez, R., Simoes, S. de M., Röper, J.-C., Eaton, S., & Zallen, J. A. (2009). Myosin II Dynamics Are Regulated by Tension in Intercalating Cells. *Developmental Cell*, *17*(5), 736–743. https://doi.org/10.1016/j.devcel.2009.09.003

Flaim, C. J., Chien, S., & Bhatia, S. N. (2005). An extracellular matrix microarray for probing cellular differentiation. *Nature Methods*, *2*, 119.

Fletcher, D. A., & Mullins, R. D. (2010). Cell mechanics and the cytoskeleton. *Nature*, *463*(7280), 485–492. PMC. https://doi.org/10.1038/nature08908

Foster, E. D., Bridges, N. D., Feurer, I. D., Eggerman, T. L., Hunsicker, L. G., & Alejandro, R. (2018). Improved Health-Related Quality of Life in a Phase 3 Islet Transplantation Trial in Type 1 Diabetes Complicated by Severe Hypoglycemia. *Diabetes Care*, *41*(5), 1001. https://doi.org/10.2337/dc17-1779

Frank, V., Kaufmann, S., Wright, R., Horn, P., Yoshikawa, H. Y., Wuchter, P., Madsen, J., Lewis, A. L., Armes, S. P., Ho, A. D., & Tanaka, M. (2016). Frequent mechanical stress suppresses proliferation of mesenchymal stem cells from human bone marrow without loss of multipotency. *Scientific Reports*, *6*(1), 24264. https://doi.org/10.1038/srep24264

Fujimoto, K., & Polonsky, K. S. (2009). Pdx1 and other factors that regulate pancreatic β-cell survival. *Diabetes, Obesity & Metabolism*, *11*(Suppl 4), 30–37. PMC. https://doi.org/10.1111/j.1463-1326.2009.01121.x

Fujita, S., Shimizu, H., & Suye, S. (2012). Control of Differentiation of Human Mesenchymal Stem Cells by Altering the Geometry of Nanofibers. *Journal of Nanotechnology*, *2012*.

Fujitani, Y., Fujitani, S., Boyer, D. F., Gannon, M., Kawaguchi, Y., Ray, M., Shiota, M., Stein, R. W., Magnuson, M. A., & Wright, C. V. E. (2006). Targeted deletion of a cis-regulatory region reveals differential gene dosage requirements for Pdx1 in foregut organ differentiation and pancreas formation. *Genes & Development*, *20*(2), 253–266. https://doi.org/10.1101/gad.1360106

Gage, B. K., Webber, T. D., & Kieffer, T. J. (2013). Initial Cell Seeding Density Influences Pancreatic Endocrine Development During in vitro Differentiation of Human Embryonic Stem Cells. *PLOS ONE*, *8*(12), e82076. https://doi.org/10.1371/journal.pone.0082076

Galea, G. L., Cho, Y.-J., Galea, G., Molè, M. A., Rolo, A., Savery, D., Moulding, D., Culshaw, L. H., Nikolopoulou, E., Greene, N. D. E., & Copp, A. J. (2017). Biomechanical coupling facilitates spinal neural tube closure in mouse embryos. *Proceedings of the National Academy of Sciences*, *114*(26), E5177. https://doi.org/10.1073/pnas.1700934114

Galli, A., Maffioli, E., Sogne, E., Moretti, S., Di Cairano, E. S., Negri, A., Nonnis, S., Norata, G. D., Bonacina, F., Borghi, F., Podestà, A., Bertuzzi, F., Milani, P., Lenardi, C., Tedeschi, G., & Perego, C. (2018). Cluster-assembled zirconia substrates promote long-term differentiation and functioning of human islets of Langerhans. *Scientific Reports*, *8*(1), 9979. https://doi.org/10.1038/s41598-018-28019-3

Gannon, M., Tweedie Ables, E., Crawford, L., Lowe, D., Offield, M. F., Magnuson, M. A., & Wright, C. V. E. (2008). Pdx-1 function is specifically required in embryonic β cells to generate appropriate numbers of endocrine cell types and maintain glucose homeostasis. *Developmental Biology*, *314*(2), 406–417. https://doi.org/10.1016/j.ydbio.2007.10.038

Ganz, A., Lambert, M., Saez, A., Silberzan, P., Buguin, A., Mège, R. M., & Ladoux, B. (2006). Traction forces exerted through N-cadherin contacts. *Biology of the Cell*, *98*(12), 721–730. https://doi.org/10.1042/BC20060039

Gao, B., Jing, C., Ng, K., Pingguan-Murphy, B., & Yang, Q. (2019). Fabrication of three-dimensional islet models by the geometry-controlled hanging-drop method. *Acta Mechanica Sinica*, *35*(2), 329–337. https://doi.org/10.1007/s10409-019-00856-z

Gao, J., He, L., Shi, Y., Cai, M., Xu, H., Jiang, J., Zhang, L., & Wang, H. (2017). Cell contact and pressure control of YAP localization and clustering revealed by super-resolution imaging. *Nanoscale*, *9*(43), 16993–17003. https://doi.org/10.1039/C7NR05818G

Gao, T., McKenna, B., Li, C., Reichert, M., Nguyen, J., Singh, T., Yang, C., Pannikar, A., Doliba, N., Zhang, T., Stoffers, D. A., Edlund, H., Matschinsky, F., Stein, R., & Stanger, B. Z. (2014). Pdx1 maintains β cell identity and function by repressing an α cell program. *Cell Metabolism*, *19*(2), 259–271. PubMed. https://doi.org/10.1016/j.cmet.2013.12.002

Gattazzo, F., Urciuolo, A., & Bonaldo, P. (2014). Extracellular matrix: A dynamic microenvironment for stem cell niche. *Matrix-Mediated Cell Behaviour and Properties*, *1840*(8), 2506–2519. https://doi.org/10.1016/j.bbagen.2014.01.010

George, N. M., Day, C. E., Boerner, B. P., Johnson, R. L., & Sarvetnick, N. E. (2012). Hippo Signaling Regulates Pancreas Development through Inactivation of Yap. *Molecular and Cellular Biology*, *32*(24), 5116. https://doi.org/10.1128/MCB.01034-12

Geron, E., Boura-Halfon, S., Schejter, E. D., & Shilo, B.-Z. (2015). The Edges of Pancreatic Islet β Cells Constitute Adhesive and Signaling Microdomains. *Cell Reports*, *10*(3), 317–325. https://doi.org/10.1016/j.celrep.2014.12.031

Geuzaine, C., & Remacle, J.-F. (2009). Gmsh: A 3-D finite element mesh generator with built-in pre- and post-processing facilities. *International Journal for Numerical Methods in Engineering*, *79*(11), 1309–1331. https://doi.org/10.1002/nme.2579

Ghanian, M. H., Farzaneh, Z., Barzin, J., Zandi, M., Kazemi-Ashtiani, M., Alikhani, M., Ehsani, M., & Baharvand, H. (2015). Nanotopographical control of human embryonic stem cell differentiation into definitive endoderm. *Journal of Biomedical Materials Research Part A*, *103*(11), 3539–3553. https://doi.org/10.1002/jbm.a.35483

Ghazizadeh, Z., Kao, D.-I., Amin, S., Cook, B., Rao, S., Zhou, T., Zhang, T., Xiang, Z., Kenyon, R., Kaymakcalan, O., Liu, C., Evans, T., & Chen, S. (2017). ROCKII inhibition promotes the maturation of human pancreatic beta-like cells. *Nature Communications*, *8*(1), 298. https://doi.org/10.1038/s41467-017-00129-y

Gilbert, P. M., Havenstrite, K. L., Magnusson, K. E. G., Sacco, A., Leonardi, N. A., Kraft, P., Nguyen, N. K., Thrun, S., Lutolf, M. P., & Blau, H. M. (2010). Substrate Elasticity Regulates Skeletal Muscle Stem Cell Self-Renewal in Culture. *Science*, *329*(5995), 1078. https://doi.org/10.1126/science.1191035

Gilman, T. (1990). Parameter for measurement of wound closure. *Wounds*, *3*, 95–101.

Gilman, T. (2004). Wound Outcomes: The Utility of Surface Measures. *The International Journal of Lower Extremity Wounds*, *3*(3), 125–132. https://doi.org/10.1177/1534734604264419

Gjorevski, N., & Nelson, C. M. (2010). Endogenous patterns of mechanical stress are required for branching morphogenesis. *Integrative Biology*, *2*(9), 424–434. https://doi.org/10.1039/C0IB00040J

Glieberman, A. L., Pope, B. D., Zimmerman, J. F., Liu, Q., Ferrier, J. P., Kenty, J. H. R., Schrell, A. M., Mukhitov, N., Shores, K. L., Tepole, A. B., Melton, D. A., Roper, M. G., & Parker, K. K. (2019). Synchronized stimulation and continuous insulin sensing in a microfluidic human Islet on a Chip designed for scalable manufacturing. *Lab on a Chip*, *19*(18), 2993–3010. https://doi.org/10.1039/C9LC00253G

Goh, S.-K., Bertera, S., Olsen, P., Candiello, J., Halfter, W., Uechi, G., Balasubramani, M., Johnson, S., Sicari, B., Kollar, E., Badylak, S. F., & Banerjee, I. (2013). Perfusion-decellularized pancreas as a natural 3D scaffold for pancreatic tissue and whole organ

engineering. *Biomaterials*, *34*(28), 6760–6772. PMC. https://doi.org/10.1016/j.biomaterials.2013.05.066

Gorin, D. R., Cordts, P. R., LaMorte, W. W., & Menzoian, J. O. (1996). The influence of wound geometry on the measurement of wound healing rates in clinical trials. *Journal of Vascular Surgery*, *23*(3), 524–528. https://doi.org/10.1016/S0741-5214(96)80021-8

Grasso, S., Hernández, J. A., & Chifflet, S. (2007). Roles of wound geometry, wound size, and extracellular matrix in the healing response of bovine corneal endothelial cells in culture. *American Journal of Physiology-Cell Physiology*, *293*(4), C1327–C1337. https://doi.org/10.1152/ajpcell.00001.2007

Greggio, C., De Franceschi, F., Figueiredo-Larsen, M., Gobaa, S., Ranga, A., Semb, H., Lutolf, M., & Grapin-Botton, A. (2013). Artificial three-dimensional niches deconstruct pancreas development in vitro. *Development (Cambridge, England)*, *140*(21), 4452–4462. PubMed. https://doi.org/10.1242/dev.096628

Guckenberger, D. J., de Groot, T. E., Wan, A. M. D., Beebe, D. J., & Young, E. W. K. (2015). Micromilling: A method for ultra-rapid prototyping of plastic microfluidic devices. *Lab on a Chip*, *15*(11), 2364–2378. PubMed. https://doi.org/10.1039/c5lc00234f

Guilak, F., Cohen, D. M., Estes, B. T., Gimble, J. M., Liedtke, W., & Chen, C. S. (2009). Control of Stem Cell Fate by Physical Interactions with the Extracellular Matrix. *Cell Stem Cell*, *5*(1), 17–26. https://doi.org/10.1016/j.stem.2009.06.016

Gumbiner, B. M., & Kim, N.-G. (2014). The Hippo-YAP signaling pathway and contact inhibition of growth. *Journal of Cell Science*, *127*(Pt 4), 709–717. PubMed. https://doi.org/10.1242/jcs.140103

Gupta, S. K., Wesolowska-Andersen, A., Ringgaard, A. K., Jaiswal, H., Song, L., Hastoy, B., Ingvorsen, C., Taheri-Ghahfarokhi, A., Magnusson, B., Maresca, M., Jensen, R. R., Beer, N. L., Fels, J. J., Grunnet, L. G., Thomas, M. K., Gloyn, A. L., Hicks, R., McCarthy, M. I., Hansson, M., & Honoré, C. (2018). NKX6.1 induced pluripotent stem cell reporter lines for isolation and analysis of functionally relevant neuronal and pancreas populations. *Stem Cell Research*, *29*, 220–231. https://doi.org/10.1016/j.scr.2018.04.010

Guruswamy Damodaran, R., & Vermette, P. (2018). Decellularized pancreas as a native extracellular matrix scaffold for pancreatic islet seeding and culture. *Journal of Tissue Engineering and Regenerative Medicine*, *0*(0), 1–8. https://doi.org/10.1002/term.2655

Gwak, S.-J., Bhang, S. H., Kim, I.-K., Kim, S.-S., Cho, S.-W., Jeon, O., Yoo, K. J., Putnam, A. J., & Kim, B.-S. (2008). The effect of cyclic strain on embryonic stem cell-derived cardiomyocytes. *Biomaterials*, *29*(7), 844–856. https://doi.org/10.1016/j.biomaterials.2007.10.050

Hakim, F., Kaitsuka, T., Raeed, J. M., Wei, F.-Y., Shiraki, N., Akagi, T., Yokota, T., Kume, S., & Tomizawa, K. (2014). High oxygen condition facilitates the differentiation of mouse and human pluripotent stem cells into pancreatic progenitors and insulin-producing cells. *The Journal of Biological Chemistry*, *289*(14), 9623–9638. PubMed. https://doi.org/10.1074/jbc.M113.524363

Hammar, E., Parnaud, G., Bosco, D., Perriraz, N., Maedler, K., Donath, M., Rouiller, D. G., & Halban, P. A. (2004). Extracellular Matrix Protects Pancreatic β-Cells Against Apoptosis. *Diabetes*, *53*(8), 2034. https://doi.org/10.2337/diabetes.53.8.2034

Han, S. J., Bielawski, K. S., Ting, L. H., Rodriguez, M. L., & Sniadecki, N. J. (2012). Decoupling substrate stiffness, spread area, and micropost density: A close spatial

relationship between traction forces and focal adhesions. *Biophysical Journal*, *103*(4), 640–648. PubMed. https://doi.org/10.1016/j.bpj.2012.07.023

Hansson, M., Tonning, A., Frandsen, U., Petri, A., Rajagopal, J., Englund, M. C. O., Heller, R. S., Håkansson, J., Fleckner, J., Sköld, H. N., Melton, D., Semb, H., & Serup, P. (2004). Artifactual Insulin Release From Differentiated Embryonic Stem Cells. *Diabetes*, *53*(10), 2603. https://doi.org/10.2337/diabetes.53.10.2603

Hardikar, A. A., Marcus-Samuels, B., Geras-Raaka, E., Raaka, B. M., & Gershengorn, M. C. (2003). Human pancreatic precursor cells secrete FGF2 to stimulate clustering into hormone-expressing islet-like cell aggregates. *Proceedings of the National Academy of Sciences*, *100*(12), 7117. https://doi.org/10.1073/pnas.1232230100

Hashemitabar, M., & Heidari, E. (2019). Redefining the signaling pathways from pluripotency to pancreas development: In vitro β-cell differentiation. *Journal of Cellular Physiology*, *234*(6), 7811–7827. https://doi.org/10.1002/jcp.27736

Heinis, M., Simon, M.-T., Ilc, K., Mazure, N. M., Pouysségur, J., Scharfmann, R., & Duvillié, B. (2010). Oxygen Tension Regulates Pancreatic β-Cell Differentiation Through Hypoxia-Inducible Factor 1α. *Diabetes*, *59*(3), 662–669. PMC. https://doi.org/10.2337/db09-0891

Heisenberg, C.-P., & Bellaïche, Y. (2013). Forces in Tissue Morphogenesis and Patterning. *Cell*, *153*(5), 948–962. https://doi.org/10.1016/j.cell.2013.05.008

Hellman, B. (1959). Actual Distribution of the Number and Volume of the Islets of Langerhans in Different Size Classes in Non-diabetic Humans of Varying Ages. *Nature*, *184*(4697), 1498–1499. https://doi.org/10.1038/1841498a0

Heng, B. C., Zhang, X., Aubel, D., Bai, Y., Li, X., Wei, Y., Fussenegger, M., & Deng, X. (2020). Role of YAP/TAZ in Cell Lineage Fate Determination and Related Signaling

Pathways. *Frontiers in Cell and Developmental Biology*, *8*, 735. https://doi.org/10.3389/fcell.2020.00735

Hering, B. J., Clarke, W. R., Bridges, N. D., Eggerman, T. L., Alejandro, R., Bellin, M. D., Chaloner, K., Czarniecki, C. W., Goldstein, J. S., Hunsicker, L. G., Kaufman, D. B., Korsgren, O., Larsen, C. P., Luo, X., Markmann, J. F., Naji, A., Oberholzer, J., Posselt, A. M., Rickels, M. R., … Turgeon, N. A. (2016). Phase 3 Trial of Transplantation of Human Islets in Type 1 Diabetes Complicated by Severe Hypoglycemia. *Diabetes Care*, *39*(7), 1230. https://doi.org/10.2337/dc15-1988

Hernández-Hernández, V., Rueda, D., Caballero, L., Alvarez-Buylla, E. R., & Benítez, M. (2014). Mechanical forces as information: An integrated approach to plant and animal development. *Frontiers in Plant Science*, *5*, 265. https://doi.org/10.3389/fpls.2014.00265

Herrera-Perez, R. M., & Kasza, K. E. (2019). Manipulating the Patterns of Mechanical Forces That Shape Multicellular Tissues. *Physiology*, *34*(6), 381–391. https://doi.org/10.1152/physiol.00018.2019

Hilderink, J., Spijker, S., Carlotti, F., Lange, L., Engelse, M., van Blitterswijk, C., de Koning, E., Karperien, M., & van Apeldoorn, A. (2015). Controlled aggregation of primary human pancreatic islet cells leads to glucose-responsive pseudoislets comparable to native islets. *Journal of Cellular and Molecular Medicine*, *19*(8), 1836–1846. PMC. https://doi.org/10.1111/jcmm.12555

Hoesli, C. A., Raghuram, K., Kiang, R. L. J., Mocinecová, D., Hu, X., Johnson, J. D., Lacík, I., Kieffer, T. J., & Piret, J. M. (2011). Pancreatic cell immobilization in alginate beads produced by emulsion and internal gelation. *Biotechnology and Bioengineering*, *108*(2), 424–434. https://doi.org/10.1002/bit.22959

Hoesli, C. A., Tremblay, C., Juneau, P.-M., Boulanger, M. D., Beland, A. V., Ling, S. D., Gaillet, B., Duchesne, C., Ruel, J., Laroche, G., & Garnier, A. (2018). Dynamics of Endothelial Cell Responses to Laminar Shear Stress on Surfaces Functionalized with Fibronectin-Derived Peptides. *ACS Biomaterials Science & Engineering*, *4*(11), 3779–3791. https://doi.org/10.1021/acsbiomaterials.8b00774

Hogrebe, N. J., Augsornworawat, P., Maxwell, K. G., Velazco-Cruz, L., & Millman, J. R. (2020). Targeting the cytoskeleton to direct pancreatic differentiation of human pluripotent stem cells. *Nature Biotechnology*, *38*(4), 460–470. https://doi.org/10.1038/s41587-020-0430-6

Hogrebe, N. J., Maxwell, K. G., Augsornworawat, P., & Millman, J. R. (2021). Generation of insulin-producing pancreatic β cells from multiple human stem cell lines. *Nature Protocols*. https://doi.org/10.1038/s41596-021-00560-y

Hohwieler, M., Illing, A., Hermann, P. C., Mayer, T., Stockmann, M., Perkhofer, L., Eiseler, T., Antony, J. S., Müller, M., Renz, S., Kuo, C.-C., Lin, Q., Sendler, M., Breunig, M., Kleiderman, S. M., Lechel, A., Zenker, M., Leichsenring, M., Rosendahl, J., … Kleger, A. (2017). Human pluripotent stem cell-derived acinar/ductal organoids generate human pancreas upon orthotopic transplantation and allow disease modelling. *Gut*, *66*(3), 473. https://doi.org/10.1136/gutjnl-2016-312423

Horb, L. D., & Slack, J. (2004). Role of cell division in branching morphogenesis and differentiation of the embryonic pancreas. *International Journal of Developmental Biology*, *44*(7), 791–796.

Hrvatin, S., O'Donnell, C. W., Deng, F., Millman, J. R., Pagliuca, F. W., DiIorio, P., Rezania, A., Gifford, D. K., & Melton, D. A. (2014). Differentiated human stem cells resemble

fetal, not adult, β cells. *Proceedings of the National Academy of Sciences of the United States of America*, *111*(8), 3038–3043. PMC. https://doi.org/10.1073/pnas.1400709111

Hsiao, C., Lampe, M., Nillasithanukroh, S., Han, W., Lian, X., & Palecek, S. P. (2016). Human pluripotent stem cell culture density modulates YAP signaling. *Biotechnology Journal*, *11*(5), 662–675. https://doi.org/10.1002/biot.201500374

Huh, D., Matthews, B. D., Mammoto, A., Montoya-Zavala, M., Hsin, H. Y., & Ingber, D. E. (2010). Reconstituting Organ-Level Lung Functions on a Chip. *Science*, *328*(5986), 1662. https://doi.org/10.1126/science.1188302

Hui, C. Y., Jagota, A., Lin, Y. Y., & Kramer, E. J. (2002). Constraints on Microcontact Printing Imposed by Stamp Deformation. *Langmuir*, *18*(4), 1394–1407. https://doi.org/10.1021/la0113567

Huveneers, S., & de Rooij, J. (2013). Mechanosensitive systems at the cadherin–F-actin interface. *Journal of Cell Science*, *126*(2), 403–413. https://doi.org/10.1242/jcs.109447

Ionescu-Tirgoviste, C., Gagniuc, P. A., Gubceac, E., Mardare, L., Popescu, I., Dima, S., & Militaru, M. (2015). A 3D map of the islet routes throughout the healthy human pancreas. *Scientific Reports*, *5*, 14634.

Jansson, L., & Hellerström, C. (1983). Stimulation by glucose of the blood flow to the pancreatic islets of the rat. *Diabetologia*, *25*(1), 45–50. https://doi.org/10.1007/BF00251896

Jaramillo, M., Mathew, S., Mamiya, H., Goh, S. K., & Banerjee, I. (2015). Endothelial cells mediate islet-specific maturation of human embryonic stem cell-derived pancreatic progenitor cells. *Tissue Engineering. Part A*, *21*(1–2), 14–25. PubMed. https://doi.org/10.1089/ten.TEA.2014.0013

Jaramillo, M., Mathew, S., Task, K., Barner, S., & Banerjee, I. (2014). Potential for Pancreatic Maturation of Differentiating Human Embryonic Stem Cells Is Sensitive to the Specific Pathway of Definitive Endoderm Commitment. *PLOS ONE*, *9*(4), e94307. https://doi.org/10.1371/journal.pone.0094307

Javaherian, S., O'Donnell, K. A., & McGuigan, A. P. (2011). A Fast and Accessible Methodology for Micro-Patterning Cells on Standard Culture Substrates Using Parafilm™ Inserts. *PLOS ONE*, *6*(6), e20909. https://doi.org/10.1371/journal.pone.0020909

Jennings, R. E., Berry, A. A., Kirkwood-Wilson, R., Roberts, N. A., Hearn, T., Salisbury, R. J., Blaylock, J., Piper Hanley, K., & Hanley, N. A. (2013). Development of the Human Pancreas From Foregut to Endocrine Commitment. *Diabetes*, *62*(10), 3514. https://doi.org/10.2337/db12-1479

Jennings, R. E., Berry, A. A., Strutt, J. P., Gerrard, D. T., & Hanley, N. A. (2015). Human pancreas development. *Development*, *142*(18), 3126. https://doi.org/10.1242/dev.120063

Jin, L., Feng, T., Shih, H. P., Zerda, R., Luo, A., Hsu, J., Mahdavi, A., Sander, M., Tirrell, D. A., Riggs, A. D., & Ku, H. T. (2013). Colony-forming cells in the adult mouse pancreas are expandable in Matrigel and form endocrine/acinar colonies in laminin hydrogel. *Proceedings of the National Academy of Sciences of the United States of America*, *110*(10), 3907–3912. PubMed. https://doi.org/10.1073/pnas.1301889110

Jin, L., Gao, D., Feng, T., Tremblay, J. R., Ghazalli, N., Luo, A., Rawson, J., Quijano, J. C., Chai, J., Wedeken, L., Hsu, J., LeBon, J., Walker, S., Shih, H.-P., Mahdavi, A., Tirrell, D. A., Riggs, A. D., & Ku, H. T. (2016). Cells with surface expression of CD133highCD71low are enriched for tripotent colony-forming progenitor cells in the

adult murine pancreas. *Stem Cell Research*, *16*(1), 40–53. https://doi.org/10.1016/j.scr.2015.11.015

Johansson, K. A., Dursun, U., Jordan, N., Gu, G., Beermann, F., Gradwohl, G., & Grapin-Botton, A. (2007). Temporal Control of Neurogenin3 Activity in Pancreas Progenitors Reveals Competence Windows for the Generation of Different Endocrine Cell Types. *Developmental Cell*, *12*(3), 457–465. https://doi.org/10.1016/j.devcel.2007.02.010

Jonkman, J. E. N., Cathcart, J. A., Xu, F., Bartolini, M. E., Amon, J. E., Stevens, K. M., & Colarusso, P. (2014). An introduction to the wound healing assay using live-cell microscopy. *Cell Adhesion & Migration*, *8*(5), 440–451. PubMed. https://doi.org/10.4161/cam.36224

Jun, Y., Lee, J., Choi, S., Yang, J. H., Sander, M., Chung, S., & Lee, S.-H. (2019). In vivo–mimicking microfluidic perfusion culture of pancreatic islet spheroids. *Science Advances*, *5*(11), eaax4520. https://doi.org/10.1126/sciadv.aax4520

Kam, Y., Guess, C., Estrada, L., Weidow, B., & Quaranta, V. (2008). A novel circular invasion assay mimics in vivo invasive behavior of cancer cell lines and distinguishes single-cell motility in vitro. *BMC Cancer*, *8*(1), 198. https://doi.org/10.1186/1471-2407-8-198

Kang, C.-W., & Huang, H. (2017). Deformation, failure and removal mechanisms of thin film structures in abrasive machining. *Advances in Manufacturing*, *5*(1), 1–19. https://doi.org/10.1007/s40436-016-0165-2

Katoh, K., Kano, Y., Amano, M., Kaibuchi, K., & Fujiwara, K. (2001). Stress fiber organization regulated by MLCK and Rho-kinase in cultured human fibroblasts. *American Journal of Physiology-Cell Physiology*, *280*(6), C1669–C1679. https://doi.org/10.1152/ajpcell.2001.280.6.C1669

Kearney, E. M., Farrell, E., Prendergast, P. J., & Campbell, V. A. (2010). Tensile Strain as a Regulator of Mesenchymal Stem Cell Osteogenesis. *Annals of Biomedical Engineering*, *38*(5), 1767–1779. https://doi.org/10.1007/s10439-010-9979-4

Keller, R., Davidson, L. A., & Shook, D. R. (2003). How we are shaped: The biomechanics of gastrulation. *Differentiation*, *71*(3), 171–205. https://doi.org/10.1046/j.1432-0436.2003.710301.x

Kelly, C., McClenaghan, N. H., & Flatt, P. R. (2011). Role of islet structure and cellular interactions in the control of insulin secretion. *Islets*, *3*(2), 41–47. https://doi.org/10.4161/isl.3.2.14805

Khadpekar, A. J., Khan, M., Sose, A., & Majumder, A. (2019). Low Cost and Lithography-free Stamp fabrication for Microcontact Printing. *Scientific Reports*, *9*(1), 1024. https://doi.org/10.1038/s41598-018-36521-x

Kiehart, D. P. (1999). Wound healing: The power of the purse string. *Current Biology*, *9*(16), R602–R605. https://doi.org/10.1016/S0960-9822(99)80384-4

Kilian, K. A., Bugarija, B., Lahn, B. T., & Mrksich, M. (2010). Geometric cues for directing the differentiation of mesenchymal stem cells. *Proceedings of the National Academy of Sciences*, *107*(11), 4872–4877.

Killaars, A. R., Walker, C. J., & Anseth, K. S. (2020). Nuclear mechanosensing controls MSC osteogenic potential through HDAC epigenetic remodeling. *Proceedings of the National Academy of Sciences*, *117*(35), 21258. https://doi.org/10.1073/pnas.2006765117

Kim, D.-H., Han, K., Gupta, K., Kwon, K. W., Suh, K.-Y., & Levchenko, A. (2009). Mechanosensitivity of fibroblast cell shape and movement to anisotropic substratum

topography gradients. *Biomaterials*, *30*(29), 5433–5444. https://doi.org/10.1016/j.biomaterials.2009.06.042

Kim, H. Y., Pang, M.-F., Varner, V. D., Kojima, L., Miller, E., Radisky, D. C., & Nelson, C. M. (2015). Localized Smooth Muscle Differentiation Is Essential for Epithelial Bifurcation during Branching Morphogenesis of the Mammalian Lung. *Developmental Cell*, *34*(6), 719–726. https://doi.org/10.1016/j.devcel.2015.08.012

Kim, J., Kim, H. N., Lim, K.-T., Kim, Y., Seonwoo, H., Park, S. H., Lim, H. J., Kim, D.-H., Suh, K.-Y., Choung, P.-H., Choung, Y.-H., & Chung, J. H. (2013). Designing nanotopographical density of extracellular matrix for controlled morphology and function of human mesenchymal stem cells. *Scientific Reports*, *3*(1), 3552. https://doi.org/10.1038/srep03552

Kim, J., Shim, I. K., Hwang, D. G., Lee, Y. N., Kim, M., Kim, H., Kim, S.-W., Lee, S., Kim, S. C., Cho, D.-W., & Jang, J. (2019). 3D cell printing of islet-laden pancreatic tissue-derived extracellular matrix bioink constructs for enhancing pancreatic functions. *Journal of Materials Chemistry B*, *7*(10), 1773–1781. https://doi.org/10.1039/C8TB02787K

Komatsu, H., Cook, C., Wang, C.-H., Medrano, L., Lin, H., Kandeel, F., Tai, Y.-C., & Mullen, Y. (2017a). Oxygen environment and islet size are the primary limiting factors of isolated pancreatic islet survival. *PLOS ONE*, *12*(8), e0183780. https://doi.org/10.1371/journal.pone.0183780

Komatsu, H., Cook, C., Wang, C.-H., Medrano, L., Lin, H., Kandeel, F., Tai, Y.-C., & Mullen, Y. (2017b). Oxygen environment and islet size are the primary limiting factors of isolated pancreatic islet survival. *PLOS ONE*, *12*(8), e0183780. https://doi.org/10.1371/journal.pone.0183780

Krentz, N. A. J., Lee, M. Y. Y., Xu, E. E., Sproul, S. L. J., Maslova, A., Sasaki, S., & Lynn, F. C. (2018). Single-Cell Transcriptome Profiling of Mouse and hESC-Derived Pancreatic Progenitors. *Stem Cell Reports*, *11*(6), 1551–1564. https://doi.org/10.1016/j.stemcr.2018.11.008

Kroon, E. (2008). Pancreatic endoderm derived from human embryonic stem cells generates glucose-responsive insulin-secreting cells in vivo. *Nat Biotechnol*, *26*. https://doi.org/10.1038/nbt1393

Kubo, A., Stull, R., Takeuchi, M., Bonham, K., Gouon-Evans, V., Sho, M., Iwano, M., Saito, Y., Keller, G., & Snodgrass, R. (2011). Pdx1 and Ngn3 Overexpression Enhances Pancreatic Differentiation of Mouse ES Cell-Derived Endoderm Population. *PLOS ONE*, *6*(9), e24058. https://doi.org/10.1371/journal.pone.0024058

Kuroda, M., Wada, H., Kimura, Y., Ueda, K., & Kioka, N. (2017). Vinculin promotes nuclear localization of TAZ to inhibit ECM stiffness-dependent differentiation into adipocytes. *Journal of Cell Science*, *130*(5), 989–1002. https://doi.org/10.1242/jcs.194779

Kurpinski, K., Chu, J., Hashi, C., & Li, S. (2006). Anisotropic mechanosensing by mesenchymal stem cells. *Proceedings of the National Academy of Sciences*, *103*(44), 16095. https://doi.org/10.1073/pnas.0604182103

LaBarge, M. A., Nelson, C. M., Villadsen, R., Fridriksdottir, A., Ruth, J. R., Stampfer, M. R., Petersen, O. W., & Bissell, M. J. (2009). Human mammary progenitor cell fate decisions are products of interactions with combinatorial microenvironments. *Integrative Biology*, *1*(1), 70–79. https://doi.org/10.1039/B816472J

Lachowski, D., Cortes, E., Robinson, B., Rice, A., Rombouts, K., & Del Río Hernández, A. E. (2018). FAK controls the mechanical activation of YAP, a transcriptional regulator

required for durotaxis. *The FASEB Journal*, *32*(2), 1099–1107. https://doi.org/10.1096/fj.201700721R

Lammert, E., Cleaver, O., & Melton, D. (2001). Induction of Pancreatic Differentiation by Signals from Blood Vessels. *Science*, *294*(5542), 564. https://doi.org/10.1126/science.1064344

Lavon, N., Yanuka, O., & Benvenisty, N. (2006). The Effect of Overexpression of Pdx1 and Foxa2 on the Differentiation of Human Embryonic Stem Cells into Pancreatic Cells. *STEM CELLS*, *24*(8), 1923–1930. https://doi.org/10.1634/stemcells.2005-0397

le Duc, Q., Shi, Q., Blonk, I., Sonnenberg, A., Wang, N., Leckband, D., & de Rooij, J. (2010). Vinculin potentiates E-cadherin mechanosensing and is recruited to actin-anchored sites within adherens junctions in a myosin II–dependent manner. *Journal of Cell Biology*, *189*(7), 1107–1115. https://doi.org/10.1083/jcb.201001149

Lebreton, F., Lavallard, V., Bellofatto, K., Bonnet, R., Wassmer, C. H., Perez, L., Kalandadze, V., Follenzi, A., Boulvain, M., Kerr-Conte, J., Goodman, D. J., Bosco, D., Berney, T., & Berishvili, E. (2019). Insulin-producing organoids engineered from islet and amniotic epithelial cells to treat diabetes. *Nature Communications*, *10*(1), 4491. https://doi.org/10.1038/s41467-019-12472-3

Lecomte, M.-J., Pechberty, S., Machado, C., Da Barroca, S., Ravassard, P., Scharfmann, R., Czernichow, P., & Duvillié, B. (2016). Aggregation of Engineered Human β-Cells Into Pseudoislets: Insulin Secretion and Gene Expression Profile in Normoxic and Hypoxic Milieu. *Cell Medicine*, *8*(3), 99–112. PubMed. https://doi.org/10.3727/215517916X692843

Lee, J., Abdeen, A. A., Wycislo, K. L., Fan, T. M., & Kilian, K. A. (2016). Interfacial geometry dictates cancer cell tumorigenicity. *Nat Mater*, *15*(8), 856–862.

Lee, W., Kalashnikov, N., Mok, S., Halaoui, R., Kuzmin, E., Putnam, A. J., Takayama, S., Park, M., McCaffrey, L., Zhao, R., Leask, R. L., & Moraes, C. (2019). Dispersible hydrogel force sensors reveal patterns of solid mechanical stress in multicellular spheroid cultures. *Nature Communications*, *10*(1), 144. https://doi.org/10.1038/s41467-018-07967-4

Legøy, T. A., Vethe, H., Abadpour, S., Strand, B. L., Scholz, H., Paulo, J. A., Ræder, H., Ghila, L., & Chera, S. (2020). Encapsulation boosts islet-cell signature in differentiating human induced pluripotent stem cells via integrin signalling. *Scientific Reports*, *10*(1), 414. https://doi.org/10.1038/s41598-019-57305-x

Leight, J. L., Liu, W. F., Chaturvedi, R. R., Chen, S., Yang, M. T., Raghavan, S., & Chen, C. S. (2012). Manipulation of 3D Cluster Size and Geometry by Release from 2D Micropatterns. *Cellular and Molecular Bioengineering*, *5*(3), 299–306. PMC. https://doi.org/10.1007/s12195-012-0236-9

Li, L.-C., Qiu, W.-L., Zhang, Y.-W., Xu, Z.-R., Xiao, Y.-N., Hou, C., Lamaoqiezhong, Yu, P., Cheng, X., & Xu, C.-R. (2018). Single-cell transcriptomic analyses reveal distinct dorsal/ventral pancreatic programs. *EMBO Reports*, *19*(10), e46148. PubMed. https://doi.org/10.15252/embr.201846148

Li, X. Y., Wu, S. Y., & Leung, P. S. (2019). Human Fetal Bone Marrow-Derived Mesenchymal Stem Cells Promote the Proliferation and Differentiation of Pancreatic Progenitor Cells and the Engraftment Function of Islet-Like Cell Clusters. *International Journal of Molecular Sciences*, *20*(17), 4083. PubMed. https://doi.org/10.3390/ijms20174083

Liang, C.-C., Park, A. Y., & Guan, J.-L. (2007). In vitro scratch assay: A convenient and inexpensive method for analysis of cell migration in vitro. *Nature Protocols*, *2*, 329.

Liu, H., Guo, D., Ruzi, A., Chen, Y., Pan, T., Yang, F., Li, J., Xu, K., Zhou, T., Qin, D., & Li, Y.-X. (2017). Testosterone improves the differentiation efficiency of insulin-producing cells from human induced pluripotent stem cells. *PloS One*, *12*(6), e0179353–e0179353. PubMed. https://doi.org/10.1371/journal.pone.0179353

Liu, H., Li, R., Liao, H.-K., Min, Z., Wang, C., Yu, Y., Shi, L., Dan, J., Hayek, A., Martinez Martinez, L., Nuñez Delicado, E., & Izpisua Belmonte, J. C. (2021). Chemical combinations potentiate human pluripotent stem cell-derived 3D pancreatic progenitor clusters toward functional β cells. *Nature Communications*, *12*(1), 3330. https://doi.org/10.1038/s41467-021-23525-x

Liu, Y.-S., Liu, Y.-A., Huang, C.-J., Yen, M.-H., Tseng, C.-T., Chien, S., & Lee, O. K. (2015). Mechanosensitive TRPM7 mediates shear stress and modulates osteogenic differentiation of mesenchymal stromal cells through Osterix pathway. *Scientific Reports*, *5*(1), 16522. https://doi.org/10.1038/srep16522

Liu, Z., Tan, J. L., Cohen, D. M., Yang, M. T., Sniadecki, N. J., Ruiz, S. A., Nelson, C. M., & Chen, C. S. (2010). Mechanical tugging force regulates the size of cell–cell junctions. *Proceedings of the National Academy of Sciences*, *107*(22), 9944. https://doi.org/10.1073/pnas.0914547107

Llacua, A., de Haan, B. J., Smink, S. A., & de Vos, P. (2016). Extracellular matrix components supporting human islet function in alginate-based immunoprotective microcapsules for treatment of diabetes. *Journal of Biomedical Materials Research Part A*, *104*(7), 1788–1796. https://doi.org/10.1002/jbm.a.35706

Lock, L. T., Laychock, S. G., & Tzanakakis, E. S. (2011). Pseudoislets in stirred-suspension culture exhibit enhanced cell survival, propagation and insulin secretion. *Journal of Biotechnology*, *151*(3), 278–286. https://doi.org/10.1016/j.jbiotec.2010.12.015

Lou, H.-Y., Zhao, W., Li, X., Duan, L., Powers, A., Akamatsu, M., Santoro, F., McGuire, A. F., Cui, Y., Drubin, D. G., & Cui, B. (2019). Membrane curvature underlies actin reorganization in response to nanoscale surface topography. *Proceedings of the National Academy of Sciences*, *116*(46), 23143. https://doi.org/10.1073/pnas.1910166116

Ludwig, B., Rotem, A., Schmid, J., Weir, G. C., Colton, C. K., Brendel, M. D., Neufeld, T., Block, N. L., Yavriyants, K., Steffen, A., Ludwig, S., Chavakis, T., Reichel, A., Azarov, D., Zimermann, B., Maimon, S., Balyura, M., Rozenshtein, T., Shabtay, N., … Barkai, U. (2012). Improvement of islet function in a bioartificial pancreas by enhanced oxygen supply and growth hormone releasing hormone agonist. *Proceedings of the National Academy of Sciences*, *109*(13), 5022. https://doi.org/10.1073/pnas.1201868109

Ludwig, T. E., Levenstein, M. E., Jones, J. M., Berggren, W. T., Mitchen, E. R., Frane, J. L., Crandall, L. J., Daigh, C. A., Conard, K. R., Piekarczyk, M. S., Llanas, R. A., & Thomson, J. A. (2006). Derivation of human embryonic stem cells in defined conditions. *Nature Biotechnology*, *24*(2), 185–187. https://doi.org/10.1038/nbt1177

Luo, Y., Shen, H., Fang, Y., Cao, Y., Huang, J., Zhang, M., Dai, J., Shi, X., & Zhang, Z. (2015). Enhanced Proliferation and Osteogenic Differentiation of Mesenchymal Stem Cells on Graphene Oxide-Incorporated Electrospun Poly(lactic-co-glycolic acid) Nanofibrous Mats. *ACS Applied Materials & Interfaces*, *7*(11), 6331–6339. https://doi.org/10.1021/acsami.5b00862

Ma, Z., Sagrillo-Fagundes, L., Tran, R., Parameshwar, P. K., Kalashnikov, N., Vaillancourt, C., & Moraes, C. (2019). Biomimetic Micropatterned Adhesive Surfaces To Mechanobiologically Regulate Placental Trophoblast Fusion. *ACS Applied Materials & Interfaces*, *11*(51), 47810–47821. https://doi.org/10.1021/acsami.9b19906

Maas, S. A., Ellis, B. J., Ateshian, G. A., & Weiss, J. A. (2012). FEBio: Finite elements for biomechanics. *Journal of Biomechanical Engineering*, *134*(1), 011005–011005. PubMed. https://doi.org/10.1115/1.4005694

Maas, S. A., LaBelle, S. A., Ateshian, G. A., & Weiss, J. A. (2018). A Plugin Framework for Extending the Simulation Capabilities of FEBio. *Biophysical Journal*, *115*(9), 1630–1637. https://doi.org/10.1016/j.bpj.2018.09.016

Macfarlane, W. M., McKinnon, C. M., Felton-Edkins, Z. A., Cragg, H., James, R. F. L., & Docherty, K. (1999). Glucose Stimulates Translocation of the Homeodomain Transcription Factor PDX1 from the Cytoplasm to the Nucleus in Pancreatic β-Cells. *Journal of Biological Chemistry*, *274*(2), 1011–1016. https://doi.org/10.1074/jbc.274.2.1011

Maldonado, M. (2015). The effects of electrospun substrate-mediated cell colony morphology on the self-renewal of human induced pluripotent stem cells. *Biomaterials.*, *50*. https://doi.org/10.1016/j.biomaterials.2015.01.037

Maldonado, M., Luu, R. J., Ico, G., Ospina, A., Myung, D., Shih, H. P., & Nam, J. (2017). Lineage- and developmental stage-specific mechanomodulation of induced pluripotent stem cell differentiation. *Stem Cell Research & Therapy*, *8*(1), 216. https://doi.org/10.1186/s13287-017-0667-2

Malta, D. F. B., Reticker-Flynn, N. E., da Silva, C. L., Cabral, J. M. S., Fleming, H. E., Zaret, K. S., Bhatia, S. N., & Underhill, G. H. (2016). Extracellular matrix microarrays to study inductive signaling for endoderm specification. *High Throughput Approaches to Screening Biomaterials*, *34*(Supplement C), 30–40. https://doi.org/10.1016/j.actbio.2016.02.014

Mamidi, A., Prawiro, C., Seymour, P. A., de Lichtenberg, K. H., Jackson, A., Serup, P., & Semb, H. (2018a). Mechanosignalling via integrins directs fate decisions of pancreatic progenitors. *Nature*, *564*(7734), 114–118. https://doi.org/10.1038/s41586-018-0762-2

Mamidi, A., Prawiro, C., Seymour, P. A., de Lichtenberg, K. H., Jackson, A., Serup, P., & Semb, H. (2018b). Mechanosignalling via integrins directs fate decisions of pancreatic progenitors. *Nature*, *564*(7734), 114–118. https://doi.org/10.1038/s41586-018-0762-2

Marshak, S., Benshushan, E., Shoshkes, M., Havin, L., Cerasi, E., & Melloul, D. (2000). Functional conservation of regulatory elements in the pdx-1 gene: PDX-1 and hepatocyte nuclear factor 3beta transcription factors mediate beta-cell-specific expression. *Molecular and Cellular Biology*, *20*(20), 7583–7590. PubMed. https://doi.org/10.1128/mcb.20.20.7583-7590.2000

Martino, F., Perestrelo, A. R., Vinarský, V., Pagliari, S., & Forte, G. (2018). Cellular Mechanotransduction: From Tension to Function. *Frontiers in Physiology*, *9*, 824. https://doi.org/10.3389/fphys.2018.00824

Mason, M. N., & Mahoney, M. J. (2008). Selective β-Cell Differentiation of Dissociated Embryonic Pancreatic Precursor Cells Cultured in Synthetic Polyethylene Glycol Hydrogels. *Tissue Engineering Part A*, *15*(6), 1343–1352. https://doi.org/10.1089/ten.tea.2008.0290

McBeath, R., Pirone, D. M., Nelson, C. M., Bhadriraju, K., & Chen, C. S. (2004). Cell Shape, Cytoskeletal Tension, and RhoA Regulate Stem Cell Lineage Commitment. *Developmental Cell*, *6*(4), 483–495. https://doi.org/10.1016/S1534-5807(04)00075-9

McGrath, M. H., & Simon, R. H. (1983). Wound Geometry and the Kinetics of Wound Contraction. *Plastic and Reconstructive Surgery*, *72*(1). https://journals.lww.com/plasreconsurg/Fulltext/1983/07000/Wound_Geometry_and_the_Kinetics_of_Wound.15.aspx

McMahon, L. A., Reid, A. J., Campbell, V. A., & Prendergast, P. J. (2008). Regulatory Effects of Mechanical Strain on the Chondrogenic Differentiation of MSCs in a Collagen-GAG Scaffold: Experimental and Computational Analysis. *Annals of Biomedical Engineering*, *36*(2), 185–194. https://doi.org/10.1007/s10439-007-9416-5

Medina, J. D., Alexander, M., Hunckler, M. D., Fernández-Yagüe, M. A., Coronel, M. M., Smink, A. M., Lakey, J. R., de Vos, P., & García, A. J. (2020). Functionalization of Alginate with Extracellular Matrix Peptides Enhances Viability and Function of Encapsulated Porcine Islets. *Advanced Healthcare Materials*, *9*(9), 2000102. https://doi.org/10.1002/adhm.202000102

Meijering, E., Dzyubachyk, O., & Smal, I. (2012). Chapter nine—Methods for Cell and Particle Tracking. In P. M. conn (Ed.), *Methods in Enzymology* (Vol. 504, pp. 183–200). Academic Press. https://doi.org/10.1016/B978-0-12-391857-4.00009-4

Micallef, S. J., Li, X., Schiesser, J. V., Hirst, C. E., Yu, Q. C., Lim, S. M., Nostro, M. C., Elliott, D. A., Sarangi, F., Harrison, L. C., Keller, G., Elefanty, A. G., & Stanley, E. G. (2012). INSGFP/whuman embryonic stem cells facilitate isolation of in vitro derived insulin-

producing cells. *Diabetologia*, *55*(3), 694–706. https://doi.org/10.1007/s00125-011-2379-y

Mihara, Y., Matsuura, K., Sakamoto, Y., Okano, T., Kokudo, N., & Shimizu, T. (2017). Production of pancreatic progenitor cells from human induced pluripotent stem cells using a three-dimensional suspension bioreactor system. *Journal of Tissue Engineering and Regenerative Medicine*, n/a-n/a. https://doi.org/10.1002/term.2228

Mihic, A., Li, J., Miyagi, Y., Gagliardi, M., Li, S.-H., Zu, J., Weisel, R. D., Keller, G., & Li, R.-K. (2014). The effect of cyclic stretch on maturation and 3D tissue formation of human embryonic stem cell-derived cardiomyocytes. *Biomaterials*, *35*(9), 2798–2808. https://doi.org/10.1016/j.biomaterials.2013.12.052

Millman, J. R., Xie, C., Van Dervort, A., Gürtler, M., Pagliuca, F. W., & Melton, D. A. (2016). Generation of stem cell-derived β-cells from patients with type 1 diabetes. *Nature Communications*, *7*, 11463.

Minteer, D. M., Gerlach, J. C., & Marra, K. G. (2014). Bioreactors addressing diabetes mellitus. *Journal of Diabetes Science and Technology*, *8*(6), 1227–1232. PubMed. https://doi.org/10.1177/1932296814548215

Miri, A. K., Mirzaee, I., Hassan, S., Mesbah Oskui, S., Nieto, D., Khademhosseini, A., & Zhang, Y. S. (2019). Effective bioprinting resolution in tissue model fabrication. *Lab on a Chip*, *19*(11), 2019–2037. https://doi.org/10.1039/C8LC01037D

Monjaret, F., Fernandes, M., Duchemin-Pelletier, E., Argento, A., Degot, S., & Young, J. (2015). Fully Automated One-Step Production of Functional 3D Tumor Spheroids for High-Content Screening. *Journal of Laboratory Automation*, *21*(2), 268–280. https://doi.org/10.1177/2211068215607058

Moraes, C., Chen, J.-H., Sun, Y., & Simmons, C. A. (2010). Microfabricated arrays for high-throughput screening of cellular response to cyclic substrate deformation. *Lab on a Chip*, *10*(2), 227–234. https://doi.org/10.1039/B914460A

Moraes, C., Sun, Y., & Simmons, C. A. (2011). (Micro)managing the mechanical microenvironment. *Integrative Biology*, *3*(10), 959–971. https://doi.org/10.1039/c1ib00056j

Moriguchi, H., & Yasuda, K. (2006). Photothermal Microneedle Etching: Improved Three-Dimensional Microfabrication Method for Agarose Gel for Topographical Control of Cultured Cell Communities. *Japanese Journal of Applied Physics*, *45*(No. 30), L796–L799. https://doi.org/10.1143/jjap.45.l796

Motté, E., Szepessy, E., Suenens, K., Stangé, G., Bomans, M., Jacobs-Tulleneers-Thevissen, D., Ling, Z., Kroon, E., & Pipeleers, D. (2014). Composition and function of macroencapsulated human embryonic stem cell-derived implants: Comparison with clinical human islet cell grafts. *American Journal of Physiology-Endocrinology and Metabolism*, *307*(9), E838–E846. https://doi.org/10.1152/ajpendo.00219.2014

Mui, K. L., Chen, C. S., & Assoian, R. K. (2016). The mechanical regulation of integrin-cadherin crosstalk organizes cells, signaling and forces. *Journal of Cell Science*, *129*(6), 1093–1100. PubMed. https://doi.org/10.1242/jcs.183699

Murrell, M., Kamm, R., & Matsudaira, P. (2011). Tension, Free Space, and Cell Damage in a Microfluidic Wound Healing Assay. *PLOS ONE*, *6*(9), e24283. https://doi.org/10.1371/journal.pone.0024283

Nair, G. G., Liu, J. S., Russ, H. A., Tran, S., Saxton, M. S., Chen, R., Juang, C., Li, M., Nguyen, V. Q., Giacometti, S., Puri, S., Xing, Y., Wang, Y., Szot, G. L., Oberholzer, J., Bhushan,

A., & Hebrok, M. (2019). Recapitulating endocrine cell clustering in culture promotes maturation of human stem-cell-derived β cells. *Nature Cell Biology*, *21*(2), 263–274. https://doi.org/10.1038/s41556-018-0271-4

Nakayama, K. H., Hou, L., & Huang, N. F. (2014). Role of Extracellular Matrix Signaling Cues in Modulating Cell Fate Commitment for Cardiovascular Tissue Engineering. *Advanced Healthcare Materials*, *3*(5), 628–641. PMC. https://doi.org/10.1002/adhm.201300620

Nam, K.-H., Kim, P., Wood, D. K., Kwon, S., Provenzano, P. P., & Kim, D.-H. (2016). Multiscale Cues Drive Collective Cell Migration. *Scientific Reports*, *6*, 29749.

Narayanan, K., Lim, V. Y., Shen, J., Tan, Z. W., Rajendran, D., Luo, S.-C., Gao, S., Wan, A. C. A., & Ying, J. Y. (2013). Extracellular Matrix-Mediated Differentiation of Human Embryonic Stem Cells: Differentiation to Insulin-Secreting Beta Cells. *Tissue Engineering Part A*, *20*(1–2), 424–433. https://doi.org/10.1089/ten.tea.2013.0257

Nardone, G., Oliver-De La Cruz, J., Vrbsky, J., Martini, C., Pribyl, J., Skládal, P., Pešl, M., Caluori, G., Pagliari, S., Martino, F., Maceckova, Z., Hajduch, M., Sanz-Garcia, A., Pugno, N. M., Stokin, G. B., & Forte, G. (2017). YAP regulates cell mechanics by controlling focal adhesion assembly. *Nature Communications*, *8*(1), 15321. https://doi.org/10.1038/ncomms15321

Naujok, O., Francini, F., Picton, S., Bailey, C. J., Lenzen, S., & Jörns, A. (2009). Changes in gene expression and morphology of mouse embryonic stem cells on differentiation into insulin-producing cells in vitro and in vivo. *Diabetes/Metabolism Research and Reviews*, *25*(5), 464–476. https://doi.org/10.1002/dmrr.965

Negi, S., Jetha, A., Aikin, R., Hasilo, C., Sladek, R., & Paraskevas, S. (2012). Analysis of Beta-Cell Gene Expression Reveals Inflammatory Signaling and Evidence of Dedifferentiation

following Human Islet Isolation and Culture. *PLOS ONE*, *7*(1), e30415. https://doi.org/10.1371/journal.pone.0030415

Nelson, C. M., Jean, R. P., Tan, J. L., Liu, W. F., Sniadecki, N. J., Spector, A. A., & Chen, C. S. (2005). Emergent patterns of growth controlled by multicellular form and mechanics. *Proceedings of the National Academy of Sciences of the United States of America*, *102*(33), 11594–11599. https://doi.org/10.1073/pnas.0502575102

Nelson, C. M., Liu, W. F., & Chen, C. S. (2007). Manipulation of Cell-Cell Adhesion Using Bowtie-Shaped Microwells. In A. S. Coutts (Ed.), *Adhesion Protein Protocols* (pp. 1–9). Humana Press. https://doi.org/10.1007/978-1-59745-353-0_1

Nelson, C. M., Raghavan, S., Tan, J. L., & Chen, C. S. (2003). Degradation of Micropatterned Surfaces by Cell-Dependent and -Independent Processes. *Langmuir*, *19*(5), 1493–1499. https://doi.org/10.1021/la026178b

Nelson, C. M., Vanduijn, M. M., Inman, J. L., Fletcher, D. A., & Bissell, M. J. (2006). Tissue geometry determines sites of mammary branching morphogenesis in organotypic cultures. *Science (New York, N.Y.)*, *314*(5797), 298–300. PubMed. https://doi.org/10.1126/science.1131000

Nelson, S. B., Schaffer, A. E., & Sander, M. (2007). The transcription factors Nkx6.1 and Nkx6.2 possess equivalent activities in promoting beta-cell fate specification in $Pdx1^{+}$ pancreatic progenitor cells. *Development*, *134*(13), 2491. https://doi.org/10.1242/dev.002691

Nostro, M. C., Sarangi, F., Yang, C., Holland, A., Elefanty, A. G., Stanley, E. G., Greiner, D. L., & Keller, G. (2015). Efficient Generation of NKX6-1(+) Pancreatic Progenitors from

Multiple Human Pluripotent Stem Cell Lines. *Stem Cell Reports*, *4*(4), 591–604. PMC. https://doi.org/10.1016/j.stemcr.2015.02.017

Nourmohammadzadeh, M., Xing, Y., Lee, J. W., Bochenek, M. A., Mendoza-Elias, J. E., McGarrigle, J. J., Marchese, E., Chun-Chieh, Y., Eddington, D. T., Oberholzer, J., & Wang, Y. (2016). A microfluidic array for real-time live-cell imaging of human and rodent pancreatic islets. *Lab on a Chip*, *16*(8), 1466–1472. PubMed. https://doi.org/10.1039/c5lc01173f

Nourse, J. L., & Pathak, M. M. (2017). How cells channel their stress: Interplay between Piezo1 and the cytoskeleton. *Seminars in Cell & Developmental Biology*, *71*, 3–12. PubMed. https://doi.org/10.1016/j.semcdb.2017.06.018

Nyegaard, S., Christensen, B., & Rasmussen, J. T. (2016). An optimized method for accurate quantification of cell migration using human small intestine cells. *Metabolic Engineering Communications*, *3*, 76–83. https://doi.org/10.1016/j.meteno.2016.03.002

Nyeng, P., Heilmann, S., Löf-Öhlin, Z. M., Pettersson, N. F., Hermann, F. M., Reynolds, A. B., & Semb, H. (2019). P120ctn-Mediated Organ Patterning Precedes and Determines Pancreatic Progenitor Fate. *Developmental Cell*, *49*(1), 31-47.e9. https://doi.org/10.1016/j.devcel.2019.02.005

Nyitray, C. E., Chavez, M. G., & Desai, T. A. (2014). Compliant 3D microenvironment improves β-cell cluster insulin expression through mechanosensing and β-catenin signaling. *Tissue Engineering. Part A*, *20*(13–14), 1888–1895. PubMed. https://doi.org/10.1089/ten.TEA.2013.0692

Offield, M. F., Jetton, T. L., Labosky, P. A., Ray, M., Stein, R. W., Magnuson, M. A., Hogan, B. L., & Wright, C. V. (1996). PDX-1 is required for pancreatic outgrowth and differentiation of the rostral duodenum. *Development*, *122*(3), 983.

Ohlsson, H., Karlsson, K., & Edlund, T. (1993). IPF1, a homeodomain-containing transactivator of the insulin gene. *The EMBO Journal*, *12*(11), 4251–4259. https://doi.org/10.1002/j.1460-2075.1993.tb06109.x

Oliver-De La Cruz, J., Nardone, G., Vrbsky, J., Pompeiano, A., Perestrelo, A. R., Capradossi, F., Melajová, K., Filipensky, P., & Forte, G. (2019). Substrate mechanics controls adipogenesis through YAP phosphorylation by dictating cell spreading. *Biomaterials*, *205*, 64–80. https://doi.org/10.1016/j.biomaterials.2019.03.009

Osafune, K., Caron, L., Borowiak, M., Martinez, R. J., Fitz-Gerald, C. S., Sato, Y., Cowan, C. A., Chien, K. R., & Melton, D. A. (2008). Marked differences in differentiation propensity among human embryonic stem cell lines. *Nature Biotechnology*, *26*(3), 313–315. https://doi.org/10.1038/nbt1383

O'Sullivan, E. S., Vegas, A., Anderson, D. G., & Weir, G. C. (2011). Islets Transplanted in Immunoisolation Devices: A Review of the Progress and the Challenges that Remain. *Endocrine Reviews*, *32*(6), 827–844. https://doi.org/10.1210/er.2010-0026

Pagliuca, F. W., Millman, J. R., Gürtler, M., Segel, M., Van Dervort, A., Ryu, J. H., Peterson, Q. P., Greiner, D., & Melton, D. A. (2014). Generation of Functional Human Pancreatic β Cells In Vitro. *Cell*, *159*(2), 428–439. https://doi.org/10.1016/j.cell.2014.09.040

Pan, F. C., & Wright, C. (2011). Pancreas organogenesis: From bud to plexus to gland. *Developmental Dynamics*, *240*(3), 530–565. https://doi.org/10.1002/dvdy.22584

Panzetta, V., Fusco, S., & Netti, P. A. (2019). Cell mechanosensing is regulated by substrate strain energy rather than stiffness. *Proceedings of the National Academy of Sciences*, *116*(44), 22004. https://doi.org/10.1073/pnas.1904660116

Paraskevas, S., Maysinger, D., Wang, R., Duguid, W. P., & Rosenberg, L. (2000). Cell Loss in Isolated Human Islets Occurs by Apoptosis. *Pancreas*, *20*(3). https://journals.lww.com/pancreasjournal/Fulltext/2000/04000/Cell_Loss_in_Isolated_Human_Islets_Occurs_by.8.aspx

Park, J., Kim, D.-H., Shah, S. R., Kim, H.-N., Kshitiz, Kim, P., Quiñones-Hinojosa, A., & Levchenko, A. (2019). Switch-like enhancement of epithelial-mesenchymal transition by YAP through feedback regulation of WT1 and Rho-family GTPases. *Nature Communications*, *10*(1), 2797. https://doi.org/10.1038/s41467-019-10729-5

Pedersen, J. K., Nelson, S. B., Jorgensen, M. C., Henseleit, K. D., Fujitani, Y., Wright, C. V. E., Sander, M., & Serup, P. (2005). Endodermal expression of Nkx6 genes depends differentially on Pdx1. *Developmental Biology*, *288*(2), 487–501. https://doi.org/10.1016/j.ydbio.2005.10.001

Pedersen, M. G., Bertram, R., & Sherman, A. (2005). Intra- and Inter-Islet Synchronization of Metabolically Driven Insulin Secretion. *Biophysical Journal*, *89*(1), 107–119. PMC. https://doi.org/10.1529/biophysj.104.055681

Peng, T., Liu, L., MacLean, A. L., Wong, C. W., Zhao, W., & Nie, Q. (2017). A mathematical model of mechanotransduction reveals how mechanical memory regulates mesenchymal stem cell fate decisions. *BMC Systems Biology*, *11*(1), 55. https://doi.org/10.1186/s12918-017-0429-x

Pennarossa, G., Santoro, R., Manzoni, E. F. M., Pesce, M., Gandolfi, F., & Brevini, T. A. L. (2018). Epigenetic Erasing and Pancreatic Differentiation of Dermal Fibroblasts into Insulin-Producing Cells are Boosted by the Use of Low-Stiffness Substrate. *Stem Cell Reviews and Reports*, *14*(3), 398–411. https://doi.org/10.1007/s12015-017-9799-0

Petersen, M. B. K., Azad, A., Ingvorsen, C., Hess, K., Hansson, M., Grapin-Botton, A., & Honoré, C. (2017). Single-Cell Gene Expression Analysis of a Human ESC Model of Pancreatic Endocrine Development Reveals Different Paths to β-Cell Differentiation. *Stem Cell Reports*, *9*(4), 1246–1261. https://doi.org/10.1016/j.stemcr.2017.08.009

Piccand, J., Meunier, A., Merle, C., Jia, Z., Barnier, J.-V., & Gradwohl, G. (2014). Pak3 promotes cell cycle exit and differentiation of β-cells in the embryonic pancreas and is necessary to maintain glucose homeostasis in adult mice. *Diabetes*, *63*(1), 203–215. PubMed. https://doi.org/10.2337/db13-0384

Piccolo, S., Cordenonsi, M., & Dupont, S. (2013). Molecular Pathways: YAP and TAZ Take Center Stage in Organ Growth and Tumorigenesis. *Clinical Cancer Research*, *19*(18), 4925. https://doi.org/10.1158/1078-0432.CCR-12-3172

Piccolo, S., Dupont, S., & Cordenonsi, M. (2014). The Biology of YAP/TAZ: Hippo Signaling and Beyond. *Physiological Reviews*, *94*(4), 1287–1312. https://doi.org/10.1152/physrev.00005.2014

Piper, K., Brickwood, S., Turnpenny, L., Cameron, I., Ball, S., Wilson, D., & Hanley, N. (2004). Beta cell differentiation during early human pancreas development. *Journal of Endocrinology*, *181*(1), 11–23. https://doi.org/10.1677/joe.0.1810011

Poh, Y.-C., Chen, J., Hong, Y., Yi, H., Zhang, S., Chen, J., Wu, D. C., Wang, L., Jia, Q., Singh, R., Yao, W., Tan, Y., Tajik, A., Tanaka, T. S., & Wang, N. (2014). *Generation of organized germ layers from a single mouse embryonic stem cell*. *5*, 4000.

Polte, T. R., Eichler, G. S., Wang, N., & Ingber, D. E. (2004). Extracellular matrix controls myosin light chain phosphorylation and cell contractility through modulation of cell shape and cytoskeletal prestress. *American Journal of Physiology-Cell Physiology*, *286*(3), C518–C528. https://doi.org/10.1152/ajpcell.00280.2003

Preibisch, S., Saalfeld, S., & Tomancak, P. (2009). Globally optimal stitching of tiled 3D microscopic image acquisitions. *Bioinformatics (Oxford, England)*, *25*(11), 1463–1465. PubMed. https://doi.org/10.1093/bioinformatics/btp184

Qin, J., Tao, T., Wang, Y., Chen, W., Li, Z., su, wentao, Guo, Y., & Deng, P. (2019). Engineering human islet organoids from iPSCs using an organ-on-chip platform. *Lab on a Chip*. https://doi.org/10.1039/C8LC01298A

Raghavan, S., Desai, R. A., Kwon, Y., Mrksich, M., & Chen, C. S. (2010). Micropatterned Dynamically Adhesive Substrates for Cell Migration. *Langmuir*, *26*(22), 17733–17738. https://doi.org/10.1021/la102955m

Rajagopal, J., Anderson, W. J., Kume, S., Martinez, O. I., & Melton, D. A. (2003). Insulin Staining of ES Cell Progeny from Insulin Uptake. *Science*, *299*(5605), 363. https://doi.org/10.1126/science.1077838

Ramachandran, K., Huang, H.-H., & Stehno-Bittel, L. (2015). A Simple Method to Replace Islet Equivalents for Volume Quantification of Human Islets. *Cell Transplantation*, *24*(7), 1183–1194. https://doi.org/10.3727/096368914X681928

Rape, A., Guo, W., & Wang, Y. (2011). The Regulation of Traction Force in Relation to Cell Shape and Focal Adhesions. *Biomaterials*, *32*(8), 2043–2051. PMC. https://doi.org/10.1016/j.biomaterials.2010.11.044

Rasmussen, C. H., Petersen, D. R., Moeller, J. B., Hansson, M., & Dufva, M. (2016). Collagen Type I Improves the Differentiation of Human Embryonic Stem Cells towards Definitive Endoderm. *PLOS ONE*, *10*(12), e0145389. https://doi.org/10.1371/journal.pone.0145389

Rasmussen, C. H., Reynolds, P. M., Petersen, D. R., Hansson, M., McMeeking, R. M., Dufva, M., & Gadegaard, N. (2016a). Enhanced Differentiation of Human Embryonic Stem Cells Toward Definitive Endoderm on Ultrahigh Aspect Ratio Nanopillars. *Advanced Functional Materials*, *26*(6), 815–823. https://doi.org/10.1002/adfm.201504204

Rasmussen, C. H., Reynolds, P. M., Petersen, D. R., Hansson, M., McMeeking, R. M., Dufva, M., & Gadegaard, N. (2016b). Enhanced Differentiation of Human Embryonic Stem Cells Toward Definitive Endoderm on Ultrahigh Aspect Ratio Nanopillars. *Advanced Functional Materials*, *26*(6), 815–823. https://doi.org/10.1002/adfm.201504204

Ravichandran, A., Lim, J., Chong, M. S. K., Wen, F., Liu, Y., Pillay, Y. T., Chan, J. K. Y., & Teoh, S.-H. (2017). In vitro cyclic compressive loads potentiate early osteogenic events in engineered bone tissue. *Journal of Biomedical Materials Research Part B: Applied Biomaterials*, *105*(8), 2366–2375. https://doi.org/10.1002/jbm.b.33772

Rezania, A., Bruin, J. E., Arora, P., Rubin, A., Batushansky, I., Asadi, A., O'Dwyer, S., Quiskamp, N., Mojibian, M., Albrecht, T., Yang, Y. H. C., Johnson, J. D., & Kieffer, T. J. (2014). Reversal of diabetes with insulin-producing cells derived in vitro from human pluripotent stem cells. *Nat Biotech*, *32*(11), 1121–1133.

Rezania, A., Bruin, J. E., Riedel, M. J., Mojibian, M., Asadi, A., Xu, J., Gauvin, R., Narayan, K., Karanu, F., O'Neil, J. J., Ao, Z., Warnock, G. L., & Kieffer, T. J. (2012). Maturation of Human Embryonic Stem Cell–Derived Pancreatic Progenitors Into Functional Islets Capable of Treating Pre-existing Diabetes in Mice. *Diabetes*, *61*(8), 2016–2029. PMC. https://doi.org/10.2337/db11-1711

Rezania, A., Bruin, J. E., Xu, J., Narayan, K., Fox, J. K., O'Neil, J. J., & Kieffer, T. J. (2013). Enrichment of human embryonic stem cell-derived NKX6.1-expressing pancreatic progenitor cells accelerates the maturation of insulin-secreting cells in vivo. *STEM CELLS*, *31*(11), 2432–2442. https://doi.org/10.1002/stem.1489

Riahi, R., Yang, Y., Zhang, D. D., & Wong, P. K. (2012). Advances in Wound-Healing Assays for Probing Collective Cell Migration. *Journal of Laboratory Automation*, *17*(1), 59–65. https://doi.org/10.1177/2211068211426550

Richardson, T., Barner, S., Candiello, J., Kumta, P. N., & Banerjee, I. (2016). Capsule stiffness regulates the efficiency of pancreatic differentiation of human embryonic stem cells. *Acta Biomaterialia*, *35*, 153–165. https://doi.org/10.1016/j.actbio.2016.02.025

Robert, T., De Mesmaeker, I., Stangé, G. M., Suenens, K. G., Ling, Z., Kroon, E. J., & Pipeleers, D. G. (2018). Functional Beta Cell Mass from Device-Encapsulated hESC-Derived Pancreatic Endoderm Achieving Metabolic Control. *Stem Cell Reports*, *10*(3), 739–750. https://doi.org/10.1016/j.stemcr.2018.01.040

Rocheleau, J. V., Walker, G. M., Head, W. S., McGuinness, O. P., & Piston, D. W. (2004). Microfluidic glucose stimulation reveals limited coordination of intracellular Ca^{2+} activity oscillations in pancreatic islets. *Proceedings of the National Academy of Sciences*

of the United States of America, *101*(35), 12899. https://doi.org/10.1073/pnas.0405149101

Rodriguez, L. G., Wu, X., & Guan, J.-L. (2005). Wound-Healing Assay. In J.-L. Guan (Ed.), *Cell Migration: Developmental Methods and Protocols* (pp. 23–29). Humana Press. https://doi.org/10.1385/1-59259-860-9:023

Rodriguez, N. M., Desai, R. A., Trappmann, B., Baker, B. M., & Chen, C. S. (2014). Micropatterned multicolor dynamically adhesive substrates to control cell adhesion and multicellular organization. *Langmuir : The ACS Journal of Surfaces and Colloids*, *30*(5), 1327–1335. PubMed. https://doi.org/10.1021/la404037s

Rodriguez-Diaz, A., Toyama, Y., Abravanel, D. L., Wiemann, J. M., Wells, A. R., Tulu, U. S., Edwards, G. S., & Kiehart, D. P. (2008). Actomyosin purse strings: Renewable resources that make morphogenesis robust and resilient. *HFSP Journal*, *2*(4), 220–237. PubMed. https://doi.org/10.2976/1.2955565

Rosado-Olivieri, E. A., Anderson, K., Kenty, J. H., & Melton, D. A. (2019). YAP inhibition enhances the differentiation of functional stem cell-derived insulin-producing β cells. *Nature Communications*, *10*(1), 1464. https://doi.org/10.1038/s41467-019-09404-6

Rosenberg, L., Wang, R., Paraskevas, S., & Maysinger, D. (1999). Structural and functional changes resulting from islet isolation lead to islet cell death. *Surgery*, *126*(2), 393–398. https://doi.org/10.1016/S0039-6060(99)70183-2

Rostovskaya, M., Bredenkamp, N., & Smith, A. (2015). Towards consistent generation of pancreatic lineage progenitors from human pluripotent stem cells. *Philosophical Transactions of the Royal Society of London. Series B, Biological Sciences*, *370*(1680), 20140365–20140365. PubMed. https://doi.org/10.1098/rstb.2014.0365

Roy, S., Darque-Ceretti, E., Felder, E., Raynal, F., & Bispo, I. (2010). Experimental analysis and finite element modelling of nano-scratch test applied on 40–120nm SiCN thin films deposited on Cu/Si substrate. *Thin Solid Films*, *518*(14), 3859–3865. https://doi.org/10.1016/j.tsf.2010.02.004

Rozario, T., & DeSimone, D. W. (2010). The Extracellular Matrix In Development and Morphogenesis: A Dynamic View. *Developmental Biology*, *341*(1), 126–140. PMC. https://doi.org/10.1016/j.ydbio.2009.10.026

Ruiz, S. A., & Chen, C. S. (2008). Emergence of Patterned Stem Cell Differentiation Within Multicellular Structures. *STEM CELLS*, *26*(11), 2921–2927. https://doi.org/10.1634/stemcells.2008-0432

Russ, H. A., Parent, A. V., Ringler, J. J., Hennings, T. G., Nair, G. G., Shveygert, M., Guo, T., Puri, S., Haataja, L., Cirulli, V., Blelloch, R., Szot, G. L., Arvan, P., & Hebrok, M. (2015). Controlled induction of human pancreatic progenitors produces functional beta-like cells in vitro. *The EMBO Journal*, *34*(13), 1759–1772. PMC. https://doi.org/10.15252/embj.201591058

Sabatini, P. V., Speckmann, T., & Lynn, F. C. (2019). Friend and foe: β-cell Ca2+ signaling and the development of diabetes. *Molecular Metabolism*, *21*, 1–12. https://doi.org/10.1016/j.molmet.2018.12.007

Sackett, S. D., Tremmel, D. M., Ma, F., Feeney, A. K., Maguire, R. M., Brown, M. E., Zhou, Y., Li, X., O'Brien, C., Li, L., Burlingham, W. J., & Odorico, J. S. (2018). Extracellular matrix scaffold and hydrogel derived from decellularized and delipidized human pancreas. *Scientific Reports*, *8*(1), 10452. https://doi.org/10.1038/s41598-018-28857-1

Saha, S., Ji, L., de Pablo, J. J., & Palecek, S. P. (2006). Inhibition of human embryonic stem cell differentiation by mechanical strain. *Journal of Cellular Physiology*, *206*(1), 126–137. https://doi.org/10.1002/jcp.20441

Sakar, M. S., Eyckmans, J., Pieters, R., Eberli, D., Nelson, B. J., & Chen, C. S. (2016). Cellular forces and matrix assembly coordinate fibrous tissue repair. *Nature Communications*, *7*(1), 11036. https://doi.org/10.1038/ncomms11036

Samols, E., Marri, G., & Marks, V. (1965). PROMOTION OF INSULIN SECRETION BY GLUCAGON. *Originally Published as Volume 2, Issue 7409*, *286*(7409), 415–416. https://doi.org/10.1016/S0140-6736(65)90761-0

Sander, M., Sussel, L., Conners, J., Scheel, D., Kalamaras, J., Dela Cruz, F., Schwitzgebel, V., Hayes-Jordan, A., & German, M. (2000). Homeobox gene Nkx6.1 lies downstream of Nkx2.2 in the major pathway of beta-cell formation in the pancreas. *Development*, *127*(24), 5533.

Sankar, K. S., Green, B. J., Crocker, A. R., Verity, J. E., Altamentova, S. M., & Rocheleau, J. V. (2011). Culturing Pancreatic Islets in Microfluidic Flow Enhances Morphology of the Associated Endothelial Cells. *PLOS ONE*, *6*(9), e24904. https://doi.org/10.1371/journal.pone.0024904

Schaffer, A. E., Taylor, B. L., Benthuysen, J. R., Liu, J., Thorel, F., Yuan, W., Jiao, Y., Kaestner, K. H., Herrera, P. L., Magnuson, M. A., May, C. L., & Sander, M. (2013). Nkx6.1 Controls a Gene Regulatory Network Required for Establishing and Maintaining Pancreatic Beta Cell Identity. *PLOS Genetics*, *9*(1), e1003274. https://doi.org/10.1371/journal.pgen.1003274

Schindelin, J., Arganda-Carreras, I., Frise, E., Kaynig, V., Longair, M., Pietzsch, T., Preibisch, S., Rueden, C., Saalfeld, S., & Schmid, B. (2012). Fiji: An open-source platform for biological-image analysis. *Nature Methods*, *9*(7), 676–682.

Schneider, D., Baronsky, T., Pietuch, A., Rother, J., Oelkers, M., Fichtner, D., Wedlich, D., & Janshoff, A. (2013). Tension Monitoring during Epithelial-to-Mesenchymal Transition Links the Switch of Phenotype to Expression of Moesin and Cadherins in NMuMG Cells. *PLOS ONE*, *8*(12), e80068. https://doi.org/10.1371/journal.pone.0080068

Schulz, T. C., Young, H. Y., Agulnick, A. D., Babin, M. J., Baetge, E. E., Bang, A. G., Bhoumik, A., Cepa, I., Cesario, R. M., Haakmeester, C., Kadoya, K., Kelly, J. R., Kerr, J., Martinson, L. A., McLean, A. B., Moorman, M. A., Payne, J. K., Richardson, M., Ross, K. G., … Robins, A. J. (2012). A Scalable System for Production of Functional Pancreatic Progenitors from Human Embryonic Stem Cells. *PLOS ONE*, *7*(5), e37004. https://doi.org/10.1371/journal.pone.0037004

Shapiro, A. M. J., Lakey, J. R. T., Ryan, E. A., Korbutt, G. S., Toth, E., Warnock, G. L., Kneteman, N. M., & Rajotte, R. V. (2000). Islet Transplantation in Seven Patients with Type 1 Diabetes Mellitus Using a Glucocorticoid-Free Immunosuppressive Regimen. *New England Journal of Medicine*, *343*(4), 230–238. https://doi.org/10.1056/NEJM200007273430401

Shapiro, A. M. J., Pokrywczynska, M., & Ricordi, C. (2017). Clinical pancreatic islet transplantation. *Nat Rev Endocrinol*, *13*(5), 268–277.

Sharma, A., Yerra, V. G., & Kumar, A. (2017). Emerging role of Hippo signalling in pancreatic biology: YAP re-expression and plausible link to islet cell apoptosis and replication. *Biochimie*, *133*, 56–65. https://doi.org/10.1016/j.biochi.2016.12.009

Sharon, N., Chawla, R., Mueller, J., Vanderhooft, J., Whitehorn, L. J., Rosenthal, B., Gürtler, M., Estanboulieh, R. R., Shvartsman, D., Gifford, D. K., Trapnell, C., & Melton, D. (2019). A Peninsular Structure Coordinates Asynchronous Differentiation with Morphogenesis to Generate Pancreatic Islets. *Cell*, *176*(4), 790-804.e13. PubMed. https://doi.org/10.1016/j.cell.2018.12.003

Sharon, N., Vanderhooft, J., Straubhaar, J., Mueller, J., Chawla, R., Zhou, Q., Engquist, E. N., Trapnell, C., Gifford, D. K., & Melton, D. A. (2019). Wnt Signaling Separates the Progenitor and Endocrine Compartments during Pancreas Development. *Cell Reports*, *27*(8), 2281-2291.e5. https://doi.org/10.1016/j.celrep.2019.04.083

Shenkman, R. M., Godoy-Silva, R., Papas, K. K., & Chalmers, J. J. (2009). Effects of energy dissipation rate on islets of Langerhans: Implications for isolation and transplantation. *Biotechnology and Bioengineering*, *103*(2), 413–423. PubMed. https://doi.org/10.1002/bit.22241

Shih, H. P., Panlasigui, D., Cirulli, V., & Sander, M. (2016). ECM Signaling Regulates Collective Cellular Dynamics to Control Pancreas Branching Morphogenesis. *Cell Reports*, *14*(2), 169–179. https://doi.org/10.1016/j.celrep.2015.12.027

Silva, P. N., Green, B. J., Altamentova, S. M., & Rocheleau, J. V. (2013). A microfluidic device designed to induce media flow throughout pancreatic islets while limiting shear-induced damage. *Lab on a Chip*, *13*(22), 4374–4384. https://doi.org/10.1039/C3LC50680K

Simpson, K. J., Selfors, L. M., Bui, J., Reynolds, A., Leake, D., Khvorova, A., & Brugge, J. S. (2008). Identification of genes that regulate epithelial cell migration using an siRNA screening approach. *Nature Cell Biology*, *10*, 1027.

Sipione, S., Eshpeter, A., Lyon, J. G., Korbutt, G. S., & Bleackley, R. C. (2004). Insulin expressing cells from differentiated embryonic stem cells are not beta cells. *Diabetologia*, *47*(3), 499–508. https://doi.org/10.1007/s00125-004-1349-z

Somers, S. M., & Grayson, W. L. (2021). Protocol for the Use of a Novel Bioreactor System for Hydrated Mechanical Testing, Strained Sterile Culture, and Force of Contraction Measurement of Tissue Engineered Muscle Constructs. *Frontiers in Cell and Developmental Biology*, *9*, 815. https://doi.org/10.3389/fcell.2021.661036

Song, J., & Millman, J. R. (2016). Economic 3D-printing approach for transplantation of human stem cell-derived β-like cells. *Biofabrication*, *9*(1), 015002–015002. PubMed. https://doi.org/10.1088/1758-5090/9/1/015002

Spaeth, J. M., Gupte, M., Perelis, M., Yang, Y.-P., Cyphert, H., Guo, S., Liu, J.-H., Guo, M., Bass, J., Magnuson, M. A., Wright, C., & Stein, R. (2017). Defining a Novel Role for the Pdx1 Transcription Factor in Islet β-Cell Maturation and Proliferation During Weaning. *Diabetes*, *66*(11), 2830. https://doi.org/10.2337/db16-1516

Speller, N. C., Morbioli, G. G., Cato, M. E., Cantrell, T. P., Leydon, E. M., Schmidt, B. E., & Stockton, A. M. (2019). Cutting edge microfluidics: Xurography and a microwave. *Sensors and Actuators B: Chemical*, *291*, 250–256. https://doi.org/10.1016/j.snb.2019.04.004

Stallcop, L. E., Álvarez-García, Y. R., Reyes-Ramos, A. M., Ramos-Cruz, K. P., Morgan, M. M., Shi, Y., Li, L., Beebe, D. J., Domenech, M., & Warrick, J. W. (2018). Razor-printed sticker microdevices for cell-based applications. *Lab on a Chip*, *18*(3), 451–462. https://doi.org/10.1039/C7LC00724H

Stendahl, J. C., Kaufman, D. B., & Stupp, S. I. (2009). Extracellular Matrix in Pancreatic Islets: Relevance to Scaffold Design and Transplantation. *Cell Transplantation*, *18*(1), 1–12. PMC.

Strale, P.-O., Azioune, A., Bugnicourt, G., Lecomte, Y., Chahid, M., & Studer, V. (2016). Multiprotein Printing by Light-Induced Molecular Adsorption. *Advanced Materials*, *28*(10), 2024–2029. https://doi.org/10.1002/adma.201504154

Strano, A., Tuck, E., Stubbs, V. E., & Livesey, F. J. (2020). Variable Outcomes in Neural Differentiation of Human PSCs Arise from Intrinsic Differences in Developmental Signaling Pathways. *Cell Reports*, *31*(10). https://doi.org/10.1016/j.celrep.2020.107732

Sugimoto, M., Takahashi, S., Kojima, M., Gotohda, N., Kato, Y., Kawano, S., Ochiai, A., & Konishi, M. (2014). What is the nature of pancreatic consistency? Assessment of the elastic modulus of the pancreas and comparison with tactile sensation, histology, and occurrence of postoperative pancreatic fistula after pancreaticoduodenectomy. *Surgery (United States)*, *156*(5), 1204–1211. Scopus. https://doi.org/10.1016/j.surg.2014.05.015

Suszynski, T. M., Avgoustiniatos, E. S., & Papas, K. K. (2014). Intraportal Islet Oxygenation. *Journal of Diabetes Science and Technology*, *8*(3), 575–580. https://doi.org/10.1177/1932296814525827

Svendsen, B., Larsen, O., Gabe, M. B. N., Christiansen, C. B., Rosenkilde, M. M., Drucker, D. J., & Holst, J. J. (2018). Insulin Secretion Depends on Intra-islet Glucagon Signaling. *Cell Reports*, *25*(5), 1127-1134.e2. https://doi.org/10.1016/j.celrep.2018.10.018

Taipale, J., & Keski-Oja, J. (1997). Growth factors in the extracellular matrix. *The FASEB Journal*, *11*(1), 51–59.

Takizawa-Shirasawa, S., Yoshie, S., Yue, F., Mogi, A., Yokoyama, T., Tomotsune, D., & Sasaki, K. (2013). FGF7 and cell density are required for final differentiation of pancreatic amylase-positive cells from human ES cells. *Cell and Tissue Research*, *354*(3), 751–759. https://doi.org/10.1007/s00441-013-1695-6

Tao, T., Wang, Y., Chen, W., Li, Z., Su, W., Guo, Y., Deng, P., & Qin, J. (2019). Engineering human islet organoids from iPSCs using an organ-on-chip platform. *Lab on a Chip*, *19*(6), 948–958. https://doi.org/10.1039/C8LC01298A

Taylor, B. L., Liu, F.-F., & Sander, M. (2013a). Nkx6.1 is essential for maintaining the functional state of pancreatic beta cells. *Cell Reports*, *4*(6), 1262–1275. PubMed. https://doi.org/10.1016/j.celrep.2013.08.010

Taylor, B. L., Liu, F.-F., & Sander, M. (2013b). Nkx6.1 Is Essential for Maintaining the Functional State of Pancreatic Beta Cells. *Cell Reports*, *4*(6), 1262–1275. https://doi.org/10.1016/j.celrep.2013.08.010

Taylor-Weiner, H., Ravi, N., & Engler, A. J. (2015). Traction forces mediated by integrin signaling are necessary for definitive endoderm specification. *Journal of Cell Science*, *128*(10), 1961. https://doi.org/10.1242/jcs.166157

Taylor-Weiner, H., Schwarzbauer, J. E., & Engler, A. J. (2013). Defined extracellular matrix components are necessary for definitive endoderm induction. *STEM CELLS*, *31*(10), 2084–2094. https://doi.org/10.1002/stem.1453

Tewary, M., Ostblom, J., Prochazka, L., Zulueta-Coarasa, T., Shakiba, N., Fernandez-Gonzalez, R., & Zandstra, P. W. (2017). A stepwise model of reaction-diffusion and positional information governs self-organized human peri-gastrulation-like patterning. *Development*, *144*(23), 4298. https://doi.org/10.1242/dev.149658

Thompson, A. J., Pillai, E. K., Dimov, I. B., Foster, S. K., Holt, C. E., & Franze, K. (2019). Rapid changes in tissue mechanics regulate cell behaviour in the developing embryonic brain. *ELife*, *8*, e39356. https://doi.org/10.7554/eLife.39356

Thompson, D. W. (1942). On growth and form. *Cambridge Univ. Press*, *1*(6), 7.

Totaro, A., Panciera, T., & Piccolo, S. (2018). YAP/TAZ upstream signals and downstream responses. *Nature Cell Biology*, *20*(8), 888–899. PubMed. https://doi.org/10.1038/s41556-018-0142-z

Toyoda, T., Kimura, A., Tanaka, H., Ameku, T., Mima, A., Hirose, Y., Nakamura, M., Watanabe, A., & Osafune, K. (2017). Rho-Associated Kinases and Non-muscle Myosin IIs Inhibit the Differentiation of Human iPSCs to Pancreatic Endoderm. *Stem Cell Reports*, *9*(2), 419–428. https://doi.org/10.1016/j.stemcr.2017.07.005

Toyoda, T., Mae, S.-I., Tanaka, H., Kondo, Y., Funato, M., Hosokawa, Y., Sudo, T., Kawaguchi, Y., & Osafune, K. (2015). Cell aggregation optimizes the differentiation of human ESCs and iPSCs into pancreatic bud-like progenitor cells. *Stem Cell Research*, *14*(2), 185–197. https://doi.org/10.1016/j.scr.2015.01.007

Tran, R., Hoesli, C. A., & Moraes, C. (2020). Accessible dynamic micropatterns in monolayer cultures via modified desktop xurography. *Biofabrication*. http://iopscience.iop.org/article/10.1088/1758-5090/abce0b

Tran, R., Moraes, C., & Hoesli, C. A. (2020a). Developmentally-Inspired Biomimetic Culture Models to Produce Functional Islet-Like Cells From Pluripotent Precursors. *Frontiers in Bioengineering and Biotechnology*, *8*, 1147. https://doi.org/10.3389/fbioe.2020.583970

Tran, R., Moraes, C., & Hoesli, C. A. (2020b). Controlled clustering enhances PDX1 and NKX6.1 expression in pancreatic endoderm cells derived from pluripotent stem cells. *Scientific Reports*, *10*(1), 1190. https://doi.org/10.1038/s41598-020-57787-0

Trappmann, B., Gautrot, J. E., Connelly, J. T., Strange, D. G. T., Li, Y., Oyen, M. L., Cohen Stuart, M. A., Boehm, H., Li, B., Vogel, V., Spatz, J. P., Watt, F. M., & Huck, W. T. S. (2012). *Extracellular-matrix tethering regulates stem-cell fate*. *11*, 642.

Trimble, E. R., Halban, P. A., Wollheim, C. B., & Renold, A. E. (1982). Functional differences between rat islets of ventral and dorsal pancreatic origin. *The Journal of Clinical Investigation*, *69*(2), 405–413. PubMed. https://doi.org/10.1172/jci110464

Tschumperlin, D. J., Dai, G., Maly, I. V., Kikuchi, T., Laiho, L. H., McVittie, A. K., Haley, K. J., Lilly, C. M., So, P. T. C., Lauffenburger, D. A., Kamm, R. D., & Drazen, J. M. (2004). Mechanotransduction through growth-factor shedding into the extracellular space. *Nature*, *429*(6987), 83–86. https://doi.org/10.1038/nature02543

Tseng, Q., Duchemin-Pelletier, E., Deshiere, A., Balland, M., Guillou, H., Filhol, O., & Théry, M. (2012). Spatial organization of the extracellular matrix regulates cell–cell junction positioning. *Proceedings of the National Academy of Sciences*, 201106377. https://doi.org/10.1073/pnas.1106377109

Ungrin, M. D., Joshi, C., Nica, A., Bauwens, C., & Zandstra, P. W. (2008). Reproducible, Ultra High-Throughput Formation of Multicellular Organization from Single Cell Suspension-Derived Human Embryonic Stem Cell Aggregates. *PLOS ONE*, *3*(2), e1565. https://doi.org/10.1371/journal.pone.0001565

Ungrin, M., & Zandstra, P. (2011). *Devices And Methods For Production Of Cell Aggregates* (Patent No. US20110086375A1).

van Dongen, S. F. M., Maiuri, P., Marie, E., Tribet, C., & Piel, M. (2013). Triggering Cell Adhesion, Migration or Shape Change with a Dynamic Surface Coating. *Advanced Materials*, *25*(12), 1687–1691. https://doi.org/10.1002/adma.201204474

Vedula, S. R. K., Peyret, G., Cheddadi, I., Chen, T., Brugués, A., Hirata, H., Lopez-Menendez, H., Toyama, Y., Neves de Almeida, L., Trepat, X., Lim, C. T., & Ladoux, B. (2015). Mechanics of epithelial closure over non-adherent environments. *Nature Communications*, *6*(1), 6111. https://doi.org/10.1038/ncomms7111

Vegas, A. J., Veiseh, O., Gürtler, M., Millman, J. R., Pagliuca, F. W., Bader, A. R., Doloff, J. C., Li, J., Chen, M., Olejnik, K., Tam, H. H., Jhunjhunwala, S., Langan, E., Aresta-Dasilva, S., Gandham, S., McGarrigle, J. J., Bochenek, M. A., Hollister-Lock, J., Oberholzer, J., … Anderson, D. G. (2016). Long-term glycemic control using polymer-encapsulated human stem cell–derived beta cells in immune-competent mice. *Nature Medicine*, *22*(3), 306–311. https://doi.org/10.1038/nm.4030

Velazco-Cruz, L., Goedegebuure, M. M., & Millman, J. R. (2020). Advances Toward Engineering Functionally Mature Human Pluripotent Stem Cell-Derived β Cells. *Frontiers in Bioengineering and Biotechnology*, *8*, 786. https://doi.org/10.3389/fbioe.2020.00786

Velazco-Cruz, L., Song, J., Maxwell, K. G., Goedegebuure, M. M., Augsornworawat, P., Hogrebe, N. J., & Millman, J. R. (2019). Acquisition of Dynamic Function in Human Stem Cell-Derived β Cells. *Stem Cell Reports*, *12*(2), 351–365. https://doi.org/10.1016/j.stemcr.2018.12.012

Veres, A., Faust, A. L., Bushnell, H. L., Engquist, E. N., Kenty, J. H.-R., Harb, G., Poh, Y.-C., Sintov, E., Gürtler, M., Pagliuca, F. W., Peterson, Q. P., & Melton, D. A. (2019).

Charting cellular identity during human in vitro β-cell differentiation. *Nature*, *569*(7756), 368–373. https://doi.org/10.1038/s41586-019-1168-5

Versaevel, M., Grevesse, T., & Gabriele, S. (2012). Spatial coordination between cell and nuclear shape within micropatterned endothelial cells. *Nature Communications*, *3*, 671.

Vignaud, T., Galland, R., Tseng, Q., Blanchoin, L., Colombelli, J., & Théry, M. (2012). Reprogramming cell shape with laser nano-patterning. *J Cell Sci*, *125*(9), 2134–2140.

Vijayraghavan, D. S., & Davidson, L. A. (2017). Mechanics of neurulation: From classical to current perspectives on the physical mechanics that shape, fold, and form the neural tube. *Birth Defects Research*, *109*(2), 153–168. https://doi.org/10.1002/bdra.23557

Villasenor, A., Chong, D. C., Henkemeyer, M., & Cleaver, O. (2010). Epithelial dynamics of pancreatic branching morphogenesis. *Development (Cambridge, England)*, *137*(24), 4295–4305. PubMed. https://doi.org/10.1242/dev.052993

Vining, K. H., & Mooney, D. J. (2017). Mechanical forces direct stem cell behaviour in development and regeneration. *Nature Reviews. Molecular Cell Biology*, *18*(12), 728–742. PubMed. https://doi.org/10.1038/nrm.2017.108

Wada, K.-I., Itoga, K., Okano, T., Yonemura, S., & Sasaki, H. (2011). Hippo pathway regulation by cell morphology and stress fibers. *Development*, *138*(18), 3907–3914. https://doi.org/10.1242/dev.070987

Waeber, G., Thompson, N., Nicod, P., & Bonny, C. (1996). Transcriptional activation of the GLUT2 gene by the IPF-1/STF-1/IDX-1 homeobox factor. *Molecular Endocrinology*, *10*(11), 1327–1334. https://doi.org/10.1210/mend.10.11.8923459

Walker, J. T., Haliyur, R., Nelson, H. A., Ishahak, M., Poffenberger, G., Aramandla, R., Reihsmann, C., Luchsinger, J. R., Saunders, D. C., Wang, P., Garcia-Ocaña, A., Bottino,

R., Agarwal, A., Powers, A. C., & Brissova, M. (2020). Integrated human pseudoislet system and microfluidic platform demonstrate differences in GPCR signaling in islet cells. *JCI Insight*, *5*(10), e137017. PubMed. https://doi.org/10.1172/jci.insight.137017

Wan, J., Huang, Y., Zhou, P., Guo, Y., Wu, C., Zhu, S., Wang, Y., Wang, L., Lu, Y., & Wang, Z. (2017). Culture of iPSCs Derived Pancreatic β-Like Cells In Vitro Using Decellularized Pancreatic Scaffolds: A Preliminary Trial. *BioMed Research International*, *2017*, 4276928–4276928. PubMed. https://doi.org/10.1155/2017/4276928

Wang, C., Baker, B. M., Chen, C. S., & Schwartz, M. A. (2013). Endothelial cell sensing of flow direction. *Arteriosclerosis, Thrombosis, and Vascular Biology*, *33*(9), 2130–2136. PubMed. https://doi.org/10.1161/ATVBAHA.113.301826

Wang, H., Abhilash, A., Chen, C. S., Wells, R. G., & Shenoy, V. B. (2014). Long-Range Force Transmission in Fibrous Matrices Enabled by Tension-Driven Alignment of Fibers. *Biophysical Journal*, *107*(11), 2592–2603. PMC. https://doi.org/10.1016/j.bpj.2014.09.044

Wang, H., Maechler, P., Ritz-Laser, B., Hagenfeldt, K. A., Ishihara, H., Philippe, J., & Wollheim, C. B. (2001). Pdx1 Level Defines Pancreatic Gene Expression Pattern and Cell Lineage Differentiation. *Journal of Biological Chemistry*, *276*(27), 25279–25286. https://doi.org/10.1074/jbc.M101233200

Wang, J., Yuan, R., Zhu, X., & Ao, P. (2020). Adaptive Landscape Shaped by Core Endogenous Network Coordinates Complex Early Progenitor Fate Commitments in Embryonic Pancreas. *Scientific Reports*, *10*(1), 1112. https://doi.org/10.1038/s41598-020-57903-0

Wang, N., Tytell, J. D., & Ingber, D. E. (2009). Mechanotransduction at a distance: Mechanically coupling the extracellular matrix with the nucleus. *Nat Rev Mol Cell Biol*, *10*(1), 75–82. https://doi.org/10.1038/nrm2594

Wang, R., & Rosenberg, L. (1999). Maintenance of beta-cell function and survival following islet isolation requires re-establishment of the islet-matrix relationship. *Journal of Endocrinology*, *163*(2), 181–190. https://doi.org/10.1677/joe.0.1630181

Wang, Y., Cheng, L., & Gerecht, S. (2014). Efficient and scalable expansion of human pluripotent stem cells under clinically compliant settings: A view in 2013. *Annals of Biomedical Engineering*, *42*(7), 1357–1372. PubMed. https://doi.org/10.1007/s10439-013-0921-4

Wang, Y., Gunasekara, D. B., Reed, M. I., DiSalvo, M., Bultman, S. J., Sims, C. E., Magness, S. T., & Allbritton, N. L. (2017). A microengineered collagen scaffold for generating a polarized crypt-villus architecture of human small intestinal epithelium. *Biomaterials*, *128*, 44–55. https://doi.org/10.1016/j.biomaterials.2017.03.005

Wang, Y., Lo, J. F., Mendoza-Elias, J. E., Adewola, A. F., Harvat, T. A., Kinzer, K. P., Lee, D., Qi, M., Eddington, D. T., & Oberholzer, J. (2010). Application of microfluidic technology to pancreatic islet research: First decade of endeavor. *Bioanalysis*, *2*(10), 1729–1744. https://doi.org/10.4155/bio.10.131

Watada, H., Kajimoto, Y., Miyagawa, J., Hanafusa, T., Hamaguchi, K., Matsuoka, T., Yamamoto, K., Matsuzawa, Y., Kawamori, R., & Yamasaki, Y. (1996). PDX-1 Induces Insulin and Glucokinase Gene Expressions in αTC1 Clone 6 Cells in the Presence of Betacellulin. *Diabetes*, *45*(12), 1826. https://doi.org/10.2337/diab.45.12.1826

Watt, F. M. (1986). The extracellular matrix and cell shape. *Trends in Biochemical Sciences*, *11*(11), 482–485. https://doi.org/10.1016/0968-0004(86)90252-5

Weber, L. M., & Anseth, K. S. (2008). Hydrogel encapsulation environments functionalized with extracellular matrix interactions increase islet insulin secretion. *Matrix Biology*, *27*(8), 667–673. https://doi.org/10.1016/j.matbio.2008.08.001

Werner, M., Blanquer, S. B. G., Haimi, S. P., Korus, G., Dunlop, J. W. C., Duda, G. N., Grijpma, Dirk. W., & Petersen, A. (2017). Surface Curvature Differentially Regulates Stem Cell Migration and Differentiation via Altered Attachment Morphology and Nuclear Deformation. *Advanced Science*, *4*(2), 1600347. https://doi.org/10.1002/advs.201600347

Wesolowska-Andersen, A., Jensen, R. R., Alcántara, M. P., Beer, N. L., Duff, C., Nylander, V., Gosden, M., Witty, L., Bowden, R., McCarthy, M. I., Hansson, M., Gloyn, A. L., & Honore, C. (2020). Analysis of Differentiation Protocols Defines a Common Pancreatic Progenitor Molecular Signature and Guides Refinement of Endocrine Differentiation. *Stem Cell Reports*, *14*(1), 138–153. https://doi.org/10.1016/j.stemcr.2019.11.010

Willmann, S. J., Mueller, N. S., Engert, S., Sterr, M., Burtscher, I., Raducanu, A., Irmler, M., Beckers, J., Sass, S., Theis, F. J., & Lickert, H. (2016). The global gene expression profile of the secondary transition during pancreatic development. *Mechanisms of Development*, *139*, 51–64. https://doi.org/10.1016/j.mod.2015.11.004

Wolfenson, H., Yang, B., & Sheetz, M. P. (2019). Steps in Mechanotransduction Pathways that Control Cell Morphology. *Annual Review of Physiology*, *81*(1), 585–605. https://doi.org/10.1146/annurev-physiol-021317-121245

Wong, J. C. Y., Gao, S. Y., Lees, J. G., Best, M. B., Wang, R., & Tuch, B. E. (2010). Definitive endoderm derived from human embryonic stem cells highly express the integrin receptors

αV and β5. *Cell Adhesion & Migration*, *4*(1), 39–45. https://doi.org/10.4161/cam.4.1.10627

Wozniak, M. A., & Chen, C. S. (2009). Mechanotransduction in development: A growing role for contractility. *Nat Rev Mol Cell Biol*, *10*(1), 34–43. https://doi.org/10.1038/nrm2592

Wright, D., Rajalingam, B., Karp, J. M., Selvarasah, S., Ling, Y., Yeh, J., Langer, R., Dokmeci, M. R., & Khademhosseini, A. (2008). Reusable, reversibly sealable parylene membranes for cell and protein patterning. *Journal of Biomedical Materials Research Part A*, *85A*(2), 530–538. https://doi.org/10.1002/jbm.a.31281

Wu, H., Uchimura, K., Donnelly, E. L., Kirita, Y., Morris, S. A., & Humphreys, B. D. (2018). Comparative Analysis and Refinement of Human PSC-Derived Kidney Organoid Differentiation with Single-Cell Transcriptomics. *Cell Stem Cell*, *23*(6), 869-881.e8. https://doi.org/10.1016/j.stem.2018.10.010

Wu, J., Rostami, M. R., Cadavid Olaya, D. P., & Tzanakakis, E. S. (2014). Oxygen transport and stem cell aggregation in stirred-suspension bioreactor cultures. *PloS One*, *9*(7), e102486–e102486. PubMed. https://doi.org/10.1371/journal.pone.0102486

Wu, Y., Aegerter, P., Nipper, M., Ramjit, L., Liu, J., & Wang, P. (2021). Hippo Signaling Pathway in Pancreas Development. *Frontiers in Cell and Developmental Biology*, *9*, 1132. https://doi.org/10.3389/fcell.2021.663906

Xia, Y., & Whitesides, G. M. (1998). Soft Lithography. *Angewandte Chemie International Edition*, *37*(5), 550–575. https://doi.org/10.1002/(SICI)1521-3773(19980316)37:5<550::AID-ANIE550>3.0.CO;2-G

Xin, X., Hussain, M., & Mao, J. J. (2007). Continuing differentiation of human mesenchymal stem cells and induced chondrogenic and osteogenic lineages in electrospun PLGA

nanofiber scaffold. *Biomaterials*, *28*(2), 316–325. PMC. https://doi.org/10.1016/j.biomaterials.2006.08.042

Xu, H., Tsang, K. S., Chan, J. C. N., Yuan, P., Fan, R., Kaneto, H., & Xu, G. (2013). The Combined Expression of Pdx1 and MafA with Either Ngn3 or NeuroD Improves the Differentiation Efficiency of Mouse Embryonic Stem Cells into Insulin-Producing Cells. *Cell Transplantation*, *22*(1), 147–158. https://doi.org/10.3727/096368912X653057

Xue, X., Sun, Y., Resto-Irizarry, A. M., Yuan, Y., Aw Yong, K. M., Zheng, Y., Weng, S., Shao, Y., Chai, Y., Studer, L., & Fu, J. (2018). Mechanics-guided embryonic patterning of neuroectoderm tissue from human pluripotent stem cells. *Nature Materials*, *17*(7), 633–641. https://doi.org/10.1038/s41563-018-0082-9

Yabe, S. G., Fukuda, S., Nishida, J., Takeda, F., Nashiro, K., & Okochi, H. (2019). Induction of functional islet-like cells from human iPS cells by suspension culture. *Regenerative Therapy*, *10*, 69–76. https://doi.org/10.1016/j.reth.2018.11.003

Yang, M. T., Fu, J., Wang, Y.-K., Desai, R. A., & Chen, C. S. (2011). Assaying stem cell mechanobiology on microfabricated elastomeric substrates with geometrically modulated rigidity. *Nat. Protocols*, *6*(2), 187–213. https://doi.org/10.1038/nprot.2010.189

Yoshie, H., Koushki, N., Kaviani, R., Tabatabaei, M., Rajendran, K., Dang, Q., Husain, A., Yao, S., Li, C., Sullivan, J. K., Saint-Geniez, M., Krishnan, R., & Ehrlicher, A. J. (2018). Traction Force Screening Enabled by Compliant PDMS Elastomers. *Biophysical Journal*, *114*(9), 2194–2199. PubMed. https://doi.org/10.1016/j.bpj.2018.02.045

Young, J., Margaron, Y., Fernandes, M., Duchemin-Pelletier, E., Michaud, J., Flaender, M., Lorintiu, O., Degot, S., & Poydenot, P. (2018). MyoScreen, a High-Throughput Phenotypic Screening Platform Enabling Muscle Drug Discovery. *SLAS DISCOVERY:*

Advancing the Science of Drug Discovery, *23*(8), 790–806. https://doi.org/10.1177/2472555218761102

Youngblood, R. L., Sampson, J. P., Lebioda, K. R., & Shea, L. D. (2019). Microporous scaffolds support assembly and differentiation of pancreatic progenitors into β-cell clusters. *Acta Biomaterialia*, *96*, 111–122. https://doi.org/10.1016/j.actbio.2019.06.032

Yourek, G., McCormick, S. M., Mao, J. J., & Reilly, G. C. (2010). Shear stress induces osteogenic differentiation of human mesenchymal stem cells. *Regenerative Medicine*, *5*(5), 713–724. PubMed. https://doi.org/10.2217/rme.10.60

Yu, Y., Gamble, A., Pawlick, R., Pepper, A. R., Salama, B., Toms, D., Razian, G., Ellis, C., Bruni, A., Gala-Lopez, B., Lu, J. (Lulu), Vovko, H., Chiu, C., Abdo, S., Kin, T., Korbutt, G., Shapiro, A. M. J., & Ungrin, M. (2018). Bioengineered human pseudoislets form efficiently from donated tissue, compare favourably with native islets in vitro and restore normoglycaemia in mice. *Diabetologia*, *61*(9), 2016–2029. https://doi.org/10.1007/s00125-018-4672-5

Yung, T., Poon, F., Liang, M., Coquenlorge, S., McGaugh, E. C., Hui, C., Wilson, M. D., Nostro, M. C., & Kim, T.-H. (2019). Sufu- and Spop-mediated downregulation of Hedgehog signaling promotes beta cell differentiation through organ-specific niche signals. *Nature Communications*, *10*(1), 4647. https://doi.org/10.1038/s41467-019-12624-5

Zaidel-Bar, R. (2013). Cadherin adhesome at a glance. *Journal of Cell Science*, *126*(2), 373–378. https://doi.org/10.1242/jcs.111559

Zhao, B., Li, L., Wang, L., Wang, C.-Y., Yu, J., & Guan, K.-L. (2012). Cell detachment activates the Hippo pathway via cytoskeleton reorganization to induce anoikis. *Genes & Development*, *26*(1), 54–68.

Zhao, L., Mok, S., & Moraes, C. (2019). Micropocket hydrogel devices for all-in-one formation, assembly, and analysis of aggregate-based tissues. *Biofabrication*, *11*(4), 045013. https://doi.org/10.1088/1758-5090/ab30b4

Zhou, J. X., Brusch, L., & Huang, S. (2011). Predicting Pancreas Cell Fate Decisions and Reprogramming with a Hierarchical Multi-Attractor Model. *PLOS ONE*, *6*(3), e14752. https://doi.org/10.1371/journal.pone.0014752

Zhou, J. X., Samal, A., d'Hérouël, A. F., Price, N. D., & Huang, S. (2016). Relative stability of network states in Boolean network models of gene regulation in development. *Biosystems*, *142–143*, 15–24. https://doi.org/10.1016/j.biosystems.2016.03.002

Zhou, Q., Law, A. C., Rajagopal, J., Anderson, W. J., Gray, P. A., & Melton, D. A. (2007). A Multipotent Progenitor Domain Guides Pancreatic Organogenesis. *Developmental Cell*, *13*(1), 103–114. https://doi.org/10.1016/j.devcel.2007.06.001

Zhu, M., Tao, H., Samani, M., Luo, M., Wang, X., Hopyan, S., & Sun, Y. (2020). Spatial mapping of tissue properties in vivo reveals a 3D stiffness gradient in the mouse limb bud. *Proceedings of the National Academy of Sciences*, *117*(9), 4781. https://doi.org/10.1073/pnas.1912656117

Zhu, Y., Liu, Q., Zhou, Z., & Ikeda, Y. (2017). PDX1, Neurogenin-3, and MAFA: critical transcription regulators for beta cell development and regeneration. *Stem Cell Research & Therapy*, *8*(1), 240. https://doi.org/10.1186/s13287-017-0694-z